Natural products as leads for the synthesis of new anticancer compounds

Thesis of: **SILVIA GAZZOLA**

Supervisor: Professor GIANLUIGI BROGGINI

Accademic year: 2015-2016

Dedicata a mia sorella e amica Kikka…

….perchè la Chimica è la filosofia di Madre Natura…

INDEX

Introduction

1. Chapter 1

1.1. Cancer

Although some promising developments have been achieved thanks to an intensive medical and pharmaceutical research, cancer remains one of the leading causes of mortality worldwide.[1] There were an estimated 14.1 million cancer cases around the world in 2012, of these 7.4 million cases were in men and 6.7 million in women. This number is expected to increase to 24 million by 2035.[2]

The word "cancer" derives from the father of medicine, Hippocrates, who used the Greek word *karkinos* (crab or crayfish) to describe solid malignant tumour due to the appearance of the cut
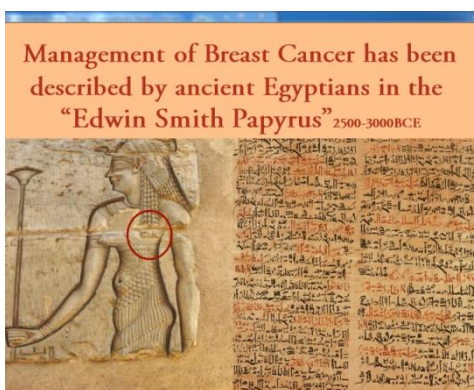
surface of them with "the veins stretched on all sides as the animal the crab has its feet, whence it derives its name". The Roman physician, Celsus (28-50 B.C.), later translated the Greek term into *cancer*, the Latin word for crab.[3] The earliest known descriptions of cancer appear in seven papyri, discovered and deciphered late in the 19th century. Two of them, known as the "Edwin Smith" and "George Ebers" papyri, contain descriptions of cancer written around 1600 B.C., and are believed to date from sources as early as 2500 B.C.

Cancer is the general name for a group of more than 100 diseases. Although there are many kinds of cancer, all cancers start because abnormal cells grow out of control. In most cases, the cancer cells form a tumor. Over time, the tumours can invade nearby normal tissue, crowd it out, or push it aside. Some cancers, like leukemia, rarely form tumours but these cancer cells involve the blood and blood-forming organs and circulate through other tissues where they grow.[4] Cancers may be caused in one of three ways, namely incorrect diet, genetic predisposition, and via the

---
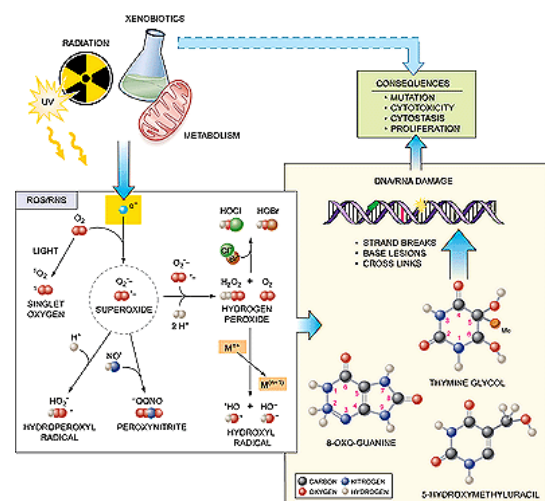
[1] a) S. Sednia, *New Approaches to Natural Anticancer Drugs*, SpringerBriefs in Pharmaceutilcal Science & Drug Development, **2015**; b) A. Jemal; F. Bray; M. M. Center; J. Ferlay; E. Ward; D. Forman, *CA-Cancer J. Clin.*, **2011**, *61*, 69; c) R. Siegel; D. Naishadham; A. Jemal, *CA-Cancer J. Clin.*, **2012,** *62*, 10.

[2] J. Ferlay; I. Soerjomataram; M. Ervik; R. Dikshit; S. Eser; C. Mathers; M. Rebelo; D. M. Parkin; D. Forman; F. Bray, *Cancer Incidence and Mortality Worldwide International Agency for Research on Cancer*, **2014**.

[3] R. W. Moss, *Galen on Cancer,* **2004**.

[4] http://www.cancer.org/cancer/cancerbasics/what-is-cancer

environment. As many as 95% of all cancers are caused by life style and may take as long as 20-30 years to develop.[5] The transformation of a normal cell into a cancerous cell is believed to proceed through many stages and one of the most important mechanism contributing to this process is considered to be oxidative damage to the DNA. If a cell containing damaged DNA divides before the DNA can be repaired, the result is likely to be a permanent genetic alteration constituting a first step in carcinogenesis. This stage may remain dormant, and the subject may only be at risk for developing cancer at a later stage. The second stage, called promotion, occurs very slowly over a period ranging from several months to years. During this stage, a change in diet and lifestyle can have beneficial effect so that person may not develop cancer during his or her lifetime. The third and final stage involves progression and spread of the disease.[6]

A significant feature of tumour cells is their abnormal cell growth and, basically, the conventional chemotherapy mostly targets one or more process involved DNA replication and cell division. That is why these compounds have high toxicity even with the normal cells, therefore a massive fraction of current research in this area is now moving towards molecular therapeutic agents targeting the key molecular abnormalities that drive malignant transformation and progression of tumours (e.g., kinases related to cell cycle progression or signal transduction).[7]

1.2. Natural sources as potential anti-cancer agents

Natural products have been the most significant source of drugs and drug leads in history.[8] Plants, in particular, have formed the basis of sophisticated traditional medicine systems, with the earliest records, dating from around 2600 B.C., documenting the uses of approximately 1000 plant-derived substances in Mesopotamia. These include oils of *Cedrus species* (cedar) and *Cupressus sempevirens* (cypress), *Glycyrrhiza glabra* (licorice), *Commiphora species* (myrrh), and *Papaver somniferum* (poppy juice), all of which are still used today for the treatment of ailments ranging from coughs and colds to parasitic infections and inflammation.[9] The ancient medical literature reports that the surgery was a common practice, however the physicians also recommended the use of some natural products, especially arising from plants. For example, the extensive use of traditional Chinese medicine has been documented over the centuries,[10] with the first record dating from about 1100 B.C. (Wu Shi Er Bing Fang, containing 52 prescriptions). Even from the ancient Western world, Dioscorides, a Greek physician (100 C.E.), accurately recorded the collection, storage, and use of medicinal herbs during his travels with Roman armies

---

[5] A. Bhanot; R. Sharma; M. N. Nooli; *J. of Phytomed.*, **2011**, *3*, 9.
[6] L. Reddy; B. Odhav; K. D. Bhoola; *Pharm. & Therap.*, **2003**, *99*, 1.
[7] K.-H Altmann; Jurg Gertsch; *Nat. Prod. Rep.,* **2007***, 24,* 327.
[8] G. Tan; C. Gyllenhaal; D. D. Soejarto; *Curr. Drug Targets*, **2006**, 265.
[9] J. K. Borchardt; *Drug New Perspect.*, **2002**, *15*, 187.
[10] K. C. Huang; *The pharmacology of Chinese Herbs, 2nd ed.* CRC Press, **1990**.

throughout the "known world", whilst Galen (130–200 C.E.) a practitioner and teacher of pharmacy and medicine in Rome, is well known for his complex prescriptions and formulae used in compounding drugs.

Plants have a long history of use in the treatment of cancer, as reported by Hartwell in his review of 1982 where he lists more than 3000 plant species that have reportedly been used against this disease.[11] To note that in many reports, the word "cancer" is undefined, or related to conditions such as "hard swellings", abscesses, warts, calluses, polyps or tumours, to name a few. Such symptoms would generally apply to skin, "tangible" or visible conditions, and may indeed sometimes correspond to a cancerous condition, but many of the claims for the efficacy of such treatment should be viewed with some skepticism because cancer, as a specific disease entity, is likely to be poorly defined in terms of folklore and traditional medicine.[12] Nevertheless, nature has played an important role as a source of effective anticancer compounds. Cragg *at al.*, in their well-known publication of 2012, demonstrate as only the 20,2% of the 128 anticancer drugs approved or in clinical trials from 01/1981 to 12/2010 are classifiable into the "totally synthetic drugs" (S) category. The residual 79.8% are either genuine natural products or are based thereon, or mimicked natural products in one form or another (Figure 1).[13]
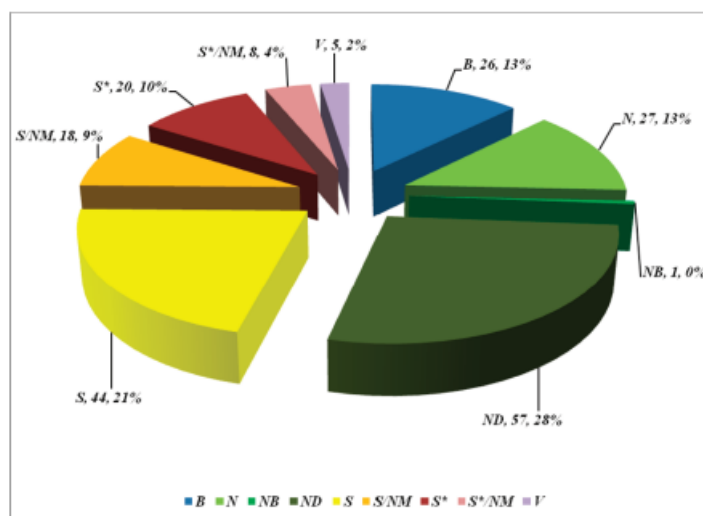
Figure 1: N: Derived from an unmodified natural product source; ND: derived from a natural product source (e.g., semisynthetics); NM: natural product mimic S: Exclusively from a synthetic source; S*: From a synthetic source, but originally modelled on a natural product parent; B: Biologics (monoclonals, etc. derived from mammalian sources); V: vaccines; NB: natural product botanical (botanical "defined mixture").

In the same review it is possible to find a huge list (filled up to 2012) of anticancer compounds arising from natural sources, which normally are classified in plant, marine or microorganism

[11] J. Hartwell; *Plants Used Against Cancer: A Survey - Quarterman Pub., Incorporated*, **1982**.

[12] G. M. Cragg; M. R. Boyd; J. H. Cardellina II; D. J. Newman; K. M. Snader; T. G. McCloud; *Ethnobotany and drug discovery: The experience of the US National Cancer Institute, in: D.J. Chadwick, J. Marsh (Eds.), Ethnobotany and the search for new drugs, ciba foundation symposium, John Wiley & Sons, Inc., New York, NY,* **1994**, *185*, 178.

[13] D. J. Newman; G. M. Cragg; *J. Nat. Prod.*, **2012**, *75*, 311.

sources. It worth to note the incredible diversity and complexity of some molecular structures associated with several different mechanisms of action on cancer cells. In the following section the most famous classes of anticancer compounds there will be listed, divided on the basis of their source (plant, marine-derived or microbial agents).

1.2.1. Plants as source of anti-cancer agents

Discovery and development of the vinca alkaloids were the start of the history of plant as source of anti-cancer agents (earnest 1950s). Vinblastine and vincristine, belonging to vinca alkaloid family, were isolated from the Madagascar periwinkle, Catharanthus roseus or also known as *Vinca rosea*. Regard their general mechanism of action, they bind specifically to β-tubulin blocking its ability to polymerize with α-tubulin into microtubules and therefore prohibiting the mitotic spindle formation.[14] This leads to the killing of actively dividing cells by inhibiting progression through mitosis. Vincristine is largely used in the treatment of haematological and lymphatic neoplasm a well as of several solid tumours (vinblastine in breast, testicular cancer ecc.) (Figure 2).[15]

Vincristina: R = CHO
Vinblastina: R = CH$_3$
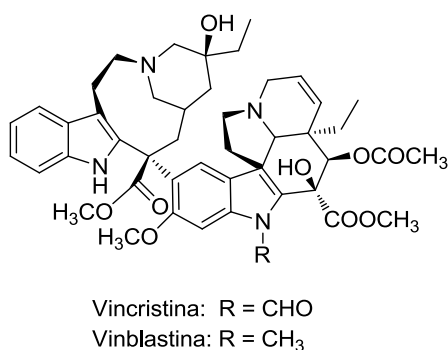
Figure 2

The vinca alkaloids are dimeric asymmetrical compounds consisting of two multi-ringed subunits, vindoline and catharantine, linked by a carbon-carbon bridge. From structural modifications of vinblastine derive the first new second-generation vinca alkaloid, vinorelbine **A**. Specifically, the carboxylic ester group of vinblastine at position 16 was converted to amide 5 in a reaction with refluxing ammonia (Eli Lilly patent) (Scheme 1).[16]

---

[14] R. L. Noble; *Biochem. Cell Biol.*, **1990**, *68*, 1344.

[15] V. T. DeVita; A. A. Serpick; P. O. Carbone; *Ann. Intern. Med.,* **1970**, *73*, 881.

[16] Eli Lilly Company, *DE Patent 22415980*, **1974**.
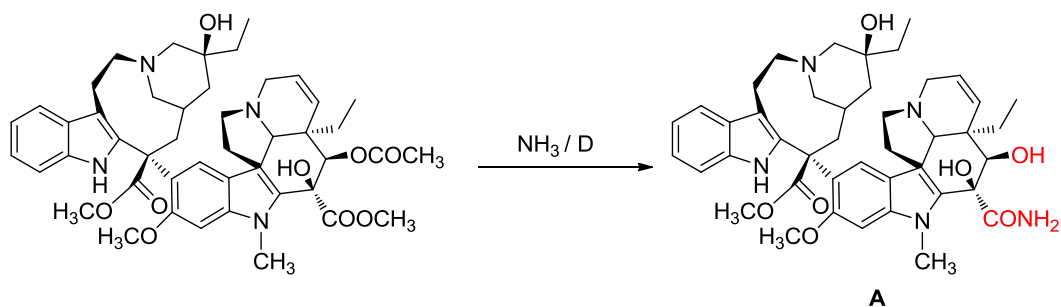
Scheme 1

Wall and co-workers in 1971 reported for the first time the structure of paclitaxel (Taxol®; Figure 3), an high cytotoxic molecule extracted from the bark of *Taxus brevifolia* which represent today the most exciting plant derived anticancer drug discovered in recent years.[17]
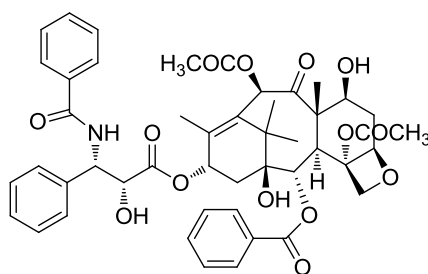
Paclitaxel

Figure 3

Its mode of action was discovered by Schiff and Horwitz in 1979 who reported in 1980 its ability by inhibiting mitosis through enhancement of the polymerization of tubulin and consequent stabilization of microtubules.[18] The lack of availability of taxol (yield of extraction: 0.14 g/Kg) have prompted extensive searches for alternative sources, such as semisynthesis, total chemical synthesis[19] and cellular culture production.[20] In particular the commercial semisynthesis of paclitaxel (by Bristol-Myers Squibb), developed by Robert Holton in 1989, starts from 10-deacetylbaccatin III **B** (easily extracted with yield 1 g/kg from the fresh leaves of English yew tree *T. baccata* L.) is based on tail addition of the so-called Ojima lactam **C** to its free hydroxyl group (Scheme 2).[21]

[17] M. C. Wani; H. L. Taylor; M. E. Wall; P. Coggon; A. T. McPhail; *J. Am. Chem. Soc.*, **1971**, *93*, 2325.

[18] P. B. Schiff; S. B. Horwitz; *Proc. Natl. Acad. Sci. U.S.A.*, **1980**, *77*, 1561.

[19] a) K. C. Nicolaou; Z. Zang; J. J. Liu; H. Ueno; P. G. Nantermet; R. K. Guy; C. F. Claiborne; J. Renaud; E. A. Couladouros; K. Paulvannan; E. J. Sorensen; *Nature*, **1994**, *367*, 630; b) R. A. Holton; C. Somoza; H. B. Kim; F. Liang; R. J. Biediger; D. Boatman; V. Shindo; C. C. Smith; S. Kim; H. Nadizadeh; Y. Suzuki; C. Tao; P. Vu; S. Tang; P. Zhang; K. K. Murthi; L. S. Gentile; J. H. Liu; *J. Am. Chem. Soc.*, **1994**, *116*, 1597.

[20] S. Kusari; S. Singh; C. Jayabaskaran; *Trends in Biotechnology*, **2014**, *32*, 6.

[21] R. A. Holton; *Metal Alkoxides.* U.S. Patent, **1993**, 5, 274, 124.
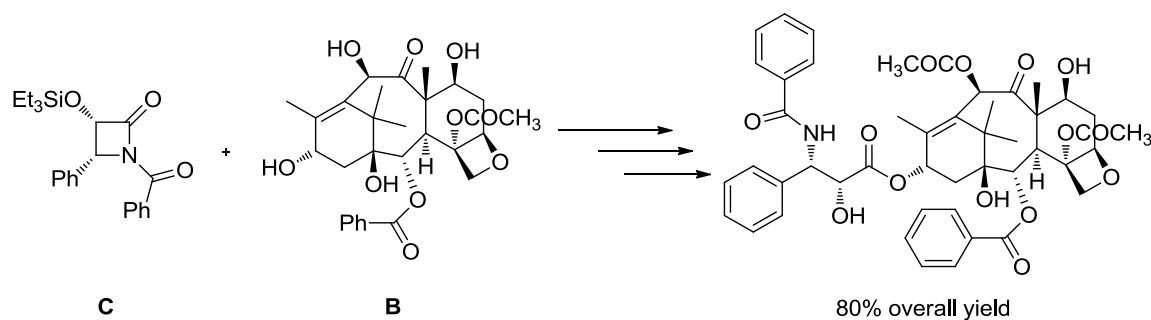
Scheme 2

Taxol® was approved for clinical use against ovarian cancer in 1992 and against breast cancer in 1994. The success of paclitaxel spawned extensive studies on the synthesis of analogues: docetaxel (Taxotere®; Figure 4), the first one to be developed, was obtained from 10-deacetylbaccatin III **B**.
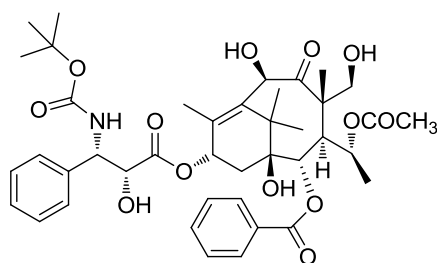
Taxotere

Figure 4

Paclitaxel and docetaxel are hydrophobic compounds characterized by a taxane ring core and unusual fourth ring at the C-4,5 position. The latter, together with a complex ester group at the C-13 position, is essential for their biological activity.

In the 1950s, the extraction of the Chinese tree *Camptotheca acuminata* led to the isolation of an high cytotoxic extract active against several solid tumours and leukaemias, but only in 1966 the active component of the extract, campthotecin, was identified and characterized.[22] Camptothecin (as its sodium salt) was dropped after it was found to be really toxic despite promising anti-tumour activity in the clinical trials. Many years later, irinotecan and belotecan, two semisynthetic camptothecin analogues, became the three clinically-active agents against colorectal and ovarian cancer (Figure 5).[23]

---

[22] M. E. Wall; M.C. Wani; C. E. Cook; K. H. Palmer; A. T. McPhail; G. A. Sim; *J. Am. Chem. Soc.,* **1966**, *88*, 3888.
[23] H. Malonne; G. Atassi; *Anticancer Drugs*, **1997**, *8*, 811.

Camptothecin   Irinotecan   Belotecan
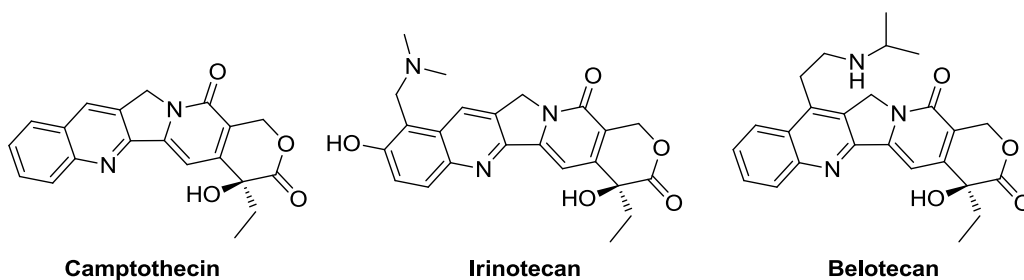
Figure 5

Camptothecin and its derivatives have a basic structure based on five-ring moiety structure with a S-conformation chiral centre in the terminal lactone ring. The configuration of stereocenter and the hydroxyl group which it is attached are fundamental for biological activity. Camptothecins cause DNA damage by stabilizing the covalent topoisomerase I-DNA complex, thus preventing religation.[24]

1.2.2. Marine organisms as source of anti-cancer agents

Covering more than 70% of the earth's surface, the world's oceans represent a huge resource for the discovery of new anticancer compounds. Marine organisms, such as sponges, bacteria or algae, are a unique reservoir for bioactive natural products, with structural features not generally found in terrestrial plant metabolites.[25] The marine organisms produce these compounds to protect themselves against predators, communicate and reproduce. In the last decade, more than 3000 new compounds have been discovered in marine environments and, among these, a number of novel marine compounds have been isolated and tested for anticancer activity.[26]

In September 2007 the complex alkaloid isolated from the colonial tunicate *Ecteinascidia turbinata*, ecteinascidin 743, was approved under the name Yondelis® for the treatment of soft tissue sarcomas (Figure 6). Moreover it is also currently in a number of clinical trials for breast, prostate, liposarcoma and paediatric sarcomas. The issue of compound supply was solved with the development of a semisynthetic route from the microbial product cyanosafracin B [48–50] (Figure 6).[27]

---

[24] Y.H. Hsiang; R. Hertzberg; S. Hecht; L.F. Liu; *J. Biol. Chem.*, **1985**, *260*, 14873.

[25] W. R. Sawadogo; R. Boly; C. Cerella; M. H. Teiten; M. Dicato; M. Diederich; *Molecules*, **2015**, *20*, 7097.

[26] H.M. Sarfaraj; F. Sheeba; A. Saba; S.K. Mohd; *Indian J. Geo-Mar. Sci.*, **2012**, *41*, 27.

[27] C. Cuevas; A. Francesch; *Nat. Prod. Rep.*, **2009**, *26*, 322.

Ecteinascidin 743

Cyanosafracin B
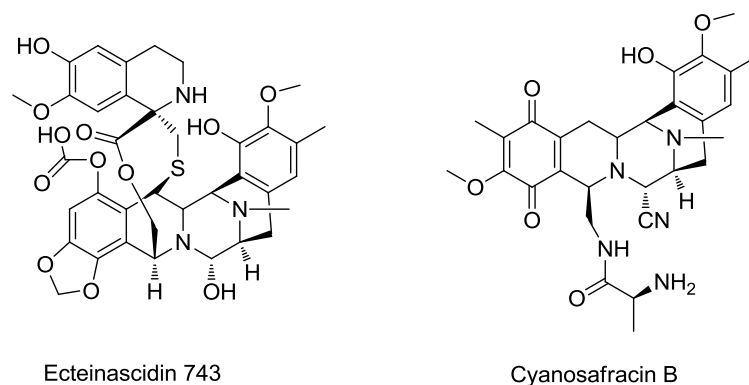
Figure 6

Another example of anticancer agents extracted from several marine sponges, and approved in November 2010 by FDA for the treatment of refractory metastatic breast cancer, is halichondrin B (Figure 7).[28]

Halichondrin B
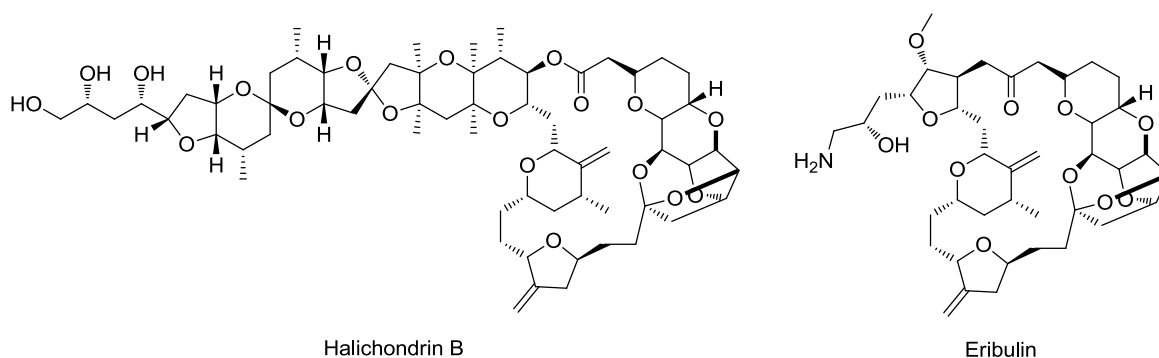
Eribulin

Figure 7

The total synthesis of the complex polyether structure was a hard challange for the drug production, but fortunately total synthetic studies revealed that the right hand half of halichondrin B (eribulin, Figure 7) retained all or most of the potency of the parent compound. Therefore a large-scale synthesis of this bioactive molecule was developed providing the necessary amount of eribulin for the clinical trials.[29] Eribulin is a microtubule dynamics inhibitor that, despite than other known classes of tubulin-targeted agents (taxanes, epothilones, and vinca alkaloid) suppresses microtubule polymerization sequestering tubulin into non-functional aggregates.[30]

Bryostatin 1 (Figure 8), the most-studied member of the family of Bryostatins, was originally isolated in the 1960s by Pettit and his collaborators from the invertebrate marine bryozoan, *Bugula neritina* taken from California coast. This marine-metabolite is a complex macrolide

[28] M. J. Yu; Y. Kishi; B. A. Littlefield; *Anticancer agents from natural products. Taylor and Francis; Boca Raton, FL*, **2005**, 241.

[29] J. Cortes; J. O'Shaughnessy; D. Loesch; J. L. Blum; L. T. Vahdat; K. Petrakova; P. Chollet; A. Manikas; V. Diéras; T. Delozier; V. Vladimirov; F. Cardoso; H. Koh; P. Bougnoux; C. E. Dutcus; S. Seegobin; D. Mir; N. Meneses; J. Wanders; C. Twelves; *Lancet.*, **2011**, *377,* 914.

[30] A.I. Spira; N.O. Iannotti; M.A. Savin; M. Neubauer; N.Y. Gabrail; R.H. Yanagihara; E.A. Zang; P.E. Cole; D. Shuster; A. Das; *Clin. Lung Cancer*, **2012**, *13*, 31.

lactone that, thank to its ability to interact with protein kinase C isozymes, it shows an excellent anticancer activity against various cancer cells lines, including lung, breast, ovarian, melanoma, sarcoma, lymphoma, and leukemia cell lines.[31]
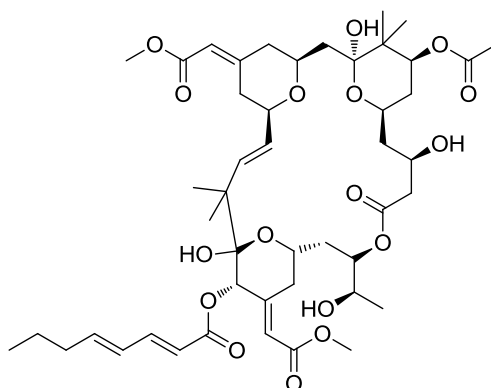
Bryostatin 1

Figure 8

The major problem for making it an available drug is the compound supply. Harvesting them from the naturally available bryozoan is impractical, and their total chemical syntheses are really long. The first total synthesis of bryostatin 1 developed by Gary E. Keck and coworkers of the University of Utah in 2011 consists of 58 steps.[32]

1.2.3. Microorganisms as source of anti-cancer agents

Some of the most important drugs of the pharmaceutical industry arise from microorganisms, an incredible productive source of structurally diverse bioactive metabolites.[33]

Antitumor antibiotics, isolated from various *Streptomyces* species, represent amongst the most important family of the cancer chemotherapeutic agents. Between them, noteworthy are the anthracyclines, which their history goes back more than 50 years, when the Italian company, Pharmitalia Research Laboratories, found a red pigment expressing antibacterial properties from microorganisms living in the soil near the Adriatic Sea. This pigment was purified and studied, and became the first recognized anthracycline antibiotic. The first anticancer anthracycline to be approved for clinical use was daunomycin in the late 1960s. This compound is still widely used in the treatment of several forms of leukemia. A second anthracycline, derived from *Streptomyces peucetius var. caesius* and called doxorubicin, remains a therapeutic milestone for the treatment of lymphoma, breast cancer, and most forms of sarcoma (Figure 9).[34]

---

[31] D. J. Newman; *Anticancer agents from natural products. 2. Taylor and Francis; Boca Raton, FL*, **2012**, 199.
[32] G. E. Keck; Y. B. Poudel; T. J. Cummins; A. Rudra; J. A. Covel; *J. Am. Chem. Soc.*, **2011**, *133*, 744.
[33] G. M. Cragg; D. J. Newman; *Biochim Biophys Acta*, **2013,** *1830,* 3670.
[34] M. S. Ewer; M. D. JDa; D. D. Von Hoff, R. S. Benjamin; *Heart Failure Clin.*, **2011**, *7*, 363.

Daunomycin   Doxorubicin
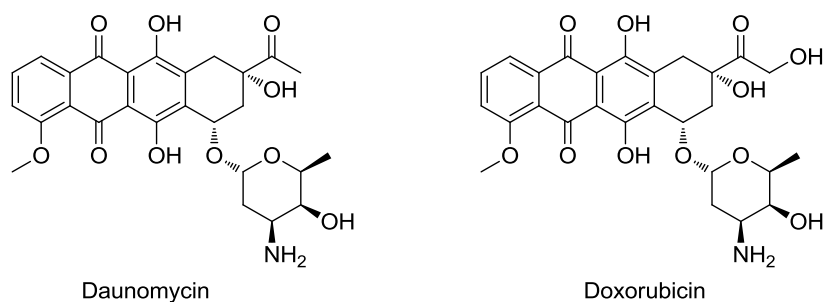
Figure 9

Other very important members of antitumor antibiotic family are, for example, bleomycins, actinomycins, the enediynes, and the staurosporines.[35]

In 1978 Baker *e co.* reported a new potential antifungal agent produced by *Streptomyces hygroscopicus*, the 31-membered macrocyclic rapamycin (Figure 10).[36]
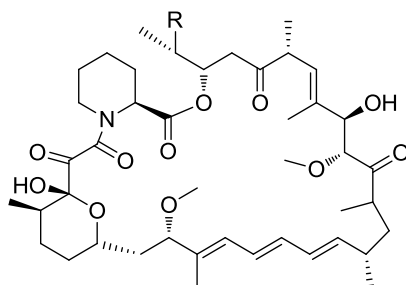
Rapamycin macrolide

Figure 10

Although the failure of rapamycin as antifungal agent, further studies highlighted its antitumour activity against several cancer cell lines. Thus the rapamycin basic structure was used as base for further modifications, leading to the development of a wide range of anticancer agents.[35]

In recent years, the rise of paclitaxel-resistant tumours in patients encouraged the researchers to look for new microtubule stabilizing agents for cancer therapy. The accurate investigation from myxobacteria led to the discovery of epothilones, some of the most interesting natural product base structures for the development of powerful anticancer drug (Figure 11).[37]

---

[35] L.-A. Giddings; D. J. Newman; *J. Ind. Microbiol. Biotechnol*, **2013**, *40*, 1181.

[36] H. Baker; A. Sidorowicz; S. N. Sehgal; C. Vezina; *J. Antibiot.*, **1978**, *31*, 539.

[37] D. M. Bollag; P. A. Mcqueney; J. Zhu; O. Hensens; L. Koupal; J. Liesch; M. Goetz; E. Lazarides; C. M. Woods; *Cancer Res.*, **1995**, *55*, 2325.
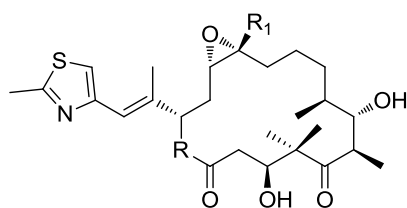
Epothilone A: R = O, R^1 = H
Epothilone B: R = O, R^1 = CH_3
Ixabepilone: R = NH, R^1 = CH_3

Figure 11

In the mid to late 1980s the 16-membered macrolides epothilones A and B were identified in the extracts of the myxobacterium *Sorangium cellulosum*. Classical fermentation and manipulation of the biosynthetic cluster have given significant quantities of different epothilones and, in addition, semi- and total syntheses are being performed by a number of research groups affording modified macrolide ring. Epothilone B (or patupilone) showed better antineoplastic activity than epothilone A in preclinical trials, therefore it has subsequently advanced to further stages of clinical development. However, reduced *in vivo* efficacy was recognized because of its poor metabolic stability and pharmacokinetic properties. Since the easy hydrolysis of lactone function by esterases was a major obstacle for clinical utility, epothilone B was modified in a lactam (ixabepilone). The aza-epothilone B was approved for against metastatic breast cancer by the FDA in 2007, and is currently in many trials from Phase I to Phase III against a variety of carcinomas.[38]

The last example of a microorganism metabolite reported in this context regard cryptophycins. Cryptophycins are a family of macrocylicic depsipeptides firstly isolated from cyanobacteria *Nostoc* sp. ATCC 53789 in 1990. Cryptophycin 1, the main antitumor activity responsible of the bacteria extract, and cryptophycin-52, the highly bioactive synthetic derivative, display remarkable cytotoxicity even against multi-drug resistance (MDR) cancer cells (Figure 12).
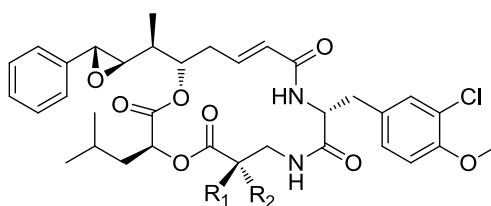
Cryptophycin 1: R^1 = Me, R^2 = H
Cryptophycin-52: R^1 = R^2 = Me

Figure 12

Their bioactivity is based on their interaction with the β-subunit of α/β-tubulin dimers inducing apoptosis due to inhibition of the microtubule dynamics. The IC_{50} of cryptophycin 1 and

---

[38] G. Hofle; H. Reichenbach; *Anticancer agents from natural products. Taylor and Francis; Boca Raton, FL,* **2012**, 513.

cryptophycin-52 show 100- to 1000-fold increased *in vitro* activity compared to paclitaxel or *Vinca* alkaloids. However, *in vivo* they display high cytotoxicity, therefore numerous synthetic analogues have been designed for structure–activity relationship (SAR) studies to improve the cancer cells selectivity. Norbert Sewald and co-workers in 2013 published a comprehensive review regarding modified cryptophycins.[39]

2. Chapter 2

2.1. Biosynthesis principles

The life of all living organisms is ensured by continuous transformation and modification of a wide number of organic compounds. The metabolic pathway is the term used to indicate the pathways in which an integrated network of enzyme-mediated and regulated chemical reaction works for this purpose. There are two kinds of metabolisms:

> ➢ primary metabolism, which describes the processes involved the formation of the crucial important molecules of life (carbohydrates, proteins, fats and nucleic acids);

> ➢ secondary metabolism, which concerns the production of compounds with more limited distribution in nature.

Despite the incredible varied features of living organisms, the primary metabolites are generated essentially through the same pathways, apart from minor variations. In contrast, the secondary metabolites are found in only specific organisms, or group of organisms, and are expression of the individuality of species. The function of these compounds is not always clear, but it is logical to assume that all of them do play some vital role of the producer. Most of the pharmacologically active natural products belong in the area of secondary metabolites.

Surprisingly, only few molecules are used by natural products biosynthesis processes as main building blocks. For instance, intermediates of acetyl coenzyme A, shikimic acid, mevalonic acid, and 1-deoxyxylulose 5-phosphate, which are furnished from the primary metabolism (Scheme 3). In addition to these, other building blocks based on amino acids are frequently employed in natural product synthesis.

---

[39] C. Weiss; B. Sammet; N. Sewald; *Nat. Prod. Rep.*, **2013**, *30*, 924.
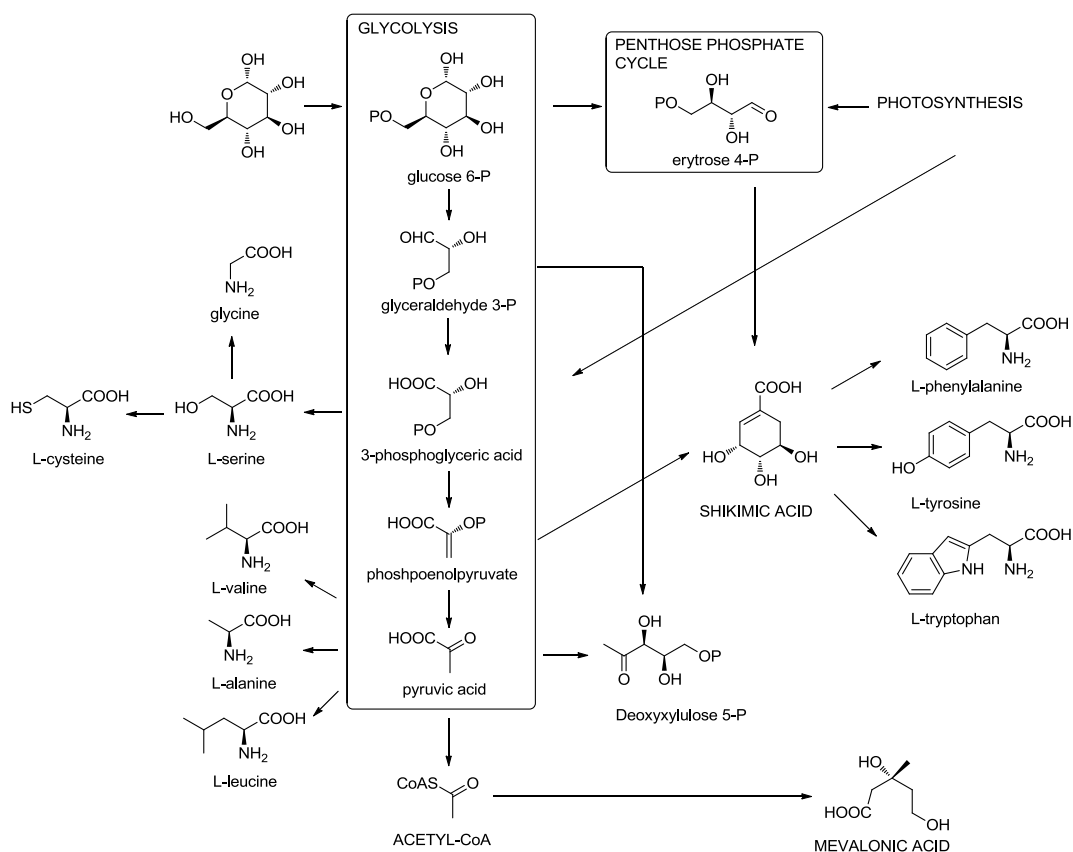
Scheme 3

The follow scheme shows the most frequently basic units that it is possible to encounter when the carbon and nitrogen skeleton of each natural product is dissected in a retrosynthesis process (Scheme 4).

Briefly:

- C_2 unit may be supplied by acetyl-CoA;
- C_5 is the so-called "isoprene unit" and it is formed from mevalonate or deoxyxylulose phosphate;
- C_6C_3 is obtained from the carbon moiety of either L-phenylalanine or L-tyrosine and it is referred to a phenylpropyl unit;
- C_6C_2N unit has the same origin of C_6C_3 unit, but carboxyl group of the amino acid is removed;
- indole.C_2CN unit arises from L-tryptophan;
- C_4N unit is produced from the non-protein amino acid L-ornithine and it is usually found as a pyrrolidine;
- C_5N unit, found as piperidine, is produced in the same way as unit above, but using L-lysine instead of L-ornithine.
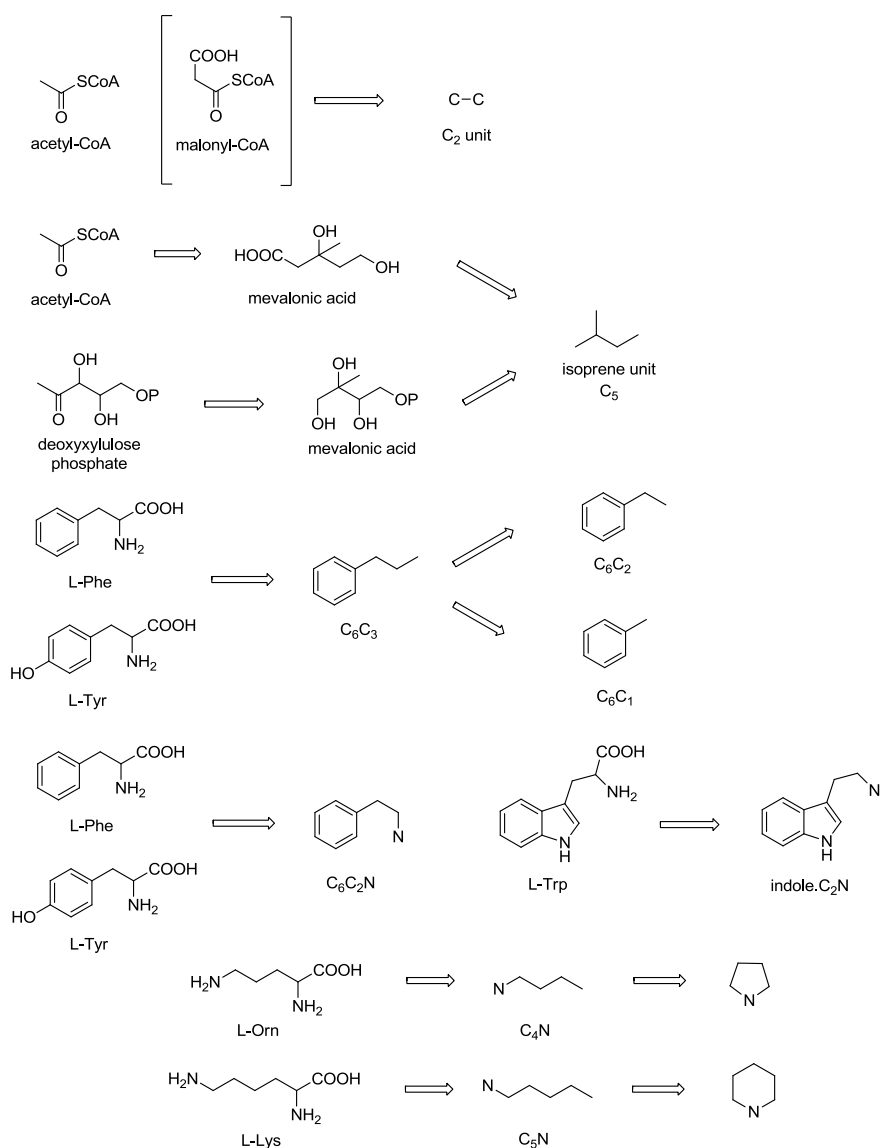
Scheme 4

Throughout the biosynthetic processes, the formation of new carbon-carbon bonds occur generally with Aldol and Claisen condensations, in most cases, between coenzyme A esters; otherwise some rearrangements are possible, such as Wagner-Meerwein rearrangement. The formation of C-N bonds is frequently achieved either by condensation reactions between amines and aldehydes or ketons affording Schiff bases, or in other cases by Mannich reactions. Also oxidation and reduction enzyme-mediated reactions are important for reaching the elaborate final product, even if these processes are not always completely understood.[40]

According to the biosynthetic strategies for their assembly in the producer organisms, therefore sharing the same scaffold elements, natural products can be divided into several structural classes, mainly in polyketides (PKSs), nonribosomal peptides (NRPs), terpenes, and alkaloids.

---

[40] P. M. Dewick; *Medicinal Natural Products: A Biosynthetic Approach*, Wiley

Polyketides constitute a large family of microbial and plant-derived bioactive natural product including linear, polycyclic, and macrocyclic structural forms. These secondary metabolites display various molecular weight and functional group modification and, moreover, they show a wide range of bioactivity such as antibiotic, antiparassitic, antiviral and antitumor activity. More details are described in the chapter 7.

Nonribosomal peptides (NRPs) are a structurally diverse class of peptides with various functions, such as cytostatic, immunosuppressive, antibacterial, or antitumor properties produced by a large multidomain enzymatic machineries called nonribosomal peptide synthetases (NRPSs). These megaenzymes is formed by catalytic domains which catalyse complex regiospecific and stereospecific reactions to assemble structurally and functionally diverse peptides in an iterative chain elongation process (Figure 13).[41] Furthermore, aside from the common amino acids, a larger variety of chemical groups, such as D- amino acids, fatty acids ecc., is found in these bioactive compounds. They contribute to structural versatility of NRPs and are known to be important for bioactivity.

a)   **b)**
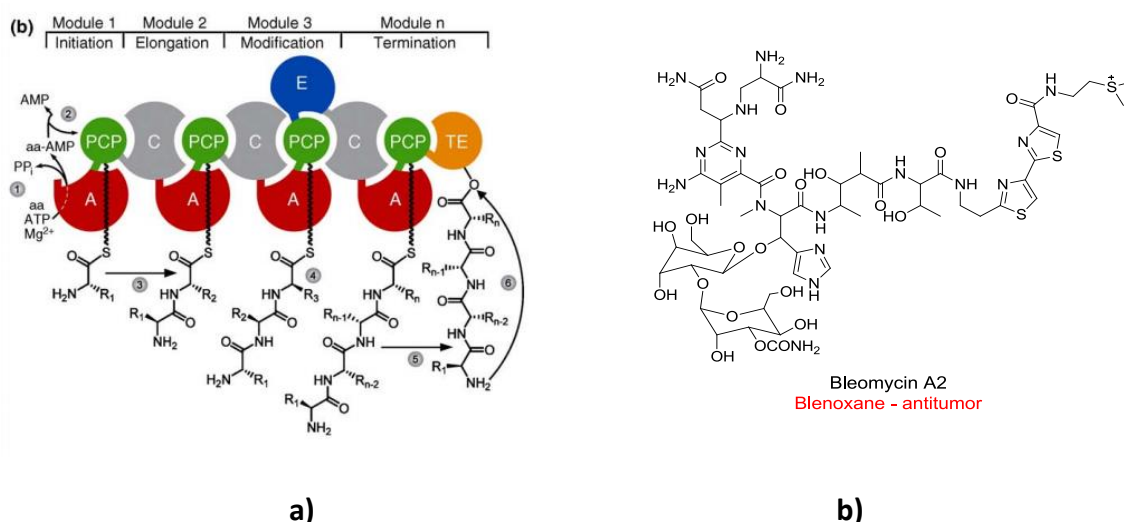
Figure 13: a) Simplified mechanism of nonribosomal peptide (NRP) synthesis. (1) The amino acid is activated as aminoacyl-AMP by the adenylation domain. (2) Transfer of the amino acid onto the PCP domain. (3) Condensation of PCP-bound amino acids. (4) Possibility of amino acid modifications, for example by epimerization domains. (5) Transesterification of the peptide chain from the terminal PCP onto the TE domain. (6) TE catalyzed product release by either hydrolysis or macrocyclization. **b+)** Example of nonribosomally assembled, clinically approved antitumour peptide.

Terpenes or isoprenoids constitute the most chemically diverse class of natural products. They are found in almost all living organisms where they have a myriad of different vital or no-vital functions (cholesterol, carotenoids). Most terpenoids are derived from successive condensations "tail-to-tail" or "head-to-tail" between the C_5 units dimethylallyl diphosphate (DMAPP) and isopentenyl diphosphate (IPP) leading to mono- (C_{10}), sesqui- (C_{15}), di- (C_{20}), sester- (C_{25}), tri- (C_{30}),

---

[41] M. Strieker; A Tanovic; M. A. Marahiel; *Current Opinion in Structural Biology*, **2010**, *20*, 234.

tetra- (C_{40}), and poly- (C_5n (n = > 8)) terpenes (Scheme 5).[42] The ability of the C_n precursor to undergo various way of cyclization and subsequent "decoration" reactions affords to the chemical diversity of terpenoids. For example Baccatin III, the diterpenoid part of the well-known anticancer drug paclitaxel, is a monocyclic diterpenoids with a 14-carbon macrocyclic ring called cembrane (compound **B**, Scheme 2).

All terpenes are formed through the reactions of IPP and DMAPP

DMAPP

Stereospecific proton loss

geranyl PP (GPP) → Monoterpenes

Repeat several times:

farnesyl PP → Sesquiterpenes

geranylgeranyl PP → Diterpenes

squalene → Triterpenes (Steroids
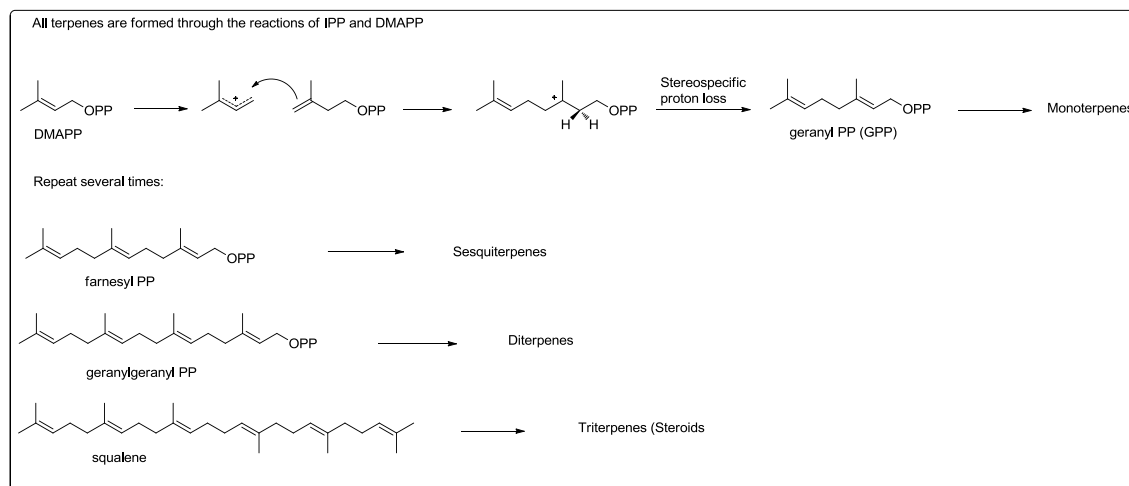
Scheme 5

The modern definition for the wide and diversify class of alkaloids has been given by S. W. Pelletier, saying:

> *"An alkaloid is a cyclic organic compound containing nitrogen in a negative oxidation state which is of limited distribution among living organisms."* [43]

For this class of natural compounds it is really difficult to find an unified classification due to the incredible differences between the members. Therefore they are grouped into many classes based on their origin and the nature of the nitrogen-containing moiety. Also the biosynthesis pathway of alkaloids could be very different between each other: commonly they are originated from the amino acids, but they are also known to arise from mixed biosynthetic processes, the most important of which include terpenoid and steroidal alkaloids.[44] Due to their huge differences, herein I will not explain more in detail their biosynthesis.

2.2. Design and synthesis of analogues of natural products

During their biosynthesis, natural products (NPs) interact with biosynthetic enzymes and proteins. Thus they have already interacted with different biological systems, such as enzymes and proteins, and that is why, essentially, all natural products have some receptor binding capacity

---

[42] E. Oldfield; F.-Y. Lin; *Angew. Chem. Int. Ed.*, **2012**, *51*, 1124.

[43] S. W. Pellettier; *Alkaloids: Chemical and Biological Perspectives, 1st Edition,* **2001**.

[44] E. Poupon; B. Nay; *Wiley-vch Verlag GmbH & Co. KGaa,* **2011**.

and they are so attractive for the drug discovery world.[45] Comparing a synthetic molecule with a second metabolite, it is noticed that there are a number of structural substantially differences between NPs from synthetic ones.[46] Jon Clardy and Christopher Walsh in their paper[47] describe the key futures of these diversities, briefly summarized in the following list:

- a larger fraction of sp^3 carbons (most of the rings are partly or completely saturated);
- more stereogenic centres often arising from C-C bond formation reactions (aldol condensations) or stereoselective reduction of a carbonyl group;
- relatively more carbon, hydrogen and oxygen, and less nitrogen and other elements;
- have more fused, bridge, and spiro rings;
- molecular masses in excess of 500 daltons and high polarities (greater water solubility). In those cases, they violate Lipinski's 'rule of five', easy rules based on calculated properties that normally help to rationalize and improve the profile of putative synthetic drugs.

When some interesting compound is identified through the High Throughput Screening (HTS) and it is extracted from the original natural source, chemists start to study a possible chemical synthesis of it in order to mimic its bioactivity. In fact, it very often happens that it is a hard challenge obtaining a renewable supply of active compounds from biological sources. However, the high level of their complexity structure can limit the total synthesis and/or the essential chemical modifications of the natural scaffold to optimize their therapeutic use.

The chemistry of NPs, as well as medicinal chemistry, has made massive progress about the reproduction of natural compounds in laboratory, developing a collection of typical reactions to achieve their respective target compounds. Regarding medicinal chemistry, a set of their common transformations used in this topic is enclosed into a medicinal chemist's toolbox". Indeed a "process chemist's toolbox" has been described to identified the typical reactions used during the scale up of the synthesis of potential new drugs arising from medicinal chemistry studies. Finally, the description of a "toolbox of a NPs chemist" was reported by Natalia Vasilevich & co in 2012. [48]

In this paper they compared the three toolboxes in a clear table, herein showed, where there are the main reactions used to reach the complexity of NPs-like compounds (Figure 14). On the basis of this analysis, there are many different issues between them, and the authors conclude saying: "*The enrichment of "the toolbox of medicinal chemistry" with reactions used during the synthesis of natural product may enable us to hit such difficult drug targets that have emerged in recent years*".

---

[45] E.Kellenberger; A. Hofmann; R. J. Quinn; *Nat. Prod. Rep.,* **2011**, *28*, 1483.
[46] K. Grabowski.; G. Schneider; *Curr. Chem. Biol.,* **2007**, *1*, 115.
[47] J. Clardy; C. Walsh; *Nature,* **2004**, *432*, 829.
[48] N. I. Vasilevich; R. V Kombarov; D. V. Genis; M. A. Kirpichenok; *J. Med. Chem.,* **2012**, *55*, 7003.

reaction type	% of total in NPs synthesis reviewed	medicinal chemistry, %	process chemistry, %
oxidation	14.6	1.9	4.9
reduction	13.1	7	11.4
addition of C-nucleophile to carbonyl yielding alkene or *sec*-alcohol	12.0	2.2	2.2
acylation of N, O, S	6.8	28.33	15.6
alkylation of N, O, S	6.1	29.23	23.9
Pd-catalyzed coupling	3.8	9	3.8
nucleophilic substitution	3.2	1.2	2.8
enolate alkylation	2.9	0.5 or less	
elimination to double bond	2.6	0.3	1.2
metathesis	1.9		
epoxide opening	1.9		
electrophilic substitution	1.9		
acetal, ketal, and hemiacetal formation	1.9		
Diels−Alder reaction	1.05		
hydroboration	1		

Figure 14

Besides single trasformations, chemistry related to NPs also provides many synthetic strategies. The first one that herein will be discuss, is the divergent strategy approach.

Divergent strategy in natural product synthesis allows the construction of array of compounds with small structural differences. When they are evaluated, they could offer precious information useful to build a detailed structure–activity relationship, which would not be available from a single-shot scrutiny of a certain molecule.[49]
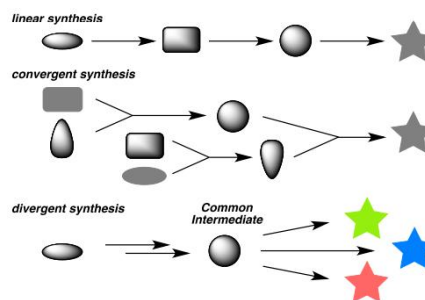
Diversity-oriented synthesis is one of the most famous divergent strategy. Originally proposed by Schreiber, it is involved the synthesis of a library of diverse small molecules covering a large portion of chemical space (multi-dimensional molecular descriptor space, where descriptors are characteristics of the compounds such as molecular weight) for biological screening. Thus DOS libraries can be used to identify new ligands for a variety of targets.[50]

Very related with DOS there is the concept of '*Diverted total synthesis*' (DTS). It was proposed by Danishefsky and it is concerned the preparation of a natural product-like compound library by the derivatization of a versatile synthetic intermediate. The story of Ixabepilone (Figure 11), the only epothilone that has been approved by FDA so far, represents one of the most famous cases of

[49] R. W. Huigens; K. C. Morrison; R. W. Hicklin; T. A. Flood; M. F. Richter; P. J. Hergenrother; *Nat. Chem.*, **2013**, *5*, 195.
[50] M. D. Burke; S. L. Schreiber; *Angew. Chem. Int. Ed.*, **2004**, *43*, 46.

diverted total synthesis.[51] Its structure has been originated from several SAR studies (structure–activity relationship) made on many semisynthetic epothilone analogs, and all of them are semisynthetic derivatives deriving from the key intermediate Epo B.

In the DTS field, the case of pironetin analogues is another important example. Pironetin is an antitumor agent that exerts its activity by binding to α-tubulin, therefore it inhibits the assembly of tubulin to microtubules. Marco *et al.* simplifying the syntheses significantly, synthesized four analogues of the NP pironetin removing the alkyl groups at C4, C8 and C10 (Figure 15).[52]
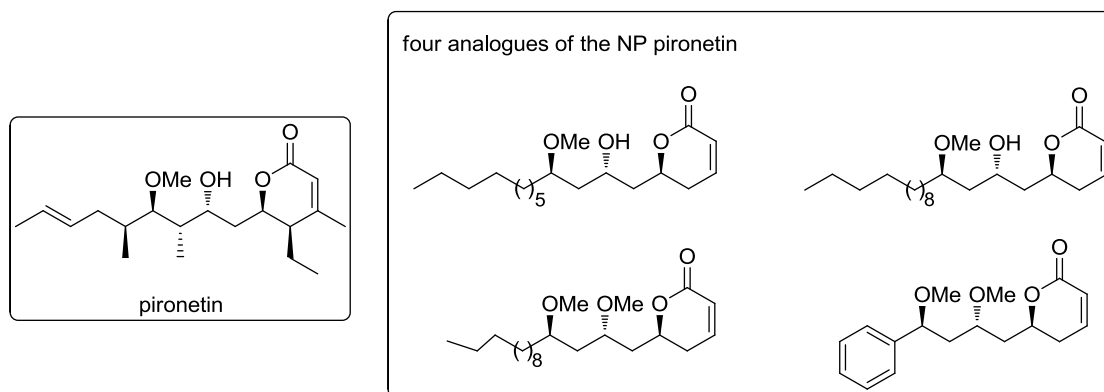

Figure 15

Through the *biology-oriented synthesis* (BIOS), a NP core scaffold of a lead bioactive compound is taken as privileged structure for the creation of a novel compound collection. Basically, the idea is that the same core scaffold could maintain the match with many target ligand sites, therefore it could have a similar bioactivity. Noscapine is a famous cough suppressant and more recently it was discovered an excellent antitumour activity as microtubule inhibitor (Figure 16). Using this synthetic approach, 18 compounds based on the tetrahydroisoquinoline scaffold were prepared and, not surprisingly, 7 of them interfere with microtubule polymerization.[53]
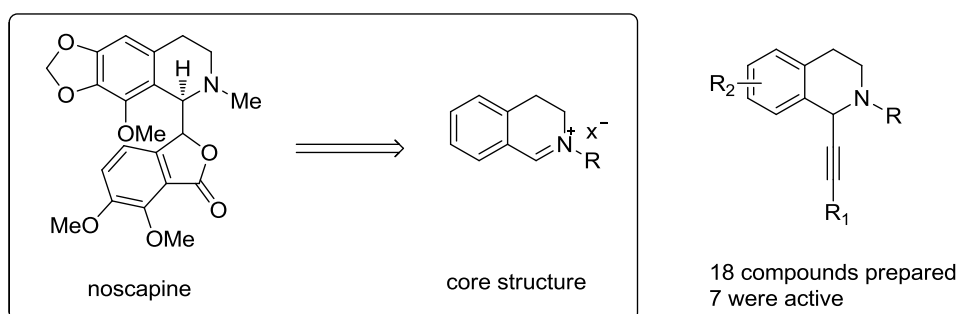

Figure 16

[51] K.-H. Altmann; F. Z. Gaugaz; R. Schiess; *Mol. Diversity*, **2011**, *15*, 383.
[52] M. Carda; J. Murga; S. Díaz-Oltra; J. García-Pla; J. Paños; E. Falomir; C. Trigili; J. F. Díaz; I. Barasoain; J. A. Marco; *Eur. J. Org. Chem.*, **2013**, 1116.
[53] S. Rizzo; H. Waldmann; *Chem. Rev.*, **2014**, *114*, 4621.

In order to create new bioactive molecules it is also possible to combine partial or whole

structures of molecules: this concept is well explained by the term *"hybrid molecules"*.[54] There are three categories of hybrid molecules: *a)* both parts act on the same target, *b)* each part acts on a different target, *c)* both parts bind to one target at closely related binding sites.[55] An interesting example, from the synthetic point of view, is the synthesis of an hybrid between epothilone B and 16-membered macrosphelide derivative, which are able to induce apoptosis

in human lymphoma U937 cells.[56] The formed compound showed significantly higher apoptosis-inducing activity than the parent macrosphelides (Figure 17).
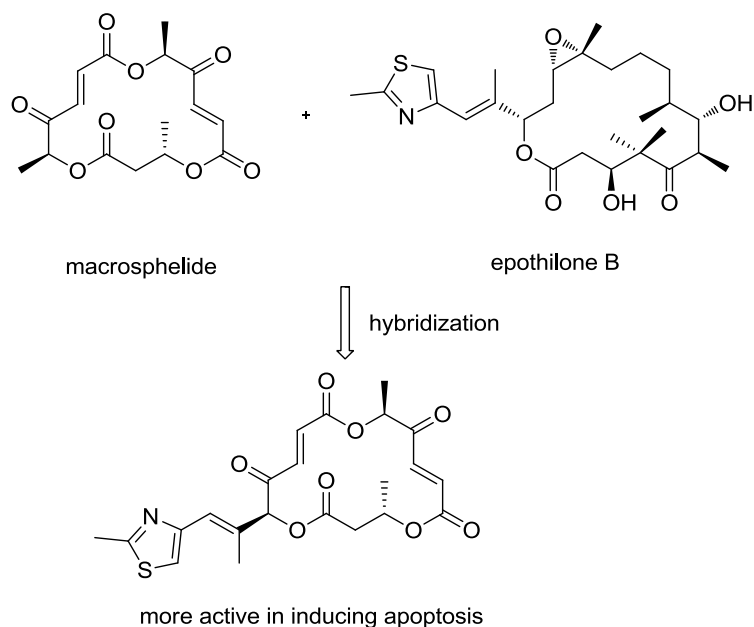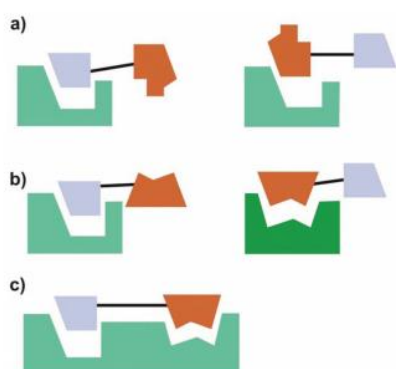

Figure 17

Finally, in many case a detailed knowledge of the whole biosynthetic process about one particular metabolite, can be employ for the synthesis of NPs analogues through a process called *mutasynthesis*. As already mentioned above, in bacteria and fungi several molecules are biosynthesized through particular megaenzymes, such as no-ribosomial-peptide synthase and polyketide synthase. Exploiting the mutasynthesis concept, a mutant organism could be generate modifying or deleting one or more genes responsible for important steps throughout the biosynthesis pathway of a bioactive natural product. Therefore it is possible to obtain a new natural compound directly from a microorganism that by total synthesis would not be available so

[54]K. Suzuki; *Chem. Rec.*, **2010**, *10*, 291.
[55]B. Meunier; *Acc. Chem. Res.*, **2007**, *41*, 69.
[56]Y. Matsuya; T. Kawaguchi; K. Ishihara; K. Ahmed; Q.-L. Zhao; T. Kondo; H. Nemoto; *Org. Lett.*, **2006**, *8*, 4609.

efficiently. Geldanamycin is a benzoquinone ansamycin antibiotic that manifests anti-cancer activity through the inhibition of HSP90-chaperone function. Kirschning and his group have been able to prepare a range of its derivatives feeding various 3-aminobenzoic acids to the mutant strain of *S. hygroscopicus* in which the synthesis of the natural starting unit was blocked (Figure 18).[57]

Figure 18

[57] S. Eichner; H. G. Floss; F. Sasse; A. Kirschning; *Chem. Bio. Chem.*, **2009**, *10*, 1801.

Contents of this thesis

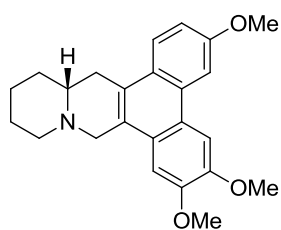The present work is focused on the design, synthesis and biological evaluation of several new potential anticancer compounds based on natural product scaffolds.

The **third chapter** will be described the synthesis and the biological evaluation of a 1,7,8,8a-tetrahydro-3*H*-oxazolo[3,4-a]pyrazin-6(5*H*)-one series in which the basic scaffold should mimic the privileged structure oxazole-piperazine unit present in several biological active compounds. Biological tests showed that the obtained compounds are endowed with an interesting antitumor activity against two human thyroid cancer cell lines, namely FTC-133 and 8305C, by promoting the apoptotic pathway and DNA fragmentation. [58]
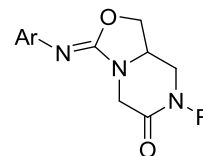
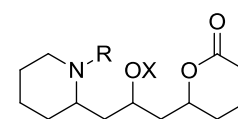Develop of two synthetic approaches to obtain the racemic mixture and the pure enantiomers of boehmeriasin A is the central topic of **chapter 4**. Boehmeriasin A is a phenanthroquinolizidine alkaloid isolated from *Boehmeria siamensis* Craib and it showed a strong cytotoxic activity at the nanomolar range against different cancer cell lines. Topoisomerases and SIRT2 are identified as biological targets and the experimental data has been supported by docking studies.[59]

(R)-boehmeriasin A

In the **chapters 5** and **6** will be discussed the results regarding the design and synthesis of new microtubule-inhibitors.
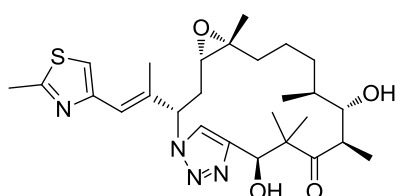
In the first one pironetin and dumetorine core are taken as natural privileged scaffold for making a hybrid molecule able to covalently bind the α-tubuline. The novel built molecule can exist in 8 different stereoisomers due to the presence of three stereocenters, therefore all of them were synthesized and evaluated on their ability to interfere with microtubule assembly in vitro.

hybrid compounds

Later, following the "diverted total synthesis" approach, the synthesis of epothilone derivative was planned in order to reach a new anticancer compound having a triazole ring instead of an amide group. The microtubule stabilizing ability of epothilones is very attractive either for the consequent high cytotoxicity showed against

[58]U. Chiacchio; V. Barbera; R. Bonfanti; G. Broggini; A. Campisi; S. Gazzola;R. Parenti; G. Romeo; *Bioorg. Med. Chem.,* **2013**, *21*, 5748.
[59] M. S. Christodoulou; F. Calogero; M. Baumann; A. Garcìa-Argaiez; S. Pieraccini; M. Sironi; F. Dapiaggi; R. Bucci; G. Broggini; S. Gazzola; S. Liekens; A. Silvani; M. Lahtela-Kakkonen; N. Martinet, A. Nonell-Canals; E. Santamaria-Navarro; I. R. Baxendale; L. Dalla Via; D. Passarella; *Eur. J. Med. Chem.*, **2015**, *92*, 766.

cancer cells or for its demonstrate neuroprotective effect in Parkinson's disease thanks to its ability to cross the blood-brain barrier.[60]

Chapter 7 gives an account of my research project carried out in my first foreign experience in the laboratories of Prof. Manuela Tosin (Warwick University, UK). The Tosin's group has developed a chemical strategy for the isolation of biosynthetic intermediates produced by polyketide synthase megaenzimes, in order to achieve a deep knowledge of biosynthetic processes of important bioactive natural products, such as antibiotics or anticancer compounds for combinatorial chemistry or mutasynthesis purpouse. Lasalocid A is a polyketide produced by type 1 polyketide synthase (PKS1) in *S. lasaliensis* that belong to the wide family of polyether antibiotics. These bioactive natural compounds are active against several critical
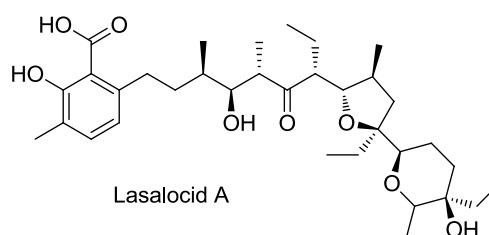
Lasalocid A

infectious diseases and, further, some of them have the ability to selectively kill cancer stem cells. A detailed investigation of Lasaloicid A biosynthesis was performed in order to *i)* identified and isolate all polyketide biosynthetic intermediates and *ii)* to study new chemical functionalizations *in vivo* on polyketide intermediates, affording novel putative bioactive molecules.[61]

---

[60]D. Cartelli; F. Casagrande; C. L. Busceti; D. Bucci; G. Molinaro; A. Traficante; D. Passarella; E. Giavini; G. Pezzoli; G. Battaglia; G. Cappelletti; *Sci Rep.*, **2013**, *3*, 1837.

[61] E. Riva; I. Wilkening; S. Gazzola; A. W. M. Li; L. Smith; P. F. Leadlay; M. Tosin; *Angew. Chem. Int. Ed.*, **2014**, *53*, 11944.
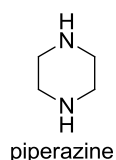
Chapter 3

Synthesis and biological evaluation of novel oxazole-pyrazine based derivatives as anticancer agents

3.1. Introduction

Due to their biological properties, nitrogen- and oxygen-containing heterocyclic compounds constitute a huge group of organic molecules present in the majority of clinically approved drugs.[62] Compounds currently investigated as natural potent drug candidates incorporate many variants of five and six-membered rings, including piperazines and oxazoles.

The piperazine scaffolds occur frequently in complex natural products, and are reported to elicit a broad spectrum of pharmacological activities like antibacterial, antifungal and anticancer activity.[63]

One of the most famous commerciable available anticancer drug containing the piperazine ring is Imatinib (Figure 19), marketed by Novartis as Gleevec (Canada, South Africa and the USA) or Glivec (Australia, Europe and Latin America). It is a potent inhibitor of the tyrosine kinase activity used in the treatment of multiple cancers of the BCR-ABL1 oncoprotein, as well as that of several receptor tyrosine kinases.[64]
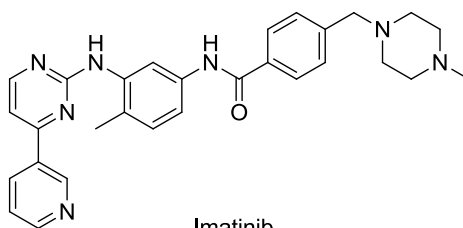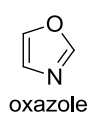

Imatinib

Figure 19

Imatinib was developed in the late 1990s by rational drug design: after the "Philadelphia chromosome" mutation and hyperactive "bcr-abl" protein were discovered, the investigators through high-throughput screening identified 2-phenylaminopyrimidine as lead compound. After previous tests, it was modified by the introduction of methyl and benzamide groups to give it enhanced binding properties, resulting in imatinib.[65]

Like piperazines, oxazole containing compounds are very common in natural products, and they play an important role in medicinal chemistry showing a broad spectrum of biological activity such as antimicrobial, antitumor, analgesics and anti-inflammatory agents.[66]

For example, telomestatin (Figure 20), is a potent telomerase inhibitor currently in clinical trials, containing linked oxazoles with a thiazoline unit.

---

[62] M. Sainsbury, *Heterocyclic Chemistry, Basic Concepts in Chemistry, Wiley Interscience and Royal Society of Chemistry, Bristol*, **2002**.
[63] *Chapter 5; piperazines, Pharm. Lib.*, **1997**, *25*, 148.
[64] P. W. Manley; F. Blasco; J. Mestan; R. Aichholz; *Bioorg. Med. Chem.*, **2013**, *21*, 3231.
[65] J. Zimmermann; E. Buchdunger; H. Mett; T. Meyer; N. B. Lydon; *Bioorg. Med. Chem. Lett.*, **1997**, *7*, 187.
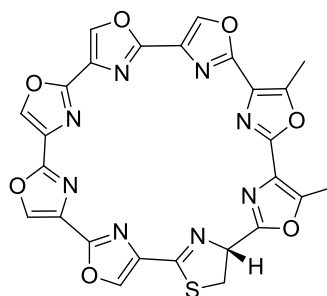[66] Z. Jin; *Nat. Prod. Rep.*, **2009**, *26*, 382.

Figure 20

Inhibiting the telomerase activity of cancer cells, telomestatin induces apoptosis once the telomeres are too short to be transcribed. Indeed, from literature it is easy to figure the pharmacological importance of oxazole derivatives out when it is present into the prospective pharmaceutical candidate: typically an improved of compound's solubility occurs, while maintaining hydrogen bond acceptors, as well as an enhancement of compound's rigidity. Furthermore, oxazole provides many sites for potential binding interactions through π- stacking with a biological target.[67]

Noteworthy natural compounds containing the oxazole ring fused into a piperazine core are (-)-quinocarcin and (-)-tetrazomine. (-)-Quinocarcin is an alkaloid that was isolated by Takahashi and Tomita in 1983 from the culture broth of *Streptomyces melunoVinuceus*.[68] It exhibited potent antitumor activities against a variety of tumor cell lines, above of all against lymphocytic leukemia). The structurally related (-)-tetrazomine is an antitumor antibiotic that displayed similar activity (Figure 21).
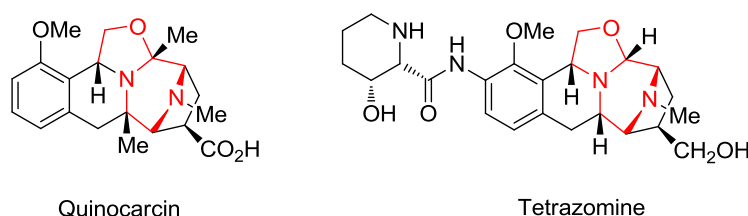

Quinocarcin   Tetrazomine

Figure 21

In both molecules seems that the oxazole ring exerts a fundamental role in the bioactivity, in fact it has been suggested that their cytotoxic activity arises from the expression of multiple mechanisms including the mediation of oxidative damage to DNA via the reduction of molecular oxygen to superoxide by the autoredox disproportionation of the fused oxazolidine.[69]

From the biological point of view, in anticancer drug discovery, small-molecular-weight compounds, that are able to activate many proteins by signal transduction cascades, have attracted significant scientific interest due to the medicinal, biochemical and biological

[67] G. Haberhauer; E. Drosdow, T. Oeser; F. Rominger; *Tetrahedron*, **2008**, *64*, 1853.

[68] K. Takahashi; K. Shimizu; *J. Antibiot.*, **1983**, 463.

[69] Y.-C. Wu; M.´l. Liron; J. Zhu; *J. Am. Chem. Soc.*, **2008**, *130*, 7148.

implications of important molecular recognition events. These events occur when an extracellular signalling molecule activates a specific receptor located on the cell surface or inside the cell and, in turn, this receptor triggers a biochemical chain of events inside the cell, creating a response (Figure 22).
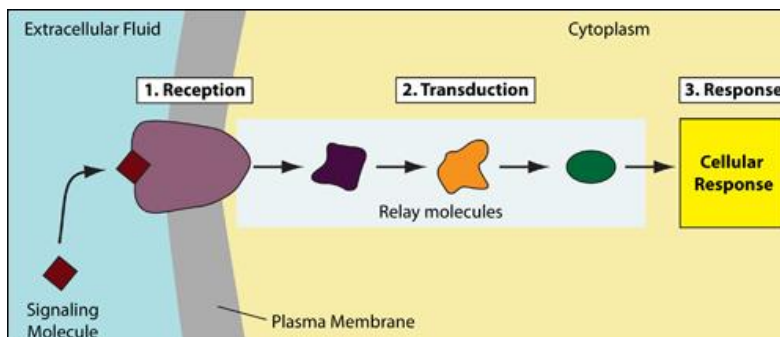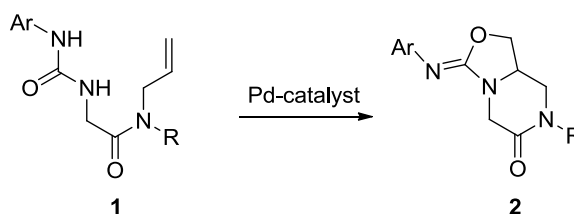

Figure 22

Depending on the cell, the response alters the cell's metabolism, shape, gene expression and thus it could induce the programmed cell death (apoptosis).

3.2. Aim of this work

As part of our medicinal chemistry program aimed at the discovery of potential anticancer agents, we have addressed our attention to the synthesis of a novel series of derivatives containing the oxazolo–piperazine pharmacophore **2** through a selective palladium-catalyzed double intramolecular domino process of alkenylureas (Scheme 6).

Scheme 6

Thanks to previous computational studies, these "small molecules" have been traced to commercial available drug sunitinib, a tyrosine kinase inhibitors used in the treatment of various thyroid cancer (Figure 23).
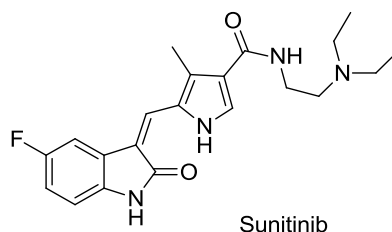

Sunitinib

Figure 23

Therefore all bicyclic products were evaluated for their antitumor activity on human follicular (FTC-133) and anaplastic (8305C) thyroid carcinoma cell lines, as representatives of two aggressive types of thyroid cancer.

3.3. Chemistry

In the field of our ongoing interest regarding the construction of hetero-polycyclic compounds through palladium catalysis,[70] we have recently reported the selective double intramolecular aminooxygenation and diamination reactions of alkenylureas to yield bicyclic products containing a piperazinone ring (Scheme 7).[71]
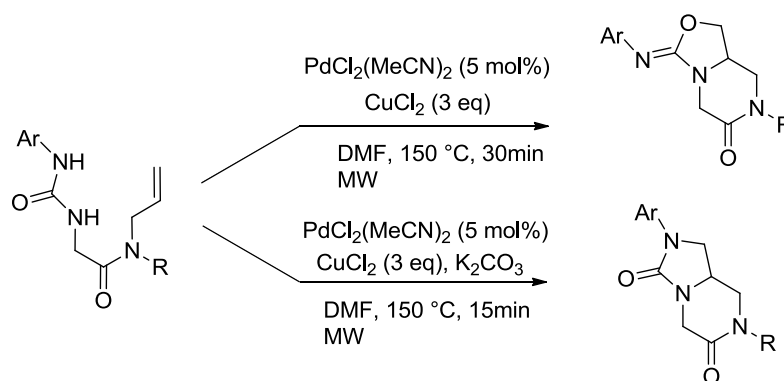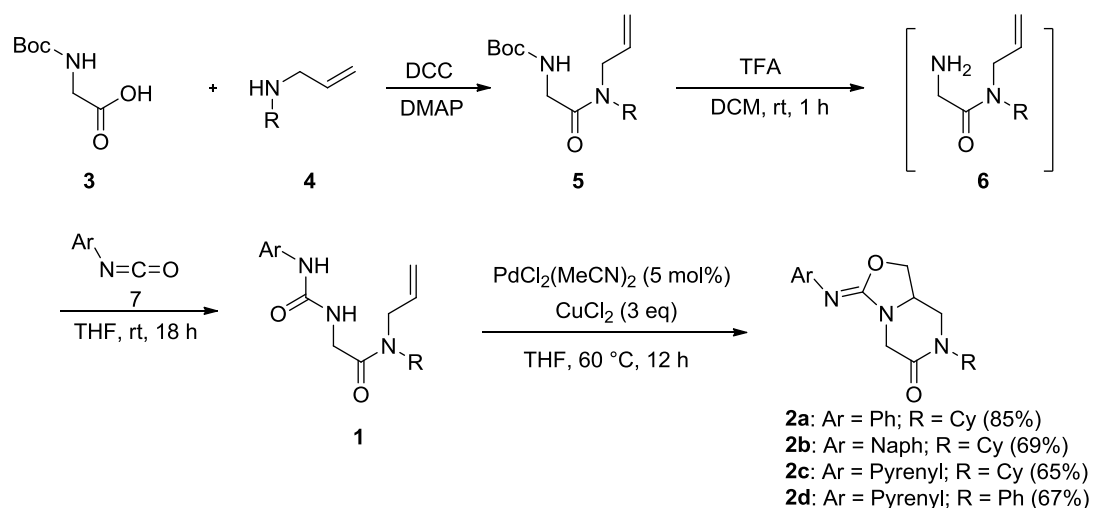
Scheme 7

These Pd(II)-catalyzed protocols under microwave irradiation provided selectively 3-arylimino-oxazolo[3,4-*a*]pyrazin-6-one and 2-aryl-imidazo[1,5-*a*]pyrazin-3,6-dione derivatives in few steps from readily available precursors. The isomeric oxazolo- and imidazo-piperazinone structures were defined thanks to ^{13}C NMR spectra, where the resonance of the methylene group of the five-membered ring resulted to be less shielded for the oxazole ring compared with the imidazole one (65-70 ppm vs. 41-46 ppm), consistent with the literature data.[72]

The aminooxygenation process, which can also be carried out in satisfactory yield by conventional heating, was used to prepare 1,7,8,8a-tetrahydro-3*H*-oxazolo[3,4-*a*]pyrazines **2a-d,** target compounds for later biological studies. Firstly, the reaction between *N*-Boc-glycine **3** with cyclohexyl- or phenyl-allylamine **4,** activated by DCC and DMAP, afforded the *N*-allyl-amides of Boc-glycine **5**. These intermediates were converted to the corresponding allylamides **6** by removal of the *t*-butoxycarbonyl group, and then treated with the respective aryl isocyanates **7**. Finally, the double cyclization of the alkenyl ureas **1a-d** was performed using PdCl$_2$(MeCN)$_2$ as catalyst and CuCl$_2$ (3 equiv) as oxidant in THF under reflux for 12 hours with high yields (Scheme 8).

[70] G. Broggini; E. Borsini; A. Fasana; G. Poli; F. Liron; *Eur. J. Org. Chem.,* **2012**, 3617.

[71] G. Broggini; V. Barbera; E. M. Beccalli; U. Chiacchio; A. Fasana; S. Galli; S. Gazzola; *Adv. Synth. Catal.* **2013**, *355*, 1640.

[72] a) T. H. Kim; G. J. Lee; *J. Org. Chem.,* **1999**, *64*, 2941; b) F. Saczewski; J. Saczewski; M. Gdaniec; *Chem. Pharm. Bull.,* **2001**, *49*, 1203; c) T. H. Kim; N. Lee; G. J. Lee; J. N. Kim; *Tetrahedron*, **2001**, *57*, 7137.

Scheme 8

In mechanicistic point of view, the aminooxygenation product could arise from an intramolecular nucleophilic attack by the oxygen atom of the urea on the σ-alkyl-complex **A** (Scheme 9). In particular, CuCl$_2$ would inhibit the palladium β-hydride elimination favouring the loss of the Pd species through the formation of a heterobimetallic σ-Pd/Cu complex.[73] The process generates the intermediate **B** and the elimination of H$^+$ furnishes the products **2a-d**.
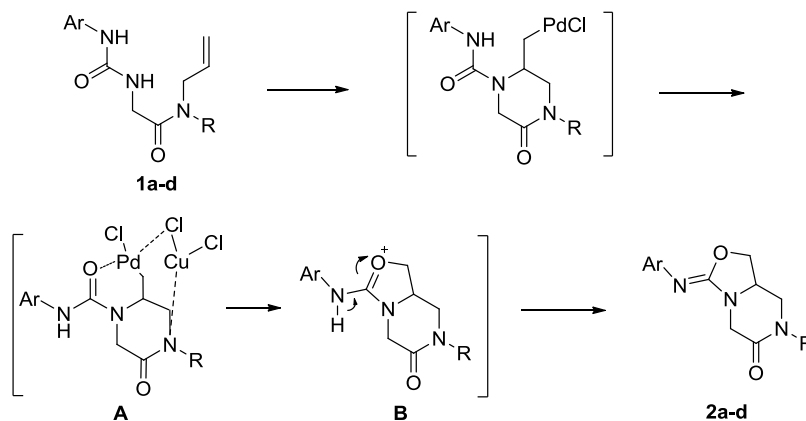
Scheme 9

---

[73] For the concept of a heterobimetallic σ-Pd/Cu complex, see: a) P. Szolcsanyi; T. Gracza; *Tetrahedron*. **2006**, *62*, 8498; b) D. Zargarian; *Organometallics,* **1991**, *10*, 2914; c) T. Hosokawa; T. Uno; S. Inui; S.-I. Murahashi; *J. Am. Chem. Soc.*, **1996**, *118*, 3990.

3.4. Biological evaluation

3.4.1. Cytotoxic effect of the compounds

The synthesized final products **2a-d** (Figure 24) were tested to investigate their potential antitumor activity on two cancer cell lines, FTC-133 and 8305C, as representative of follicular and anaplastic thyroid human cancer, respectively.
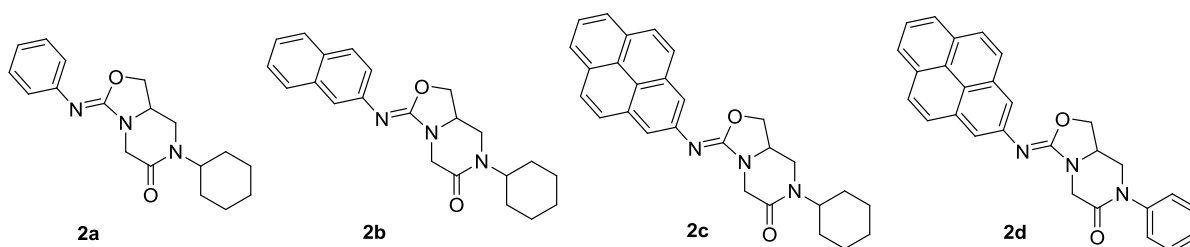

2a   **2b**   **2c**   **2d**

Figure 24

The cell viability was monitored by MTT assays.

The MTT colorimetric assay uses the tetrazolium yellow dye 3-(4,5-dimethylthiazol-2-yl)-2,5-diphenyltetrazolium bromide (MTT) to quantify the metabolic activity of cells. In fact this molecule is easily reduced by NAD(P)H-dependent cellular oxidoreductase enzymes to its insoluble formazan, which has a purple colour (Scheme 10).

MTT   Mithochondrial reductase →   formazan
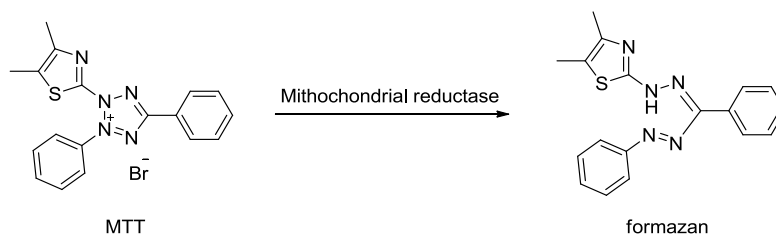
Scheme 10

Rapidly dividing cells like tumour cells exhibit high rates of MTT reduction, that is why this assay can be useful for measuring cytotoxicity (loss of viable cells) or cytostatic activity (shift from proliferation to quiescence) of potential medicinal agents and toxic materials.

In preliminary experiments, FTC-133 and 8305C cell line cultures were exposed to different concentrations (5–100 μM) of the synthesized compounds **2a-d.** Using the respective untreated cell cultures as controls, it was found that 50 μM is the optimal concentration for having a significant reduction in cellular viability in both FTC-133 and 8305C cell lines after 24 h of treatment. Analysing the IC_{50} values (50% cytotoxic inhibitory concentration) reported in Table 1, it is evident that all compounds displayed cytotoxic effects on the both cell lines, at

concentrations ranging from 44 to 80 μM and that FTC-133 cells were more susceptible to treatment with compounds **2a-d**, than the 8305C cells.

Table 1: Concentrations (μM) of compounds 2a-d that induced 50% decrease (IC$_{50}$) in FTC-133 and 8305C cell proliferation[a]

Cell lines	Untreated cells	2a	2b	2c	2d
FTC-133	>100	50.03 ± 3.90	44.79 ± 4.27	48.32 ± 2.98	74.21 ± 3.93
8305C	>100	70.66 ± 2.13	61.03 ± 3.71	68.45 ± 3.71	80.28 ± 4.52

[a] FTC–133 and 8305C cell lines were incubated with drug compounds in concentration ranging from 5 to 100 μM at 37 °C in a 5% CO$_2$ atmosphere for 24 h. Viability was determined by the MTT assay. Each data represents mean ± SD from four independent experiments, performed in triplicate.

3.4.2. Evaluation of the apoptotic pathway activation

In mammals the apoptosis can be initiated by three different pathways, each of these converges
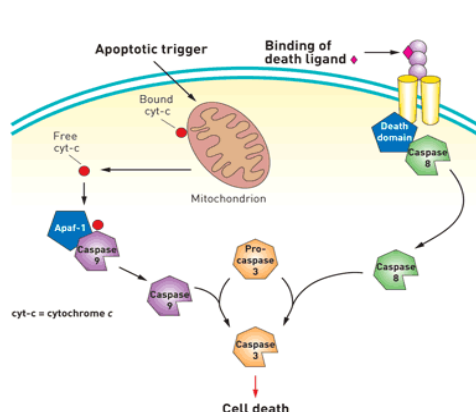
to a common execution phase of apoptosis that requires proteolytic activation of caspases-3, a cysteine-aspartic protease, from its inactive proenzymes (Figure 25). [74]

To investigate whether the new compounds could activate the caspase-3 dependent apoptotic pathway process in the treated cancer cells, the amount of caspase-3 was evaluated after 24 h of cell incubation at 50 μM concentration of **2a-d** using fluorescent

microscope analysis. Significant enhancement of caspase-3 positive cells was detected after 24 hours of treatment in FTC-133 and 8305C cell lines, when compared to the untreated control. The effect appeared more evident in FTC-133 cell lines, with compound **2d** showing the lowest activity with respect **2a-c** (Figure 25).

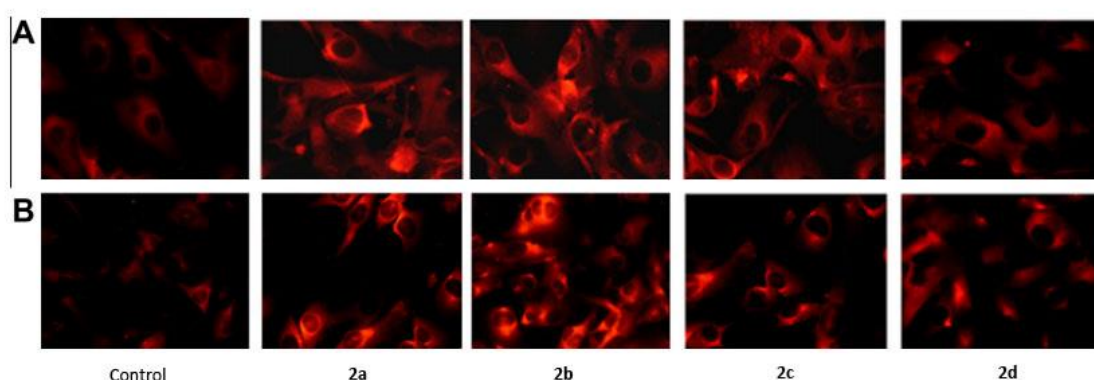**Figure 25:** Fluorescent microscope analysis of caspase-3 cleavage in (**A**) FCT-133 and (**B**) 8305C human thyroid cancer cell lines, untreated (control) and treated with 50 μM **2a-d** for 24 h. Scale bars = 50 μm.

---

[74] S. Ghavami; M. Hashemi; S. R. Ande; B. Yeganeh; W. Xiao; M. Eshraghi; C. J. Bus; K. Kadkhoda; E. Wiechec; A. J. Halayko; M. Los; *J. Med. Genet.*, **2009**, *46*, 497.

Table 2 show the quantification and statistical analysis of caspase-3 immunolabeling in FCT–133 and 8305C human thyroid cancer cell line cultures untreated (Control) and treated with 50 μM **2a-d** for 24 h.

Table 2

	% Caspase-3 positive FTC-133 cell lines	% Caspase-3 positive 8305C cell lines
Treatment	24 h	24 h
Control	2.51 ± 1	3.22 ± 1
2a	88.68 ± 1	75.88 ± 1
2b	90.56 ± 2	78.56 ± 2
2c	89.24 ± 2	68.30 ± 3
2d	29.30 ± 3	18.24 ± 2

3.4.3. Evaluation of DNA fragmentation and molecule/DNA labeling

The apoptosis process involves also the DNA fragmentation. The synthesized compounds were tested to prove the DNA fragmentation and the eventual molecule/DNA labeling in untreated and treated FTC-133 and 8305C thyroid cancer cell lines. We observed that all the molecules tested, and prevalently **2a-c** compounds, were able to induce DNA fragmentation in treated cancer cell lines. The effect appeared more evident in FTC-133 cancer cell lines. Furthermore, to assess the molecule/ DNA labeling, gel electrophoresis was performed in absence or in presence of SYBR Green I, a well-known fluorescent dye that binds specifically to double-stranded DNA (Figure 26). Molecule/DNA labeling was detected only in presence of the fluorescent dye. The obtained data show that all the molecules induced DNA fragmentation at a different degree.
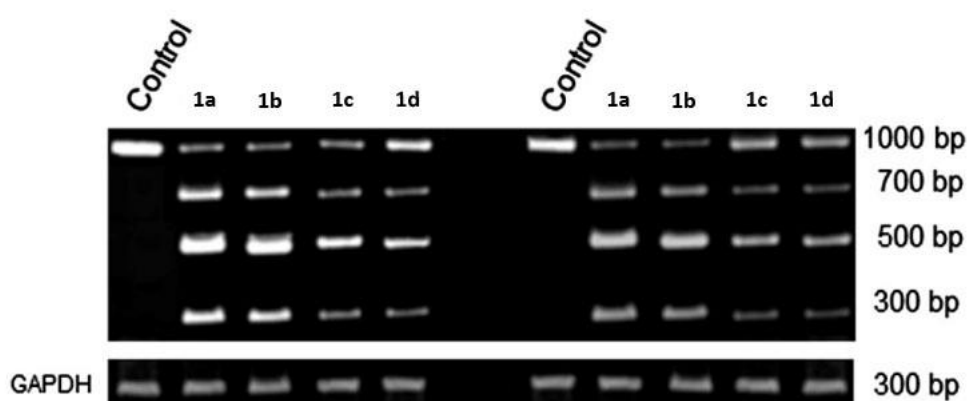

Figure 26: DNA fragmentation in untreated or treated FTC-133 (left) and 8305C (right) cells with 50 μM of **2a-d** for 24 h. Gel electrophoresis was performed in presence of SIBER Green I. Glyceraldehyde-3-phosphate dehydrogenase-1 (GAPDH-1) gene was used as a reference gene to normalize target gene expression.

3.5. Conclusion

In summary, with this work we developed an efficient synthesis of a series of oxazolo[3,4-*a*]pyrazin-6(3*H*)-ones through a procedure based on a double intramolecular domino process catalyzed by PdCl$_2$(MeCN)$_2$/ CuCl$_2$ performed on different alkenyl ureas.

Biological tests indicate that the obtained compounds have an interesting antitumor activity against two thyroid human cell lines, by activating caspase-3 dependent apoptotic pathway and DNA fragmentation with a prevalent action on follicular type.

3.6. Experimental part

3.6.1. Synthesis

Flash column chromatography was performed employing 230 – 400 mesh silica gel. Analytical thin layer chromatography was performed on silica gel 60 F254. Melting points were measured with a Büchi B-540 apparatus and are uncorrected. IR spectra were recorded on a Nicolet 550 FT-IR spectrophotometer. Nuclear magnetic resonance spectra were acquired on Varian instrument at 200 or 500 MHz for ^{1}H NMR and 125 MHz for ^{13}C NMR. ^{13}C spectra were ^{1}H decoupled and multiplicities were determined by the APT pulse sequence. EI mass spectra were recorded at an ionizing voltage of 6 KeV on a VG 70-70 EQ. Elemental analyses were executed on a Perkin–Elmer CHN Analyzer Series II 2400.

General procedure for the preparation of alkenyl ureas 1
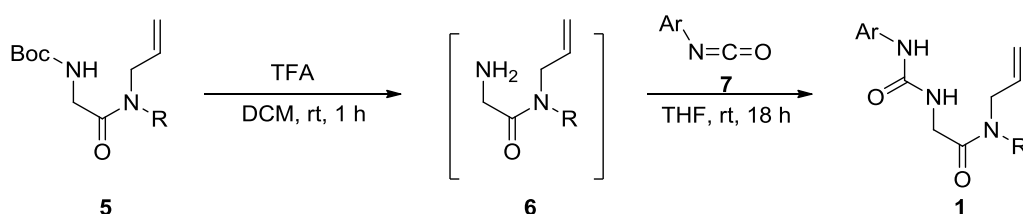
Trifluoroacetic acid (3 mL) was added to a solution of allyl-amide **5** (1 mmol) in CH_2Cl_2 (3 mL). The mixture was stirred at room temperature for 1 h. The solvent was evaporated to dryness and the residue was taken with a 1 M solution of NaOH up to pH 13. The mixture was extracted with CH_2Cl_2 (3 10 mL) and the organic layer was dried over Na_2SO_4. Concentration at reduced pressure gave a colourless oil, which was dissolved in THF (5 mL) and treated with the appropriate isocyanate **7** (1 mmol). The solution was stirred at room temperature overnight and then the solvent was evaporated to give a crude residue that was chromatographed on silica gel column.

N-Allyl-N-cyclohexyl-2-(3-phenylureido)-acetamide (1a)
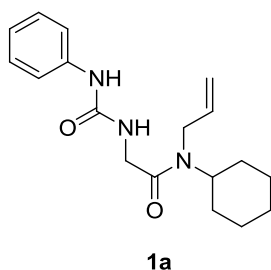
Eluent: light petroleum–AcOEt 3:2. White solid; yield 82%, mp 97–99 °C. IR (nujol): ν= 3301, 1750, 1654 cm^{-1}. ^{1}H NMR (500 MHz, CDCl$_3$, mixture of two rotamers in 7:6 ratio) major rotamer: δ 1.07–1.82 (m, 10H), 3.91 (d, J = 4.8 Hz, 2H), 4.13 (s, 2H), 4.34–4.46 (m, 1H), 5.06–5.26 (m, 2H), 5.72–5.87 (m, 1H), 6.45 (br s, 1H), 7.00–7.03 (m, 1H), 7.24–7.28 (m, 2H), 7.32–7.36 (m, 2H) 7.64 (br s, 1H) ppm; minor rotamer: δ 1.07–1.82 (m, 10H), 3.47–3.59 (m, 1H), 3.94 (d, J = 5.1 Hz, 2H), 4.23 (s,

2H), 5.06–5.26 (m, 2H), 5.72–5.87 (m, 1H), 6.45 (br s, 1H), 7.00–7.03 (m, 1H), 7.24–7.28 (m, 2H), 7.32–7.36 (m, 2H), 7.64 (br s, 1H) ppm; ^{13}C NMR (125 MHz, CDCl$_3$) major rotamer: δ 25.3, 25.5, 29.7, 44.7, 46.1, 52.4, 117.5, 118.5, 121.1, 128.8, 129.1, 137.7, 155.5, 164.4 ppm; minor rotamer: δ 25.3, 25.4, 29.3, 44.5, 46.1, 47.6, 116.8, 118.5, 121.1, 128.8, 129.1, 138.3, 155.6, 164.4 ppm. MS: m/z 315 (M+). Anal. Calcd for C$_{18}$H$_{25}$N$_3$O$_2$: C, 68.54; H, 7.99; N, 13.32; Found C, 68.72; H, 7.73; N, 13.41.

N-Allyl-*N*-cyclohexyl-2-(3-naphthalen-1-ylureido)-acetamide (1b)
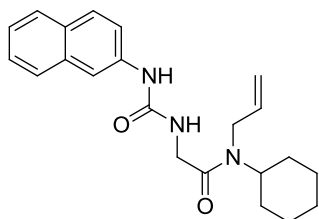
1b

Eluent: light petroleum–AcOEt 3:2. Beige solid; yield 75%, mp 173–174 °C. IR (nujol): ν = 3287, 1745, 1656 cm^{-1}. ^{1}H NMR (500 MHz, CDCl$_3$, mixture of two rotamers in 4:3 ratio) major rotamer: δ 1.02–1.79 (m, 10H), 3.74 (d, J = 4.8 Hz, 2H), 4.11 (s, 2H), 4.19–4.32 (m, 1H), 4.98–5.16 (m, 2H), 5.56–5.72 (m, 1H), 6.73 (br s, 1H), 7.42–7.50 (m, 3H), 7.63 (br s, 1H), 7.82–7.86 (m, 2H), 8.08–8.13 (m, 2H) ppm; minor rotamer: δ 1.02–1.79 (m, 10H), 3.39– 3.45 (m, 1H), 3.81 (d, J = 5.4 Hz, 2H), 4.20 (s, 2H), 4.98–5.16 (m, 2H), 5.56–5.72 (m, 1H), 6.81 (br s, 1H), 7.42–7.50 (m, 3H,), 7.67 (br s, 1H), 7.82–7.86 (m, 2H), 8.08–8.13 (m, 2H) ppm; ^{13}C NMR (125 MHz, CDCl$_3$) major rotamer: δ 25.3, 25.5, 29.6, 42.6, 44.8, 54.3, 114.1, 116.9, 121.3, 122.0, 125.2, 125.8, 126.0, 128.3, 128.5, 134.1, 134.3, 157.0, 169.6 ppm; minor rotamer: δ 25.3, 25.4, 29.2, 42.4, 44.3, 56.4, 114.1, 116.1, 121.1, 121.9, 125.1, 125.5, 125.9, 128.3, 128.5, 133.7, 134.5, 156.9, 168.4 ppm; MS: m/z 365 (M$^+$); Anal. Calcd for C$_{22}$H$_{27}$N$_3$O$_2$: C, 72.30; H, 7.45; N, 11.50; Found C, 72.09; H, 7.61; N, 11.73. 4.1.3.

N-Allyl-*N*-cyclohexyl-2-(3-pyren-1-ylureido)-acetamide (1c)
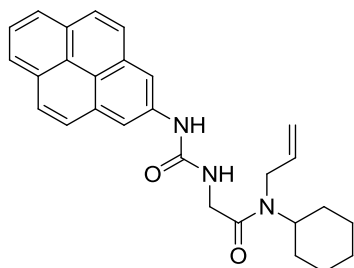

1c

Eluent: light petroleum–AcOEt 3:2. Brown solid; yield 70%, mp 97–99 °C; ^{1}H NMR (200 MHz, CDCl$_3$): δ 1.02–1.79 (m, 10H), 3.58– 3.69 (m, 1H), 3.94–4.02 (m, 1H), 4.44 (d, 1H), 4.53 (d, 1H), 5.10– 5.37 (m, 2H), 5.72–5.90 (m, 2H), 7.34 (br d, 1H), 8.00–8.24 (m, 9H), 8.70 (d, 1H) ppm; ^{13}C
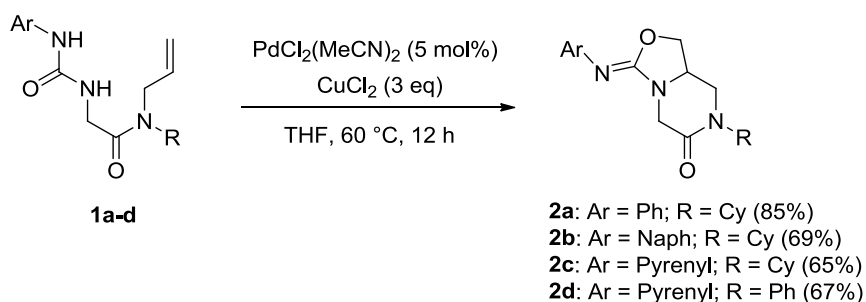
NMR (125 MHz, CDCl$_3$): δ 24.9, 25.8, 29.2, 29.7, 43.1, 46.0, 52.5, 118.4, 121.4, 122.8, 124.5, 124.8, 125.0, 125.3, 125.9, 126.5, 127.3, 127.5, 128.0, 129.0, 129.7, 131.0, 131.3, 131.7, 132.1, 140.1, 157.0, 169.3 ppm; MS: m/z 439 (M$^+$); Anal. Calcd for C$_{28}$H$_{29}$N$_3$O$_2$: C, 76.51; H, 6.65; N, 9.56; Found C, 76.39; H, 6.88; N, 9.59.

N-Allyl-N-phenyl-2-(3-pyren-1-ylureido)-acetamide (1d)


1d
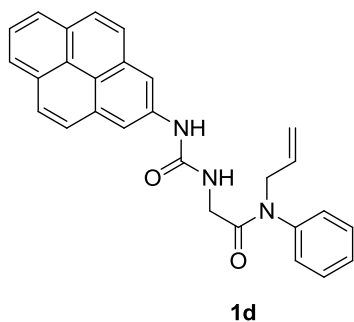
Eluent: light petroleum–AcOEt 3:2. Brown solid; yield 67%, mp 103–105 °C; ^{1}H NMR (200 MHz, CDCl$_3$): δ 3.81 (d, J = 4.4 Hz, 1H), 4.15 (d, J = 6.3 Hz, 2H), 4.90–4.99 (m, 2H), 5.61–5.74 (m, 1H), 6.30 (br s, 1H), 7.01–7.05 (m, 2H), 7.23–7.27 (m, 4H), 7.81 (br s, 1H), 7.98–8.05 (m, 3H), 8.11–8.30 (m, 6H) ppm; ^{13}C NMR (125 MHz, CDCl$_3$): δ 24.9, 25.8, 29.2, 43.1, 45.8, 52.5, 118.4, 121.2, 122.8, 124.7, 124.7, 125.0, 125.3, 126.0, 126.5, 127.2, 127.5, 128.0, 128.6, 129.8, 130.9, 131.3, 132.1, 140.2, 156.9, 169.2 ppm; MS: m/z 433 (M$^+$); Anal. Calcd for C$_{28}$H$_{23}$N$_3$O$_2$: C, 77.58; H, 5.35; N, 9.69; Found C, 77.76; H, 6.11; N, 9.92.

General procedure for synthesis of 3-arylimino-1,7,8,8atetrahydro-3H-oxazolo[3,4-a]pyrazin-6(5H)-ones 2a–d

1a-d

2a: Ar = Ph; R = Cy (85%)
2b: Ar = Naph; R = Cy (69%)
2c: Ar = Pyrenyl; R = Cy (65%)
2d: Ar = Pyrenyl; R = Ph (67%)

A solution of the appropriate alkenyl urea **1a-d** (1 mmol) in dry THF (3 mL) was added to a suspension of PdCl$_2$(MeCN)$_2$ (13 mg, 0.05 mmol) and CuCl$_2$ (402 mg, 3.0 mmol) in dry THF (3 mL). The reaction was heated at 60 °C for 12 h. After addition of brine, the mixture was extracted with CH$_2$Cl$_2$ (3 10 mL). The organic layer was dried over Na$_2$SO$_4$ and the solvent was evaporated under reduced pressure to give a crude product that was purified by silica gel column chromatography.

Cyclohexyl-3-phenylimino-1,7,8,8a-tetrahydro-3H-oxazolo[3,4-a]pyrazin-6(5H)-ones (2a)

2a
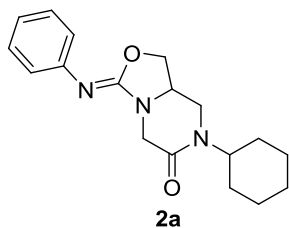
Eluent: light petroleum–AcOEt 3:7. White solid; yield 85%, mp 155–156 °C. IR (nujol): ν= 1757, 1585 cm^{-1}. ^{1}H NMR (500 MHz, CDCl$_3$): δ 1.25–1.82 (m, 10H), 3.15 (dd, J = 11.1, 9.3 Hz, 1H), 3.28 (dd, J = 12.0, 3.8 Hz, 1H), 3.82–3.87 (m, 1H), 3.88 (d, J = 17.8 Hz, 1H), 4.02 (dd, J = 8.6, 4.4 Hz, 1H), 4.43 (dd, J = 8.6, 7.4 Hz, 1H), 4.46–4.52 (m, 1H), 4.53 (d, J = 17.8 Hz, 1H) 6.89–6.98 (m, 1H), 7.05 (d, J = 7.6 Hz, 2H), 7.20–7.24 (m, 2H) ppm; ^{13}C NMR (125 MHz, CDCl$_3$): δ 25.3, 25.4, 25.6, 29.3, 29.6, 43.6, 46.4, 51.6, 52.6, 67.9, 122.5, 123.4, 128.5, 146.6, 150.9, 164.3 ppm; MS: m/z 313 (M$^+$). Anal. Calcd for C$_{18}$H$_{23}$N$_3$O$_2$: C, 68.98; H, 7.40; N, 13.41; Found C, 69.09; H, 7.17; N, 13.66.

**7-Cyclohexyl-3-(naphthalen-1-ylimino)-1,7,8,8a-tetrahydro-3H-oxazolo[3,4-a]pyrazin-6(5H)-ones (2b)**

2b
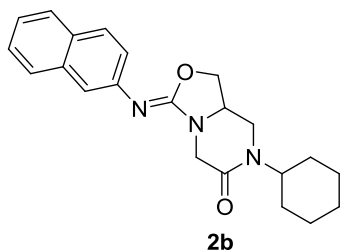
Eluent: light petroleum–AcOEt 3:7. White solid; yield 69%, mp 175–176 °C. IR (nujol): ν = 1753, 1581 cm^{-1}. ^{1}H NMR (500 MHz, CDCl$_3$): δ 1.05–1.82 (m, 10H), 3.24 (dd, J = 11.3, 10.6 Hz, 1H), 3.34 (dd, J = 12.0, 3.9 Hz, 1H), 3.92–3.98 (m, 1H), 4.02-4.07 (m, 2H), 4.47 (dd, J = 8.7, 7.2 Hz, 1H), 4.53–4.60 (m, 1H), 4.75 (d, J = 18.3 Hz, 1H), 7.19–7.21 (m, 1H), 7.36–7.45 (m, 3H), 7.52 (d, J = 8.2 Hz, 1H), 7.29–7.32 (m, 1H), 8.19–8.22 (m, 1H) ppm; ^{13}C NMR (125 MHz, CDCl$_3$): δ 25.3, 25.4, 25.6, 29.3, 29.7, 43.6, 46.6, 51.7, 52.6, 67.8, 117.4, 122.6, 124.1, 124.9, 125.7, 125.8, 127.7, 129.3, 134.3, 142.8, 150.9, 164.4 ppm; MS: m/z 363 (M$^+$); Anal. Calcd for C$_{22}$H$_{25}$N$_3$O$_2$: C, 72.70; H, 6.93; N, 11.56; Found C, 72.63; H, 7.19; N, 11.80.

**7-Cyclohexyl-3-(pyrenyl-1-ylimino)-1,7,8,8a-tetrahydro-3H-oxazolo[3,4-a]pyrazin-6(5H)-ones (2c)**Z

2c
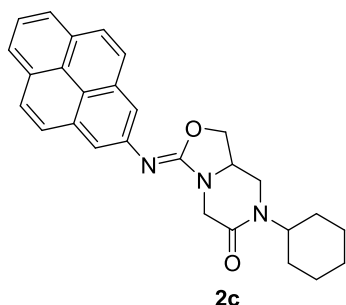
Eluent: light petroleum–AcOEt 3:7. Yellow bright solid; yield 65%, mp 132–134 °C. ^{1}H NMR (500 MHz, CDCl$_3$): δ 1.05–1.82 (m, 10H), 3.34 (dd, J = 11.3, 10.6 Hz, 1H), 3.40 (dd, J = 12.0, 3.9 Hz, 1H), 4.02–4.07 (m, 1H), 4.16–4.12 (m, 2H), 4.56–4.60 (m, 2H), 4.85 (d, J = 18.3 Hz, 1H), 7.19–7.21 (m, 1H), 7.36–7.45 (m, 3H), 7.52 (d, J = 8.2 Hz, 1H), 7.29–7.32 (m, 1H), 8.19–8.22 (m, 2H), 8.45 (d, 1H) ppm; ^{13}C NMR (125 MHz, CDCl$_3$): δ 25.3, 25.4, 25.6, 29.3, 29.7, 43.7, 46.7, 51.9, 52.6, 68.0, 120.4, 123.6, 124.1, 124.2, 125.0, 125.4, 125.5, 125.7, 126.2, 127.0, 127.4, 131.6, 142.1, 151.8, 164.4 ppm; MS: m/z 437 (M$^+$); Anal. Calcd for C$_{28}$H$_{27}$N$_3$O$_2$: C, 76.86; H, 6.22; N, 9.60; Found C, 77.05; H, 6.07; N, 9.87.

7-Phenyl-3-(pyrenyl-1-ylimino)-1,7,8,8a-tetrahydro-3H-oxazolo[3,4-a]pyrazin-6(5H)-ones (2d)

2d
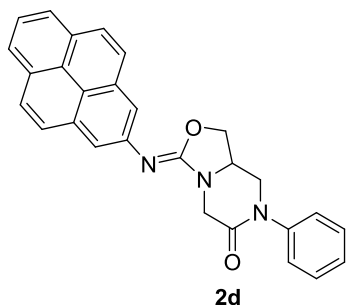
Eluent: light petroleum–AcOEt 3:7. Light yellow solid; yield 67%, mp 93–96 °C. ^{1}H NMR (500 MHz, CDCl$_3$): δ 3.58–3.66 (m, 2H), 3.89–3.94 (m, 1H), 4.06–4.09 (m, 2H), 4.52–4.55 (m, 2H), 5.04 (d, J = 18.8 Hz, 1H), 7.32 (d, 2H) 7.44 (t, 2H) 7.86 (d, J = 7.9 Hz 1H), 7.90–8.01 (m, 4H), 8.1–8.06 (m, 3H), 8.49 (d, J = 9.2 Hz, 1H) ppm; ^{13}C NMR (125 MHz, CDCl$_3$): δ 29.7, 31.6, 46.7, 46.9, 51.7, 52.8, 67.7, 96.1, 120.3, 123.6, 124.1, 124.3, 124.7, 125.0, 125.1, 125.5, 125.7, 125.8, 126.2, 126.3, 127.0, 127.4, 127.5, 127.6, 129.4, 129.5, 131.5, 131.6, 140.9, 141.9, 150.8, 165.0 ppm; MS: m/z 431 (M$^+$); Anal. Calcd for C$_{28}$H$_{21}$N$_3$O$_2$: C, 77.94; H, 4.91; N, 9.74; Found C, 78.01; H, 4.76; N, 9.48. 4.3.

3.6.2. Biological assay

Materials: Dulbecco's modified Eagle medium (DMEM) and Minimum Essential Medium (MEM) containing 2 mM GlutaMAX (GIBCO), Ham's F12 (GIBCO), nonessential amino acids, heat inactivated Fetal Bovine Serum (FBS, GIBCO), Normal Goat Serum (NGS, GIBCO), Streptomycin and penicillin antibiotics, Trypsin–EDTA 0.05% solution were from Invitrogen (Milan, Italy). Lab-Tek™ Chamber Slides II, 3-(4,5-dimethylthiazol-2-yl)-2,5-diphenyltetrazolium bromide salts (MTT), agarose, and other chemicals of analytical grade were obtained from Sigma–Aldrich (Milano, Italy).

Mouse monoclonal antibody against caspase-3 was from Becton–Dickinson (Milan, Italy). Tetrarhodamine isothiocyanate (TRITC)-conjugated anti-mouse IgG polyclonal antibody, were from Chemicon (Prodotti Gianni, Milan, Italy). QIAamp DNA Mini kit was from Qiagen.

Cell cultures: FTC-133 and 8305C cell lines were suspended in appropriate medium and plated in flasks at a final density of 2 x 106 cells or in Lab-Tek™ Chamber Slides II at a final density 0.5 x 105 cells/ well. Specifically the medium for FTC-133 cell lines was: DMEM containing 2 mM Gluta-MAX, 10% FBS, streptomycin (50 μg/mL), penicillin (50 U/mL); whereas the medium for 8305C cell lines was: MEM containing 2 mM Gluta-MAX, 10% FBS, streptomycin (50 μg/mL), penicillin (50 U/mL), and 1% nonessential amino acids. Cell lines were then incubated at 37 °C in humidified atmosphere containing 5% CO_2 and the medium was replaced every 2 or 3 days. When the cultures were about 85–90% confluent, cells were trypsinized by 0.05% trypsin and 0.53 mM EDTA at 37 °C in humidified atmosphere containing 5% CO_2 for 5 min. Trypsinization was stopped by adding 20% FBS, resuspended and plated in flasks fed with fresh basic complete media. Cells were seeded again at 1:4 density ratio and incubated at 37 °C in humidified atmosphere containing 5% CO_2.

Treatment of the cells: FTC-133 and 8305C were replated on to Lab-Tek™ Chamber Slides II at a final density of 1 104 cells/well, and fed in fresh complete medium. In preliminary experiments, we exposed the both cultures in the absence or the presence of different concentrations of **2a-d** (5, 10, 25, 50, 75, 100 μM) for 12, 24 h, in order to establish the optimal concentrations and their exposure times to all synthesized compounds. For this purpose, MTT test and morphological characterization were utilized.[75] We found that for the both cultures the optimal concentration of all synthesized compounds was 50 μM and the optimal exposure time was 24 h.

---

[75] A. Campisi; D. Caccamo; G. Raciti; G. Cannavò; V. Macaione; M. Currò; S. Macaione; A. Vanella; R. Ientile; *Brain Res.*, **2003**, *978*, 24.

MTT bioassay Cell survival analysis was performed by MTT reduction assay, evaluating mitochondrial dehydrogenase activity.[76] Cells were set up 6 105 cells per well of a 96-multiwell, flat-bottomed, 200 μL microplate, and maintained at 37 °C in a humidified 5% CO_2/95% air mixture. At the end of treatment time, 20 μL of 0.5% MTT in (pH 7.4) PBS were added to each microwell. After 1 h of incubation with the reagent, the supernatant was removed and replaced with 200 μL of dimethyl sulfoxide (DMSO). The optical density of each well was measured with a microplate spectrophotometer reader (Titertek Multiskan; Flow Laboratories, Helsinki, Finland) at 570 nm.

Immunocytochemistry: Expression of caspase-3 in FTC-133 and 8305C cells was identified by immunocytochemical procedures. Untreated or **2a-d** treated FTC-133 and 8305C were fixed by exposing to 4% paraformaldehyde in 0.1 M PBS for 20 min. Then, cells were washed three times with PBS and incubated for 1 h at 37 °C in humidified air and 5% CO_2 with 1% NGS in PBS to block unspecific sites. The cells were successively incubated overnight at 37 °C in humidified air and 5% CO_2 with mouse monoclonal antibody against caspase-3 (1:200). Finally, the slides were washed three times with PBS, mounted in PBS/glycerol (50:50), and analyzed on a Leica fluorescent microscopy (Germany). No nonspecific staining of hMSCs was observed in control incubations in which the primary antibody was omitted.

DNA labelling assay: DNA extraction from both untreated and treated FTC-133 and 8305C cells with 75 μM of **2a-d** for 24 h was performed according to the user's manual. Gel electrophoresis separates DNA fragments by size in an 2% agarose gel. DNA is visualized by including in the gel an intercalating dye, SYBER Green I. GAPDH-1 as housekeeping gene was used.

Statistical analysis: data were statistically analysed using one-way analysis of variance (one-way ANOVA) followed by post hoc Holm–Sidak test to estimate significant differences among groups. Data were reported as mean ± SD of four experiments in duplicate, and differences between groups were considered to be significant at $p < 0.05$.

---

[76] a) A. Campisi; D. Caccamo,; G. LiVolti; M. Currò; G. Parisi; R. Avola; A. Vanella; R. Ientile; *FEBS Lett.*, **2004**, *578,* 80; b) A. Campisi; M. Spatuzza; A. Russo; G. Raciti; A. Vanella; S. Stanzani; R. Pellitteri; *Neurosci. Res.*, **2012**, *72*, 289.

Chapter 4

Boehmeriasin A as new lead compound for the inhibition of topoisomerases and SIRT2

4.1. Introduction

Since the first isolation of tylophorine in 1935 from the perennial climbing plant *Tylophoria indica*, the class of phenanthroizidine alkaloids has grown considerably. The main future of these pentacyclic plant-derived small molecules is the presence of a highly oxygenated phenanthrene ring fused to a saturated *N*-heterocycle (Figure 27).
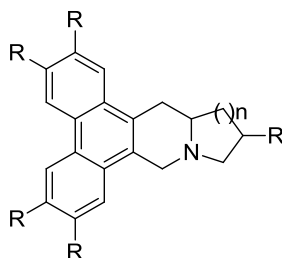
Phenanthroindolizidines   n = 1
Phenanthroquinolizidines   n = 2

Figure 27

Historically, the plant extracts have been used in herbal medicine and the isolated compounds have displayed a range of promising therapeutic activity such as anti-viral, anti-inflammatory and anti-cancer activity. The phenanthroindolizidines are much more prevalent in natural sources than the corresponding quinolizidines. In fact, cryptopleurine, which was isolated as early as 1948 from the bark of *Cryptocarya* pleurosperma, was considered for a long time to be the sole example of this rare class of alkaloids. This family was later enriched by isolation other derivatives, among whom Boehmeriasin A and B (Figure 28).[77]
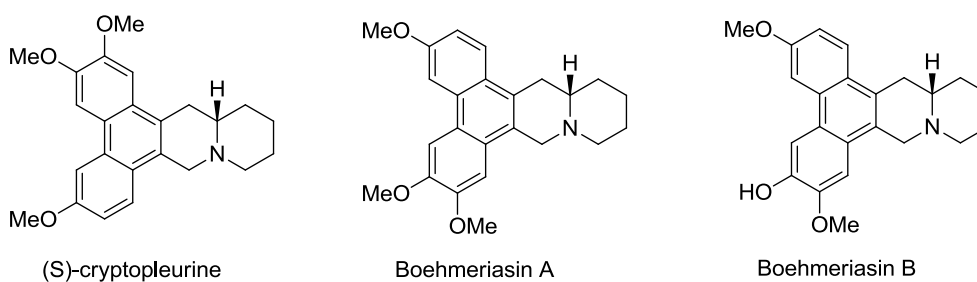

(S)-cryptopleurine
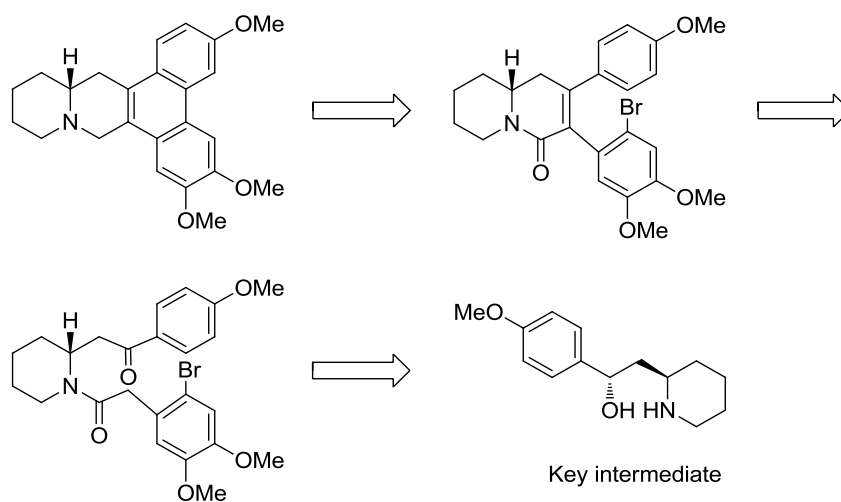
Boehmeriasin A

Boehmeriasin B

Figure 28

The structural difference between phenanthroindolizidine and phenanthroquinolizidine alkaloids lies in the size of the E-ring. The presence of the six-membered ring in the phenanthroquinolizidine skeleton led to a significant increase in cytotoxicity in comparison to phenanthroindolizidine skeleton, which has a five-membered ring. Despite their therapeutic potential, no compounds in these classes have fully passed clinical trials so far, due to their main

---

[77] D. Dumoulin; S. Lebrun; A. Couture; E. Deniau; P. Grandclaudon; *Eur. J. Org. Chem.*, **2010**, 1943.

drawbacks, including low in vivo anti-cancer activity, central nervous system toxicity and low natural availability.[78]

Boehmeriasin A and B were isolated from the aqueous ethanolic extract of *Boehmeria siamensis* Craib by Luo et al. in 2003. I*n vitro* tests showed that boehmeriasin A possesses a strong cytotoxic activity, more potent than Paclitaxel, against 12 different cancer cell lines with GI_{50} values in the range 0.2-5 ng/mL for all but one cell lines. Boehmeriasin B showed lower activity.[79]

As a consequence of its promising biological profile, coupled with its low natural abundance and unusual architecture, Boehmeriasin A continues to be target for synthesis, modification, and structure-activity relationship (SAR) studies with the hope that a new drug will emerge. Recently, few synthetic methodology have been developed for the elaboration of the phenanthroquinazolidine scaffold of Boehmeriasin. Two important examples are shown to follow. In 2010 A. Couture at al. reported the first asymmetric synthesis of Boehmeriasin A in which the key intermediate with the piperidine template was achieved through two alternative and elaborate synthetic pathways. A subsequent acylation/oxidation/aldol condensation/radical cyclization sequence completed the assembly of the title (*R*)-configured natural product (Scheme 11).[77]


Scheme 11

Afterward, both enantiomers of boehmeriasin A were synthesized by Georg in seven steps each using a chiral pool approach. Key steps in the syntheses were a one-flask, two-step protocol to generate the quinolizine core and a C-H functionalization reaction between tetrahydroquinolizinones and an aryltrifluoroborate (Scheme 12).[80]

[78]a) S.R. Chemler; *Curr. Bioact. Compd.*, **2009**, *5*, 2.

[79] a) Y. Luo; Y. Liu; D. Luo; X. Gao; B. Li; G. Zhang; *Planta Med.*, **2003**, *69*, 842; b) J. P. Michael; *Nat. Prod. Rep.*; **2005**, *22*; 603.

[80] M. W. Leighty; G. I. Georg; *ACS Med. Chem. Lett.*; **2011**, *2*, 313.

Scheme 12
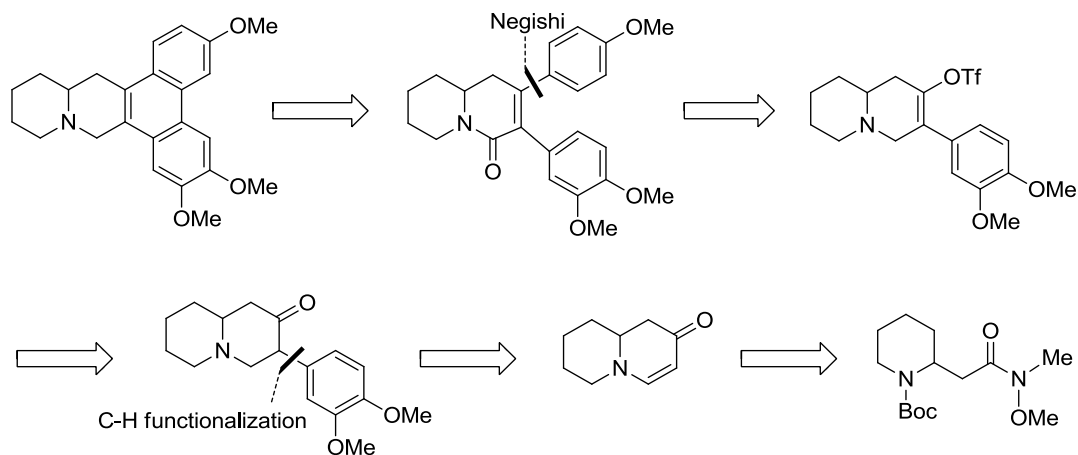
4.2. Aim of this work

In this context, we planned two synthetic approaches to obtain the racemic mixture and the pure enantiomers of boehmeriasin A which, in spite of previous reported preparations, present an increased efficacy and simplicity, relevant features for large-scale synthesis and analogue preparation.
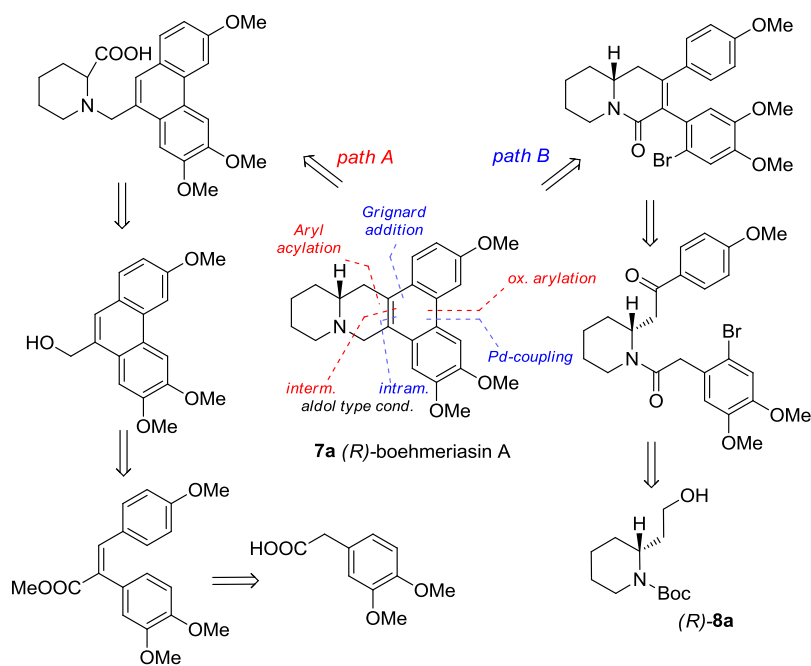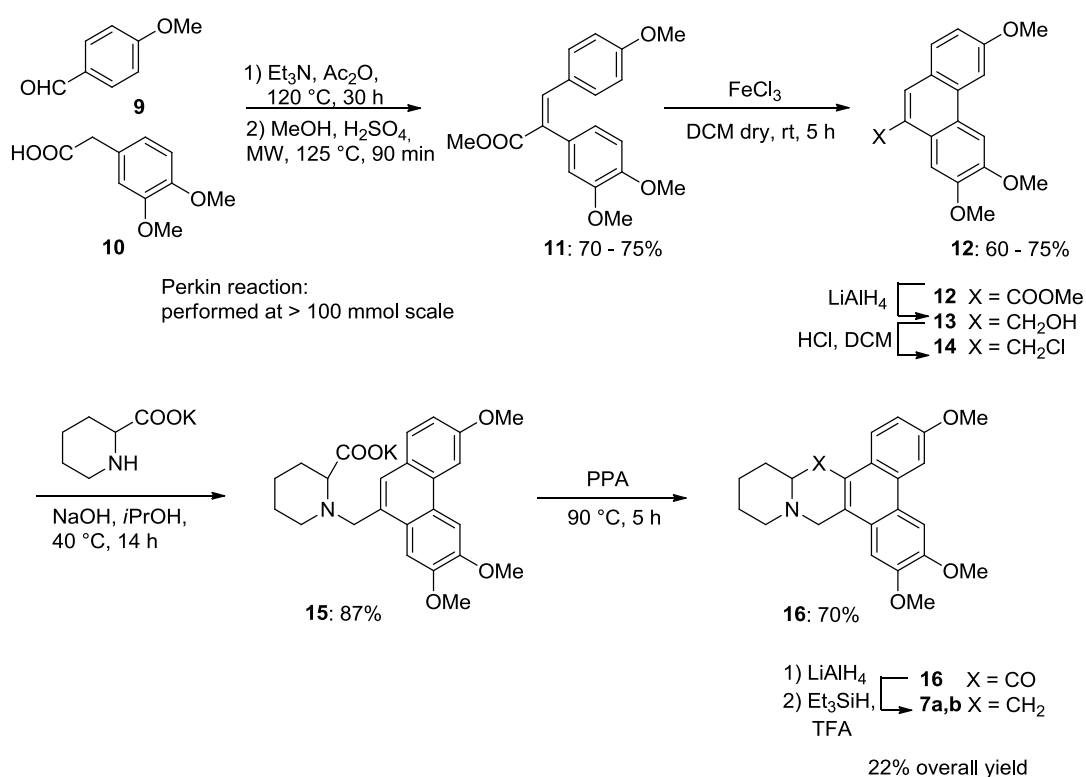

Scheme 13

Further, we wanted to test their biological activity and identify the biological target with the help of virtual screening (Hurakan tool) and docking studies.

4.3. Chemistry

As shown in the retrosynthetic plan in Scheme 13, the first step would be the formation of the phenanthrene nucleus and then, through a further cyclization, the quinolizidine ring (path A) or (path B). This would permit the generation of the nitrogen containing bicyclic system in a stereospecific way by an intramolecular aldol type reaction followed by an intramolecular arylation reaction.

4.3.1. Racemic preparation

First of all, Boehmeriasin A was prepared as racemic mixture with a simple and robust synthetic pathway, which has been allowed to prepare gram quantities of the desired natural product (Scheme 14).

Scheme 14

The synthesis started with a Perkin reaction between commercially available 4-methoxybenzaldehyde **9** and 3,4-dimethoxyphenylacetic acid **10**. This reaction can be easily performed at >100 mmol scale. Next, a microwave-assisted Fischer esterification delivered the corresponding ester **11** in quantitative yield and then the quinolizidine ring **12** was obtained through a ferrous chloride mediated oxidative biaryl coupling. Also this transformation can be performed on multigram scale in an efficient way, even if the generation of stoichiometric amounts of insoluble inorganic secondary products requires close reaction monitoring and specific work-up strategies in order to achieve a reproducible reaction outcome. The ester functionality was reduced using LiAlH$_4$ and chlorodehydroxylation of the resulting benzylic alcohol

13 with concentrated HCl cleanly affords the benzylic chloride **14**. A selective nucleophilic substitution was performed with the potassium salt of racemic pipecolic acid, furnishing the desired adduct **15**. A Friedel-Crafts acylation in neat polyphosphoric acid was used to prepare the pentacyclic scaffold **16** of boehmeriasin A in good yield. This reaction afforded an instable material under basic conditions, therefore was necessary to maintain the pH during the aqueous work-up below 8. Finally, removal of the ketone functionality was accomplished in a two-step fashion firstly using LiAlH$_4$ followed by dehydroxylation under TFA/triethylsilane conditions. In summary, this sequence allowed the preparation of racemic boehmeriasin A **7a,b** in a short 7 step sequence and in 22% overall yield.

Indeed, the resolution of the racemic natural product by chiral HPLC was evaluated. For analytical purposes a short chiral HPLC column (AD, 5 cm) in direct phase (10% ethanol and 90% hexane) was used in order to achieve resolution of the racemic boehmeriasin A (Figure 29).
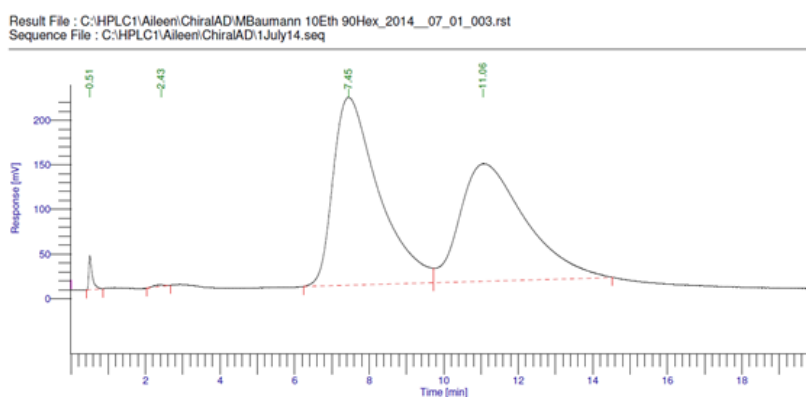

Figure 29

The successful resolution let us to be confident regard the possibility to separate the two enantiomers also on a preparative scale using a larger AD column. However, we firstly preferred to carry out an asymmetric synthesis of both (*S*)- and (*R*)-boehmeriasin A.

4.3.2. Enantioselective synthesis

In this second approach we developed an enantioselective synthesis using enantiopure piperidinethanol **8** as the starting material, which can be produced at gram scale through an enzymatic process (Scheme 15, (*S*)-enantiomer shown). [81]

---

[81] M. Angoli; A. Barilli; G. Lesma; D. Passarella; S. Riva; A. Silvani; B. Danieli; *J. Org. Chem.*, **2003**, *68*, 9525.
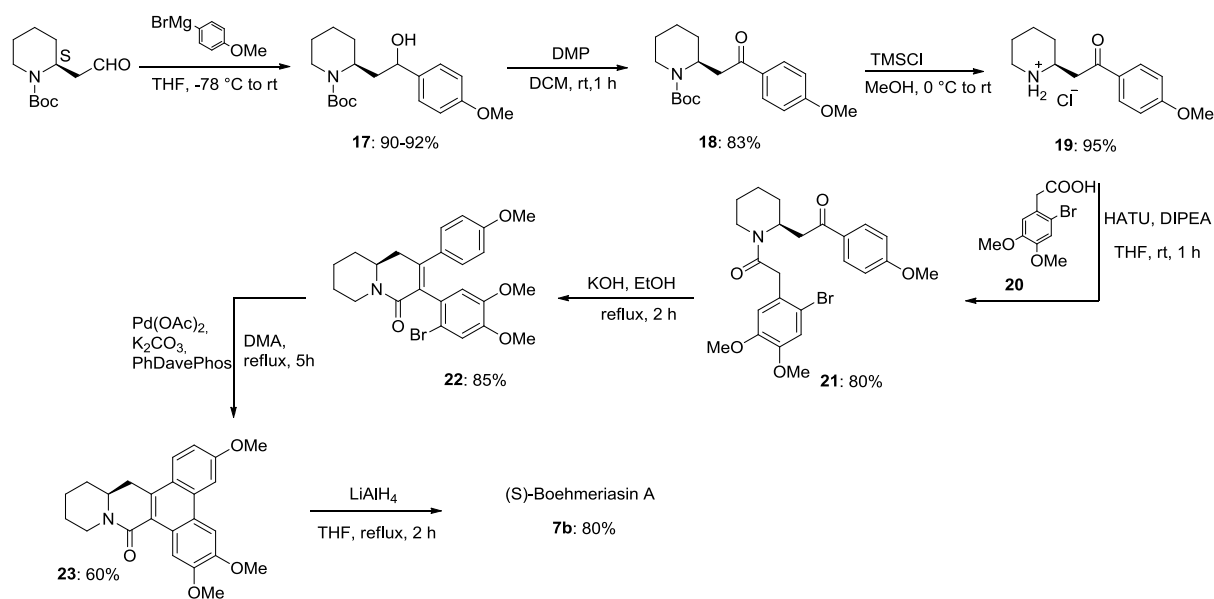
Scheme 15

After oxidation of the alcohol **8b**, the aldehyde was treated with 4-methoxyphenyl-magnesium bromide affording the secondary alcohol **17** in high yield. Dess-Martin periodinane was used as excellent oxidant to generate the intermediate **18**, and the deprotection of the Boc group (**19**) and *N*-acylation with the easily prepared 2-bromo-4,5-dimethoxyphenylacetic acid (**20**) afforded the compound **21** in 63% (3 steps). An intramolecular aldoltype condensation in the presence of KOH furnished the desirable intermediates **22** as mixture of atropisomers (85%, 1:1 ratio). To obtain the phenanthroquinolizidine skeleton a palladium catalysed intramolecular coupling was investigated (Table 3).

Table 3:
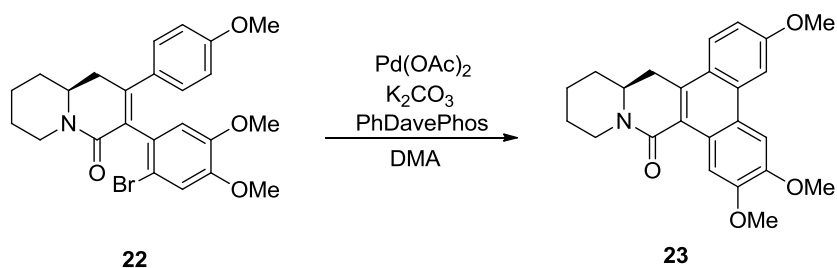
entry	Pd(OAc)$_2$ (mmol)	Ligand (mmol)	K$_2$CO$_3$ (mmol)	Time (h)	Temperature (°C)	Yield (%)
1	0.05	0.1	2	16 h	125	-
2	0.05	0.1	2	5	125	29
3	0.05	0.1	2	5	155	11
4	0.24	0.3	2	5	125	60

The reaction carried out with Pd(OAc)$_2$ as catalyst, 2'-(diphenylphosphino)-*N,N'* -dimethyl- (1,1'-*biphenyl*)-2-amine as the ligand and K$_2$CO$_3$ in dimethylacetamide at 125 °C for 5 h, furnished **23** in

60% yield. Finally, a reduction with LiAlH$_4$ completed the synthesis of boehmeriasin A with 80% of yield.

HPLC analysis confirmed that the purity of both enantiomers was in accordance with the e.e. of the starting materials **8**.

4.4. Biological evaluation

4.4.1. Anti proliferative activity

With the enantiomers of boehmeriasin A and the racemic mixture in our hands, we wanted to evaluate their anti proliferative activity on three selected cancer cell lines (human lymphoblastic leukaemia (CEM), human cervical carcinoma (HeLa) and mouse lymphocytic leukaemia (L1210) cells) and on two endothelial cell lines (human microvascular endothelial cells (HMEC-1) and bovine aortic endothelial cells (BAEC)). The chose reference compounds has been combretastatin A4P (CA-4P), that is a vascular-targeting agent which inhibits the proliferation of the tumour cells, and endothelial cells with IC$_{50}$ values around 80 nM and 3 nM, respectively (Table 4).

Table 4: Anti-proliferative activity of (*R*)- and (*S*)-boehmeriasin A in comparison with combretastatin A4P.

Compound	Tumor cell lines (IC$_{50}$[a] [nM])			Endothelial cell lines (IC$_{50}$[a] [nM])	
	HeLa	CEM	L1210	HMEC-1	BAEC
(*R*)-7	66 ± 56	185 ± 156	19 ± 10	7.4 ± 1.1	23 ± 13
(*S*)-7	182 ± 164	201 ± 127	111 ± 11	82 ± 66	23 ± 6
rac.-7	76 ± 52	119 ± 71	71 ± 23	29 ± 8	9.0 ± 2.1
CA-4P	79 ± 3	95 ± 6	82 ± 12	2.9 ± 0	3.9 ± 0.1

[a] 50% inhibitory concentration. CA-4P: combretastatin A4P. CEM: human lymphoblastic leukemia. HeLa: human cervical carcinoma. L1210: mouse lymphocytic leukemia cells. HMEC-1: human microvascular endothelial cells. BAEC: bovine aortic endothelial cells.

In accordance with other results reported in the literature,[79] both enantiomers showed potent cytostatic activity against the different tumour cells, with IC$_{50}$ values in the nanomolar range. Interestingly, **(*R*)-7** proved to be significantly more potent than the (*S*)-enantiomer against HeLa and L1210 cells. Both compounds also inhibited the proliferation of endothelial cells, with IC$_{50}$ values of 23 nM in BAEC and 82 nM for the (*R*)- and (*S*)-enantiomers in HMEC- 1, respectively. Together, these data confirm the inhibitory activity of (*R*)- and (*S*)-boehmeriasin A against both tumour and endothelial cells, the (*R*)-enantiomer being up to 11-fold more potent than the (*S*)-enantiomer in selected cell lines. The anti-proliferative activity of the racemic mixture was comparable to the activity of the (*R*)- enantiomer, being equally active in HeLa cells, about 2-fold more active in CEM cells and BAEC and 3e4-fold less active in L1210 cells and HMEC-1.

4.4.2. Virtual screening

The specific cellular target of the Boehmeriasin A, as well as of the others phenanthroquinolizidine alkaloids, is still unknown. For developing and optimizing this scaffold into therapeutic drugs, the identification of the biological target is fundamental to have a starting point to identify the eventual and proper alterable region of the molecule through structure and activity relationship studies (SAR).

The use of a virtual screening would have helped us to identify the biological target that could justify the anti-proliferative activity on different cell lines. Hurakan software[82] is a 3D ligand-based virtual screening tool that compares the input molecule with the structures present in the reference database. In particular Hurakan uses ChemblDB[83] as a reference database which contains molecules, targets and biological activities of many compounds and thus it is able to compare the behaviour of the molecules instead of comparing their structure. In this way, Hurakan predicts the biological profile of an input molecule and, in the case of Boehmeriasin A, it predicted 13 proteins for the *R*-enantiomer and 15 proteins for the *S*-enantiomer (Table 5).

Table 5: Target proteins for (*R*)- and (*S*)-boehmeriasin A

entry	(*R*)-Boehmeriasin A	(*S*)-Boehmeriasin A
1	Proto-oncogene c-JUN	Proto-oncogene c-JUN
2	DNA polymerase eta	Serotonin 2a (5-HT2a) receptor
3	Aryl hydrocarbon receptor nuclear translocator	Aryl hydrocarbon receptor nuclear translocator
4	Hypoxia-inducible factor 1 alpha	Alpha-1a adrenergic receptor
5	Chromobox protein homolog 1	Hypoxia-inducible factor 1 alpha
6	Cruzipain	Acetylcholinesterase
7	Sphingomyelin phosphodiesterase	DNA topoisomerase II alpha
8	Arachidonate 15-lipoxygenase, type II	DNA topoisomerase II beta
9	DNA dC->dU-editing enzyme APOBEC-3F	DNA topoisomerase I
10	Lysine-specific demethylase 4A	Acetylcholinesterase
11	Peptidyl-prolyl cis-trans isomerase NIMA-interacting 1	DNA dC->dU-editing enzyme APOBEC-3F
12	Nonstructural protein 1	Lysine-specific demethylase 4A
13	Nuclear factor erythroid 2-related factor 2	DNA polymerase eta
14		Nuclear factor erythroid 2-related factor 2
15		Cholinesterase

[82] E. Santamaría-Navarro; A. Nonell-Canals; Hurakan, Ligand-based 3D Screening Software, **2013**. Available at: www.mindthebyte.com.
[83] A.P. Bento; A. Gaulton; A. Hersey; L.J. Bellis; J. Chambers; M. Davies; F.A. Kruger; Y. Light; L. Mak; S. McGlinchey; M. Nowotka; G. Papadatos; R. Santos; J.P. Overington; *Nucleic Acids Res.*, **2014**, *42*, D1083.

Among all these probably target proteins, topoisimerases (entry 7-9, (*S*)-boehmeriasin) attracted our attention, since many famous chemotherapy drugs, called topoisomerase inhibitors, work by interfering with eukaryotic topoisomerases and inducing the apoptosis.

Topoisomerases are enzymes that regulate the overwinding or underwinding of DNA. The winding
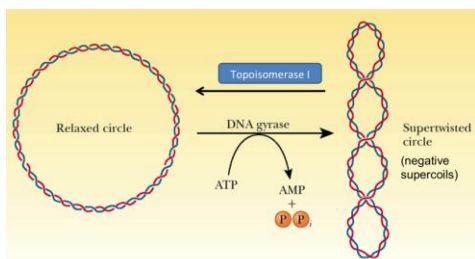

problem of DNA arises due to the intertwined nature of its double-helical structure. During DNA replication and transcription, DNA becomes overwound ahead of a replication fork. If left unabated, this tension would eventually stop the ability of the enzymes involved in these mechanisms to continue the replication process. In order to prevent and correct these types of topological problems caused by the double helix, topoisomerases bind to either single-stranded or double-stranded DNA and cut the phosphate backbone of the DNA.[84]

Based on this scenario, we were driven to evaluate the effect of both enantiomers of boehmeriasin A on topoisomerases.

4.4.3. Topoisomerases inhibition

We tested the effect of (*R*)- and (*S*)-boehmeriasin A on the relaxation of supercoiled plasmid DNA, that is an enzyme that relaxes supercoiled DNA giving rise to a series of topoisomers, representing differently relaxed forms (Topo II).

The test compounds were assayed at 10, 25 and 50 µM concentration, while *m*-AMSA, taken as reference drug, was used at 10 µM. In Figure 31 is evident that both enantiomers of boehmeriasin A exhibit a comparable and dose-dependent effect on enzymatic activity. At 10 µM both (*R*)- and (*S*)-enantiomers are unable to exert a significant inhibitory activity, while at 50 µM, the higher concentration taken into account, the topoisomerase-mediated relaxation is completely inhibited (Figure 30).
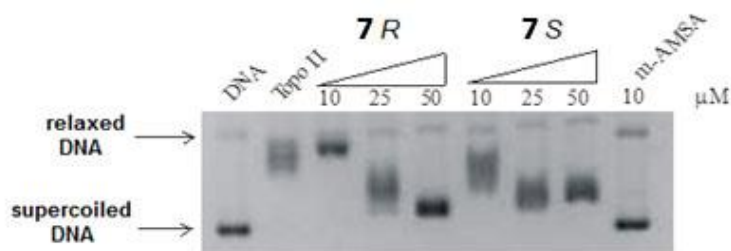

Figure 30

---

[84] J. J. Champoux; *Annu. Rev. Biochem.*, **2001**, *70*, 369.

Similar experiments were performed to assay the effect on topoisomerase I relaxation activity, and the results indicate a higher inhibitory effect compared to the data obtained on topoisomerase II. Indeed, at 10 μM concentration both (R)- and (S)-boehmeriasin A completely inhibit the relaxation mediated by topoisomerase I (Figure 31).
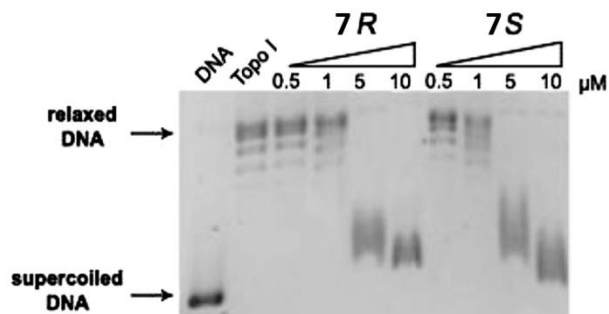

Figure 31

The topoisomerase enzymes can be inhibit at different stage of their activity. Some anti-proliferative agents, called topoisomerase poisons, interfere by stabilizing a biological intermediate into a lethal agent. This intermediate is called "cleavable complex" and it is a biochemical species arising from the cut of DNA strands, and subsequent formation of covalent bonds between each protein subunits and the newly formed 5'-phosphate ends of the DNA. This complex is considered "cleavable", since removal or disruption of the protein would result in a permanent double-strand break. The stabilization prevents the resealed of the breaks and the release of the topoisomerases.[85] Experimentally, the occurrence of cleavable complex can be demonstrate by the enzyme-dependent formation of linear (topo-II) or nicked (topo-I) DNA from supercoiled DNA. To verify whether both enantiomers of behmeriasin A would be involved in the stabilization of cleaveble complex, first a biological assay was performed on topoisomerase II in the presence of 100 μM of (R)- and (S)-boehmeriasin A and 10 μM m-AMSA used as reference because is a well-known topoisomerase II poison (Figure 32).

---

[85] W. B. Pratt, *The Anticancer drugs*, Oxford University Press, **1994**.
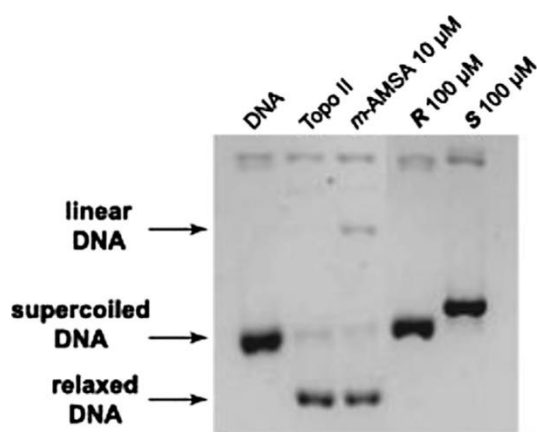
Figure 32

The results show that both derivatives do not stabilize the formation of the cleavage complex, although tested at a significantly higher concentration compared to that of the reference drug. Otherwise, as expected, *m*-AMSA, induces the formation of a detectable amount of linear DNA.

Considering topoisomerase I, the bioassay reported in Figure 34, using the topoisomerase I poison camptothecin (CPT) as reference compound, also show the inability of both (*R*)- and (*S*)-boehmeriasin A to act as a poison at the considered concentration (0.5 μM). By contrast, in the same experimental results, camptothecin induces the formation of the corresponding nicked DNA (Figure 33).
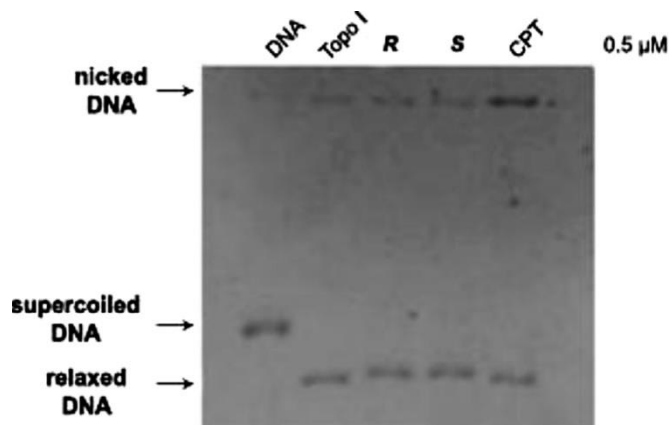
Figure 33

The polycyclic structure of Boehmeriasin A, which contains a phenanthrene moiety that could act as a DNA intercalant, along with the lack of poisoning effects, suggests that the ability of (*R*)- and (*S*)-boehmeriasin A to interfere with topoisomerase-mediated relaxation activity could come from the capacity of the compounds to form a molecular complex with DNA.

To gain better insight into the interactions between boehmeriasin A and the topoisomerases, molecular dockings studies were carried out.

The structure of topoisomerase I/DNA complex has been crystallised in complex with camptothecin, while topoisomerase II-beta/DNA has been obtained in complex with amsacrine, both well-known topoisomerase inhibitors, which are bound into the enzyme mediated DNA cleavage site intercalating between DNA base pairs.

The pockets formed by camptothecin and amsacrine upon binding to DNA in complex with topoisomerase I and II, respectively have been chosen as the putative binding sites of boehmeriasin A. Both (*R*)- and (*S*)- enantiomers have been docked. Docking simulations on topoisomerase I showed that both boehmerasin enantiomers display good binding affinity to the target. Cluster analysis showed two major clusters, comprising 50% and 36% of the docked structures of the (*S*)- enantiomer, and two minor clusters. All these clusters are almost isoenergetic, with binding energy around -14 kcal/mol (Figure 34a). The (*R*)-boehmeriasin A, on the other hand, displayed one dominant cluster, comprising 98% of the docking decoys (Figure 34b).

| a) | b) |
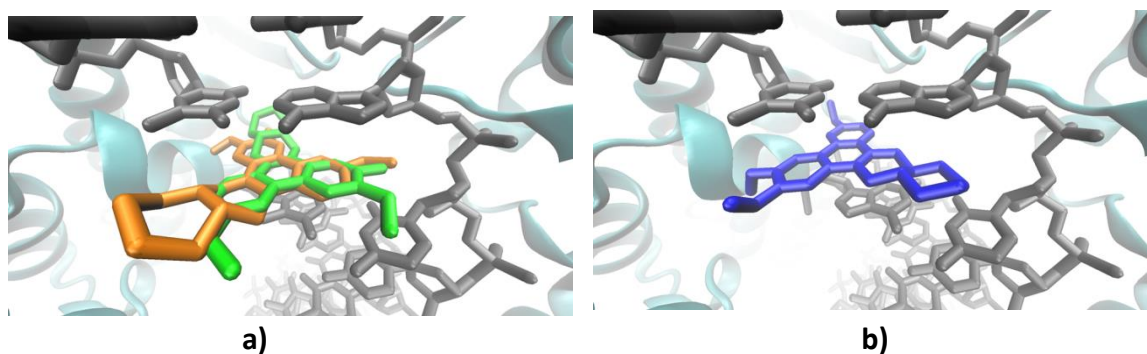
Figure 34: a) Docked structure of (*S*)-boehmeriasin A. The best fit structure of the principal cluster is depicted in orange, while the best fit structure of secondary cluster is green. Boehmerasin is intercalated between DNA bases of the nucleic acid double helix complexed with topoisomerase I; **b)** Docked structure of (*R*)-boehmeriasin A (blue molecule).

Cluster analysis of the docking results on the topoisomerase II showed only one cluster for the (*S*)-enantiomer, with the phenantrene moiety stacked between the DNA bases (Figure 35a). The (*R*)-enantiomer showed two distinct clusters: the principal one populated by 66% of the docked structures and the secondary one containing 34% of the docked structures (Figure 35b).
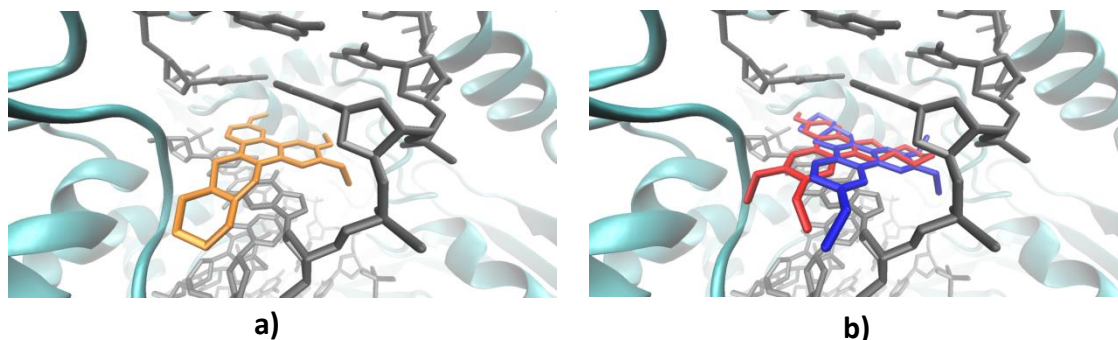
Figure 35: **a)** Docked structure of (*S*)-boehmeriasin A (orange molecule). The phenanthrene moiety is intercalated between base pairs of the DNA in complex with topoisomerase II; **b)** docked structure of (*R*)-boehmeriasin A. The best fit structure of the principal cluster is depicted in red, while the best fit structure of secondary cluster is in blue. A very similar binding energy corresponds to these structurally different poses.

A slight preference toward topoisomerase II can, on the other hand, be inferred on the basis of the docking results. It is worth noting that in all of the docked conformations both (*S*)- and (*R*)-enantiomers of boehmeriasin A do not display any significant contact with either one of the topoisomerase isoforms that have been tested, but seem to mainly interact with the DNA strand through stacking interactions.

4.4.4. Sirtuins inhibition

The similar structure of boehmeriasin A with known sirtuin inhibitors[86] drove us to study its activity against sirtuins.

Sirtuins are NAD-dependent protein deacetylase of which there are seven isoforms (SIRT1–7). They are fundamental for the modulation of multiple and diverse biological processes such as cell cycle control, microtubule dynamics, cell differentiation and so on. Recently, multiple research groups have pursued the identification and development of small-molecule compounds that modulate sirtuins, which can also be potentially useful as therapeutic agents because upregulated SIRT1 has been described in cancers.[87] Indeed, sirtuin 2 (SIRT2), has been shown to be a key regulator of cell division and differentiation.[88]

Both enantiomers were screened in vitro against SIRT1 and SIRT2 at 200 μM concentration For SIRT1 (*R*)- and (*S*)-boehmeriasin A showed no inhibition. Interestingly, for SIRT2 (*R*)-boehmeriasin A gave ~65% inhibition, whereas (S)-boehmeriasin A gave only 41% inhibition (Table 6).

[86] D. Rotili; D. Tarantino; V. Carafa; E. Lara; S. Meade; G. Botta; A. Nebbioso; J. Schemies; M. Jung; A.G. Kazantsev; M. Esteller; M.F. Fraga; L. Altucci; A. Mai; *ChemMedChem*, **2010**, *5*, 674.

[87] T. Liu; P.Y. Liu; G.M. Marshall; *Cancer Res.*, **2009**, *69*, 1702.

[88] T. Kozako; T. Suzuki; M. Yoshimitsu; N. Arima; S. Honda; S. Soeda; *Molecules*, **2014**, *19*, 20295.

Table 6: Evaluation of (R)- and (S)-boehmeriasin A against SIRT1 and SIRT2

Compound	SIRT1[a]	SIRT2[a]
(*R*)-7	12 ± 1.4	65 ± 1.6
(*S*)-7	10 ± 4.2	41 ± 0.56

[a] Inhibition % at 200 µM inhibitor concentration.

Docking studies were performed also for the interaction between boehmeriasin A and SIRT1 and SIRT2.

In SIRT1, both enantiomers of boehmeriasin A were docked into the place of the nicotinamide-moiety (so called C-pocket in sirtuins) showing π-interactions with His363 or Phe273 but they could not adopt a good orientation in the binding pocket (Figure 36).
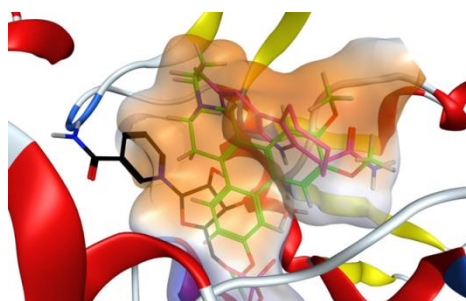
Figure 36: (R)-Boehmeriasin A (green) in the putative binding site of SIRT2. NAD^{+} (black) and Ex-527(purple) is also presented based on their position in SIRT1.

As for SIRT2, (*R*)-boehmeriasin A was docked into the C-pocket having an interaction of the phenyl-ring with Ile169 and showed good complementarity with the binding site. Whereas (*S*)-boehmeriasin A had no interactions with SIRT2, but showed also complementary binding (Figure 37). Based on the modelling there was no clear difference in the putative binding modes of the enantiomers.
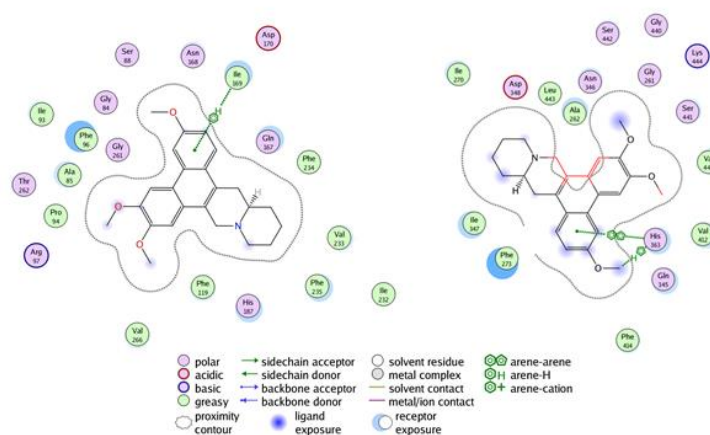
Figure 37: (*R*)-boehmeriasin A interacts with Ile169 in SIRT2. Boehmeriasin A doesn't orientate properly in the putative binding site of SIRT1.

4.5.Conclusion

In conclusion two efficient and innovative approaches were performed for the synthesis of both enantiomers as well as of racemic boehmeriasin A. Indeed biological assays confirmed the high anti-proliferative activity in three endothelial and two cancer cell lines of the two enantiomers. Thanks to biological assays, accompanied by virtual screening and docking studies, we could identify the interaction between with DNA and SIRT2 and boehmeriasin that presumably are the responsible for their biological activity. These results offer new suggestions for the design and practical synthesis of new topoisomerase and SIRT2 inhibitors based on the boehmeriasin A scaffold.

4.6. Experimental part

4.6.1. Synthesis

Racemic preparation of Boehmeriasin A

(*E*)-Methyl 2-(3,4-dimethoxyphenyl)-3-(4-methoxyphenyl) acrylate (11)
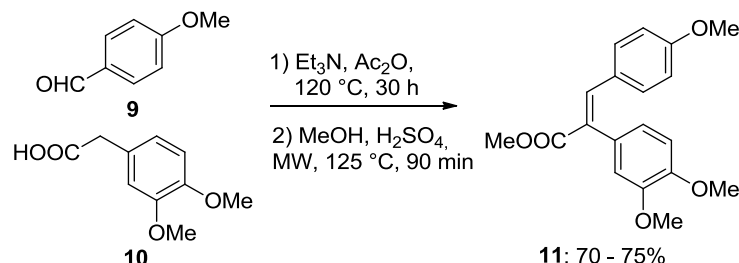
4-Methoxybenzaldehyde **9** (13.6 g, 100 mmol) and 3,4- dimethoxyphenylacetic acid **10** (19.6 g, 100 mmol) were dissolved in a mixture of triethylamine (10 mL) and acetic anhydride (20 mL) and heated at 120 °C for 30 hours. After the reaction mixture was cooled to room temperature, ethyl acetate (150 mL) was added leading to precipitation of a yellow solid. After filtration and drying this material was charged into 20 mL microwave vessels (~4 g each), filled with 7 mL methanol and 0.1 mL conc. sulphuric acid and sealed with the appropriate cap. Each of these samples was heated in a Biotage Microwave Synthesizer for 90 min at 125 °C. Upon cooling to room temperature the desired ester product precipitated as pale yellow solid and was isolated by filtration.

Yield (over 2 steps) 70 and 75%; mp 106.7 e 107.9 °C; ^{1}H NMR (400 MHz, CDCl$_3$): δ 7.77 (s, 1H), 7.02 (d, *J* = 8.8 Hz, 2H), 6.89 (d, *J* = 8.0 Hz, 1H), 6.78 (dd, *J* = 8.0, 1.6 Hz, 1H), 6.73 (d, *J* = 1.6 Hz, 1H), 6.69 (d, *J* = 8.8 Hz, 2H), 3.92 (s, 3H), 3.80 (s, 3H), 3.78 (s, 3H), 3.75 (s, 3H); ^{13}C NMR (100 MHz, CDCl$_3$,): δ 52.3, 55.2, 55.8, 55.9, 111.4, 112.8, 113.7, 122.1, 127.3, 128.6, 129.6, 132.4, 140.2, 148.6, 149.1, 160.3, 168.7; MS: m/z 351.8 [M+Na]$^+$; HR-MS: calculated for C$_{19}$H$_{21}$O$_5$: 329.1389, found 329.1393.

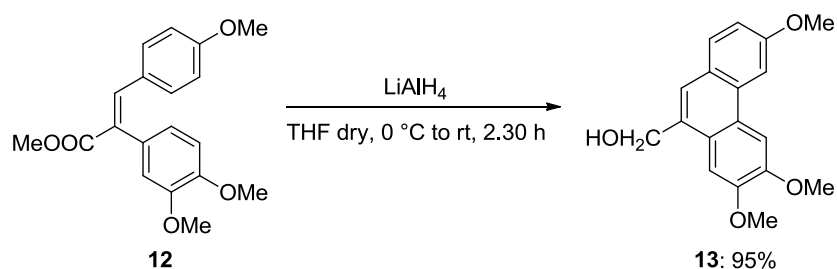**Methyl-3,6,7-trimethoxyphenanthrene-9-carboxylate (12)**
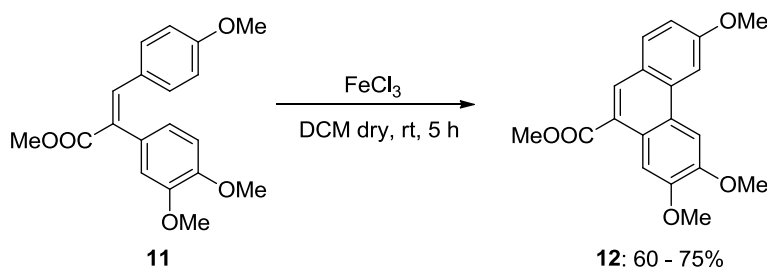
(*E*)-Methyl 2-(3,4-dimethoxyphenyl)-3-(4-methoxyphenyl) acrylate (**11**) (4 g, 12.2 mmol) was dissolved in DCM (40 mL) at room temperature. To this solution anhydrous FeCl$_3$ (5 g, 31 mmol) was added portion-wise. The resulting reaction mixture was stirred at room temperature for 3

hours after which more anhydrous FeCl$_3$ (1 g, 6 mmol) was added. After a total reaction time of 5 h, complete consumption of substrate was achieved (monitored by ^{1}H NMR). Methanol (~30 mL) was added to this crude mixture resulting in a homogeneous red-brownish solution, which was subsequently extracted with DCM/water giving the desired phenanthrene product as dark brown foam after evaporation of the solvents. Filtration of the dried organic layer over a plug of silica gel (10 g), prior to solvent removal, yields the desired product as light brown foam.

Yield commonly varied from 60 to 75% (>90% purity). ^{1}H NMR (400 MHz, CDCl$_3$): δ 8.64 (s, 1H), 8.43 (s, 1H), 7.85 (s, 1H), 7.84 (d, J = 8.8 Hz, 1H), 7.79 (d, J = 2.4 Hz, 1H), 7.20 (dd, J = 8.8, 2.4 Hz, 1H), 4.10 (s, 3H), 4.08 (s, 3H), 4.02 (s, 3H), 4.01 (s, 3H) ppm; ^{13}C NMR (100 MHz, CDCl$_3$): δ 52.0, 55.5, 55.8, 55.9, 103.2, 103.7, 106.9, 116.0, 121.6, 124.2, 125.0, 125.2, 131.3, 131.8, 133.4, 148.9, 149.9, 160.2, 168.2 ppm; MS: m/z 327 [M]$^+$; HR-MS: calculated for C$_{19}$H$_{19}$O$_5$: 327.1232, found 327.1240.

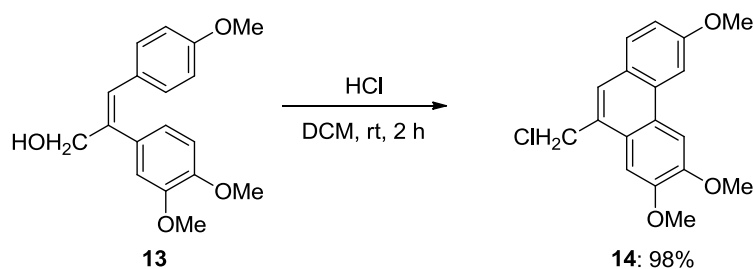**(3,6,7)-Trimethoxyphenanthren-9-yl)-methanol (13)**

12   **13**: 95%

Methyl 3,6,7-trimethoxyphenanthrene-9-carboxylate (**12**) (3.26 g, 10.0 mmol) was dissolved in THF (20 mL) and cooled to 0 °C. To this vigorously stirred solution, LiAlH$_4$ (880 mg, 25 mmol) was added in small portions over a period of 10 min. After 30 min the ice bath was removed allowing the reaction mixture to warm to room temperature where it was maintained for 2 h. Upon quenching of the reaction mixture with sat. NH$_4$Cl (2 mL) a greyish slurry was obtained which was filtered over a plug of silica (eluent DCM). The desired reduction product was obtained after removal of the volatiles as a pale yellow amorphous solid.

Yield 95%. ^{1}H NMR (700 MHz, CDCl$_3$): δ 7.79 (s, 1H), 7.73 (d, J = 2.1 Hz, 1H), 7.69 (d, J = 9.1 Hz, 1H), 7.51 (s, 1H), 7.45 (s, 1H), 7.15 (dd, J = 9.1, 1.2 Hz, 1H), 5.01 (s, 2H), 4.06 (s, 3H), 4.01 (s, 3H), 3.99 (s, 3H,), 1.92 (br. s, 1H) ppm; ^{13}C NMR (175 MHz, CDCl$_3$): δ 55.5, 55.8, 55.9, 64.6, 103.7, 103.9, 104.8, 115.4, 124.4, 124.8, 125.5, 125.7, 130.1, 131.1, 131.3, 148.7, 149.3, 158.3 ppm; MS: m/z 281.0 [MOH]$^+$; HR-MS: calculated for C$_{18}$H$_{17}$O$_3$ (MOH) 281.1178, found 281.1186.
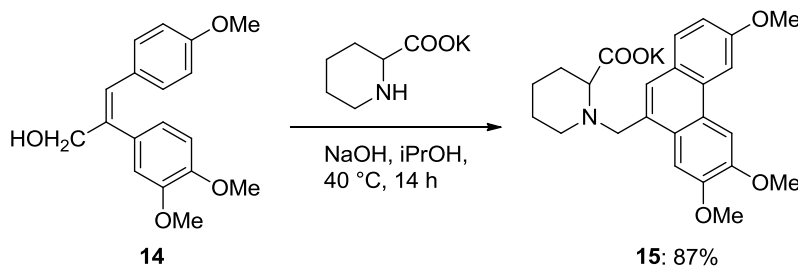
10-(Chloromethyl)-2,3,6-trimethoxyphenanthrene (14)

13   HCl, DCM, rt, 2 h   **14**: 98%

To a vigorously stirred solution of (3,6,7)-trimethoxyphenanthren-9-yl-methanol (**13**) (3.0 g, 10 mmol, in DCM) was added conc. HCl (37%, 5 mL) changing the colour of the initial pale yellow solution to dark brown. After 2 h at room temperature the reaction is directly extracted (DCM/H_2O) giving the title compound **14** as brown solid after removal of the solvent.

Yield 98%. ^{1}H NMR (400 MHz, CDCl$_3$): δ 7.76 (s, 1H), 7.70 (d, J = 2.4 Hz, 1H), 7.66 (d, J = 8.4 Hz, 1H), 7.51 (s, 1H), 7.40 (s, 1H), 7.14 (dd, J = 8.4, 2.4 Hz, 1H), 4.92 (s, 2H), 4.05 (s, 3H), 4.04 (s, 3H), 3.96 (s, 3H) ppm; ^{13}C NMR (, 100 MHz, CDCl$_3$): δ 46.1, 55.5, 55.9, 55.9, 103.8, 104.7, 115.6, 125.0, 125.1, 125.2, 126.8, 127.9, 127.9, 130.4, 131.7, 148.9, 149.4, 158.8 ppm; MS: m/z 316.1 [radical cation]; HR-MS: calculated for $C_{18}H_{18}O_3Cl$ 317.0944, found 317.0931.

Potassium 1-[(3,6,7-trimethoxyphenanthren-9-yl)methyl] piperidine-2-carboxylate (15)

14   NaOH, iPrOH, 40 °C, 14 h   **15**: 87%

A suspension containing rac-pipecolic acid (750 mg, 5.8 mmol) and potassium hydroxide (1.0 g, 17.9 mmol) in isopropanol (6 mL) was stirred at room temperature for 30 minutes. To this mixture 10-(chloromethyl)-2,3,6- trimethoxyphenanthrene (**14**) (1.6 g, 5 mmol) was added portionwise over 30 min generating a light brown slurry. The mixture was stirred at 40 °C for 14 hours before cooling to rt. Filtration and washing of this crude material, with a minimal amount of cold isopropanol (3 mL), yielded the title compound **15** as light brown solid which was used in the subsequent step without further purification.

Yield 87%. ^{1}H NMR (700 MHz, d[6]-DMSO): δ 8.81 (s, 1H), 7.94 (br s, 2H), 7.73 (d, J = 8.4 Hz, 1H), 7.39 (s, 1H), 7.11 (dd, J = 8.4, 2.8 Hz, 1H), 4.58 (d, J = 12.6 Hz, 1H), 3.97 (s, 3H), 3.96 (s, 3H), 3.92 (s, 3H), 3.03 (d, J = 12.6 Hz, 1H), 2.54 (m, 1H), 2.49 (m, 1H), 1.68-1.73 (m, 2H), 1.50-1.58 (m, 2H), 1.25-1.30 (m, 1H), 1.10-1.18 (m, 2H) ppm; ^{13}C NMR (175 MHz, d[6]-DMSO): δ 24.6, 25.9, 30.9, 51.4,

55.9, 56.1, 56.7, 60.5, 71.8, 103.8, 104.2, 109.6, 115.9, 124.5, 125.5, 126.0, 127.8, 130.0, 131.0, 131.3, 149.0, 149.2, 158.1, 177.7 ppm.

3,6,7-Trimethoxy-12,13,14,14a-tetrahydro-9H-dibenzo[f,h]pyrido[1,2-b]isoquinolin-15(11H)-one (16)
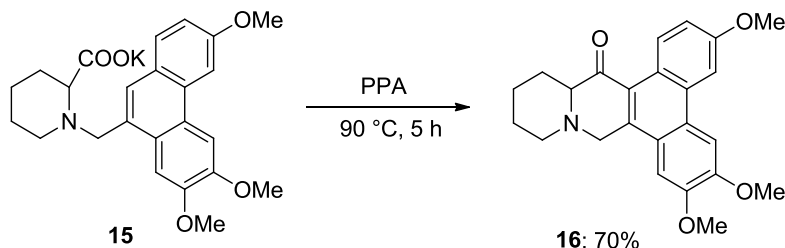
Potassium 1-((3,6,7-trimethoxyphenanthren-9-yl)methyl) piperidine-2-carboxylate (**15**) (900 mg, 2.0 mmol) was added to polyphosphoric acid (~3 g) and stirred at 90 °C for 5 h. Within 30 min, a thick black solution was obtained which was maintained at this temperature until full conversion of the substrate (monitored by LC-MS). The reaction mixture was then cooled to room temperature and carefully quenched by addition of methanol (the temperature cannot rise above 40°C). The resulting solution was then neutralized by careful addition of a saturated solution of potassium carbonate. Extractive work-up of this material with DCM/H_2O gave a crude product which was purified by column chromatography (15% EtOAc/Hex) providing the title compound **16** as a pale yellow solid.

Yield 70%. ^{1}H NMR (700 MHz, CDCl$_3$): δ 9.26 (d, J = 9.8 Hz, 1H), 7.24 (s, 1H), 7.72 (d, J = 1.4 Hz, 1H), 7.22 (1H, dd, J = 9.8, 1.4 Hz), 7.11 (s, 1H), 4.36 (d, J = 15.4 Hz, 1H), 4.07 (s, 3H), 4.01 (s, 3H), 3.97 (s, 3H), 3.65 (d, J = 15.4 Hz, 1H), 3.19 (d, J = 10.5 Hz, 1H), 2.77 (d, J = 10.5 Hz, 1H), 2.47 (d, J = 13.3 Hz, 1H), 2.40 (t, J = 13.3 Hz, 1H), 1.96 (d, J = 13.3 Hz, 1H), 1.70-1.77 (m, 1H), 1.66 (tq, J = 13.3, 2.8 Hz, 1H), 1.60 (q, J = 13.3 Hz, 1H), 1.45 (tq, J = 13.3, 2.8 Hz, 1H) ppm; ^{13}C NMR (175 MHz, CDCl$_3$): δ 23.9, 24.9, 27.4, 54.8, 55.3, 55.8, 55.9, 56.0, 68.9, 103.7, 104.3, 115.6, 122.7, 123.0, 123.1, 127.3, 129.3, 130.9, 139.3, 149.5, 151.0, 157.8, 197.3 ppm; MS: m/z 392.0 [M]$^+$; HR-MS: calculated for C$_{24}$H$_{26}$O$_4$N 392.1861, found 392.1855.

3,6,7-Trimethoxy-11,12,13,14,14a,15-hexahydro-9H-dibenzo-[f,h]pyrido[1,2-b]isoquinoline (Rac-7)
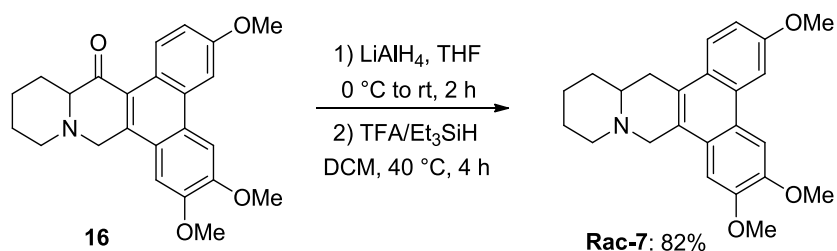
To a solution of **16** (391 mg, 1.0 mmol) in THF (5 mL, cooled to 0 °C), LiAlH₄ (100 mg, 2.6 mmol) was added portionwise. After 10 min the mixture was allowed to warm to room temperature where it was stirred for 2 hours, prior to careful quenching by addition of aqueous NH₄Cl solution. After aqueous extraction with DCM the combined organic layers were dried over anhydrous Na₂SO₄ and evaporated under reduced pressure to give the intermediate aminoalcohol product as yellow oil which was not purified further. This crude material was redissolved in DCM (2 mL) and combined with TFA (0.3 mL) and Et₃SiH (0.3 mL). After stirring for 4 h at 40 °C the reaction had reached completion (monitored by LC-MS) and was quenched by addition of aqueous NaHCO₃ solution. The crude product was isolated after aqueous extraction as yellow foam. Final purification was accomplished by flash column chromatography furnishing racemic boehmeriasin A (**Rac-7**) as solid after evaporation of the solvents.

Yield: 82%. IR (neat): ν 2931.1, 1610.4, 1511.5, 1467.9, 1253.9, 1201.9, 1138.6, 1038.7 cm⁻¹. MS: m/z 377.9 (M⁺); HR-MS: calculated for C₂₄H₂₈O₃N 378.2069, found 378.2055.

HPLC conditions: (AD 5 cm, EtOH: Hexane 1:9, 1 ml/min, 22 °C) can be used in order to achieve resolution of racemic boehmeriasin A.

Enantioselective synthesis of Boehmeriasin A

1-(4-Methoxyphenyl)-2-(1-*tert*-butoxycarbonylpiperidin-2-yl)ethanol (17)

17a,b: 90-92%
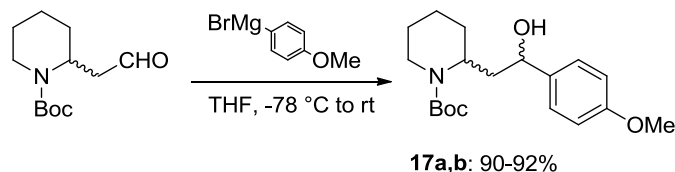
To a solution of aldehyde (0.34 g, 1.5 mmol) in THF (13 mL) at 78 °C, (4-methoxyphenyl)magnesium bromide (6 mL, 3 mmol) was added, and the new solution was stirred for 10 min at 78 °C and then overnight at room temperature. After the completion of the reaction, the solvent was evaporated in vacuum, sat. NH₄Cl was added and the aqueous layer was extracted 3 times with EtOAc. The combined organic layers were washed with water and brine, dried with Na₂SO₄, filtered and evaporated. The residue was purified by flash column chromatography (Hex/EtOAc 7:3) to provide the two diastereomer alcohols **17** as oils.

<u>**17a** (*R*-COH) and **17b** (*S*-COH)</u>

Yields 92e95%; **17a** (*R*-COH): [α]_D = + 35.9 (*c* 0.90 in CHCl₃), **17b** (*S*-COH): [α]_D = - 36.6 (*c* 0.92 in CHCl₃); ¹H NMR (400 MHz, CDCl₃): δ 7.32 (d, *J* = 8.4 Hz, 2H), 6.90 (d, *J* = 8.4 Hz, 2H), 4.61 (m, 1H), 4.41 (m, 1H), 4.04 (m, 1H), 3.82 (s, 3H), 2.80 (t, *J* = 11.6 Hz, 1H), 2.20 (td, *J* = 14.0, 2.0 Hz, 1H), 1.78-1.47 (m, 8H), 1.52 (s, 9H) ppm; ¹³C NMR (100 MHz, CDCl₃): δ 19.9, 26.2, 29.1, 29.9, 40.2, 40.9,

47.4, 56.0, 70.2, 81.1, 114.4, 127.5, 136.9, 155.6, 159.0 ppm; HR-MS: calculated for $C_{19}H_{30}NO_4$ 336.2175, found **17a**: 336.2156; HR-MS found **17b**: 336.2179.

17a (*S*-COH) and **17b** (*R*-COH)

Yields 92e95 %; **17a** (*S*-COH): $[\alpha]_D$ = + 71.9 (*c* 1.06 in CHCl$_3$), **17b** (*R*-COH): $[\alpha]_D$ = - 73.3 (*c* 0.98 in CHCl$_3$); ^{1}H NMR (400 MHz, CDCl$_3$): δ 7.32 (d, *J* = 8.4 Hz, 2H), 6.89 (d, *J* = 8.4 Hz, 2H), 4.71 (m, 1H), 4.38 (m, 1H), 3.94 (m, 1H), 3.82 (s, 3H), 2.82 (td, *J* = 13.2, 1.6 Hz, 1H), 2.12 (dt, *J* = 14.4 Hz J ¼ 6.8 Hz, 1H), 1.85 (dt, *J* = 14.4, 5.6 Hz, 1H), 1.62-1.51 (m, 6H), 1.48 (s, 9H), 1.43-1.40 (m, 1H) ppm; ^{13}C NMR (100 MHz, CDCl$_3$): δ 19.8, 26.0, 29.2, 30.4, 40.2, 40.9, 49.3, 56.0, 73.0, 80.4, 114.4, 127.7, 137.6, 156.2, 159.6 ppm; HR-MS: found **17a** 336.2160, HR-MS: found **17b** 336.2158.

1-(4-Methoxyphenyl)-2-(1-*tert*-butoxycarbonylpiperidin-2- yl)ethanone (18)

17 **18a,b**: 83%
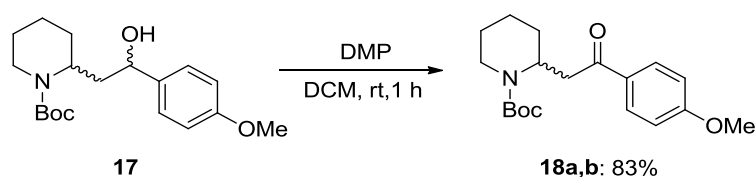
To a solution of alcohol **17** (0.22 g, 0.65 mmol) in DCM (8.4 mL), Dess-Martin periodinane (0.34 g, 0.78 mmol) was added and the new mixture was stirred for 1 h at room temperature. After the completion of the reaction, the solvent was evaporated in vacuum, 10% K$_2$CO$_3$ was added and the aqueous layer was extracted 3 times with EtOAc. The combined organic layers were washed with water and brine, dried with Na$_2$SO$_4$, filtered and evaporated. The residue was purified by flash column chromatography (Hex/EtOAc 7:3) to provide ketone **18** as oil.

Yield 83%; **18a**: $[\alpha]_D$ = - 34.2 (*c* 0.95 in CHCl$_3$), **18b**: $[\alpha]_D$ = +35.6 (*c* 1.00 in CHCl$_3$); ^{1}H NMR (400 MHz, CDCl$_3$): δ 8.00 (d, *J* = 8.8 Hz, 2H), 6.96 (d, *J* = 8.8 Hz, 2H), 4.82 (m, 1H), 4.05 (m, 1H), 3.89 (s, 3H), 3.18 (dd, *J* = 14.0, 6.4 Hz, 1H), 3.12 (dd, *J* = 14.0, 6.4 Hz, 1H), 2.90 (td, *J* = 13.0, 2.3 Hz, 1H), 1.64 (m, 5H), 1.41 (s, 10H) ppm; ^{13}C NMR (100 MHz, CDCl$_3$): δ 18.9, 25.3, 28.1, 28.4, 39.0, 39.4, 48.4, 55.5, 79.6, 113.8, 130.1, 130.6, 154.8, 163.6, 197.0 ppm; HR-MS: calculated for $C_{19}H_{28}NO_4$ 334.2018, found **18a** 334.2009; HR-MS: found **18b** 334.2006.

1-(4-Methoxyphenyl)-2-(piperidin-2-yl)ethanone hydrochloride (19)

18a,b **19a,b**: 95%
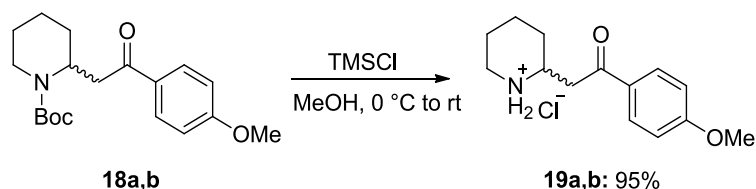
To a cooled solution at 0 °C of ketone **18** (0.31 g, 0.94 mmol) in MeOH (7.5 mL), TMSCl (0.59 mL, 5.7 mmol) was added and the solution was stirred overnight at room temperature. After the completion of the reaction, the solvent was evaporated in vacuum, to provide ketone **19** as oil.

Yield 95%; **19a**: $[\alpha]_D$ = +17.5 (*c* 1.14 in CHCl$_3$); **19b**: $[\alpha]_D$ = - 18.5 (*c* 1.25 in CHCl$_3$); ^{1}H NMR (400 MHz, CDCl$_3$): δ 9.73 (s, 1H), 9.30 (s, 1H), 7.92 (d, *J* = 8.0 Hz, 2H), 6.86 (d, *J* = 8.0 Hz, 2H), 3.84 (s, 3H), 3.78e3.72 (m, 1H), 3.70e3.64 (m, 1H), 3.55e3.47 (m, 2H), 2.97e2.91 (m, 1H), 2.00e1.80 (m, 5H), 1.58e1.50 (m, 1H) ppm; ^{13}C NMR (100 MHz, CDCl$_3$): δ 22.8, 23.1, 29.1, 41.6, 45.8, 54.7, 56.2, 114.6, 129.7, 131.4, 164.7, 195.7 ppm.

2-(2-Bromo-4,5-dimethoxyphenyl)-1-(2-(2-(4-methoxyphenyl)-2-oxoethyl)piperidin-1-yl)ethanone (21)
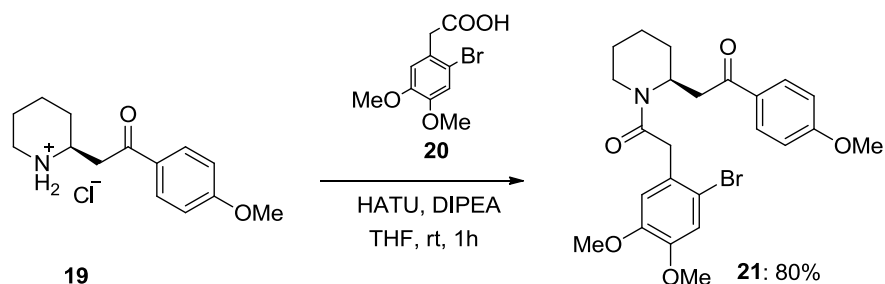
To a solution of 2-bromo-4,5-dimethoxyphenylacetic acid **20** (0.25 g, 0.90 mmol) in THF (23 mL), HATU (0.39 g, 0.99 mmol) and DIPEA (0.31 mL, 1.8 mmol) were added and the new mixture was stirred for 30 min at rt. Then, the solution was cooled at 0 °C and a solution of compound **19** (0.24 g, 0.90 mmol) in THF (12 mL) and DIPEA (200 mL) was added and the new solution was stirred for 1 h at rt. After the completion of the reaction, the solvent was evaporated in vacuum, sat. NH$_4$Cl was added and the aqueous layer was extracted 3 times with DCM. The combined organic layers were washed with water and brine, dried with Na$_2$SO$_4$, filtered and evaporated. The residue was purified by flash column chromatography (Hex/EtOAc 3:7) to provide compound **21** as oil.

Yield 80%; **21a**: $[\alpha]_D$ = - 1.2 (c 0.82 in CHCl$_3$); **21b**: $[\alpha]_D$ = + 1.3 (c 0.86 in CHCl$_3$); ^{1}H NMR (400 MHz, CDCl$_3$, amide rotamers 1:1): rotamer a δ 8.05 (d, *J* = 8.8 Hz, 2H), 7.03 (s, 1H), 6.97 (d, *J* = 8.8 Hz, 2H), 6.83 (s, 1H), 5.33-5.28 (m, 1H), 4.00 (d, *J* = 16.0 Hz, 1H), 3.90 (s, 3H), 3.87 (s, 3H), 3.85 (s, 3H), 3.78-3.72 (m, 2H), 3.26 (, d, *J* = 6.8 Hz, 2H), 3.23-3.20 (m, 1H), 1.78-1.56 (m, 5H), 1.46-1.30 (m, 1H) ppm; rotamer b δ 7.93 (d, *J* = 8.8 Hz, 2H), 6.96 (s, 1H), 6.95 (d, *J* = 8.8 Hz, 2H), 6.83 (s, 1H), 4.78-4.74 (m, 1H), 4.67-4.64 (m, 1H), 3.87 (s, 3H), 3.85 (s, 3H), 3.81 (s, 3H), 3.78-3.72 (m, 2H), 3.18-3.09 (m, 2H), 2.70 (td, *J* = 13.0, 2.4 Hz, 1H), 1.78-1.56 (m, 5H), 1.46-1.30 (m, 1H) ppm; ^{13}C NMR (100 MHz, CDCl$_3$): rotamer a δ 20.0, 26.3, 30.0, 39.6, 41.5, 42.7, 47.4, 56.2, 56.7, 114.0, 115.3, 116.0, 128.1, 130.5, 131.5, 149.0, 149.2, 164.5, 170.4, 197.5 ppm; rotamer b δ 19.3, 26.2, 27.9, 38.3, 39.2, 41.1, 50.4, 56.7, 113.5, 114.6, 115.0, 116.0, 127.7, 130.3, 131.0, 149.0, 149.2, 164.3, 170.1, 196.4 ppm; HR-MS: calculated for C$_{24}$H$_{29}$BrNO$_5$ 490.1229, found **21a** 490.1215, HR-MS: found **21b** 490.1210.

3-(2-Bromo-4,5-dimethoxyphenyl)-2-(4-methoxyphenyl)-1,6,7,8,9,9a-hexahydroquinolizin-4-one (22)
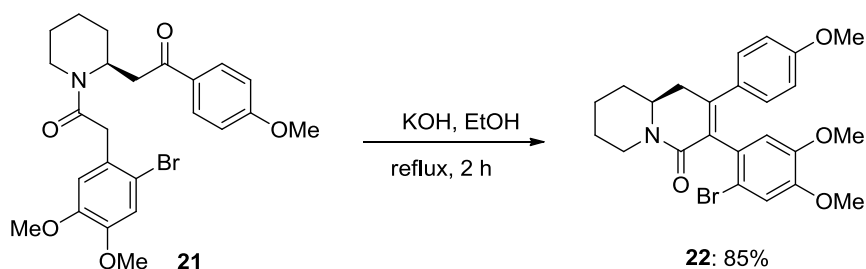

A solution of compound **21** (0.37 g, 0.76 mmol) in 5% ethanolic KOH (15.8 mL) was refluxed for 2 hours. After the completion of the reaction, the solvent was evaporated in vacuum, sat. NH_4Cl was added and the aqueous layer was extracted 3 times with DCM. The combined organic layers were washed with water and brine, dried with Na_2SO_4, filtered and evaporated. The residue was purified by flash column chromatography (Hex/EtOAc 4:6) to provide atropisomer compounds **22** as oils.

Yield 85%; **22a (mode 1):** $[\alpha]_D$ = + 57.6 (*c* 0.89 in CHCl$_3$); **22b (mode 1):** $[\alpha]_D$ = - 58.4 (*c* 0.62 in CHCl$_3$); ^{1}H NMR (400 MHz, CDCl$_3$): δ 7.01 (d, *J* = 8.4 Hz, 2H), 7.00 (s, 1H), 6.70 (d, *J* = 8.4 Hz, 2H), 6.46 (s, 1H), 4.56 (br d, *J* = 13.6 Hz, 1H), 3.86 (s, 3H), 3.76 (s, 3H), 3.68 (m, 1H), 3.65 (s, 3H), 2.86-2.69 (m, 3H), 1.95-1.84 (m, 3H), 1.58-1.44 (m, 3H) ppm; ^{13}C NMR (100 MHz, CDCl$_3$): δ 23.9, 25.4, 34.1, 38.3, 43.5, 54.1, 55.8, 56.6, 56.7, 114.0, 115.5, 115.6, 116.1, 129.6, 131.2, 131.3, 132.2, 146.3, 148.7, 149.3, 159.8, 166.8 ppm; ESI-MS 392: [M-Br]; HR-MS: calculated for $C_{24}H_{27}BrNO_4$ 472.1123, found **22a** 472.1110, HR-MS: found **22b** 472.1109.

22a (mode 2): $[\alpha]_D$ = - 39.2 (*c* 1.09 in CHCl$_3$); **22b (mode 2):** $[\alpha]_D$ = + 40.4 (*c* 1.10 in CHCl$_3$); ^{1}H NMR (400 MHz, CDCl$_3$): δ 7.04 (d, *J* = 8.8 Hz, 2H), 6.99 (s, 1H), 6.71 (d, *J* = 8.8 Hz, 2H), 6.50 (s, 1H), 4.62 (br d, *J* = 13.6 Hz, 1H), 3.85 (s, 3H), 3.76 (s, 3H), 3.70 (s, 3H), 3.67-3.60 (m, 1H), 3.09 (dd, *J* = 17.2, 6.4 Hz, 1H), 2.69-2.63 (m, 2H), 1.97-1.92 (m, 1H), 1.89-1.82 (m, 1H), 1.76-1.73 (m, 2H), 1.70-1.59 (m, 2H) ppm, ^{13}C NMR (100 MHz, CDCl$_3$): δ 24.4, 25.1, 32.5, 36.1, 44.6, 53.5, 55.2, 55.9, 56.1, 113.4, 115.0, 115.2, 115.8, 128.9, 130.4, 130.5, 131.9, 145.7, 148.0, 148.6, 159.2, 166.1 ppm; HR-MS: found **22a** 472.1113, HR-MS: found **22b** 472.1111.

3,6,7-Trimethoxy-11,12,13,14,14a,15-hexahydro-9H-phenanthro[9,10-b]quinolizin-9-one (23)

22 → **23**: 60%

Pd(OAc)$_2$,
K$_2$CO$_3$,
PhDavePhos

DMA, reflux, 5 h
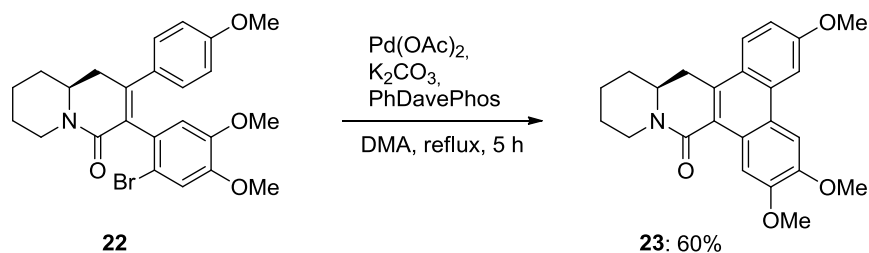
To a solution of compound **22** (0.12 g, 0.24 mmol) in DMA (5.3 mL), Pd(OAc)$_2$ (13 mg, 0.058 mmol), 2'-(diphenylphosphino)-N,N' -dimethyl-(1,1'-biphenyl)-2-amine (28 mg, 0.072 mmol) and K$_2$CO$_3$ (0.066 g, 0.48 mmol) were added and the new mixture was heated at 125 C for 5 h. After the completion of the reaction, H$_2$O was added and the aqueous layer was extracted 3 times with EtOAc. The combined organic layers were washed with water and brine, dried with Na$_2$SO$_4$, filtered and evaporated. The residue was purified by flash column chromatography (Hex/EtOAc 4:6) to provide compound **17** as oil.

Yield 60%; **23a**: $[\alpha]_D$ = - 108.4 (c 0.44 in CHCl$_3$), **23b:** $[\alpha]_D$ = +110.2 (c 0.65 in CHCl$_3$); ^{1}H NMR (CDCl$_3$, 400 MHz): δ 9.41 (s, 1H), 8.01 (d, J = 8.8 Hz, 1H), 7.88 (d, J = 3.2 Hz, 1H), 7.87 (s, 1H), 7.23 (dd, J = 9.2, 2.4 Hz, 1H), 4.74 (br d, J = 11.6 Hz, 1H), 4.12 (s, 6H), 4.05 (s, 3H), 3.64-3.56 (m, 1H), 3.52 (dd, J = 16.4, 4.8 Hz, 1H), 3.05 (dd, J = 16.0, 5.2 Hz, 1H), 2.90 (td, J = 13.2, 3.2 Hz, 1H), 2.01 (br d, J = 10.0 Hz, 1H), 1.93-1.91 (m, 2H), 1.67-1.48 (m, 3H) ppm, ^{13}C NMR (100 MHz, CDCl$_3$): δ 23.6, 25.4, 33.4, 36.6, 43.5, 53.5, 56.2, 56.5, 56.6, 103.7, 105.1, 109.5, 116.1, 120.3, 123.4, 125.2, 126.4, 127.2, 134.0, 135.1, 149.0, 150.2, 160.2, 168.2 ppm; EI-MS: 391 [M]. HR-MS calculated for C$_{24}$H$_{26}$NO$_4$ 392.1861, found **23a** 392.1850; HR-MS: found **23b** 392.1847.

3,6,7-Trimethoxy-11,12,13,14,14a,15-hexahydro-9H-dibenzo[f,h]pyrido[1,2-b]isoquinoline, boehmeriasin A [7a and 7b]

23 → **7a,b**: 80%

LiAlH$_4$

THF, reflux, 2 h
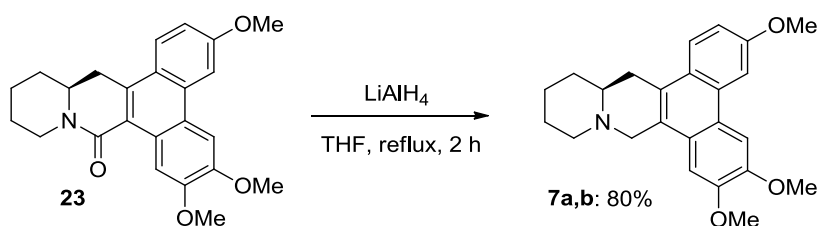
To a cooled at 0 °C suspension of LiAlH$_4$ (0.020 g, 0.49 mmol) in THF (5 mL), a solution of compound **23** (48 mg, 0.12 mmol) in THF (2.5 mL) was added dropwise and the new mixture was refluxed for 2 h. After the completion of the reaction, the reaction mixture was cooled at 0 °C, and carefully quenched by addition of 10% NaOH aqueous solution and after the THF was evaporated in vacuum. Then, the aqueous layer was extracted 3 times with EtOAc. The combined organic layers were washed with water and brine, dried with Na$_2$SO$_4$, filtered and evaporated. The residue

was purified by flash column chromatography (DCM/MeOH 9.6:0.4) to provide boehmeriasin A (**7**) as solid.

Yield 80%; **7a**: $[\alpha]_D$ = - 79.2 (*c* 0.12 in MeOH), **7b**: $[\alpha]_D$ = + 80.6 (*c* 0.10 in MeOH), ^{1}H NMR (400 MHz, CDCl$_3$): δ 7.92-7.90 (m, 3H), 7.22 (dd, *J* = 8.8, 2.4 Hz, 1H), 7.14 (s, 1H), 4.64 (d, *J* = 15.2 Hz, 1H), 4.12 (s, 3H), 4.07 (s, 3H), 4.03 (s, 3H), 3.58 (d, *J* = 15.2 Hz, 1H), 3.30 (d, *J* = 11.2 Hz, 1H), 3.18 (dd, *J* = 16.4, 2.8 Hz, 1H), 2.94 (dd, *J* = 16.4, 6.0 Hz, 1H), 2.41-2.29 (m, 2H), 2.03 (d, *J* = 13.2 Hz, 1H), 1.92-1.78 (m, 3H), 1.56-1.45 (m, 2H) ppm; ^{13}C NMR (100 MHz, CDCl$_3$): δ 25.1, 26.7, 34.4, 35.3, 56.2, 56.7, 56.8, 57.1, 58.2, 103.8, 104.7, 105.3, 115.4, 123.9, 124.9, 125.7, 125.9, 126.6, 130.9, 148.9, 150.1, 158.2 ppm; HR-MS: calculated for $C_{24}H_{28}O_3N$ 378.2069, found **7a** 378.2057; Anal. Calcd for $C_{24}H_{27}NO_3$: C, 76.36; H, 7.21; N, 3.71; Found **7a**: C, 75.58; H, 7.02; N, 3.56; HR-MS: found **7b** 378.2058; Found **7b**: C, 75.53; H, 7.04; N, 3.53.

4.6.2. Virtual screening

(*R*)-And (*S*)-boehmeriasin A were used as input structures for Hurakan running the jobs on default parameters.

4.6.3. Biological assay

Cell proliferation

- **Endothelial cells.** Bovine aortic endothelial cells (BAEC) and human dermal microvascular endothelial cells (HMEC-1) were seeded in 48-well plates at 10,000 cells/well and 20,000 cells/well, respectively. After 24 h, 5-fold dilutions of the compounds were added. The cells were allowed to proliferate 3 days (or 4 days for HMEC-1) in the presence of the compounds, trypsinized, and counted by means of a Coulter counter (Analis, Belgium).

- **Tumour cells.** Human cervical carcinoma (HeLa) cells were seeded in 96- well plates at 15,000 cells/well in the presence of different concentrations of the compounds. After 4 days of incubation, the cells were trypsinized and counted in a Coulter counter. Suspension cells (Mouse leukaemia L1210 and human lymphoid Cem cells) were seeded in 96-well plates at 60,000 cells/well in the presence of different concentrations of the compounds. L1210 and Cem cells were allowed to proliferate for 48 h or 96 h, respectively and then counted in a Coulter counter. The 50% inhibitory concentration (IC$_{50}$) was defined as the compound concentration required to reduce cell proliferation by 50%. Combretastatin A-4 phosphate was added as reference compound.

Analysis of *in vitro* sirtuin inhibition - SIRT1 and SIRT2 *in Vitro* Assay. The compounds were studied using the Fluor de Lys fluorescence assays which are described in the BioMol product sheet (Enzo Life Sciences). In assays the BioMol KI177 substrate was used for SIRT1 and the KI179 substrate for SIRT2. The determined Km value of SIRT1 for KI177 was 58 μM and the Km of SIRT2

for KI179 was 198 μM.[89] The Km values of SIRT1 and SIRT2 were 558 μM and 547 μM for NAD+ reported by BioMol, respectively. Briefly, assays were carried out using the Fluor de Lys acetylated peptide substrate at 0.7 Km and NAD+ (Sigma N6522 or BioMol KI282) at 0.9 Km, recombinant GST-SIRT1/2-enzyme and SIRT assay buffer (KI286). GST-SIRT1 and GST-SIRT2 were produced as described previously.[90] The buffer together with Fluor de Lys acetylated peptide substrate, NAD+ and DMSO/compounds in DMSO (2.5 mL in 50 mL total reaction volume; DMSO from Sigma, D2650) were preincubated for 5 min at room temperature. Then enzyme was added to start the reaction. The reaction mixture was incubated for 1 h at 37 °C and after that, Fluor de Lys developer (KI176) and 2 μM nicotinamide (KI283) in SIRT assay buffer (total volume 50 mL) were added. The incubation was continued for 45 min at 37 °C. Finally, fluorescence readings were obtained using EnVision 2104 Multilabel Reader (PerkinElmer) with excitation wavelength 370 nm and emission 460 nm. The Fluor de Lys fluorescence assays of sirtuins are regularly performed with compounds from our own collections to calibrate data between assay runs.

Topoisomerase-mediated DNA relaxation: Supercoiled pBR322 plasmid DNA (0.25 mg, Fermentas Life Sciences) was incubated with 1U topoisomerase II (human recombinant topoisomerase II a, USB Corporation) or 2U topoisomerase I (human recombinant topoisomerase I, TopoGen) and the test compounds as indicated, for 60 min at 37 °C in 20 μL reaction buffer. Reactions were stopped by adding 4 mL stop buffer (5% sodium dodecyl sulphate (SDS), 0.125% bromophenol blue, and 25% glycerol), 50 mg/mL proteinase K (Sigma) and incubating for a further 30 min at 37 °C. The samples were separated by electrophoresis on a 1% agarose gel at room temperature. The gels were stained with ethidium bromide 1 mg/mL in TAE buffer (0.04 M Triseacetate and 0.001 M EDTA), transilluminated by UV light, and fluorescence emission was visualized by a CCD camera coupled to a Bio-Rad Gel Doc XR apparatus.

Topoisomerase II-mediated DNA cleavage: Reaction mixtures (20 μL) containing 10 mM TriseHCl (pH = 7.9), 50 mM NaCl, 50 mM KCl, 5 mM $MgCl_2$, 0.1 mM EDTA, 15 μg/mL bovine serum albumin, 1 mM ATP, 0.25 μg pBR322 plasmid DNA (Fermentas Life Sciences), 10 U topoisomerase II (human recombinant topoisomerase II a, USB Corporation) and test compounds were incubated for 60 min at 37 °C. Reactions were stopped by adding 4 μL stop buffer (5% SDS, 0.125% bromophenol blue and 25% glycerol), 50 μg/mL proteinase K (Sigma) and incubating for a further 30 min at 37 °C. The samples were separated by electrophoresis on a 1% agarose gel containing ethidium bromide 0.5 μg/mL at room temperature in TBE buffer (0.09 M Triseborate and 0.002 M EDTA),

[89] P. H. Kiviranta; T. Suuronen; E. A. A. Wallen; J. Leppanen; T. H. Nyronen; T. Jarvinen; A. Poso; *J. Med. Chem.*, **2004**, *47*, 6292.

[90] P. H. Kiviranta; J. Leppanen; V. M. Rinne; T. Suuronen; O. Kyrylenko; S. Kyrylenko; E. Kuusisto; A. J. Tervo; t. Jarvinen; A. Salminen; A. Poso; E. A. A. Wallen; *Bioorg. Med. Chem. Lett.*, **2007**, *17*, 2448.

transilluminated by UV light, and fluorescence emission was visualized by a CCD camera coupled to a Bio-Rad Gel Doc XR apparatus.

Topoisomerase I-mediated DNA cleavage: Reaction mixtures (20 μL) containing 35 mM Tris-HCl (pH = 8.0), 72 mM KCl, 5 mM MgCl$_2$, 5 mM DTT, 5 mM spermidine, 0.01% bovine serum albumin, 20 ng pBR322 plasmid DNA (Fermentas Life Sciences), 5 U topoisomerase I (human recombinant topoisomerase I, TopoGen) and test compounds were incubated for 60 min at 37 °C. Reactions were stopped by adding 4 μL of stop buffer (5% SDS, 0.125% bromophenol blue and 25% glycerol), 50 μg/ mL proteinase K (Sigma) and incubating for a further 30 min at 37 °C. The samples were separated by electrophoresis on a 1% agarose gel containing ethidium bromide 0.5 μg/mL (Sigma) at room temperature in TBE buffer (0.09 M Triseborate and 0.002 M EDTA), transilluminated by UV light, and fluorescence emission was visualized by a CCD camera coupled to a Bio-Rad Gel Doc XR apparatus.

4.6.4. Docking studies

Topoisomerase: (*R*)- and (*S*)-Boehmeriasin A were docked in the enzyme mediated DNA cleavage site in the crystal structure of the topoisomerase I and of the topoisomerase II-beta, both in complex with DNA using AutoDock 4.2 software.

Sirtuins: (*R*)- and (*S*)-Boehmeriasin A were docked in the crystal structure of SIRT1 complex with Ex-527(PDB id 4I5I) and the homology model of SIRT2 using Schrodinger's Glide software.

Chapter 5

Synthesis of pironetin-dumetorine hybrids as new tubulin binders

5.1. Introduction

Natural compounds that target microtubules have proven to be one of the best classes of cancer chemotherapeutic drugs available in clinics to date.[91] Microtubules (MTs) are cylinders of linear polymers (protofilaments), formed by the polymerization of the αβ-tubulin heterodimers which are arranged head to tail in a polar fashion (Figure 38).[92]

α−tubulin   β−tubulin   α and β tubulin heterodimers

Section of a Microtubule
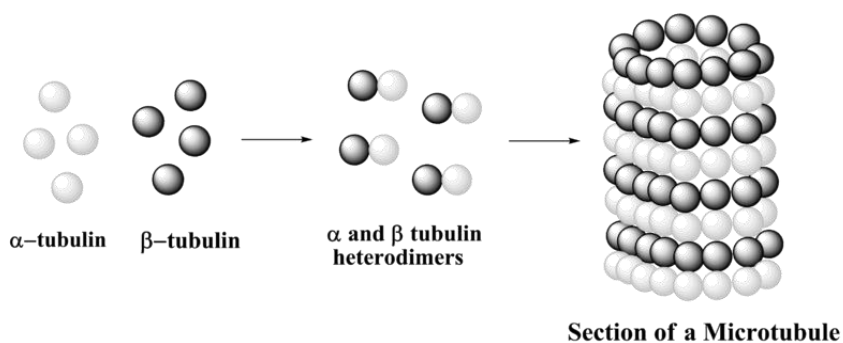
Figure 38

In eukaryotes, microtubules are one of the major components of the cytoskeleton, and thus they are fundamental in many biological processes, such as structural support, motility, intracellular transport, and DNA segregation. They are also involved in chromosome separation during the mitosis because they are the major constituents of mitotic spindles, the subcellular structure that separates chromosomes between daughter cells.

Their wide bioactivity in all cells is regulated in large part by their dynamic instability, referred to the individual microtubule ability to switch between growing and shrinking phases at the ends (Figure 39).

Minus end   Plus end

Polymerization

Rescue   **Catastrophe**

○ GTP-α-tubulin
○ GDP-β-tubulin
● GTP-β-tubulin
○ Nucleating material

Depolymerization
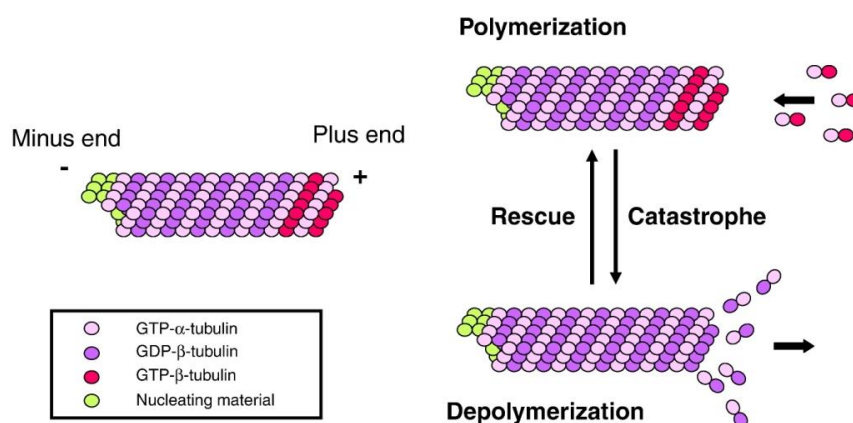
Figure 39

---

[91] E. Mukhtar; V. M. Adhami; H. Mukhtar; *Mol Cancer Ther.*, **2014**, *13*, 275.
[92] L. A. Amos; *Org .Biomol. Chem.*, **2004**, *2*, 2153.

Cell division is required for tumour growth, both directly, by cancer cell division, and indirectly, by endothelial cell division as a step in angiogenesis and tumour vascularisation. Some of the discovered natural compounds able to interfere with microtubules, blocking the cell cycle and inducing apoptosis, act by inhibiting the polymerisation of tubulin, while others inhibit depolymerisation.[93]

A large number of drugs are known to be able to bind β-tubulin and in this context it is possible to identify three well established drug binding domains: *i)* the vinca domain, *ii)* the taxane site and *iii)* the colchicine site (Figure 40).[94]
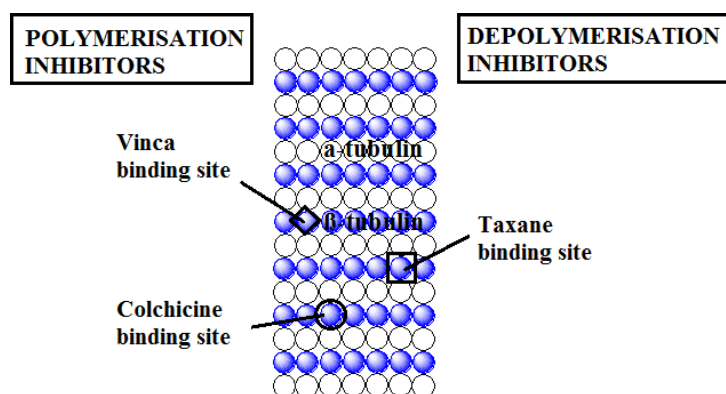
Figure 40

By contrast, the number of molecules that bind to α-tubulin is very small. The first reported example is pironetin, a potent microtubule polymerization inhibitor, isolated from the fermentation broth of *Streptomyces Discodermolide*,[95] followed, a short time later, by the peptide-like hemiasterlin family (Figure 41).[96]

Pironetin   Hemiasterlin
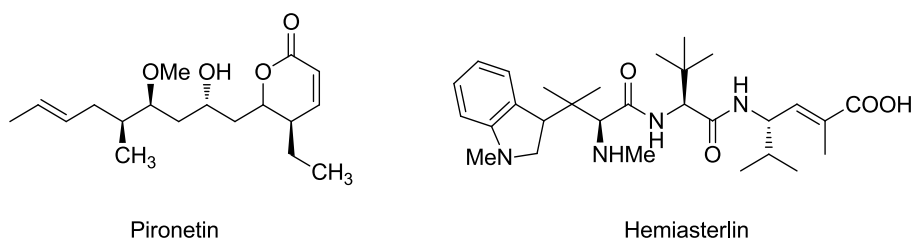
Figure 41

This polyketide has a unique structure containing the pharmacophoric alkenyl-5,6-dihydro-2*H*-pyran-2-one moiety and an alkyl chain, which is simpler than the structure of other M phase inhibitors. From the analyses of structure-activity relationship, it was revealed that pironetin binds to Lys352 of α-tubulin by Michael addition on α,β-unsuturated-pyranone ring. In addition, it

---

[93]a) N.G. Vindya; N. Sharma; M. Yadav; K.R. Ethiraj*; Curr. Top. Med. Chem.*, **2015**, *15*, 73; b) E.C. Breen; J.J. Walsh; *Curr. Med. Chem.*, **2010**, *17*, 609.

[94] K. H. Downing; *Annu. Rev. Cell. Dev. Biol.*, **2000**, *16*, 89.

[95] F. Sarabia; M. García-Castro; A. Sánchez-Ruiz; *Curr. Bioact. Compd.*, **2006**, *2*, 269.

[96] H. J. Anderson; J. E. Coleman; R. J. Andersen; M. Roberge; *Cancer Chemother. Pharmacol.*, **1997**, *39*, 223.

has been suggested that the Asn258 residue of α-tubulin fixes the pironetin molecule through two hydrogen bonds with the pyrone carbonyl and the methoxy oxygen atom (Figure 42).[97]
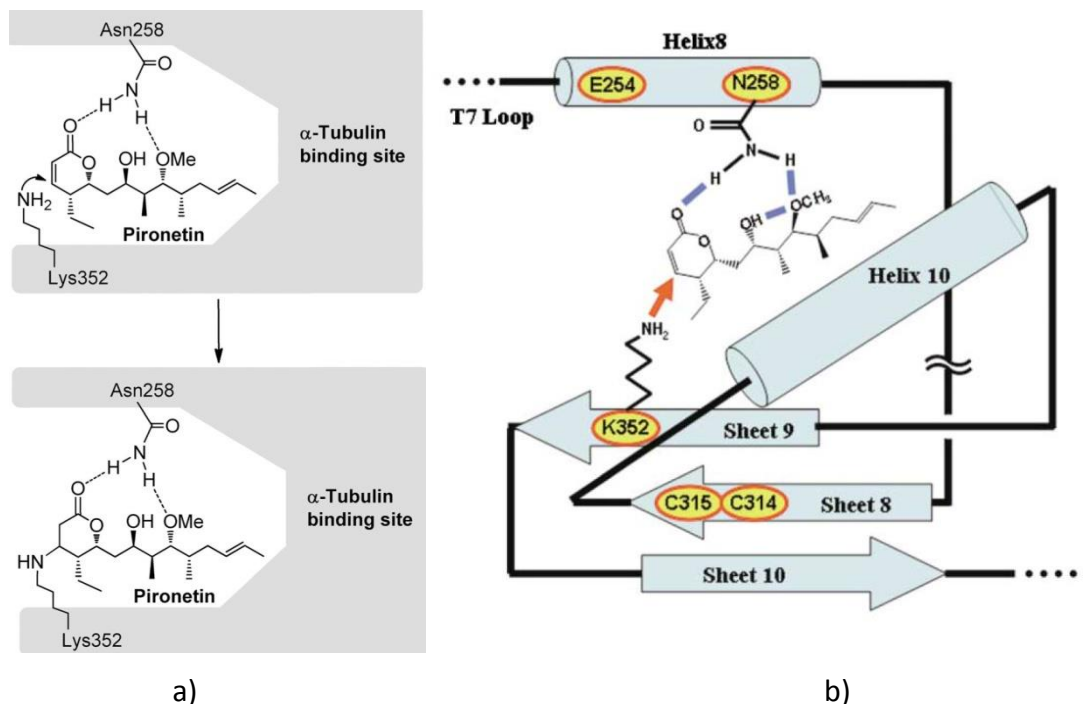
Figure 42: a) Schematic model of the cavalent union of pironetin with its binding site at the α−tubulin suface; **b)** secondary structure around the pironetin binding site on α−tubulin and binding model.

Since it is known that most of the compounds containing α,β-unsaturated lactone covalently bind to sulfhydryl group of cysteine residue of proteins, pironetin is a unique compound which binds specific lysine residue on α-tubulin. These features of pironetin suggest that it is possible to create a new drug useful for cancer therapy from pironetin as a lead compound. In this context, several efforts have been done by J. Alberto Marco and his group in the design and development of novel α-tubulin-binding pironetin analogues during last years.[98]

5.2. Aim of this work

This project was born in collaboration with the group Daniele Passarella of the university of Milan, which in the last years has addressed its attention toward the total synthesis of 2-piperidinyl alkaloids, such as (+)- dumetorine (Figure 43).[99] Dumetorine was isolated in 1985 from the tubers

[97] a)T. Usui; H. Watanabe; H. Nakayama; Y. Tada; N. Kanoh; M. Kondoh; T. Asao; K. Takio; H. Watanabe; K. Nishikawa; T. Kitahara; H. Osada; *Chem. Bio.*, **2004**, *11*, 799; b) H. Watanabe; H. Watanabe; T. Usui; M. Kondoh; H. Osada; T. Kitahara; *J. Antibiot.*, **2000**, *53*, 540.
[98] a) J. Paños; S. Díaz-Oltra; M. Sánchez-Peris; J. García-Pla; J. Murga; E. Falomir; M. Carda; M. Redondo-Horcajo; J. F. Díaz; I. Barasoain; J. A. Marco; *Org. Biomol. Chem.*, **2013**, *11*, 5809; b) M. Carda; J. Murga; S. Díaz-Oltra; J. García-Pla; J. Paños; E. Falomir; C. Trigili; J. F. Díaz; I. Barasoain; J. A. Marco; *Eur. J. Org. Chem.*, **2013**, 1116; c) J. A. Marco; J. García-Pla; M. Carda; J. Murga; E. Falomir; C. Trigili, S. Notararigo; J. F. Díaz; I. Barasoain; *Eur. J. Med. Chem.*, **2011**, *46*, 1630.
[99] a) E. Riva; A. Rencurosi; S. Gagliardi; D. Passarella; M. Martinelli; *Chem. Eur. J.*, **2011**, *17*, 6221; b) D. Passarella; S. Riva; G. Grieco; F. Cavallo; B. Checa; F. Arioli; E. Riva; D. Comi; B. Danieli; *Tetrahedron: Asymmetry*, **2009**, *20*, 192.

of *Dioscorea dumetorum Pax*, a West African yam whose extracts have found a notable use in folk medicine and arrow poisons.[100]

Based on this background, we decided to prepare a new pironetin-like compound with the ability to bind selectively α-tubulin. The molecule target was designed as a hybrid **20** between pironetin and dumetorine, given that it is possible to identify a similar lactonic moiety in both of them. Indeed, the nitrogen atom of the piperidinic ring of dumetorine could mimic the hydroxylic group bound to C9 in the pironetin, important in terms of hydrogen bonds with tubulin residues (Figure 43).
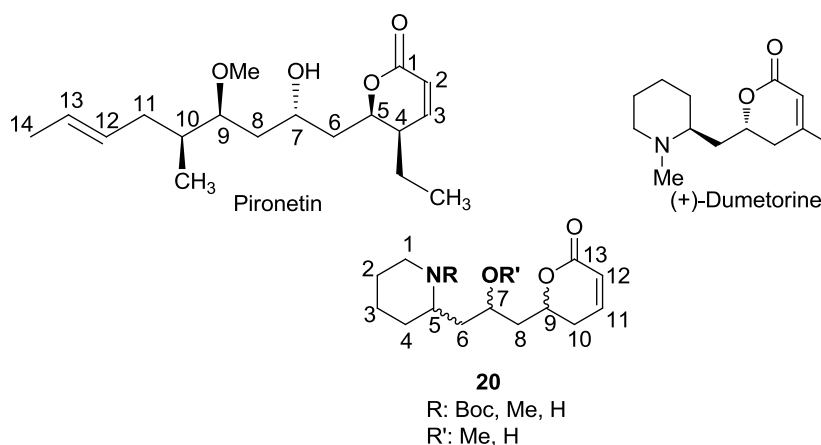
Figure 43

The presence of 3 stereocentres opens the way toward 8 stereoisomers that could interact in different ways with the biological target. Our purpose is to identify the most bioactive stereoisomer and, as an extension of the project, connect it to a β-tubulin binder in order to achieve a cytotoxic TBMs with a potential ability to bind to either α- or β-tubulin and produce a microtubule-destabilizing effect.

5.3. Docking studies

Previous docking studies were performed by Professor S. Pieraccini from University of Milan in order to support the disegn of the novel compound. First of all, they allowed to highlight a similar orientation of the hybrid **20** compared with pironetin on the binding site of α-tubulin: the lactonic ring is direct toward the enter of the binding task, while the piperidinic ring fills the position of the pironetin alkyl chain. Also, our molecule would seem to form a major number of hydrogen bonds with tubulin than pironetin, whereby a stronger interaction is expected (Figure 44).

---

[100] D. G. Corley; M. S. Tempesta; M. M. Iwu; *Tetrahedron Lett.*, **1485**, *26*, 1615.
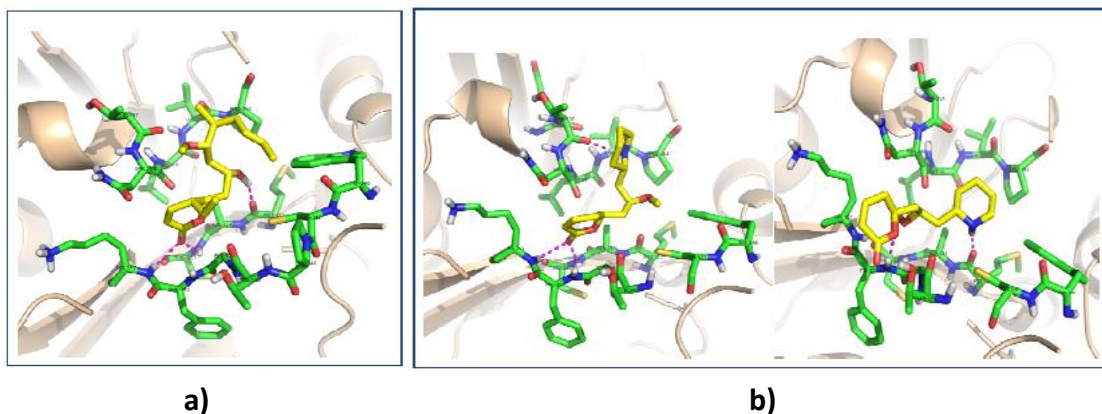
Figure 44: a) Docked structure of pironetin in the binding task of α-tubulin; **b)** docked structures of hybrid in the binding task of α-tubulin.

Molecular dockings of the eight possible stereoisomers **38b-45b** were performed (Figure 45).
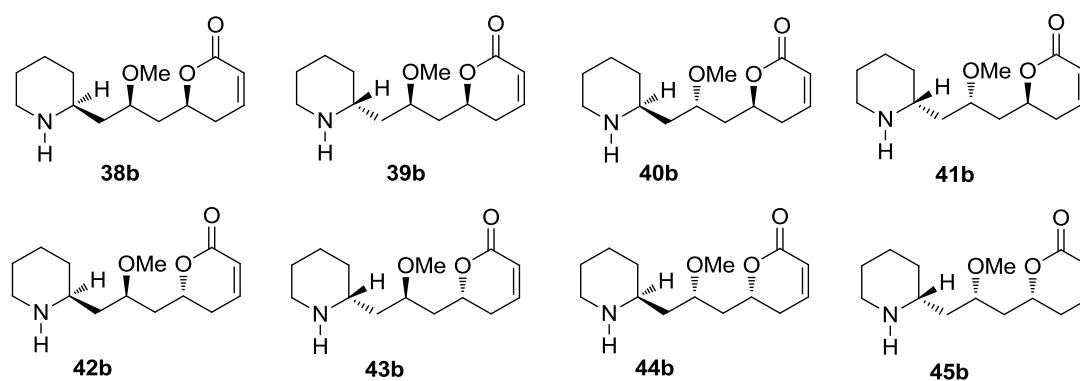
Figure 45

The docked compounds show different orientation and a moderate affinity for the putative binding site. One of the main features in common between most of the docked molecules (except **41b** and **45b**) is the formation of an H-bond involving the N-H group of the piperidinic ring with either Val260 or with Thr257 backbone oxygen and a hydrophobic interaction with Pro261 (Figure 46).

a)

b)

c)

d)
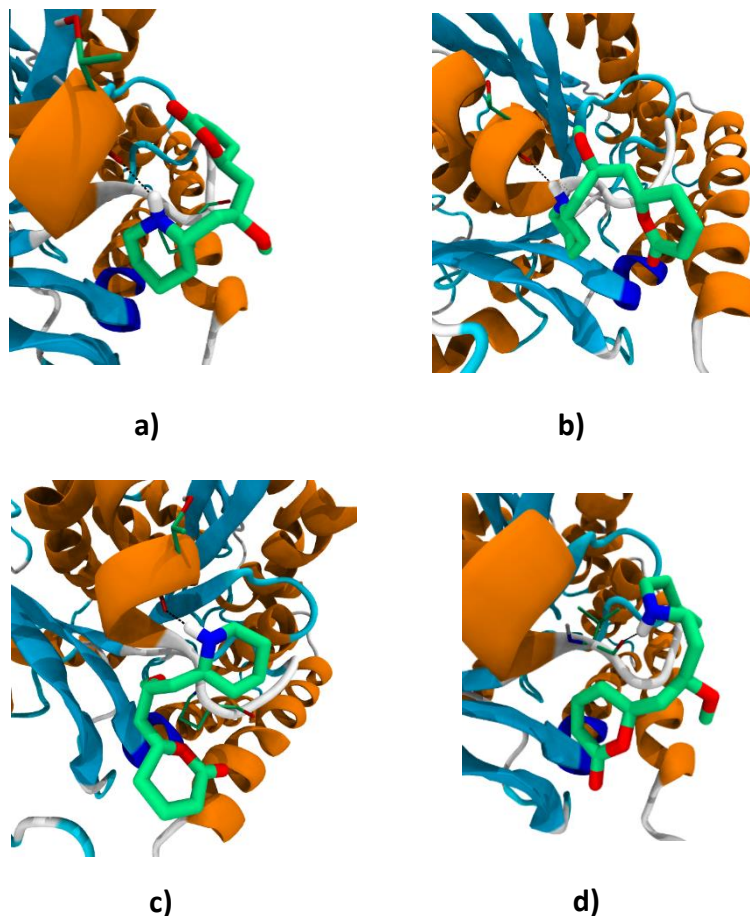
Figure 46: a) Docking pose of compound **38b**. The piperidine N-H group forms an H-bond with Thr257 backbone oxygen; **b)** Docking pose of compound **40b**. N-H group of piperdine forms an H-bond with Thr257 backbone oxygen. Indeed it also presents a hydrophobic interaction between piperidine ring and Pro261; **c)** Docking pose of compounds **42b** and **44b**. The docked structures show an H-bond between piperidine N-H group and Thr257 backbone oxygen; **d)** Piperidine N-H groups of compounds **39b** and **43b** interact with Val260 backbone oxygen. There is a hydrophobic interaction between the lactones and Pro261.

Compounds **41b** and **45b** have the same orientation within the binding site and preferentially exhibit an intramolecular interaction (Figure 47) between the carbonyl of the lactone ring and the amino group of piperidine.
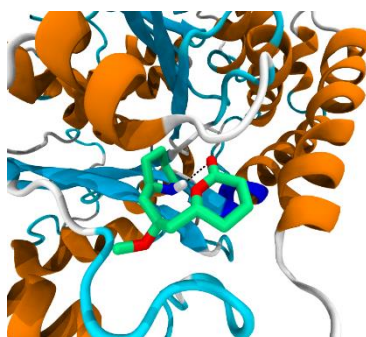
Figure 47: Compounds **41b** and **45b** have a peculiar behaviour, they exhibit an intramolecular interaction between the carbonyl of the lactone and the N-H group of the piperidine.

Albeit the exhibited affinity of the the proposed pironetine derivatives is not impressive, pironetin binding site seems to be a plausible putative binding site for all of them due to the flexibility of the skeleton. Therefore experimental investigations are needed to check the reality and potency of these interactions.

5.4. Chemistry

As consequence of the computational results, we planned the preparation of the eight stereoisomers according to the retrosynthetic scheme showed in Scheme 16.
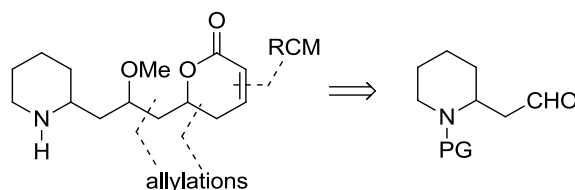
Scheme 16

The preparation is based on the reactivity and the versatility of aldehyde **21** (previously used as enantiopure compound in boehmeriasin A synthesis). The use of allylmagnesium bromide in the presence of enantiopure DIP-Cl[101] induces the formation of the allylic alcohols **22a-25a** with complete stereocontrol at C2' (numbering system of the target compound) with the formation of two distereoisomers. By this way the use of (-)-DIP-Cl furnished the distereoisomers **22a** and **23a** while the use of (+)-DIP-Cl led to the compounds **24a** and **25a** (Scheme 17).
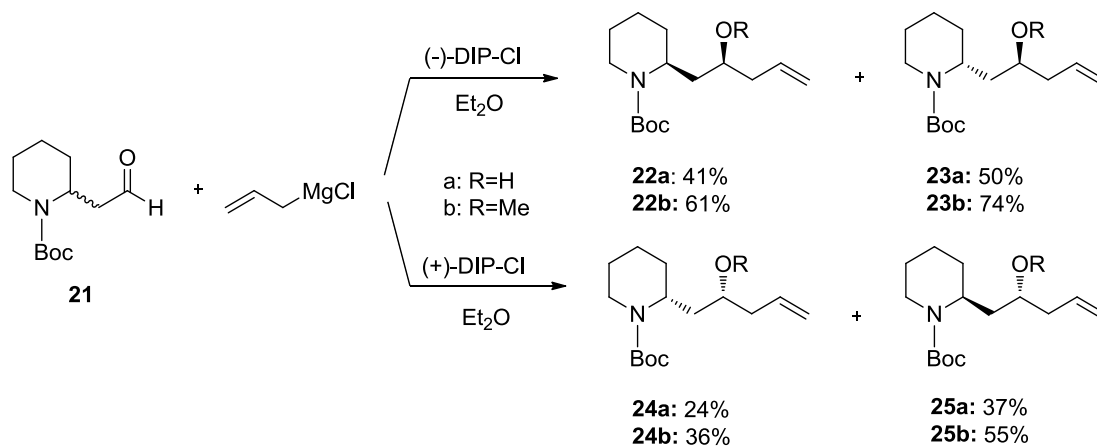
Scheme 17

The hydroxylic group of compounds **22a-25a** was protected as methyl ether forming **22b-25b** which were treated with ozonolysis conditions in order to achieve the corresponding aldehydes **26-29** (Scheme 18).

---

[101] M. V. R. Reddy; H. C. Brown; P. V. Ramachandran; *J. Orgmet. Chem.*, **2001**, *624*, 239.
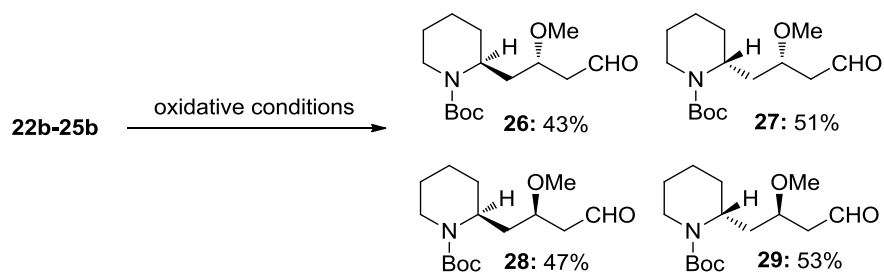
Scheme 18

The formation of the third stereogenic center is based on the replication of the stereocontrolled allylation reaction able to generate **30a-37a**. Subsequently, the compounds **30b-37b** were obtained treating the secondary alcohol with acryloyl chloride (Scheme 19).
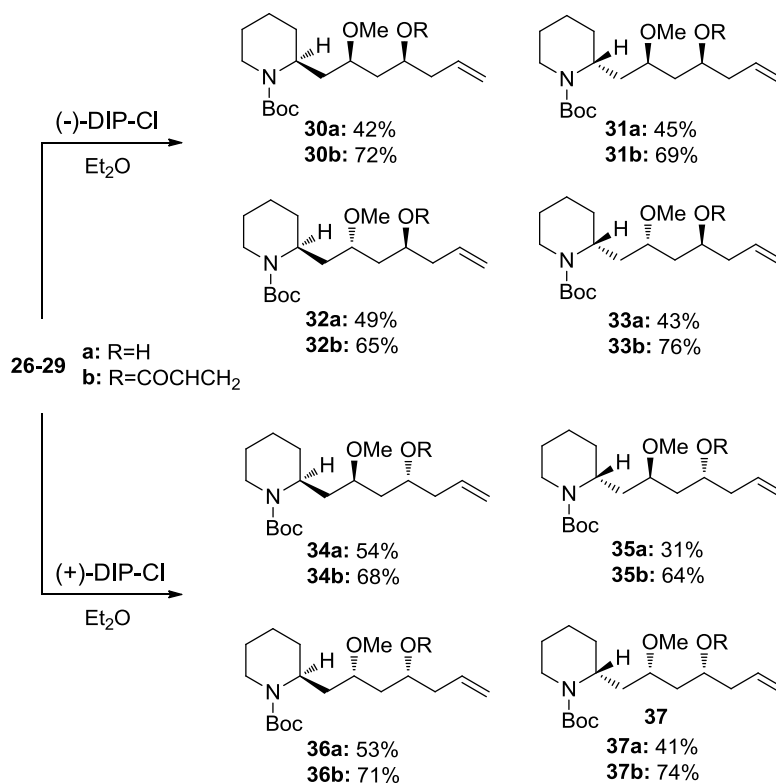
Scheme 19

The target compounds **38b-45b** were achieved as salt of acid trifluoracetic carrying out ring closing methatesis reactions, in the presence of Hoveyda-Grubbs-II catalyst, and, then, treating **38a-45a** with TFA for the cleavage of the piperidinic nitrogen (Scheme 20).

38a: 75%
38b: 91%

39a: 68%
39b: 82%

40a: 69%
40b: 85%

41a: 77%
41b: 87%

42a: 81%
42b: 85%

43a: 76%
43b: 90%

44a: 71%
44b: 89%

45a: 64%
45b: 92%

30b-37b

1) Hoveyda-Grubbs 2nd
Toluene, reflux, 4h

2) TFA
CH$_2$Cl$_2$, rt, 30 min
a: R=Boc
b: R=H
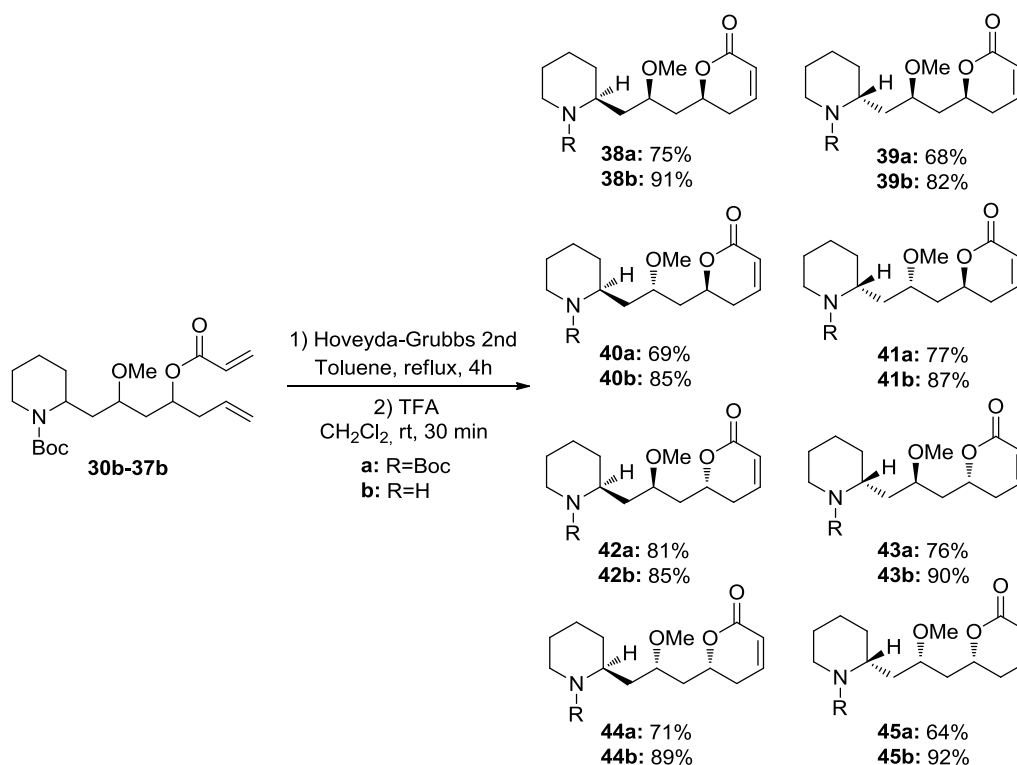
Scheme 20

5.5. Biological evaluation

To get an insight into its potential biological activity of compounds **38b-45b**, we investigated their ability to interfere with microtubule assembly in vitro (Figure 48).
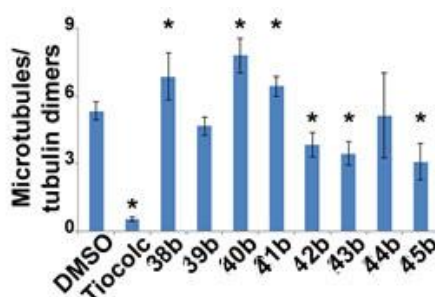
Figure 48: Effects of compounds **38b-45b** on tubulin polymerisation. The histogram represent the ratio between microtubules and tubulin dimers obtained in control conditions (DMSO), In the presence of 10 μM thiocolchicine (TioColc), and in presence of 50 μM compounds (**38b-45b**). *$p<0.05$ according to ANOVA, Fisher post hoc test.

Thiocolchicine (10 μM) was used as reference compound since its ability to inhibit the tubulin assembly to form microtubules. In comparison, the new pironetin derivatives appear to moderately impact microtubule formation. **38b** and **40b** significantly increase the ratio between microtubules and tubulin dimers, whereas the **42b**, **43b** and **45b** inhibit microtubule assembly.

5.6.Conclusion

In summary, the obtainment of the eight stereoisomers of the target compound has been completed. The enantiopure grade of them is under analysis by HPLC. The biological tests showed a possible influence of the obtained compounds on tubulin polymerization even if with a not relevant inhibition properties. Thus, the present work could suggest the synthesis of new tubulin-inhibitors based on the designed hybrid.

Once figure the best candidate out, a future work could be bind it to a well-known β-tubulin inhibitor in order to create a bivalent molecule. In fact, due to synergic interactions, it finally could be result a good microtubule-inhibitor.

5.7. Experimental part

5.7.1. Synthesis

General procedure for diasteroselective allylation: synthesis of 22a-25a

Allylmagnesium bromide (commercial 1M solution in Et$_2$O, 2.86 mL, 2.86 mmol) was added dropwise under nitrogen atmosphere to a solution of suitable enantiopure DIP-Cl (1.06 g, 3.3 mmol) in dry THF (13.5 mL) at -78°C. The reaction mixture was allowed to warm to 0 °C and stirred at that temperature for 1 h. The solution was then allowed to stand until magnesium chloride precipitated. The supernatant solution was then carefully transferred via canula to another flask and, after its cooling at −78°C, a solution of the racemic aldehyde **21** (0.500 g, 2.20 mmol) in dry THF (6.5 mL) was added dropwise. The resulting solution was further stirred at the same temperature for 1 h and then 16 h at room temperature. The reaction was quenched with NaH$_2$PO$_4$ buffer solution at pH 7 (13.5 mL), MeOH (13.5 mL) and 30% H$_2$O$_2$ (6.7 mL). After stirring for 30 minutes, the mixture was washed with saturated aqueous NaHCO$_3$ and extracted with Et$_2$O. The combined organic phases were dried over anhydrous Na$_2$SO$_4$, and filtered. The solvent was evaporated under vacuum, and the residue was purified by column chromatography on silica gel (hexane /EtOAc, 4:1). The reaction performed with (-)-DIP-Cl afforded **22a** and **23a** as a yellow oil (90% overall yield), while the reaction carried out with (+)-DIP-Cl gave **24a** and **25a** in 90% overall yield.

(*S*)-*Tert*-butyl 2-((*S*)-2-hydroxypent-4-enyl)piperidine-1-carboxylate (22a)
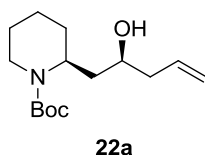
Yield: 41%. [α]$_D$ = -33.0 (*c* 1.0, CHCl$_3$). IR: (neat): ν= 1674 cm^{-1}; ^{1}H NMR (400 MHz, CDCl$_3$): δ 1.35-1.59 (m, 6H), 1.42 (s, 9H,), 1.73-1.76 (m, 1H), 2.01 (dt, *J* = 12.5, 1.8 Hz, 1H), 2.16-2.23 (m, 1H), 2.27-2.33 (m, 1H), 2.66 (dt, *J* = 12.7, 2.0 Hz, 1H), 3.39 (br s, 1H), 3.95 (br s, 1H), 4.47 (br s, 1H), 5.05 (d, *J* = 9.7 Hz, 1H), 5.08 (d, *J* = 17.4 Hz, 1H), 5.81-5.91 (m, 1H) ppm; ^{13}C NMR (100 MHz, CDCl$_3$): δ 19.4, 25.3, 28.6, 29.2, 36.9, 39.3, 41.1, 46.2, 67.1, 80.2, 116.6, 135.5, 167.1 ppm.

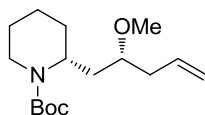### (R)-Tert-butyl-2-((R)-2-hydroxypent-4-en-1-yl)piperidine-1-carboxylate (24a)

24a
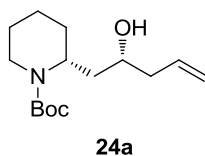
Yield: 24%. $[\alpha]_D$ = + 35.0 (c 0.8, CHCl$_3$). IR: (neat): ν = 1674 cm^{-1}. <u>NMR as **22a**</u>

(R)-Tert-butyl-2-((S)-2-hydroxypent-4-en-1-yl)piperidine-1-carboxylate (23a)

23a
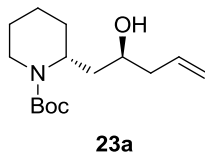
Yield: 50%. $[\alpha]_D$ = + 15.3 (c 0.9, CHCl$_3$); IR: (neat): ν = 1674 cm^{-1}; ^{1}H NMR (400 MHz, CDCl$_3$): δ 1.35-1.59 (m, 6H), 1.42 (s, 9H), 1.77-1.82 (m, 1H), 2.14-2.21 (m, 1H), 2.27-2.32 (m, 1H), 2.79 (dt, J = 12.8, 0.2 Hz, 1H), 3.65 (tt, J = 7.5, 2.4 Hz, 1H), 3.92 (m, 1H), 4.32 (br s, 1H), 5.07 (d, J = 9.8 Hz, 1H), 5.09 (d, J = 17.3 Hz, 1H), 5.75-5.85 (m, 1H) ppm; ^{13}C NMR (100 MHz, CDCl$_3$): δ 18.9, 25.4, 28.4, 29.3, 36.9, 38.8, 41.8, 48.0, 71.3, 79.6, 117.4, 135.3, 160.1 ppm.

(S)-Tert-butyl-2-((R)-2-hydroxypent-4-en-1-yl)piperidine-1-carboxylate (25a)

25a
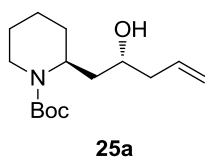
Yield: 37%. $[\alpha]_D$ = - 13.8 (c 13.3, CHCl$_3$). IR: (neat): ν = 1674 cm^{-1}. <u>NMR as **23a**</u>

General procedure for methylation: synthesis of 22b-25b
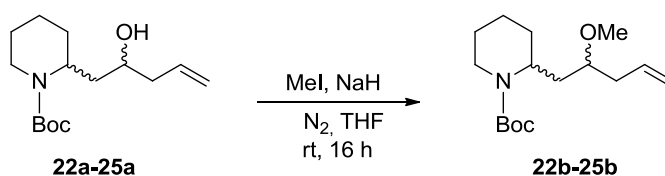
22a (0.319 g, 1.18 mmol) was dissolved in anhydrous THF (7 mL) and the solution was added dropwise to a suspension of sodium hydride (0.095 g, 3.90 mmol) in dry THF (3 mL) cooled at -78°C and it was stirred for 1 h. Then methyl iodide (0.3 mL, 4.70 mmol) was added and the reaction mixture was stirred 1 h at -78 °C and 16 h at room temperature. The mixture was quenched with cold water (10 mL) and the aqueous layer was extracted with Et$_2$O. The organic layer was dried with Na$_2$SO$_4$ and the solvent was removed under vacuum. The residue was purified by column chromatography on silica gel (hexane/EtOAc, 4:1) to give **22b** (74%) as yellow oil. In order to obtain the other compounds **23b**, **24b** and **25b** the reaction was performed in the same way.

(*S*)-*Tert*-butyl-2-((*S*)-2-methoxypent-4-en-1-yl)piperidine-1-carboxylate (22b)

22b
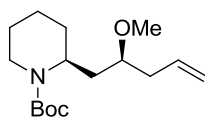
Yield: 61%. [α]$_D$ = - 36.0 (*c* 3.64, CHCl$_3$). IR: (neat): ν = 1677 cm^{-1}. ^{1}H NMR (400 MHz, CDCl$_3$): δ 1.37-1.64 (m, 6H), 1.46 (s, 9H), 1.83-1.90 (m, 1H), 2.21-2.33 (m, 2H), 2.70 (t, *J* = 13.2 Hz, 1H), 3.11-3.17 (m, 1H), 3.35 (s, 3H), 3.97 (br s, 1H), 4.44 (br s, 1H), 5.08 (d, *J* = 17.1 Hz, 1H), 5.10 (d, *J* = 9.2 Hz, 1H), 5.73-5.83 (m, 1H) ppm; ^{13}C NMR (100 MHz, CDCl$_3$): δ 19.4, 25.7, 25.7, 28.5, 29.5, 34.5, 37.7, 47.6, 56.9, 77.9, 79.1, 117.3, 134.5, 155.1 ppm.

(*R*)-*Tert*-butyl 2-((*R*)-2-methoxypent-4-enyl)piperidine-1-carboxylate (24b)

24b

Yield: 55%. [α]$_D$ = +33.0 (*c* 0.5, CHCl$_3$). IR: (neat): ν = 1677 cm^{-1}. <u>NMR as **22b**</u>

(*R*)-*Tert*-butyl 2-((*S*)-2-methoxypent-4-enyl)piperidine-1-carboxylate (23b)

23b
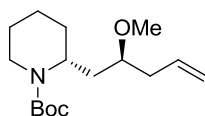
Yield: 74%. [α]$_D$ = + 23.4 (*c* 2.7, CHCl$_3$). IR: (neat): ν = 1677 cm^{-1}; ^{1}H NMR (400 MHz, CDCl$_3$): δ 1.33-1.59 (m, 6H), 1.43 (s, 9H), 1.88-1.96 (m, 1H), 2.28 (dddd, *J* = 12.3, 12.3, 6.4, 1.2 Hz, 1H), 2.35 (dddd, *J* = 12.3, 12.3, 6.4, 1.2 Hz, 1H), 2.78 (t, *J* = 13,3 Hz, 1H), 3.14-3.19 (m, 1H), 3.29 (s, 3H), 3.96 (m, 1H), 4.32 (br s, 1H), 5.03-5.09 (m, *2*H), 5.74-5.84 (m, 1H) ppm; ^{13}C NMR (100 MHz, CDCl$_3$): δ 23.6, 24.9, 30.2, 33.7, 35.1, 39.2, 44.7, 47.9, 53.9, 73.9, 80.8, 118.5, 132.4, 153.9 ppm.

(*S*)-*Tert*-butyl-2-((*R*)-2-methoxypent-4-en-1-yl)piperidine-1-carboxylate (25b)

25b
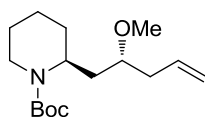
Yield: 36%. [α]$_D$ = - 19.0 (*c* 0.9, CHCl$_3$). IR: (neat): ν = 1677 cm^{-1}. <u>NMR as **23b**</u>

General procedure for ozonolysis: synthesis of 26-29
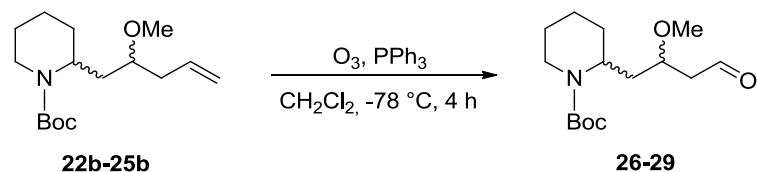
Olefin **22b** (0.470 g, 1.66 mmol) was dissolved in dry CH_2Cl_2 (19 mL) and cooled to -78 °C. A stream of ozone-oxygen was bubbled through the solution until persistence of the bluish color. Dry N_2 was then bubbled through the solution for 10 min at the same temperature. After addition of PPh_3 (0.870 g, 3.32 mmol), the reaction mixture was stirred waiting the completion of the reaction. Then the solvent was removed under vacuum and the residue was purified by column chromatography on silica gel (hexane/EtOAc, 7:3) to give **26** (43%) as orange oil. In order to obtain the other compounds **27**, **28** and **29** the reaction was performed in the same way.

(S)-Tert-butyl 2-((R)-2-methoxy-4-oxobutyl)piperidine-1-carboxylate (26)
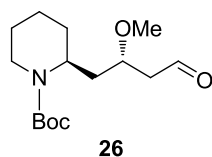
Yield: 43%. $[\alpha]_D$ = - 21.3 (c 3.45, CHCl$_3$); IR (neat): ν = 1679, 1719 cm^{-1};^{1}H NMR (400 MHz, CDCl$_3$): δ 1.37-1.65 (m, 6H), 1.46 (s, 9H), 1.88 (ddd, J = 14.0, 9.3, 4.4 Hz, 1H), 2.63 (ddd, J = 6.3, 4.3, 2.1 Hz, 2H), 2.75 (t, J = 12.7 Hz, 1H), 3.36 (s, 3H), 3.59-3.65 (m, 1H), 3.98 (br s, 1H), 4.43 (br s, 1H), 9.81 (t, J = 2.1 Hz, 1H) ppm; ^{13}C NMR (100 MHz, CDCl$_3$): δ 19.1, 25.6, 28.5, 29.0, 33.6, 38.8, 48.0, 56.6, 74.4, 76.2, 79.5, 155.0, 201.4 ppm.

**(R)-Tert-butyl 2-((S)-2-methoxy-4-oxobutyl)piperidine-1-carboxylate (29)**
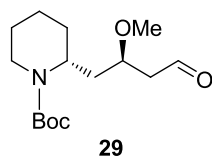
Yield: 53%. $[\alpha]_D$ = + 19.1 (c 0.5, CHCl$_3$). IR: (neat): ν = 1679, 1719 cm^{-1}. NMR as **26**

(R)-Tert-butyl 2-((R)-2-methoxy-4-oxobutyl)piperidine-1-carboxylate (27)
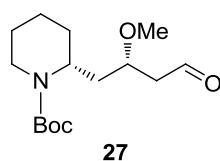
Yield: 51%. $[\alpha]_D$ = + 28.8 (*c* 2.65, CHCl₃); IR (neat): ν = 1678, 1719 cm⁻¹; ¹H NMR (400 MHz, CDCl₃):

δ 1.37-1.66 (m, 6H), 1.44 (s, 9H), 2.09-2.19 (m, 1H), 2.59 (ddd, *J* = 16.4, 7.5, 2.8 Hz, 1H), 2.75-2.82

(m, 2H), 3.32 (s, 3H), 3.64 (ddd, *J* = 12.4, 7.7, 5.1 Hz, 1H), 4.00-4.02 (m, 1H), 4.34 (br s, 1H), 9.78 (s,

1H) ppm; ¹³C NMR (100 MHz, CDCl₃): δ 19.2, 25.7, 28.6, 29.1, 33.7, 38.8, 48.0, 56.8, 60.5, 74.3,

79.7, 155.0, 201.6 ppm.

(*S*)-*Tert*-butyl 2-((*S*)-2-methoxy-4-oxobutyl)piperidine-1-carboxylate (28)
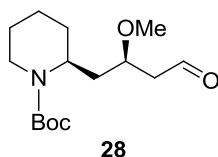
Yield: 47%. $[\alpha]_D$ = - 26.5 (*c* 0.5, CHCl₃). IR: (neat): ν = 1679, 1719 cm⁻¹. <u>NMR as **27**</u>

General procedure for diasteroselective allylation: synthesis of 30a-37a
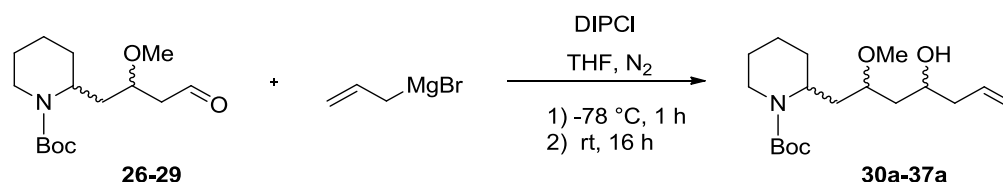
Allylmagnesium bromide (commercial 1M solution in Et₂O, 0.87 mL, 0.87 mmol) was added

dropwise under nitrogen atmosphere to a solution of the suitable enantiopure DIP-Cl (0.323 g,

1.01 mmol) in dry THF (5 mL) at -78 °C. The reaction mixture was allowed to warm to 0 °C and

stirred at that temperature for 1 hour. The solution was then allowed to stand until magnesium

chloride precipitated. The supernatant solution was then carefully transferred via canula to

another flask and after cooling up to -78 °C, a solution of aldehyde **26-29** (0.190 g, 0.67 mmol) in

dry THF (2.5 mL) was added dropwise. The resulting solution was further stirred at the same

temperature for 1 h and then 16 h at room temperature. The reaction was quenched with

NaH₂PO₄ buffer solution at pH 7 (5.1 mL), MeOH (5.1 mL) and 30% H₂O₂ (2.5 mL). After stirring for

30 minutes, the mixture was washed with saturated aqueous NaHCO₃ and extracted with Et₂O.

The combined organic phases were dried over anhydrous Na₂SO₄, and filtered. The solvent was

evaporated under vacuum, and the residue was purified by column chromatography on silica gel

(Hexane /EtOAc, 7:3) to give the **30a-37a,** respectively, (80%) as a yellow oil.

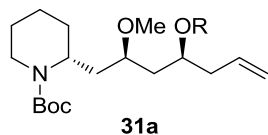**(*S*)-*Tert*-butyl 2-((2*R*,4*S*)-4-hydroxy-2-methoxyhept-6-enyl)piperidine-1-carboxylate (30a)**
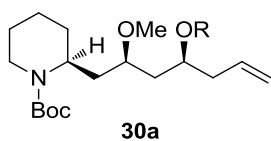
Yield: 42%. $[\alpha]_D$ = - 21.4 (*c* 0.7, CHCl$_3$); IR (neat): ν = 1687 cm^{-1}; ^{1}H NMR (400 MHz, CDCl$_3$): δ 1.34-1.63 (m, 8H), 1.45 (s, 9H), 1.74-1.76 (m, 2H), 2.22 (t, *J* = 6.6 Hz, 2H), 2.72-2.78 (m, 1H), 3.35-3.41 (m, 1H), 3.36 (s, 3H), 3.78-3.84 (m, 1H), 3.95 (br s, 1H), 4.33 (br s, 1H), 5.07-5.12 (m, 2H), 5.83 (ddt, *J* = 17.5, 10.5, 7.1 Hz, 1H) ppm; ^{13}C NMR (100 MHz, CDCl$_3$): δ 19.3, 25.7, 28.4, 28.6, 34.5, 38.9, 40.7, 42.4, 48.0, 56.5, 68.31, 70.3, 79.6, 117.7, 135.0, 155.1 ppm.

(*R*)-*Tert*-butyl 2-((2*S*,4*R*)-4-hydroxy-2-methoxyhept-6-enyl)piperidine-1-carboxylate (37a)
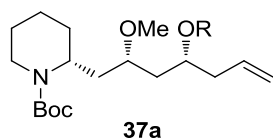
Yield: 41%. $[\alpha]_D$ = + 24.3 (*c* 0.1, CHCl$_3$). IR: (neat): ν = 1687 cm^{-1}. <u>NMR as **30a**</u>

(*R*)-*Tert*-butyl 2-((2*R*,4*S*)-4-hydroxy-2-methoxyhept-6-enyl)piperidine-1-carboxylate (31a)

Yield: 45%. $[\alpha]_D$ = - 9.2 (*c* 0.3, CHCl$_3$); IR (neat): ν = 1687 cm^{-1}; ^{1}H NMR (400 MHz, CDCl$_3$): δ 1.37-1.66 (m, 8H), 1.45 (s, 9H), 1.77-1.84 (m, 1H), 2.14-2.19 (m, 1H), 2.23 (t, *J* = 6.1 Hz, 2H), 2.80 (t, *J* = 13.2 Hz, 1H), 3.29-3.40 (m, 1H), 3.34 (s, 3H), 3.81-3.87 (m, 1H), 4.01 (br s, 1H), 4.30 (br s, 1H), 5.07-5.12 (m, 2H), 5.82-5.97 (m, 1H) ppm; ^{13}C NMR (100 MHz, CDCl$_3$): δ 19.2, 25.7, 28.6, 29.5, 33.7, 39.1, 41.0, 42.2, 47.3, 56.2, 68.3, 71.2, 79.8, 117.4, 135.1, 155.3 ppm.

(*S*)-*Tert*-butyl 2-((2*S*,4*R*)-4-hydroxy-2-methoxyhept-6-enyl)piperidine-1-carboxylate (36a)
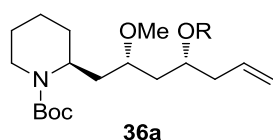
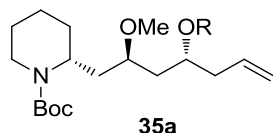Yield: 53%. $[\alpha]_D$ = +10.5 (*c* 0.04, CHCl$_3$). IR: (neat): ν = 1687 cm^{-1}. <u>NMR as **31a**</u>

(*S*)-*Tert*-butyl 2-((2*S*,4*S*)-4-hydroxy-2-methoxyhept-6-enyl)piperidine-1-carboxylate (32a)
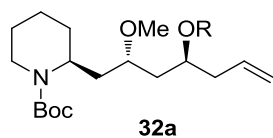
Yield: 49%. $[\alpha]_D$ = + 17.8 (*c* 0.1, CHCl$_3$). IR (neat): ν = 1687 cm^{-1}; ^{1}H NMR (400 MHz, CDCl$_3$): δ 1.33-1.66 (m, 8H), 1.45 (s, 9H), 1.76-1.84 (m, 1H), 2.15-2.19 (m, 1H), 2.23-2.25 (m, 2H), 2.80 (t, *J* = 13.8 Hz, 1H), 3.30-3.39 (m, 1H), 3.33 (s, 3H), 3.81-3.85 (m, 1H), 4.01 (br s, 1H), 4.30 (br s, 1H), 5.06-5.13
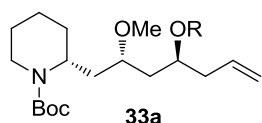
(m, 2H), 5.87 (ddt, J = 17.3, 10.2, 7.1 Hz, 1H) ppm; ^{13}C NMR (100 MHz, CDCl$_3$): δ 19.3, 25.8, 28.6, 29.4, 34.4, 38.9, 40.8, 42.3, 47.8, 57.1, 68.1, 71.1, 79.7, 117.5, 135.1, 155.0 ppm.

### (*R*)-Tert-butyl 2-((2*R*,4*R*)-4-hydroxy-2-methoxyhept-6-enyl)piperidine-1-carboxylate (35a)


Yield: 31%. $[\alpha]_D$ = + 15.7 (*c* 0.07, CHCl$_3$). IR: (neat): ν = 1687 cm^{-1}. <u>NMR as **32a**</u>

(*R*)-*Tert*-butyl 2-((2*S*,4*S*)-4-hydroxy-2-methoxyhept-6-enyl)piperidine-1-carboxylate (33a)

Yield: 43%. $[\alpha]_D$ = + 22.4 (*c* 1.4, CHCl$_3$). IR (neat): ν = 1687 cm^{-1}. ^{1}H NMR (400 MHz, CDCl$_3$): δ 1.31-1.66 (m, 15H),1.69- 1.84 (m, 3H), 2.16-2.29 (m, 2H), 2.64-2.82 (m, 1H), 3.33-3.47 (m, 5H), 3.89-4.02 (m, 3H), 4.27-4.42 (s, 1H), 5.04-5.15 (m, 2H), 5.75-5.91 (m, 1H) ppm; ^{13}C NMR (100 MHz, CDCl$_3$): δ 19.3, 25.8, 28.7, 29.3, 34.2, 38.9, 40.6, 42.5, 48.0, 57.3, 68.2, 70.3, 79.5, 117.7, 135.0, 155.1 ppm.

(*S*)-*Tert*-butyl 2-((2*R*,4*R*)-4-hydroxy-2-methoxyhept-6-enyl)piperidine-1-carboxylate (34a)
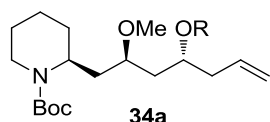
Yield: 54%. $[\alpha]_D$ = - 21.6 (*c* 0.02, CHCl$_3$). IR: (neat): ν = 1687 cm^{-1}. <u>NMR as **33a**</u>

General procedure for acroylation: synthesis of 30b-37b
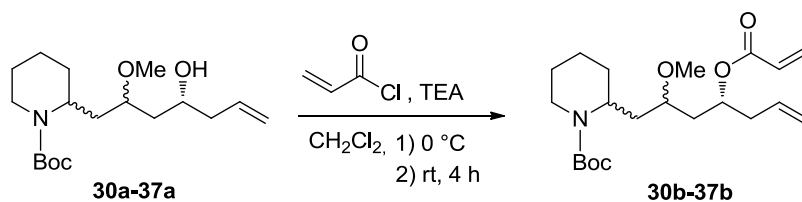

Acryloyl chloride (0.14 mL, 1.71 mmol) and TEA (0.48 mL, 3.42 mmol) were added sequentially to a cooled solution (0 °C) of compound **30a-37a** (0.140 g, 0.42 mmol) dissolved in dry CH$_2$Cl$_2$ (0.73 mL). The reaction was stirred for 4 hours at room temperature, then it was quenched with water (3 mL) and satd. aqueos NaCl (3 mL). The aqueous layer was extracted with CH$_2$Cl$_2$, and the organic layers were dried with Na$_2$SO$_4$ and filtered. The solvent was evaporated under vacuum, and the residue was purified by column chromatography on silica gel (Hexane /EtOAc 3:2) to give **30b-37b** (70%) as yellow oil.

**(*S*)-*Tert*-butyl 2-((2*R*,4*S*)-4-(acryloyloxy)-2-methoxyhept-6-enyl)piperidine-1-carboxylate (30b)**

30b
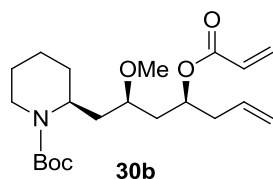
Yield: 72%. [α]$_D$ = -7.7 (*c* 0.7, CHCl$_3$); IR (neat): ν = 1677, 1719 cm^{-1}; ^{1}H NMR (400 MHz, CDCl$_3$): δ = 0.86-0.97 (m, 2H), 1.45 (s, 9H), 1.51-1.72 (m, 6H), 1.88-1.98 (m, 2H), 2.33-2.45 (m, 2H), 2.70 (t, *J* = 13.6 Hz, 1H), 3.09-3.15 (m, 1H), 3.30 (s, 3H), 3.95 (br s, 1H), 4.44 (br s, 1H), 5.06-5.12 (m, 3H), 5.72-5.82 (m, 1H), 5.82 (dd, *J* = 10.6, 1.5 Hz, 1H), 6.10 (dd, *J* = 17.3, 10.4 Hz, 1H), 6.39 (dd, *J* = 17.3, 1.5 Hz, 1H) ppm; ^{13}C NMR (100 MHz, CDCl$_3$): δ 19.2, 25.7, 28.5, 29.6, 34.6, 37.2, 38.7, 39.1, 47.0, 56.4, 70.6, 75.4, 78.9, 118.1, 128.6, 130.6, 133.3, 154.4, 165.6 ppm.

(*R*)-*Tert*-butyl 2-((2*S*,4*R*)-4-(acryloyloxy)-2-methoxyhept-6-enyl)piperidine-1-carboxylate (37b)

37b
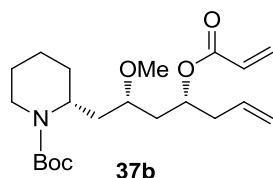
Yield: 74%. [α]$_D$ = +9.1 (*c* 0.03, CHCl$_3$). IR: (neat): ν = 1677, 1719 cm^{-1}. <u>NMR as **30b**</u>

(*R*)-T*ert*-butyl 2-((2*R*,4*S*)-4-(acryloyloxy)-2-methoxyhept-6-enyl)piperidine-1-carboxylate (31b)


31b
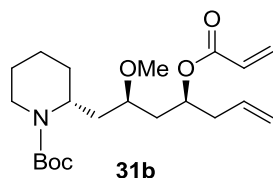
Yield: 69%. [α]$_D$ = + 20.4 (*c* 0.5, CHCl$_3$); IR (neat): ν = 1677, 1719 cm^{-1}; ^{1}H NMR (400 MHz, CDCl$_3$): δ 0.82-0.94 (m, 2H), 1.35-1.59 (m, 6H), 1.45 (s, 9H), 1.86-1.97 (m, 2H), 2.30-2.44 (m, 2H), 2.79 (t, 1H, *J* = 12.6 Hz), 3.21 (tt, 1H, *J* = 12.3, 6.2 Hz), 3.26 (s, 3H), 3.97 (br s, 1H), 4.35 (br s, 1H), 5.05-5.10 (m, 2H), 5.12-5.18 (m, 1H), 5.72-5.82 (m, 2H), 5.79 (dd, *J* = 10.4, 1.5 Hz, 1H), 6.10 (dd, *J* = 17.3, 10.4 Hz, 1H), 6.38 (dd, *J* = 17.3, 1.5 Hz, 1H) ppm; ^{13}C NMR (100 MHz, CDCl$_3$): δ 19.0, 25.6, 28.5, 28.7, 29.3, 33.5, 37.5, 39.3, 47.3, 56.8, 70.8, 75.7, 79.1, 118.2, 128.4, 130.5, 133.4, 154.7, 165.8 ppm.

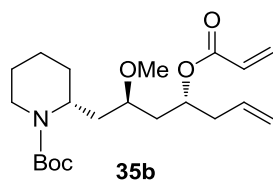**(*S*)-*Tert*-butyl 2-((2*S*,4*R*)-4-(acryloyloxy)-2-methoxyhept-6-enyl)piperidine-1-carboxylate (36b)**

36b
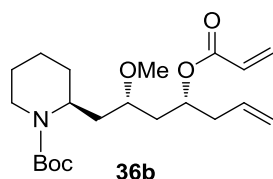
Yield: 71%. [α]$_D$ = +15.4 (c 0.005, CHCl$_3$). IR: (neat): ν = 1677, 1719 cm^{-1}. <u>NMR as **31b**</u>

(S)-Tert-butyl 2-((2S,4S)-4-(acryloyloxy)-2-methoxyhept-6-enyl)piperidine-1-carboxylate (32b)


32b
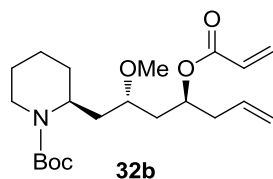
Yield: 65%. [α]$_D$ = +12.3 (c 0.5, CHCl$_3$); IR (neat): ν = 1677, 1719 cm^{-1}; ^{1}H NMR (400 MHz, CDCl$_3$): δ 0.89-0.94 (m, 2H), 1.46 (s, 9H), 1.44-2.00 (m, 8H), 2.30-2.45 (m, 2H), 2.76-2.82 (m, 1H), 3.21 (tt, J = 12.3, 6.2 Hz, 1H), 3.26 (s, 3H), 3.97 (br s, 1H), 4.35 (br s, 1H), 5.05-5.10 (m, 2H), 5.12-5.18 (m, 1H), 5.71-5.82 (m, 2H), 6.10 (dd, J = 17.3, 10.4 Hz, 1H), 6.39 (ddd, J = 17.3, 2.9, 1.5 Hz, 1H) ppm; ^{13}C NMR (100 MHz, CDCl$_3$): δ 18.9, 25.6, 28.6, 28.9, 33.2, 37.0, 38.5, 39.0, 47.4, 55.7, 70.9, 75.3, 79.2, 117.9, 128.8, 130.4, 133.5, 154.8, 165.6 ppm.

(R)-Tert-butyl 2-((2R,4R)-4-(acryloyloxy)-2-methoxyhept-6-enyl)piperidine-1-carboxylate (35b)


35b

Yield: 64%. [α]$_D$ = -16.5 (c 0.002, CHCl$_3$). IR: (neat): ν = 1677, 1719 cm^{-1}. <u>NMR as **32b**</u>

**(R)-Tert-butyl 2-((2S,4S)-4-(acryloyloxy)-2-methoxyhept-6-enyl)piperidine-1-carboxylate (33b)**

33b
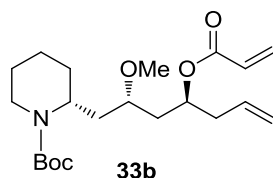
Yield: 78%. [α]$_D$ = +11.49 (c 0.8, CHCl$_3$). IR (neat): ν = 1677, 1719 cm^{-1}. ^{1}H NMR (300 MHz, CDCl$_3$): δ 1.20-1.65 (m, 19H), 1.65-1.86 (m, 1H), 2.29–2.44 (m, 2H), 2.66-2.81 (m, 1H), 3.05-3.17 (m, 1H), 3.31 (s, 3H), 3.89-4.03 (m, 1H), 4.26-4.50 (m, 1H), 5.01-5.28 (m, 2H), 5.69-5.85 (m, 2H), 6.03-6.17 (m, 1H), 6.33-6.45 (m, 1H) ppm; ^{13}C NMR (100 MHz, CDCl$_3$): δ 18.9, 25.5, 28.4, 28.7, 29.5, 34.7, 38.6, 39.1, 47.6, 57.1, 70.6, 75.6, 79.1, 117.9, 128.6, 130.4, 133.1, 165.5 ppm.

(S)-Tert-butyl 2-((2R,4R)-4-(acryloyloxy)-2-methoxyhept-6-enyl)piperidine-1-carboxylate (34b)


34b
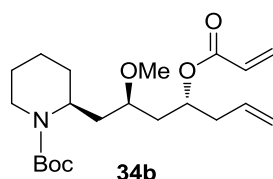
Yield: 68%. $[\alpha]_D$ = -9.4 (c 0.01, CHCl$_3$). IR: (neat): ν = 1677, 1719 cm^{-1}. <u>NMR as **33b**</u>

**General procedure for ring closing methatesis reaction: synthesis of 38a-45a**
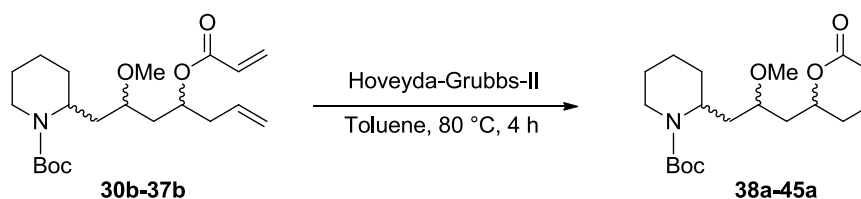
A solution of Hoveyda-Grubbs-II catalyst (0.014 g, 0.02 mmol) in dry CH$_2$Cl$_2$ (3.2 mL) was added dropwise to a solution of compound **30b** (0.085 g, 0.22 mmol) dissolved in dry CH$_2$Cl$_2$ (9.4 mL). The reaction was stirred for 4 h at room temperature, then the solvent was removed under vacuum. The residue was purified by column chromatography on silica gel (Hexane /EtOAc, 3:2) to give **18a** (75%) as dark oil.

**(S)-*Tert*-butyl 2-((R)-2-methoxy-3-((S)-6-oxo-3,6-dihydro-2H-pyran-2-yl)propyl)piperidine-1-carboxylate (38a)**
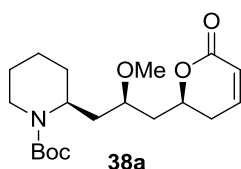
Yield: 75%. $[\alpha]_D$ = -50.20 (c 0.6, CHCl$_3$). IR (neat): ν = 1677, 1721 cm^{-1}. ^{1}H NMR (400 MHz, CDCl$_3$): δ 1.38-1.71 (m, 6H), 1.46 (s, 9H), 1.84-1.92 (m, 2H), 1.99-2.07 (m, 2H), 2.31-2.41 (m, 2H), 2.73 (t, J = 13.3 Hz, 1H), 3.32 (s, 3H), 3.32-3.37 (m, 1H), 3.96 (br s, 1H), 4.43 (br s, 1H), 4.59 (dt, J = 11.4, 6.2 Hz, 1H), 6.02 (d, J = 9.9 Hz, 1H), 6.88 (m, 1H) ppm; ^{13}C NMR (100 MHz, CDCl$_3$): δ 19.6, 25.8, 28.7, 28.9, 29.94, 30.2, 34.6, 40.6, 56.6, 58.0, 74.9, 75.5, 79.7, 121.7, 146.3, 155.3, 164.7 ppm.

(R)-*Tert*-butyl 2-((S)-2-methoxy-3-((R)-6-oxo-3,6-dihydro-2H-pyran-2-yl)propyl)piperidine-1-carboxylate (45a):
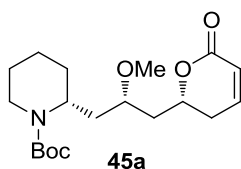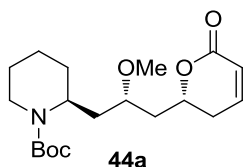

Yield: 64%. $[\alpha]_D$ = + 47.6 (c 0.002, CHCl$_3$). IR: (neat): ν = 1677, 1721 cm^{-1}. <u>NMR as **33b**</u>

(*R*)-*Tert*-butyl 2-((*R*)-2-methoxy-3-((*S*)-6-oxo-3,6-dihydro-2*H*-pyran-2-yl)propyl)piperidine-1-carboxylate (39a)
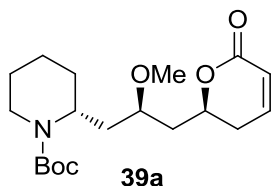

Yield: 68%. $[\alpha]_D$ = - 15.9 (*c* 0.7, CHCl$_3$); IR: (neat): ν = 1677, 1721 cm^{-1}; ^{1}H NMR (400 MHz, CDCl$_3$): δ 1.36-1.58 (m, 7H), 1.44 (s, 9H), 1.91-2.15 (m, 3H), 2.32-2.38 (m, 2H), 2.76-2.82 (m, 1H), 3.24-3.31 (m, 1H), 3.28 (s, 3H), 3.96 (br s, 1H), 4.35 (br s, 1H), 4.55-4.62 (m, 1H), 6.00 (d, *J* = 9.8 Hz, 1H), 6.86 (ddd, *J* = 9.2, 4.5 Hz, 1H) ppm; ^{13}C NMR (100 MHz, CDCl$_3$): δ 19.3, 25.7, 28.7, 29.5, 29.9, 30.2, 34.4, 40.7, 54.0, 57.7, 74.8, 75.0, 79.5, 121.6, 145.2, 155.1, 164.4 ppm.

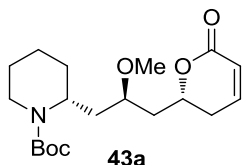**(*S*)-*Tert*-butyl 2-((*S*)-2-methoxy-3-((*R*)-6-oxo-3,6-dihydro-2*H*-pyran-2-yl)propyl)piperidine-1-carboxylate (44a)**

Yield: 71%. $[\alpha]_D$ = + 11.1 (*c* 0.023, CHCl$_3$). IR: (neat): ν = 1677, 1721 cm^{-1}. <u>NMR as **39a**</u>

(*S*)-*Tert*-butyl 2-((*S*)-2-methoxy-3-((*S*)-6-oxo-3,6-dihydro-2*H*-pyran-2-yl)propyl)piperidine-1-carboxylate (40a)
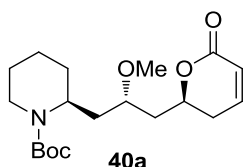

Yield: 69%. $[\alpha]_D$ = - 15.8 (*c* 0.4, CHCl$_3$); IR: (neat): ν = 1677, 1721 cm^{-1}; ^{1}H NMR (400 MHz, CDCl$_3$): δ 1.37-1.59 (m, 7H), 1.46 (s, 9H), 1.92-2.17 (m, 3H), 2.32-2.40 (m, 2H), 2.74-2.83 (m, 1H), 3.23-3.27 (m, 1H), 3.29 (s, 3H), 3.98 (br s, 1H), 4.36 (br s, 1H), 4.61 (td, *J* = 15.4, 6.5 Hz, 1H), 6.01 (d, *J* = 9.8 Hz, 1H), 6.87 (td, *J* = 9.2, 4.2 Hz, 1H) ppm; ^{13}C NMR (100 MHz, CDCl$_3$): δ 19.1, 25.6, 28.5, 28.7, 28.9, 29.4, 33.0, 38.0, 47.5, 55.9, 75.2, 75.4, 79.3, 121.4, 145.0, 155.0, 164.4 ppm.

**(*R*)-T*ert*-butyl 2-((*R*)-2-methoxy-3-((*R*)-6-oxo-3,6-dihydro-2*H*-pyran-2-yl)propyl)piperidine-1-carboxylate (43a)**

Yield: 76%. $[\alpha]_D$ = + 13.3 (*c* 0.001, CHCl$_3$). IR: (neat): ν = 1677, 1721 cm^{-1}. <u>NMR as **40a**</u>

(*R*)-*Tert*-butyl 2-((*S*)-2-methoxy-3-((*S*)-6-oxo-3,6-dihydro-2*H*-pyran-2-yl)propyl)piperidine-1-carboxylate (41a)
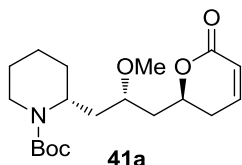

Yield: 77%. $[\alpha]_D$ = + 6.8 (*c* 0.038, CHCl$_3$); IR: (neat): ν = 1677, 1721 cm^{-1}; ^{1}H NMR (400 MHz, CDCl$_3$): δ 1.19-1.77 (m, 17H), 1.78-1.94 (m, 2H), 1.95-2.11 (m, 1H), 2.29-2.48 (m, 2H), 2.67-2.83 (m, 1H), 3.38 (s, 3H), 3.40-3.52 (m, 1H), 3.88-4.05 (m, 1H), 4.56-4.72 (m, 1H), 6.02 (dt, 1H, *J*= 9.8, 1.6 Hz), 6.84-6.92 (m, 1H) ppm; ^{13}C NMR (100 MHz, CDCl$_3$): δ 19.2, 25.7, 28.6, 28.7, 29.8, 30.2, 34.5, 40.7, 56.6, 57.7, 74.8, 75.0, 79.5, 121.6, 145.0, 155.0, 164.4 ppm.

(*S*)-*Tert*-butyl 2-((*R*)-2-methoxy-3-((*R*)-6-oxo-3,6-dihydro-2*H*-pyran-2-yl)propyl)piperidine-1-carboxylate (42a)
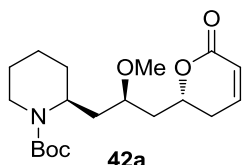

Yield: 81%. $[\alpha]_D$ = - 4.7 (*c* 0.006, CHCl$_3$). IR: (neat): ν = 1677, 1721 cm^{-1}. <u>NMR as **41a**</u>

**General procedure for the cleavage of Boc-group: synthesis of 38b-45b**
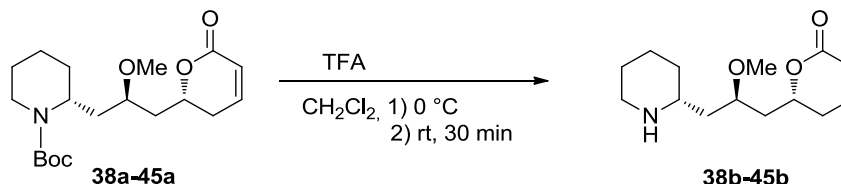
To a stirred solution of compound **38a** (0.352 g, 1 mmol) in CH$_2$Cl$_2$ (2 mL) was added TFA (2 mL) at 0 °C. The reaction mixture was stirred for 30 min. at room temperature. Upon completation, the reaction was quenched with NH$_4$OH 5M at pH 9. The organic layer was dried with Na$_2$SO$_4$ and concentrated under reduced pressure to give **38b** (92%) as colorless oil.

(*S*)-6-((*R*)-2-Methoxy-3-((*S*)-piperidin-2-yl)propyl)-5,6-dihydro-2*H*-pyran-2-one (38b)
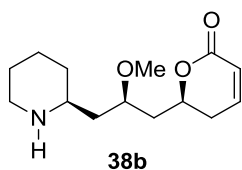

Yield: 91%. [α]$_D$ = -21.2 (*c* 0.8, CHCl$_3$). IR: (neat): ν = 1730 cm^{-1}; ^{1}H NMR (400 MHz, CDCl$_3$): δ 1.33-1.80 (m, 9H), 2.12 (ddd, *J* = 7.2, 7.2, 5.7 Hz, 2H), 2.31-2.38 (m, 2H), 2.70 (dt, *J* = 14.6, 2.6 Hz, 1H), 2.84-2.88 (m, 1H,), 3.16-3.19 (m, 1H), 3.32 (s, 3H), 3.60-3.67 (m, 1H), 4.30 (br s, 1H), 4.50-4.57 (m, 1H), 6.00 (d, *J* = 9.8 Hz, 1H), 6.87 (ddd, *J* = 9.4, 5.1, 3.2 Hz, 1H) ppm; ^{13}C NMR (100 MHz, CDCl$_3$): δ 23.9, 24.5, 29.7, 31.6, 38.2, 39.3, 46.1, 54.0, 56.3, 74.1, 75.0, 121.4, 145.3, 164.4 ppm.

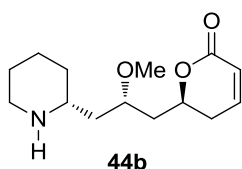**(*R*)-6-((*S*)-2-Methoxy-3-((*R*)-piperidin-2-yl)propyl)-5,6-dihydro-2*H*-pyran-2-one (45b)**
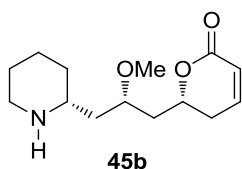
Yield: 92%. [α]$_D$ = + 24.8 (*c* 0.005, CHCl$_3$). IR: (neat): ν = 1730 cm^{-1}. <u>NMR as **38b**</u>

(*S*)-6-((*R*)-2-Methoxy-3-((*R*)-piperidin-2-yl)propyl)-5,6-dihydro-2*H*-pyran-2-one (39b)
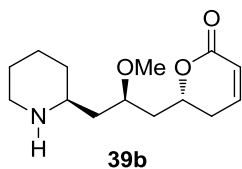
Yield: 82%. [α]$_D$ = - 13.9 (*c* 1.0, CHCl$_3$); IR: (neat): ν = 1730 cm^{-1}; ^{1}H NMR (400 MHz, CDCl$_3$): δ 1.31-1.80 (m, 8H), 2.11 (ddd, *J* = 12.9, 9.6, 6.0 Hz, 1H), 2.31-2.40 (m, 2H), 2.61-2.67 (m, 2H), 3.06-3.09 (m, 1H), 3.26 (br s, 1H), 3.31 (s, 3H), 3.57-3.63 (m, 1H), 4.53 (ddd, *J* = 12.5, 10.6, 5.3 Hz, 1H), 6.01 (d, *J* = 9.9 Hz, 1H), 6.87 (ddd, *J* = 12.9, 9.6, 6.0 Hz, 1H) ppm; ^{13}C NMR (100 MHz, CDCl$_3$): δ 24.6, 25.7, 29.7, 32.7, 38.3, 40.5, 46.9, 55.8, 56.0, 75.0, 75.5, 121.3, 145.1, 164.2 ppm.

(*R*)-6-((*S*)-2-Methoxy-3-((*S*)-piperidin-2-yl)propyl)-5,6-dihydro-2*H*-pyran-2-one (44b)

Yield: 89%. [α]$_D$ = + 12.7 (*c* 0.001, CHCl$_3$). IR: (neat): ν = 1730 cm^{-1}. <u>NMR as **39b**</u>

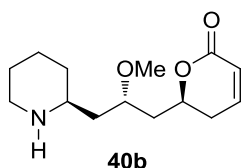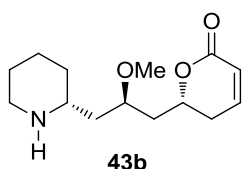**(S)-6-((S)-2-Methoxy-3-((S)-piperidin-2-yl)propyl)-5,6-dihydro-2H-pyran-2-one (40b)**
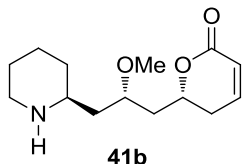

Yield: 85%. $[\alpha]_D$ = - 9.8 (c 0.5, CHCl₃). IR: (neat): ν = 1730 cm⁻¹. ¹H NMR (400 MHz, CDCl₃): δ 1.33-1.80 (m, 8H), 1.86-1.93 (m, 1H), 2.29-2.38 (m, 2H), 2.62-2.72 (m, 2H), 3.09-3.15 (m, 1H), 3.33 (s, 3H), 3.57-3.67 (m, 1H), 4.02 (br s, 1H), 4.57-4.64 (m, 1H), 6.00 (dd, J = 9.8, 1.9 Hz, 1H), 6.84-6.88 (m, 1H) ppm; ¹³C NMR (100 MHz, CDCl₃): δ 22.0, 22.3, 29.1, 30.0, 37.7, 40.0, 45.1, 55.8, 62.1, 74.8, 75.0, 120.9, 145.8, 160.5 ppm.

(R)-6-((R)-2-Methoxy-3-((R)-piperidin-2-yl)propyl)-5,6-dihydro-2H-pyran-2-one (43b)

Yield: 90%. $[\alpha]_D$ = + 6.3 (c 0.001, CHCl₃). IR: (neat): ν = 1730 cm⁻¹. <u>NMR as **40b**</u>

(S)-6-((S)-2-Methoxy-3-((R)-piperidin-2-yl)propyl)-5,6-dihydro-2H-pyran-2-one (41b)

Yield: 87%. $[\alpha]_D$ = - 21.8 (c 0.2, CHCl₃); IR: (neat): ν = 1730 cm⁻¹; ¹H NMR (400 MHz, CDCl₃): δ 2.43-2.01 (m, 10H), 2.32-2.38 (m, 3H), 2.80-2.85 (m, 1H), 3.02 (br s, 1H), 3.34 (br s, 1H), 3.36 (s, 3H), 3.65-3.72 (m, 1H), 4.57-4.65 (m, 1H), 6.01 (dd, J = 10.3, 1.6 Hz, 1H), 6.88 (ddd, J = 9.5, 5.2, 3.1 Hz, 1H) ppm; ¹³C NMR (100 MHz, CDCl₃): δ 23.0, 23.2, 30.0, 37.7, 38.6, 40.3, 44.9, 54.2, 57.2, 74.1, 74.8, 121.2, 145.3, 164.1 ppm.

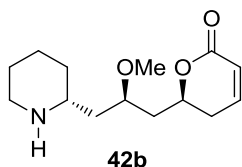**(R)-6-((R)-2-Methoxy-3-((S)-piperidin-2-yl)propyl)-5,6-dihydro-2H-pyran-2-one (42b)**

Yield: 85%. $[\alpha]_D$ = + 21.7 (c 0.009, CHCl₃). IR: (neat): ν = 1730 cm⁻¹. <u>NMR as **41b**</u>

5.7.2. Biological assay

Tubulin purification and assembly assay: Tubulin was purified from bovine brain purchased from a local slaughterhouse, conserved before use in ice-cold PBS and used as soon as possible. According to Castoldi and Popov (2003), pure tubulin was obtained by two cycles of polymerization-depoly-merization in a high-molarity PIPES buffer 1mK-PIPES, pH 6.9, 2 mm EGTA and 1 mm $MgCl_2$), and protein concentration was determined by the MicroBCA assay kit (Pierce). The test the effects on tubulin assembly, **38b-45b** were dissolved in dimethyl sulfoxide (DMSO), added at 50 μM to a reaction mixtures (20 μm tubulin, 10% glycerol, 1 mm GTP in BRB80 buffer) and incubated for 30 minutes at 37 °C. As control conditions were used either unmodified thiocolchicine (10 μM) or DMSO alone. At the end of polymerization, unpolymerized and polymerized fractions of tubulin were separated by centrifugation at 16500xg for 30 minutes at 258 °C. The collected microtubules were resuspended in SDS-PAGE sample buffer (2% w/v SDS, 10% v/v glycerol, 5% v/v b-mercaptoethanol, 0.001% w/v bromophenol blue, and 62.5 mm Tris, pH 6.8) and the unpolymerized tubulin was diluted 3:1 with 4X SDS-PAGE sample buffer. Equal proportions of each fraction were resolved by a 7.5% SDS-gel and stained with Coomassie blue. Densitometric analyses of stained gels were performed by using ImageJ software (National Institute of Health), and data were elaborated using STATISTICA (StatSoft Inc., Tulsa, OK). Significant differences were assessed by one-way ANOVA with Fisher HSD post hoc test. Experiments were done in triplicate and data are expressed as means ± SEM.

Chapter 6

Design and synthesis of triazole-epothilones

6.1. Introduction

After the elucidation of taxol's biological mechanism in 1979,[18] it took more than a decade before other microtubule-stabilizing agents with no-taxol-like structures were discovered. Among these new microtubule stabilizers, the most notable are the epothilones, which are myxobacterial-derived macrolides first isolated from the myxobacterium *Sorangium cellulosum Sc 90* by Reichenbach and Höfle.[102]

Originally, the major products isolated from the fermentation broth were epothilone A and epothilone B, but many other members of this natural products family have subsequently been obtained from myxobacteria (Figure 49).[103]
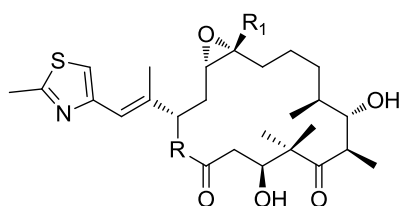
Epothilone A: R = O, R1 = H
Epothilone B: R = O, R1 = CH$_3$

Figure 49

Structurally, Epothilones A and B are 16-membered polyketide macrolactones that have a methylthiazole moiety connected to the macrocycle by a short olefinic spacer. The polyketide backbone of the molecule is synthesized by a type I modular polyketide synthase (PKS) through nine PKS modules, whereas the thiazole ring is derived from a cysteine incorporated by a single nonribosomal peptide synthetase (NRPS) (Figure 50).[104]

---

[102] K. Gerth; N. Bedorf; G. Höfle; H. Irschik; H. Reichenbach; *J Antibiot.*, **1996**, *49*, 560.

[103] I. H. Hardt; H. Steinmetz; K. Gerth; F. Sasse; H. Reichenbach; G. Höfle; *J. Nat. Prod.*, **2001**, *64*, 847.

[104] I. Molnár; T. Schupp; M. Ono; R.E. Zirkle; M. Milnamow; B. Nowak-Thompson; N. Engel; C. Toupet; A. Stratmann; D.D. Cyr; J. Gorlach; J.M. Mayo; A. Hu; S. Goff; J. Schmid; J.M. Ligon; *Chem.& Biol.*, **2000**, *7*, 97.
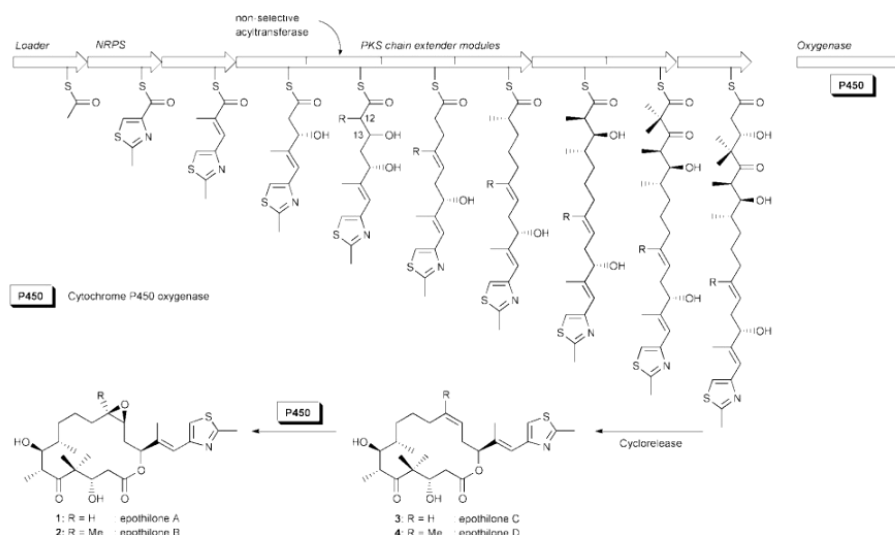
Figure 50: Structure of the epothilone biosynthetic gene cluster from Sorangium cellulosum. NRPS = non-ribosomal peptide synthase, PKS = polyketide synthase

Epothilones, in contrast to taxol, can inhibit the growth of multidrug-resistant cancer cell lines at concentrations similar to or only slightly higher than those required against drug-sensitive cancer cells, including cells whose developed a taxol resistance mediated by specific tubulin mutations. As anticipate in the *paragraph 1.1.3*, Epo A and B were quickly adopted as attractive targets for total synthesis as lead structures for anticancer drug discovery.

Thanks to biological tests, it was possible to gain that the lactone ring of the epothilones was sensitive to esterase cleavage. In fact, the incubation of epothilone B in mouse plasma led to loss of its cytotoxic activity and resulted in a metabolite with a mass 18 units higher than the parent drug.

This feature prompt toward the synthesis of the lactam analogues of epothilone B, the most potent member of the family, with the goal of improving metabolic stability. The key insight into the semisynthetic approach to the epothilone lactam was represented by the fact that the epothilone lactone is allylic and therefore possibly susceptible to a palladium-catalyzed ring opening to form a π-allylpalladium complex, which could be trapped by a nitrogen nucleophile. The reaction of unprotected epothilone B with NaN_3 in the presence of $Pd(PPh_3)_4$ led to azido acids **46** as a single diastereomer. The azide is formed with net retention of configuration likely through anti-attack by palladium and then reaction with azide from the face opposite the palladium. The one-pot process including the reduction of the azide with trimethyl phosphine and macrolactam formation with EDCI/HOBt, provides the desired lactam, later to be named ixabepilone, in 23% overall yield (Scheme 21).

Epothilone B

Ixabepothilone B

46
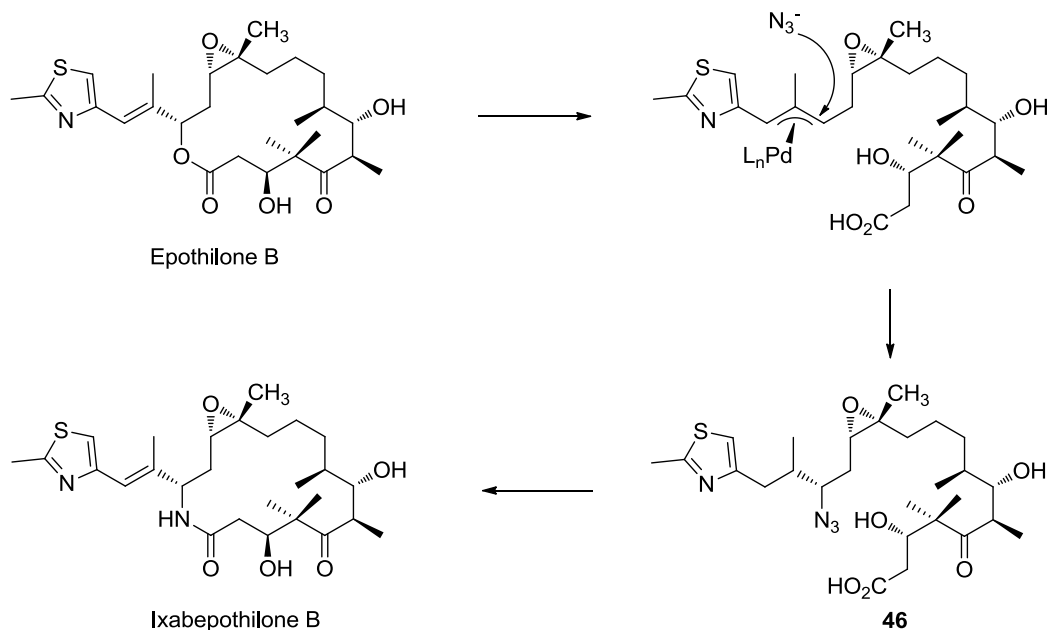
Scheme 21

In vivo studies established that the lactam analogue exhibits antitumor activity similar to that of Taxol in Taxol-sensitive tumor models and also more potent than Taxol in Taxol-resistant tumor models. In addition, it provides major stability to hydrolysis on incubation in both mouse and human sera. Based on its highly profile, Epo B lactam in 2007 was approved by the FDA for the treatment of metastatic or advanced breast cancer.[105]

6.1.1. Binding site and structure-activity relatioship

Apart from Taxol, the epothilones were the first natural products known to stabilize microtubules triggering apoptosis. Furthermore, their significantly higher activity and their undiminished effectiveness against multiresistant tumor cells have raised the possibility that epothilones could potentially replace taxanes. After the publication of the electron-crystallographic structure of the epothilone A/tubulin complex,[106] and the NMR-generated structures through molecular dynamics modelling procedures, the interactions of epothilone A with β−tubulin were described in detail for the first time. As expected, epothilone binds within a cavity on the surface of β-tubulin. This binding site, overlapping with that of Taxol, is partly constituted by the so-called M-loop, which is also essential for lateral contacts between protofilaments in the Zn^{2+}-induced tubulin layers and in microtubules. Stabilization of the M-loop, and therefore of lateral contacts between protofilaments, ultimately stabilizes growing microtubules, preventing their depolymerization once formed (Figure 51).

[105] a) K.-H. Altmann; F. Z. Gaugaz; R. Schiess; *Mol. Divers.* **2011,** *15*, 383; b) John T. Hunt; *Mol. Cancer. Ther.,* **2009**, *8 ;*275.
[106] J. H. Nettles; H. Li; B. Cornett; J. M. Krahn; J. P. Snyder; K. H. Downing; *Science*, **2004**, *305*, 866.
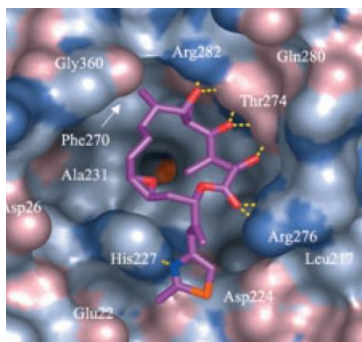
Figure 51: The Taxol/epothilone binding cavity in β-tubulin from the corresponding electron-crystallographically obtained structures with bound epothilone. For β-tubulin the surface of the molecule is depicted (C: gray, O: dark pink, N: gray-blue). Epothilone A (C: violet, O: red, N: blue) are represented as stick models.

Direct comparison of epothilone binding with Taxol binding indicates that the smaller epothilone molecule fills only about half of the Taxol-binding cavity in β-tubulin. The hypotheses concerning a common pharmacophore can thus finally be laid to rest, since the Taxol/β-tubulin interactions differ fundamentally from those in the epothilone A/tubulin complex.[107]

In addition to these results, the extensive chemical synthesis–chemical biology study of hundreds of epothilone analogues was helpful for a structure– activity relationship analysis (Figure 52).
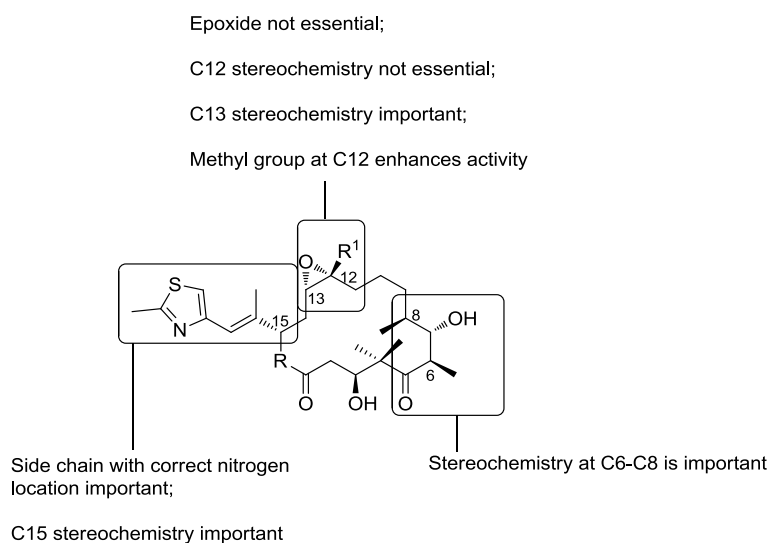

Figure 52

The configurations at C6–C8 are essential for the biological activity, probably because this region strongly influences the overall conformation of the macrocycle through steric and/or stereoelectronic effects. There was initially some speculation that the epoxide oxygen of epothilone played a role as a hydrogen bond acceptor, but after independent reports by several groups it became clear that the epoxide moiety is not essential for biological activity. However, a substituent at C12, particularly a methyl group, consistently enhances the activity. The side chain

---

[107] D. W. Heinz; W.-D. Schubert; G. Hofle; *Angew. Chem. Int. Ed,.* **2005**, *44*, 1298.

is also highly important for biological activity, and finally, the stereochemistry at C15 play a fundamental role, with C15 epimers being lacking of any biological activity.

6.2. Aim of this work

The chemistry and biology of epothilones have been extensively studied, and numerous analogs or derivatives have been discovered that retain potent in *vitro* activity.[108] Our interest is focused on developing strategies for the total synthesis of novel triazole-epothilones derivative **47** for chemical and biological studies as microtubule-inhibitors (Figure 53).
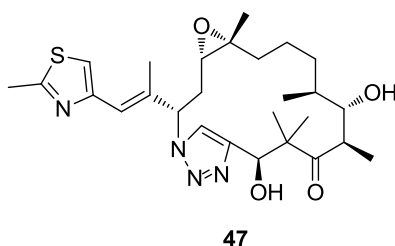

47

Figure 53

Since the lattam derivative ixabepilone is the best candidate in this class so far, the idea of the introduction of a triazole moiety into the epothilone arised from the already well-known concept of biososterism defined by Langmuir in 1919. The main criteria for isosterism is that two isosteric molecules must present similar, if not identical, volumes and shapes. Triazoles are not encountered in nature but they have found increasing importance in the field of drug research as a bioisostere of the amide linkage and have been established to be resistant against enzymatic degradation.[109]

6.3. Docking studies

Previous docking studies, performed by Prof. Sironi and Dott. Pieraccini of Milan University, indicate that triazole analoge **47** and ixabepilone share the same binding site on β-tubulin with very similar hydrophobic interaction with the biological target. In both molecules a weak Hydrogen bond is present between the OH group on C7 and an arginine residue for ixabepilone and an istidine residue for the triazole-epothilone.

Indeed, the three nitrogen atoms of triazole ring are directed to the inside of macrocyle (Figure 54).

---

[108] K. C. Nicolaou; A: Ritzén; K. Namoto; *Chem. Comm.*, **2001**, 1523.

[109] a) W. S. Horne; M. K. Yadav; C. D. Stout; M. R. Ghadiri; *J. Am. Chem. Soc.*, **2004**, *126*, 15366.
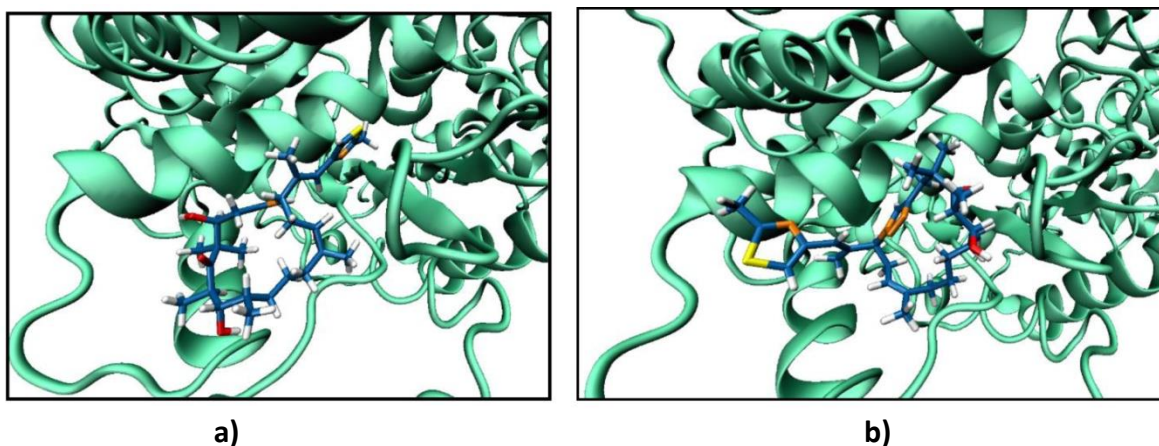
Figure 54: Docked structures of **a)** ixabepilone in the β-tubulin binding site and of **b)** triazole-epothilone **47** on the β-tubulin binding site.

Indeed, Figure 55 shows that the triazole ring induces a modification in term of arrangement of thiazolic chain of macrocycle compared with the commercial one.
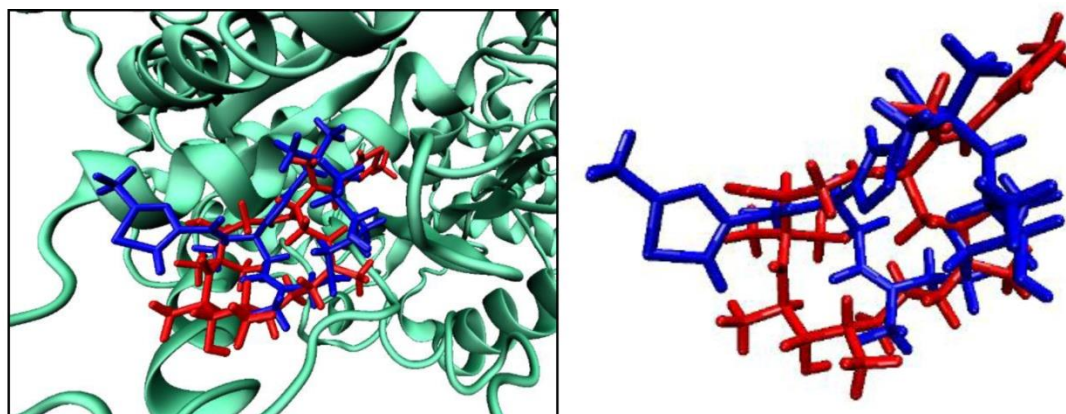

Figure 55: overlapping docked structures of ixabepilone (red) and triazole-epothilone **47** (blue)

6.4. Chemistry

Inspection of the structure of triazole-epothilone **47** revealed the intriguing possibility of applying the Huisgen cycloaddition between fragments **E** and **F** to yield the triazole derivative **C**, which can react with **D** in an aldol condensation giving **B**. The Ring Closing Metathesis (RCM) reaction to bis(terminal) olefin **B** affords the bicyclic product **A**, which could be converted to the analogue of natural product **47** by simple epoxidation, as retrosynthetically outlined in Scheme 22.

Scheme 22
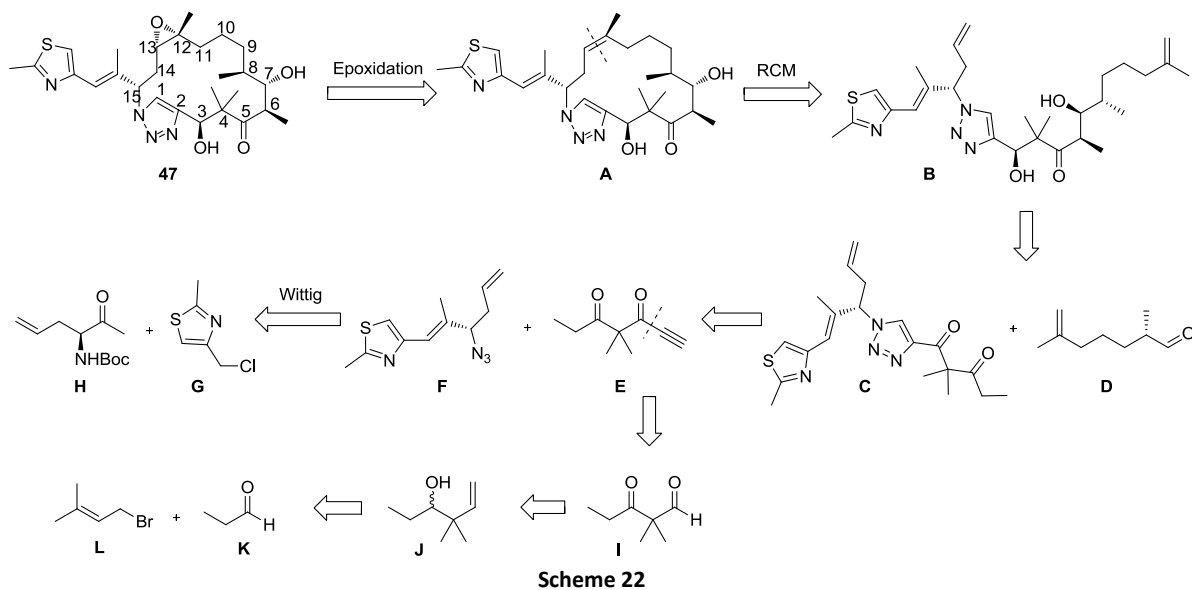
Proceeding with the retrosynthetic analysis, the witting reaction was identified as a method to permit disconnection of **F** to its components, chloromethyl-thiazole **G** and the enantiopure allyl-compound **H**. The alkyne moiety **E** allowed the indicated disconnection, defining aldehyde **I** and vinyl magnesium bromide as potential intermediates. Aldehyde **I** could then be derived from intermediate **J**, whose aldol-type condensation of the two commercial available products **L** and **K** was straightforward.

In conclusion, this retrosynthetic analysis led to identify 4 main intermediate fragments:

- ➢ Fragment **C15 – C19** (intermediate **F**)
- ➢ Fragment **C1 – C6** (Intermediate **E**)
- ➢ Fragment **C13 – C6** (Intermediate **C**)
- ➢ Fragment **C7-C13** (Intermediate **D**)

6.4.1.Synthesis of fragment F

Fragment **F** is summarized in Scheme 23. Starting from the commercially available *L*-allylglycine, protection and conversion to the aldehyde **50** using DIBAL-H was followed by an alkylation with methyl-magnesium bromide to yield the secondary alcohol **51**. (Scheme 23).

Synthesis of **52**
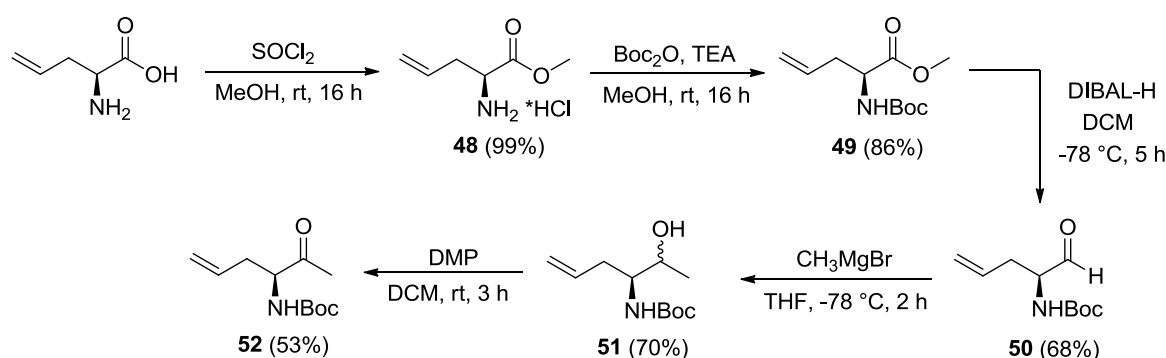
Synthesis of ylide **54**

Wittig reaction

Scheme 23

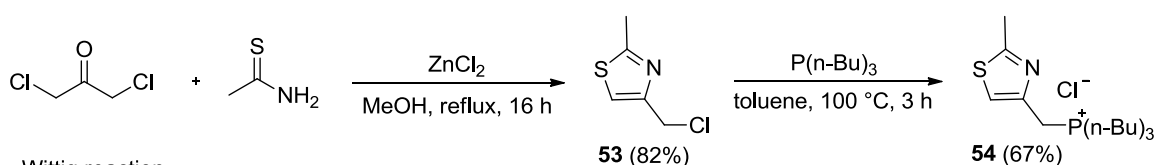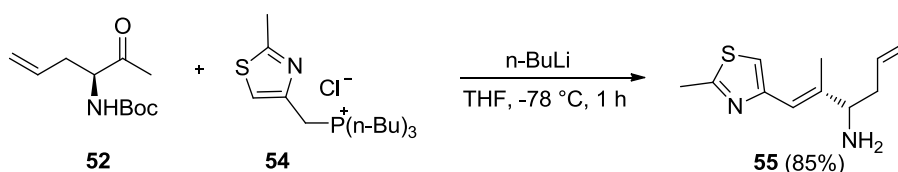The compound **52** was then obtained through an oxidation reaction with Dess Martin periodinane in 53% of yield. This participated in a Wittig coupling with the easily prepared ylide **54** giving the compound **55**. The *E*-configuration of double bond was confirmed by NOESY experimental where the presence of a cross peak between the hydrogen of NH group and the hydrogen of CH of double bond indicates their proximity. Finally, the free amine group was converted to azide **57** with the transfer agent 1*H*-imidazole-1-sulfonyl azide, which corresponds to the C15–C19 region of the epothilone derivative (Scheme 24).
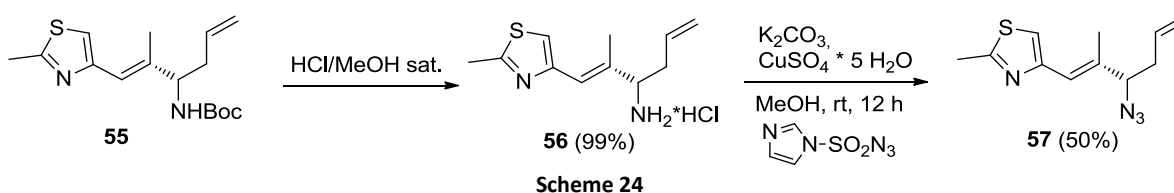
Scheme 24

6.4.2. Synthesis of fragment E

The synthesis of the fragment **E** was performed following the published procedure by Ramachandran.[110] The reaction between dimethylallylmagnesium bromide and propionaldehyde furnished the alcohol **58** which was oxidised to the corresponding chetone **59**. The terminal double bond was then converted to aldehyde by ozonolisis reaction, followed by a Grignard

---

[110] P. V. Ramachandran; J. S. Chandra; B. Prabhudas; D. Pratihar; M.V. R. Reddy; *Org. Biomol. Chem.*, **2005**, *3*, 3812.

reaction in order to introduce the alkyne function into the molecule (**61**). A final oxidation with DMP gave the alkyne **62** in 80% of yield (Scheme 25).
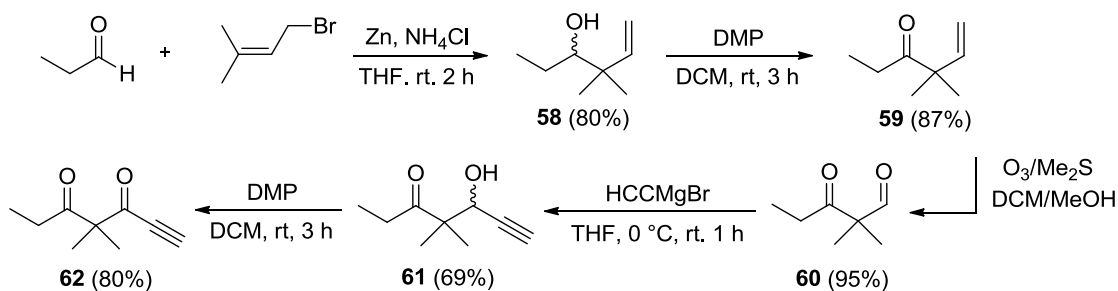
Scheme 25

6.4.3. Synthesis of fragment C

The key intermediate **C** containing the triazole ring was obtained thanks to a Huisgen 1,3-dipolar cycloaddition between the alkyne compound **62** and the azide **57** (Scheme 26).

Scheme 26

The formation of triazoles from azides and terminal alkynes catalyzed by Cu(I) is normally a robust reaction, which could be performed under a wide variety of conditions and with almost any source of solvated Cu(I). The most impor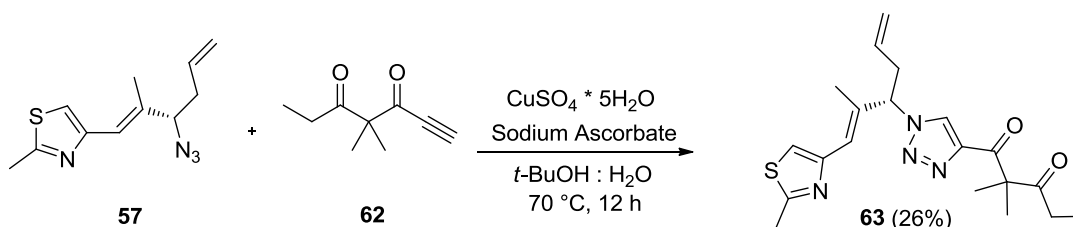tant factor seems to be maintaining the Cu(I) at a high level at all times during reaction. This is why the use of a Cu(II) source with addition of a reducing agent in a large excess has been one of the preferred methods.[111] Therefore, following the Sharpless conditions, in our case the reaction was performed with copper(II) sulphate pentahydrate as catalyst, sodium ascorbate as reducing agent in 1:1 mixture of *t*-BuOH and water at 70 °C for 12 hours. The yield was not satisfactory (only 26%), but the starting material were recovered. The same reaction was carried out by microwave activation using THF:H$_2$O 1:1 as solvent but it furnished an inseparable mixture of 1,4- and 1,5-triazole derivatives only.

6.4.4. Synthesis of fragment D

The synthesis of fragment C7-C13, representing the intermediate **D**, was accomplished starting from the commercial available compound **64**. A Wittig reaction with methyl-triphenylphosphine converted the ketone group to a terminal olefin **65**. Then, an Evans asymmetric alkylation was chosen for the introduction of the chiral center. For that, the olefin **65** was treated with oxalyl

---

[111] M. Meldal; C. W. Tornøe; *Chem. Rev.,* **2008**, *108*, 2952.

chloride to generate in *situ* the acyl chloride of carboxylic acid and then with (*R*)-(+)-4-isopropyl-2-oxazolidinone obtaining **66** (Scheme 27)**.**
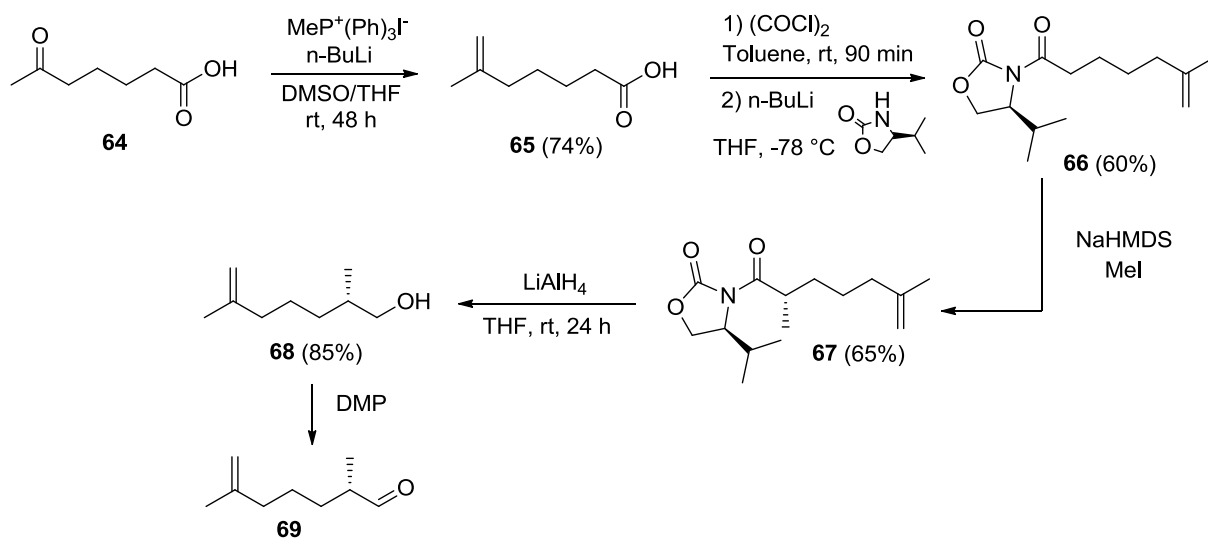
Scheme 27

Its enolate was generated by the action of NaHMDS in THF at -78 °C, followed by the reaction with excess methyl iodide to afford alkylation product **67**, which was isolated in 67% yield (diastereoselectivity of the alkylation 10:1 by ^{1}H NMR spectroscopy of the crude product). Reductive removal (LiAlH$_4$) of the auxiliary furnished alcohol **68**, which should be converted to the aldeyde **69** by Dess-Martin oxidation (reaction doesn't carry out).[112]

6.5. Conclusion

In order to reach the final epothilone derivatives **47** other reactions are necessary. In particular:

1. Regio- and stereoselective reduction of carbonilic group on C3 affording **70**. This reaction may be performed using (+)-DipCl on the alkyne derivative **62**, as reported in literature,[110] or through a hydrogenation process catalysed by [RuCl$_2$(R)-BINAP)]$_2$[Net$_2$], method already used for an analogue of the intermediate **63** (Scheme 28).[113]

[112] D. Schinzer; A. Bauer; J. Schieber; *Chem. Eur. J.* **1999**, *5*, 2492.
[113] K.C. Nicolaou; A. Ritzen; K. Namoto; *Chem. Comm.*, **2001**, 1523.
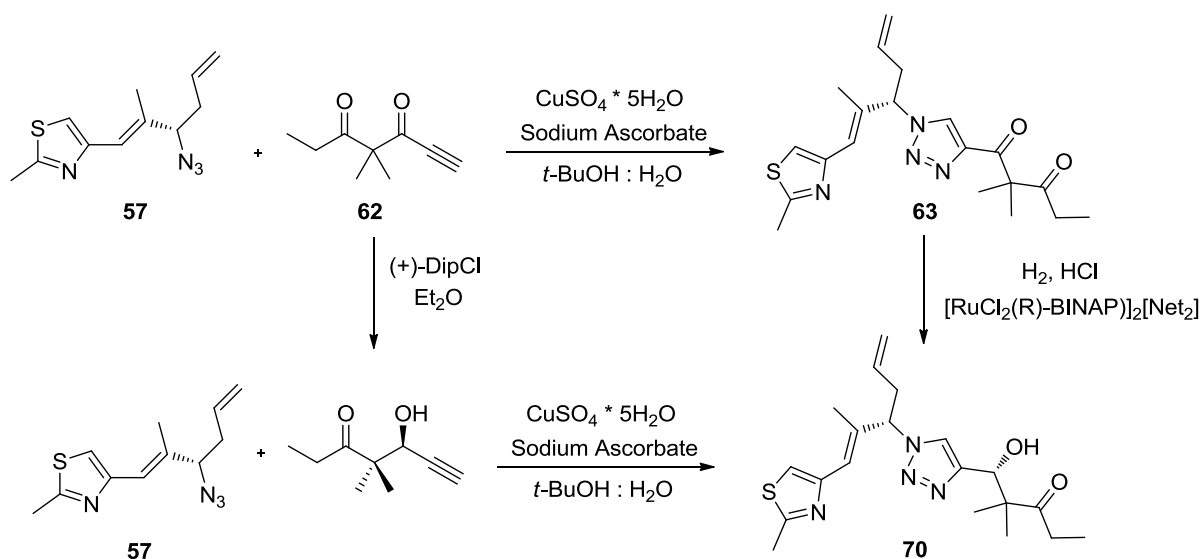
Scheme 28

Aldol condensation between **69** and **70** affording the bis(terminal) olefin **71** using the conditions reported by K. C. Nicolau in the synthesis of epothilone B (Scheme 29).[114]
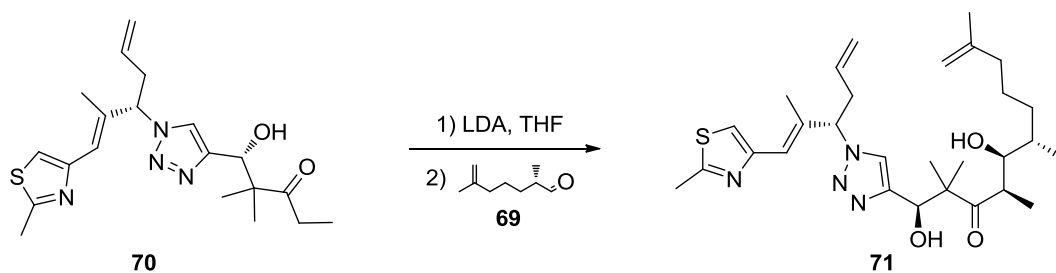
Scheme 29

2.　　Ring closing metathesis reaction on compound **71** in order to form the macrolactone **72**, followed by epoxidation of endocyclic double bond (Scheme 30).

---

[114] K.C. Nicolaou; Y. He; F. Roschangar; F. Sarabian; S. Ninkovic; Z.Yang; J.I. Trujillo; *J. Am. Chem. Soc.,* **1997**, *119,* 7960.
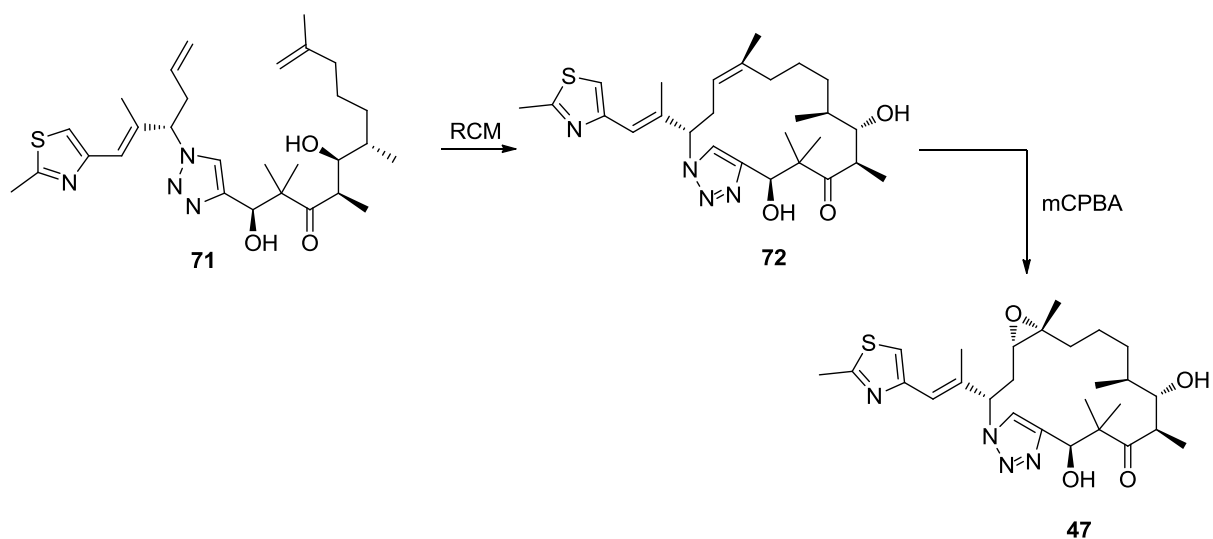
Scheme 30

Upon completed the synthesis, biological assay will be performed to check the antimicrotubule activity either on cancer cells or in Parkinson's disease, in which recently is emerged the role of microtubule dysfunction and the positive response obtained from black mice daily treating with EpoD.[115]

[115] D. Cartelli; F. Casagrande; C. L. Busceti; D. Bucci; G. Molinaro; A. Traficante; D. Passarella; E. Giavini; G. Pezzoli; G. Battaglia; G. Cappelletti; *Sci. Rep.*, **2013**, *3*, 1837.

6.6. Experimental part

6.6.1. Synthesis of fragment F

Compound 49 was prepared following the reported procedure.[116]

(S)-2-(Tert-butoxycarbonylamino)-4-pentenal (50)

To a solution of **49** (1.03 g, 4.5 mmol) at -78 °C in 34 mL of CH_2CL_2, DIBAL-H was added dropwise and then the solution was stirred for 4 hours at the same temperature under inert atmosphere. After the r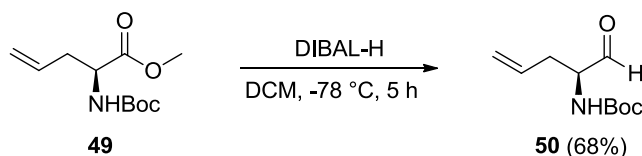eaction was completed, 434 μL of MeOH and 1.7 mL of a saturated solution of Na_2SO_4 were added at -78 °C and the mixture was stirred at room temperature overnight. Finally, 2.26 g of Na_2SO_4 were added, the mixture was filtered, and the solvent was evaporated under vacuum. The residue was purified by column chromatography on silica gel (Hexane /EtOAc 4:1) to give **50** as colourless oil.

Yield: 68%. $[\alpha]_D$ = + 3.0 (c 1.05, $CHCl_3$); ^{1}H NMR (300 MHz, $CDCl_3$): δ 1.44 (s, 9H), 2.44-2.62 (m, 2H), 4.25-4.27 (m, 1H), 5.06-5.19 (m, 3H), 5.63-5.78 (m, 1H), 9.59 (s, 1H) ppm; ^{13}C NMR (75 MHz, $CDCl_3$): δ 28.3, 33.7, 59.0, 77.4, 119.5, 131.9, 199.6 ppm.

(S)-3-(Tert-butoxycarbonylamino)-hex-5-en-2-ol (51)
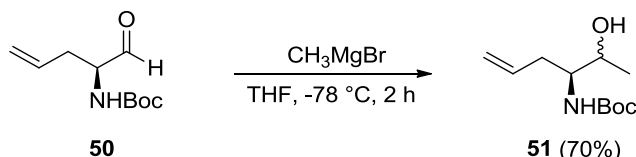
To a solution of **50** (607 mg, 3 mmol) in 30 mL of Et_2O, methylmagnesium bromide (2.28 mL, 6.8 mmol) was added at -78 °C and the mixture was stirred 1 hour at 0 °C. The reaction was quenched with 20 mL of saturated solution of NH_4Cl, the phases were separated and the aqueous layer was extracted with Et_2O (3x15 mL). The unified organic phases were dried over Na_2SO_4 and the solvent was evaporated under vacuum. The residue was purified by column chromatography on silica gel (Hexane /EtOAc 3:1) to give **51** as colourless oil.

Yield: 70%. ^{1}H NMR (300 MHz, $CDCl_3$): δ 1.15-1.21 (m, 3H), 1.42 (s, 9H), 2.05-2.37 (m, 2H), 3.50 (bs, 1H), 3.65 (bs, 1H), 3.78-3.85 (m, 1H), 4.74 (bs, 1H), 5.05-5.13 (m, 2H), 5.72-5.86 (m, 1H), ppm; ^{13}C NMR (75 MHz, $CDCl_3$): δ 20.5, 28.4, 36.9, 55.3, 68.9, 79.4, 117.7, 134.7, 156.5 ppm.

---

[116] Patent: GLAXO WELLCOME MANUFACTURING PTE LTD, *WO2009/133135 A1*, **2009**.

(S)-3-(Tert-butoxycarbonylamino)-hex-5-en-2-one (52)
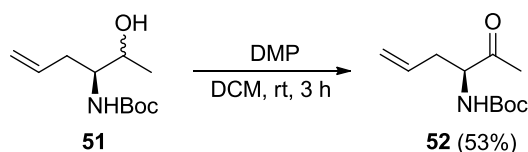
To a solution of alcohol **51** (450 mg, 2.1 mmol) in DCM (30 mL), Dess-Martin periodinane (1.24 g, 2.9 mmol) was added and the new mixture was stirred for 2 h at room temperature. After the completion of the reaction, the solvent was evaporated in vacuum, the residue was recovered with 15 mL of Et_2O and washed with a solution composed by 8 g of $Na_2S_2O_3$ in 20 mL 80% solution of $NaHCO_3$. The phases were separated and the aqueous layer was extracted 3 times with Et_2O. The combined organic layers were washed with $NaHCO_3$ (20 mL), water (2x15 mL) and brine 2x10 mL), dried with $Na_2SO_4$, filtered and evaporated. The residue was purified by flash column chromatography (Hex/EtOAc 3:1) to provide ketone **52** as light yellow oil.

Yield: 53%. $[\alpha]_D$ = + 2.27 (c 1.13, MeOH); ^1H NMR (300 MHz, $CDCl_3$): δ 1.42 (s, 9H), 2.18 (s, 3H), 2.34-2.63 (m, 2H), 4.31-4.37 (m, 1H), 5.08-5.19 (m, 3H), 5.58-5.71 (m, 1H) ppm; ^{13}C NMR (75 MHz, $CDCl_3$): δ 27.2, 28.3, 35.7, 59.3, 79.8, 119.0, 132.2, 155.3, 206.5 ppm; MS: m/z 236 [M+Na]$^+$.

Compound 53 was prepared following the reported procedure.[117]

Tributyl((2-methylthiazol-4-yl)methyl)phosphonium chloride (54)
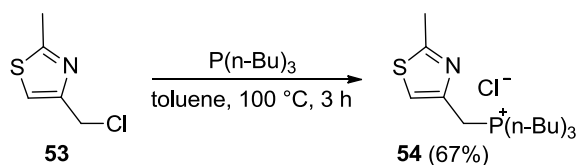
To a solution of **53** (275 mg, 1.9 mmol) in 3 mL of dry toluene, P(n-Bu)$_3$ (0.918 mL, 3.7 mmol) was added under nitrogen atmosphere. The reaction was stirred at 100 °C for 3 hours. Then, the solvent was evaporated under vacuum and the residue was purified by column chromatography on silica gel (DCM/MeOH 9:1) to give **54** as white solid.

The NMR data are consistent with those reported in literature.[118]

(3S,1E)-3-(Tert-butoxycarbonyl)amino-2-methyl-1-(2-methylthiazol-4-yl)hexa-1,5-diene (55)
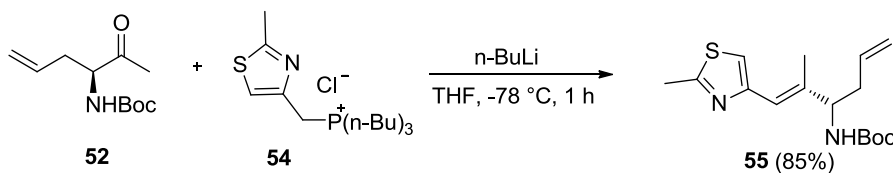
[117] J.-C. Jung; R. Kache; K. K. Vines; Y.-S. Zheng; P. Bijoy; M. Valluri; M. A. Avery; *J. Org. Chem*, **2004**, *69*, 9269.
[118] J. Mulzer; A. Mantoulidis; E. Oehler; *J. Org. Chem.*, **2000**, *65*, 7456,

To a solution of **54** (371 mg, 1.1 mmol) in 3 mL of dry THF, *n*-BuLi (0.662 mL, 1.1 mmol) was added dropwise at 0 °C under nitrogen atmosphere and the mixture was stirred for 15 minutes. Then, **52** was added at 0 °C and the temperature was allowed to rise up to rt. After 1 hour the reaction was completed (checked with TLC) and it was quenched with saturated solution of NH_4Cl (6 mL). The phases were separated and the aqueous layer was extracted 3 times with AcOEt. The combined organic layers were dried over Na_2SO_4, filtered and evaporated. The residue was purified by flash column chromatography (Hex/EtOAc 3:1) to provide ketone **55** as light yellow oil.

Yield: 85%. $[\alpha]_D$ = - 21.5 (*c* 0.625, MeOH); ^{1}H NMR (400 MHz, $CDCl_3$): δ 1.48 (s, 9H), 2.07 (s, 3H), 2.35-2.46 (m, 2H), 2.76 (s, 3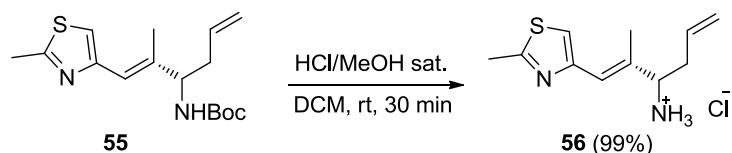H), 4.24 (bs, 1H), 4.72 (bs, 1H), 5.10-5.18 (m, 2H), 5.72-5.83 (m, 1H), 6.49 (s, 1H), 6.96 (s, 1H) ppm; ^{13}C NMR (100 MHz, $CDCl_3$): δ 16.1, 18.9, 28.4, 38.1, 56.8, 79.5, 115.4, 118.0, 118.3, 134.0, 140.4, 155.3, 164.9 ppm; MS: m/z 331 [M+Na]$^+$.

(*3S,1E*)-2-methyl-1-(2-methylthiazol-4-yl)hexa-1,5-dien-3-aminium chloride (55)

To a solution of **55** (114 mg, 0.5 mmol), the saturated solution of HCl in MeOH was added and the reaction was stirred for 30 minutes at room temperature. After completion, checked by TLC (Hex/AcOEt 2:1), the solvent was removed under vacuum. The crude product was used in the next step without further purification.

Yield: 99%. ^{1}H NMR (300 MHz, CD_3OD): δ 2.08 (s, 3H), 2.58-2.65 (m, 2H), 2.95 (s, 3H), 4.03 (t, *J* = 7.4 Hz, 1H), 5.20-5.30 (m, 3H), 5.71-5.85 (m, 1H), 6.59 (s, 1H), 7.81 (s, 1H) ppm; ^{13}C NMR (75 MHz, CD_3OD): δ 15.1, 19.4, 41.3, 58.1, 115.4, 116.0, 119.2, 123.1, 132.7, 138.1, 154.8, 168.1 ppm.

(*3S,1E*)-3-Azido-2-methyl-1-(2-methylthiazol-4-yl)hexa-1,5-diene (57)
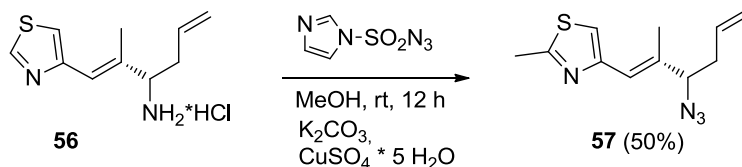
The salt **56** (39 mg, 0.2 mmol) was dissolved in MeOH (0.7 mL) and K_2CO_3 (125 mg, 0.9 mmol), $CuSO_4$ pentahydrate (0.4 mg, 0.02 mmol), and 1*H*-imidazole-1-sulfonyl azide (50 mg, 0.24 mmol) were added. The reaction was stirred at room temperature for 12 hours, then the solvent was removed under vacuum. The residue was purified by flash column chromatography (Hex/EtOAc 9:1) to provide azide **57** as yellow oil.

Yield: 50%. IR: (neat): ν = 2094 cm^{-1}; ^{1}H NMR (300 MHz, CDCl$_3$): δ 2.07 (s, 3H), 2.31-2.44 (m, 2H), 2.74 (s, 3H), 4.01-4.06 (m, 1H), 5.08-5.17 (m, 2H), 5.68-5.82 (m, 1H), 6.54 (s, 1H), 7.01 (s, 1H) ppm.

6.6.2. Synthesis of fragment **C**

Compound 62 was prepared following the reported procedure.[110]

Synthesis of (3S,1E)-2,2-dimethyl-1-(1-(2-methyl-1-(2-methylthiazol-4-yl)hexa-1,5-dien-3-yl)-1H-1,2,3-triazol-4-yl)pentane-1,3-dione (63)
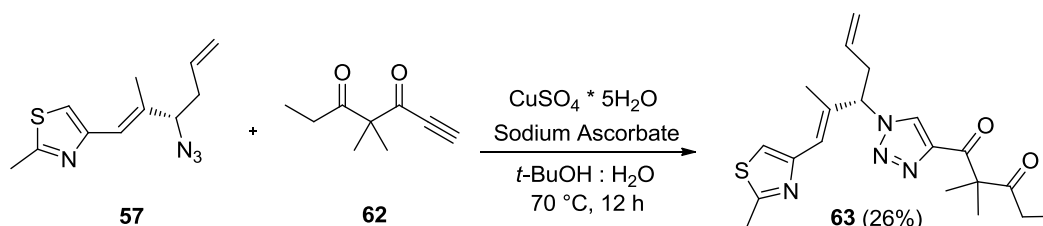

To a solution of **57** (19 mg, 0.08 mmol) and **62** (61 mg, 0.4 mmol) in *t*-BuOH:H$_2$O (1:1, 1 mL), CuSO$_4$*5H$_2$O and sodium ascorbate were added and the mixture was heated at 70 °C for 12 hours. Then the *t*-BuOH was evaporated under vacuum, water was added and the residue was extracted with DCM (3x5 mL). The combined organic layers were dried over Na$_2$SO$_4$, filtered and evaporated. The residue was purified by flash column chromatography (Hex/EtOAc 3:1) to provide triazole **63** as yellow oil.

Yield: 26%. ^{1}H NMR (400 MHz, CDCl$_3$): δ 1.09 (t, *J* = 1.4 Hz, 3H), 1.5 (s, 6H), 2.03 (s, 3H), 2.65 (q, *J* = 1.4 Hz, 2H), 2.80 (s, 3H), 2.92-2.99 (m, 1H), 3.05-3.12 (m, 1H), 5.11-5.20 (m, 3H), 5.67-5.77 (m, 1H) 6.71 (s, 1H), 7.09 (s, 1H), 8.13 (s, 1H) ppm; ^{13}C NMR (100 MHz, CDCl$_3$): δ 7.9, 15.0, 18.6, 22.4, 29.7, 36.3, 60.0, 68.9, 117.6, 119.3, 122.3, 126.2, 132.1, 136.4, 145.8, 150.4, 166.3, 194.3, 211.2 ppm; MS: m/z 409 [M+Na]$^+$.

6.6.3. Synthesis of fragment **D**

Compound 66 was prepared following the reported procedure.[119]

Compound 68 was prepared following the reported procedure.[112]

---

[119] M. M. Alhamadsheh; S. Gupta; R. A. Hudson; L. Perera; L. M. V. Tillekeratne; *Chem. Eur. J.*, **2008**, *14*, 570.

Chapter 7

In vivo trapping of polyketide intermediates from a Type I Polyketide Synthase

7.1. Introduction

7.1.1. Polyketide synthase

Polyketides are a large family of natural products found in bacteria, fungi and plants, which exhibit a staggering range of functional and structural diversity and boast a wide range of medicinally important activities, including antibiotic, anticancer, antifungal, antiparasitic and immunosuppressive properties (Figure 56).[120]

Daunomycin   Erytromycin A
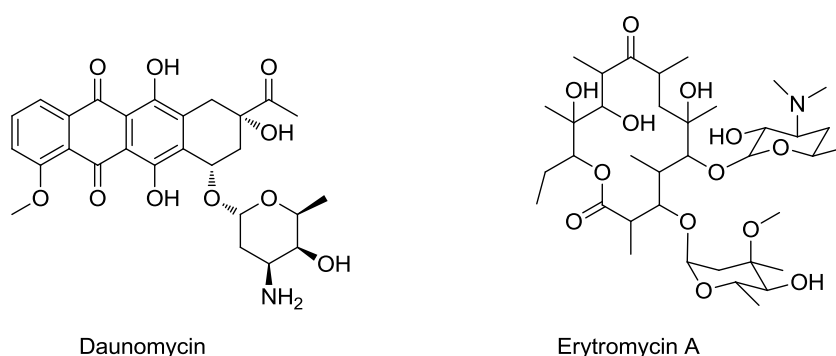
Figure 56

Even before the full extent of their utility was known, scientists became interested in how these complicated molecules are assembled. The unique structures of thousands of polyketides arise from coordinated, multistep action of enzymes organized in assembly lines, termes polyketide synthases (PKSs). The chemical logic for their assembly is that a small set of monomer units are incorporated into a linear oligomer by successive rounds of decarboxylative Claisen condensations between a thioesterified malonate derivative and an acyl thioester. Tipically the monomers are acetylCoA, malonyl-CoA, methylmalonyl-CoA, with the carboxyl group activated for capture by nucleophiles (Figure 57).[121]

malonyl-CoA   methylmalonyl-CoA   acetyl-CoA
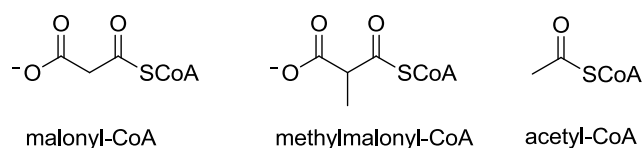
Figure 57

Three types of bacterial PKSs are known to date: type I, type II and type III PKS, but in this thesis only type I will be described.

The modular system is the classic bacterial type I PKS, best exemplified by the PKS responsible for assembling the 6-deoxyerythronolide B (6-DEB) scaffold of erythromycin A (Figure 58).

---

[120] B. Shen; *Curr. Opin. Chem. Bio.*, **2003**, 7:285
[121] M. A. Fischbach; C. T. Walsh; *Chem. Rev.*, **2006**, *106*, 3468.

Figure 58

This PKS assembles seven precursors consisting of one propionyl-CoA starter unit and six (2*S*)-methylmalonyl-Coenzyme A (CoA) extender units into 6-DEB. The role each of these type of precursors plays in p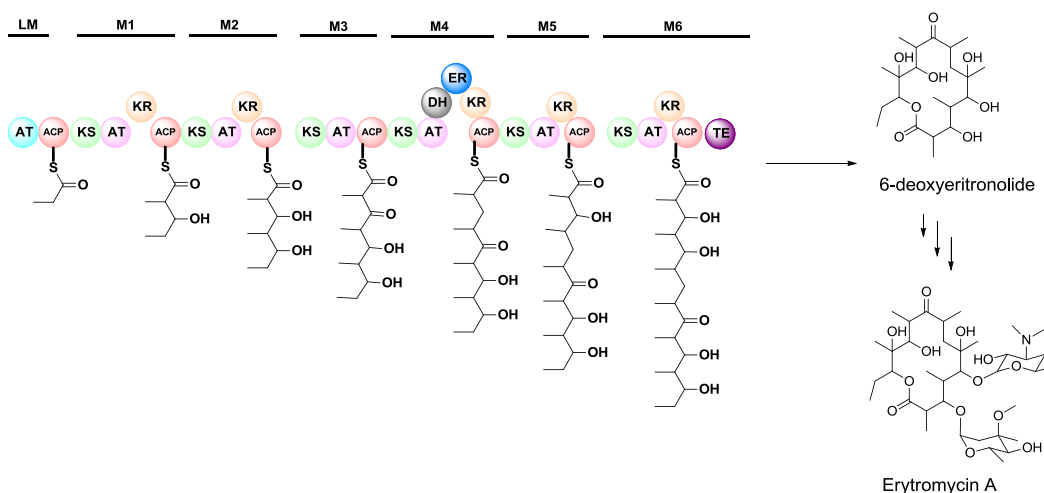olyketide assembly is readily apparent from the unit names: the starter unit is the initiating precursor for polyketide synthesis, while the extender units elongate the polyketide backbone to completion. A set of catalytic domains, grouped together as a "module," controls the incorporation of each precursor into the polyketide backbone. For modular type I PKSs, the number of modules is equivalent to the number of precursors incorporated into the polyketide. While the modules that incorporate the starter unit can have variable catalytic domains, the modules that incorporate extender units typically consist of three core domains for polyketide extension and up to three auxiliary domains involved in β-keto processing. The core domains are the ketosynthase (KS), acyltransferase (AT), and acyl carrier protein (ACP). The AT domain is the "gate keeper" of the module and recognizes the specific extender unit to be incorporated into the growing polyketide chain and covalently tethers the malonyl derivative of the extender unit onto the sulfidryl group of the ACP prosthetic group: the 4'-phosphopantetheinyl moiety of CoA. The KS domain catalyses the decarboxylative Claisen condensation between a neighboring ACP-linked malonate derivative and an ACP-linked acyl thioester to extend the polyketide chain. The remaining optional domains (ketoreductase [KR], dehydratase [DH], and enoylreductase [ER]) alter the oxidation state of the β-keto group formed after the KS-catalyzed condensation (Scheme 31).
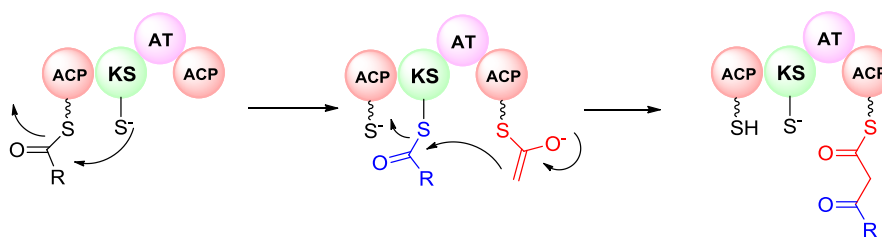
Scheme 31: During PK biosynthesis, decarboxylation of the downstream (methyl)malonyl-S-T yields a nucleophilic thioester enolate, which attacks the upstream acyl-S-T thioester in a Claisen condensation to form a C-C bond. KS: ketosynthase; AT: acyltransferase.

As already said above, the enormous structural diversity seen in the polyketide backbones of natural products comes predominantly from the diversity of starter and extender units, variations in the number of extender units incorporated, alterations in the oxidation state of the β-keto groups, and cyclization versus hydrolysis for chain termination.[122]

The basic knowledge of PKS system provides context for more efficient efforts in combinatorial biosynthesis to create collections of natural product variants with novel structure and function. Although the enormous progress made in the determination of their structures and mechanisms through the manipulation of the gene clusters encoding putative PKSs (e.g. domain deletion or 'relocation'), much more remains to be discovered.

7.1.2. Polyether antibiotics

Polyether antibiotics are a unique class of polyketides that are broadly used in veterinary medicine as anticoccidial drug. They include monensin and salinomycin among others, and all are produced by *Streptomyces* species (Figure 59).

Monensin

Salinomycin
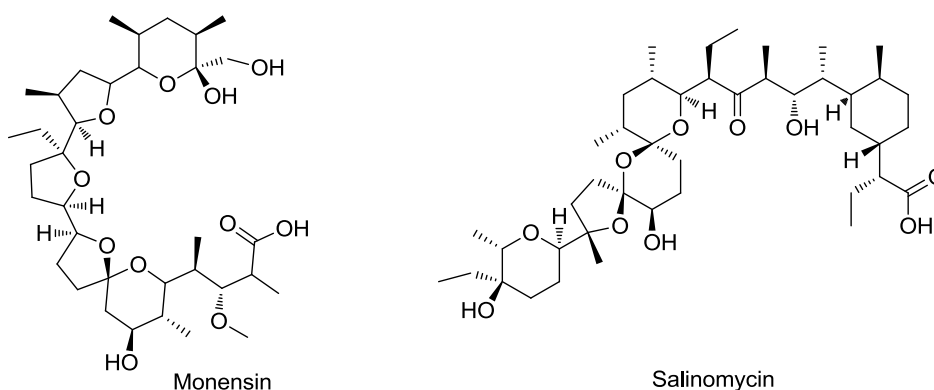
Figure 59

Due to their ability to form complexes with metal cations (host-guest complexes) and transport these complexes across lipid bilayers and cell membranes, they are widely used as anticoccidial drug but also they have shown biological activities against a variety of critical infectious disease targets including protozoa, bacteria, and viruses, as well as to selectively kill cancer stem cells.

---

[122] B. S. Moore; C. Hertweck; *Nat. Prod. Rep*, **2002**, *19*, 70.

According to the results of X-ray studies, the metal cation sites in a cage formed by oxygen atoms of the ionophore. Typically, the complexation of the cation is connected with formation of a pseudocyclic structure which is stabilized by intramolecular hydrogen bonds formed between the carboxylic group and the hydroxyl groups. The ring of ionophore molecule is wrapped around this hydrophilic cage rendering the whole complex lipophilic. The mechanism of transport of a cation by polyether ionophores is attributed to their ability to exchange protons and cations in an electroneutral process. In this type of transport of the cations (M^+), the polyether ionophore anion ($I-COO^-$) binds the metal cation or proton (H^+) to give a neutral salt ($I- COO-M^+$) or a neutral polyether ionophore in acidic form ($I-COOH$), respectively, and only uncharged molecules containing either the metal cation or proton can move through the cell membrane. The whole process leads to changes in Na^+/K^+ gradient and to an increase in the osmotic pressure inside the cell, causing swelling and vacuolization, and finally death of the bacteria cell.[123]

The wide range of biological activity mentioned above basically depends on the structural diversity, dictated by the number of ether rings and/or the manner of ring closure. Following initial Westley's speculation[124] Cane, Celmer, and Westley proposed a simple model for polyether biosynthesis involving the initial formation of an all-trans unsaturated polyketide that would undergo oxidative cyclization by stereospecific epoxidation, epoxide hydrolysis, and a cascade of nucleophilic hydroxy cyclizations.[125] This hypothesis was then validated by the isolation of (*E*,*E*,*E*)-polyketide triene precursor to monensin from a blocked mutant of *Streptomyces cinnamonensis*.[126]

7.2. Aim of this work

7.2.1. Background of the project

Lasalocid A is one of the simplest polyether composed of THF and THP rings produced by *Streptomyces lasaliensis* by type I polyketide synthase (Figure 60).[127]

[123] J. Rutkowski; B. Brzezinski; *BioMed Research International*, **2013**, 1.

[124] J. W. Westley; J. F. Blount; R. H. Jr. Evans; A. Stempel; J. Bergel; *J. Antibiot.*, **1974**, *27*, 597.

[125] D. E.Cane; W. D.Celmer; J. W.Westley; *J.Am.Chem.Soc.,* **1983**, *105*, 3594.

[126] A. Bhatt; C. B. W. Stark; B. M. Harvey; A. R. Gallimore; Y. A. Demydchuk; J. B. Spencer; J. Staunton; P. F. Leadlay; *Angew. Chem. Int. Ed.*, **2005**, *44*, 7075.

[127] M.-H. Abdulla; D. S. Ruelas; B. Wolff; J. Snedecor; K.-C. Lim; F. Xu; A. R. Renslo; J. Williams; J. H. McKerrow; C. R. Caffrey; *PLoS Neglected Trop. Dis.*, **2009**, *3*, 1.
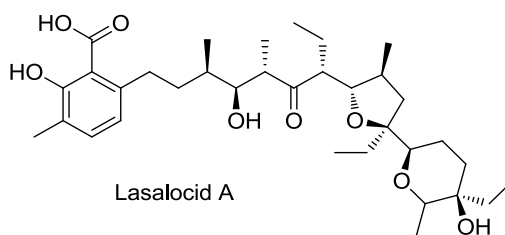
Lasalocid A

Figure 60

Its biosynthesis involves the formation of a dodecaketide from the decarboxylative condensation of malonate, methylmalonate, and ethylmalonate units. Firstly, Westley et al. suggested that the stereoselective bis(epoxidation) of a putative dodecaketide acid precursor, prelasalocid, and a subsequent epoxide hydrolysis and cyclization cascade, would lead to lasalocid A and its stereoisomer isolasalocid (Scheme 32).

Prelasalocid

epoxidation
LasC

endo-tet
LasB

exo-tet
LasB

Lasalocid A

Isolasalocid
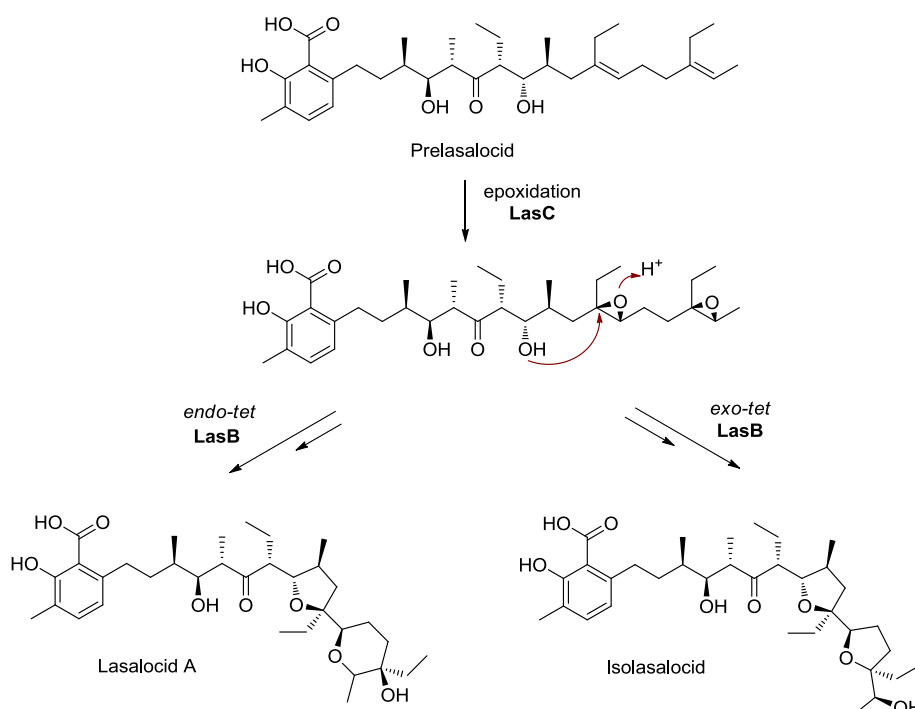
Scheme 32

However, genetic and proteomic approaches are not always applicable or successful to gain insight better to the biomechanism, especially when iterative catalytic activities by single enzymes are involved, like in this case.

In the laboratories of Manuela Tosin and coworkers, in which I spent 6 months during my PhD, has been recently developed a chemical strategy for the off-loading of intermediates from PKSs.[128] This employs nonhydrolysable synthetic mimics of malonate units normally recruited for

[128]a) M. Tosin; D. Spiteller; J. B. Spencer; *ChemBioChem.*, **2009**, *10,* 1714; b) M. Tosin; L. Betancor; E. Stephens; W. M. A. Li; J. B. Spencer; P. F. Leadlay; *ChemBioChem.*, **2010**, *11*, 539; c) M. Tosin; Y. Demydchuk; J. S. Parascandolo; C. Blasco-Per; F. J. Leeper; P. F. Leadlay; *Chem. Commun.*, **2011**, *47*, 3460.

polyketide formation, in particular carba(dethia) cysteamine analogues such as **73a** (Scheme 33 (b)).
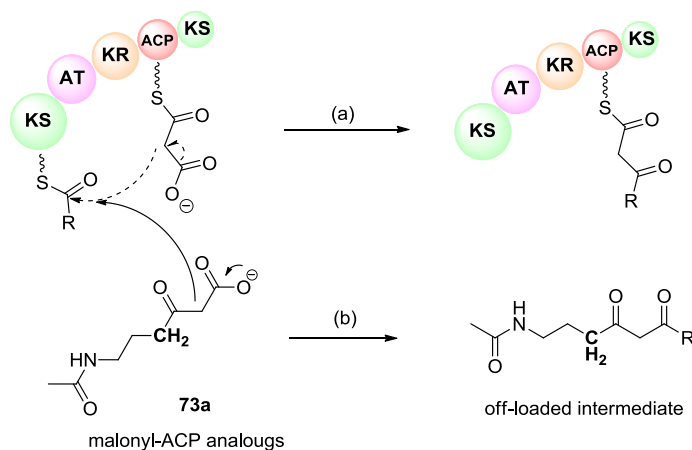
Scheme 33: (a) Methylmalonyl-ACP decarboxylative condensation leading to polyketide formation (type I modular PKS); **(b)** a smallmolecule nonhydrolysable mimic of methylmalonyl-ACP (methylmalonyl carba(dethia)-N-acetyl cysteamine, **73** intervenes, causing the off-loading of intermediates.

As the polyketide backbone is assembled by sequential decarboxylation and condensation of the natural malonate units ((**a**), Scheme 33), the carba(dethia) substrates compete with the integral acyl carrier protein (ACP) domains for the growing polyketide chain, causing the premature off-loading of truncated intermediates ((**b**), Scheme 33). Unable to be reloaded onto the enzyme, these species diffuse out of the active site and become available for LC-MS characterization. This approach has proved successful also *in vivo* studies, where the PKS catalytic activities can be interrogated in their natural context and in relation to environmental signals/responses.

In particular, *S. lasaliensis* as well as engineered mutant strains bearing a deletion in either the epoxidase LasC or the epoxide hydrolase LasB genes, has been fed with methylester of **73a** (10 mM concentration) over 3–5 days. The protection of carboxylic function is essential to increase cell permeation (charged molecule would not readily be taken up by cells) and to avoid spontaneous decarboxylation. The ester were hydrolysed by endogenous esterases to the active biosynthetic probes **73a** in situ.
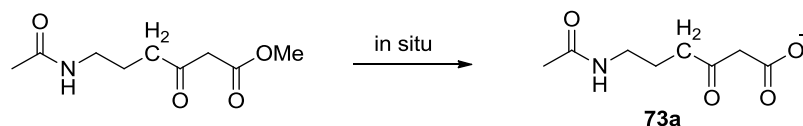
Scheme 34

Micro-LC/HRMS analyses of the ethyl acetate extracts of these bacterial cultures provide direct evidence for the off-loading of a series of intermediates from lasalocid A PKS (Scheme 35).

The total ion current and the [M+H]⁺, [M+Na]⁺, [M+NH₄]⁺ extracted ion traces (5 ppm mass accuracy) for the putative intermediate **74a**

Scheme 35: *In vivo* release of derivatives of intermediates from the lasalocid A polyketide synthase by using the synthetic chain terminators **73a** generated in situ by the hydrolysis of the corresponding methyl esters. The stereochemistry of the derivatives has yet to be established.

In the extracts of the wild-type strain grown in the presence of the malonyl carba(dethia) substrate **73a**, derivatives of a fully cyclized dodecaketide **74a**, a putative linear undecaketide diene **75a**, and its oxidized counterpart **76a** were identified. The postulated structure of these compounds is supported by HRMSn experiments and MS/MS analysis. The isolation and characterization of the putative undecaketide diene **75a** and its oxidized counterparts **76a**, suggest that epoxidation, not clear yet before these experiments, occurs on an enzyme-bound substrate, possibly on the ACP11-bound undecaketide or on the preceding ACP10 bound decaketide.

Indeed, a distinctive feature of lasalocid A is the unusual presence of an aromatic template formed by a modular PKS and it would be important to define the mechanism and the timing of its formation. The obtained results from feeding experiment using methylester of **73a** suggested that aromatization may follow ether ring formation and occur as soon as a dodecaketide chain is formed, before chain release from the PKS, but further work is needed to confirm it.[129]

---

[129] M. Tosin; L. Smith; P. F. Leadlay; *Angew. Chem. Int. Ed.*, **2011**, *50*, 11930.

7.2.2. My project

In order to improve the chemical strategy described above in term of number and amount of captured biosynthetic intermediates, aim of my work was to develop a novel synthetic chain terminator (**77**) capable of capturing polyketide biosynthetic intermediates *in vivo*. The idea was synthetize a chemical probe having a long hydrophobic chain to mimic the length of 4'-phosphopantetheinyl moiety normally bound to the ACP domain (Figure 61).
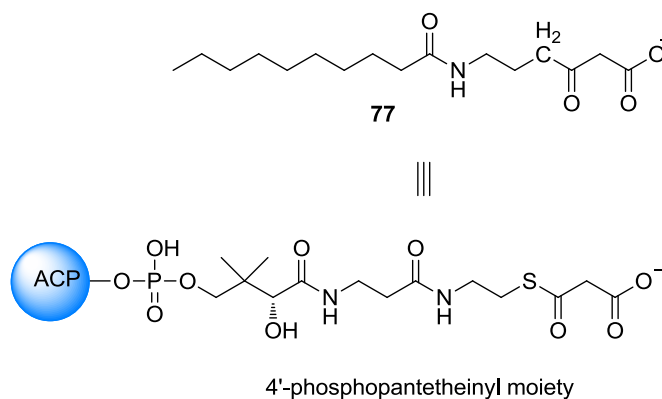

4'-phosphopantetheinyl moiety

Figure 61

Firstly, the carboxylic function was protected as methyl ester. However, previous studies showed as the hydrolysis in *situ* by endogenous esterases has been estimated to be in the range of 5-50% over five days of culturing, depending on the adopted feeding protocol. Therefore a second generation of ACP analogue was investigate to check whether, by changing the nature of the ester protection, a higher concentration of the active probes could be achieved *in vivo*, and whether this would ultimately lead to a more efficient intermediate capture.

In exploring possible protecting groups that would be easily hydrolysed *in vivo*, we considered the use of acetoxymethyl ester moiety, obtaining the compound **78** (Figure 62).
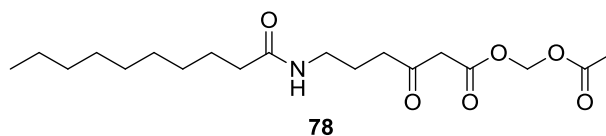

Figure 62

Acetoxymethyl (AM) esters are widely employed in prodrugs and chemical probes in eukaryotic cells to mask hydrophilic/charged bioactive functionalities, allowing effective compound cellular uptake through membrane permeation.[130] Their hydrolysis *in situ* by nonspecific cellular esterases results in the formation of hemiacetals that spontaneously decompose to 'unmask' the bioactive compounds within cells.

---

[130] P. D. Jobsis; E. C. Rothstein; R. S. Balaban; *J Microsc*. **2007**, *226*, 74.

7.3. Result

7.3.1. Chemistry

The malonyl-carba(dethia)-cysteamine analogue **77** was prepared from γ-aminobutyric acid GABA **80** according to Scheme 36. Selective acetylation of **80** with decanoyl chloride **79** and treatment of the free carboxylate with Meldrum's acid and DMAP led to the formation of the cyclic adduct **82**, which was purified by silica gel chromatography. Finally, the reaction at reflux of 16 in dry methanol afforded β-ketoester **77** in 85% of yield.
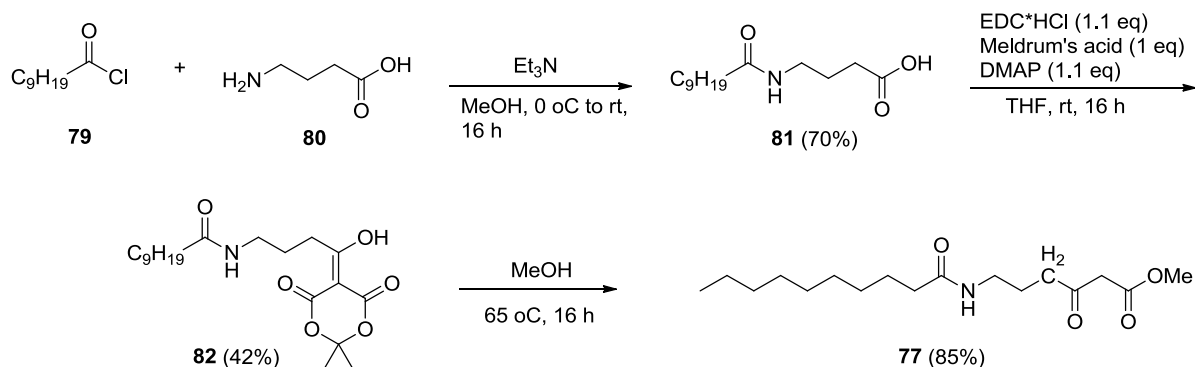
Scheme 36

The target AM ester probe **78** was prepared according to Scheme 37. Briefly, the carbonyl groups of the methyl esters **77** were protected by conversion to thioketal **83** by reaction with 1,2-ethanediol and boron trifluoride diethyl etherate. **83** were then hydrolysed to the corresponding carboxylates by treatment with potassium trimethyl silanolate, and converted to the acetoxymethyl ester **85** by reaction with bromomethyl acetate in dry THF. Finally, the desired compounds **78** was achieved by treatment of **85** with [bis-(trifluoroacetoxy)iodo]benzene.

Scheme 37
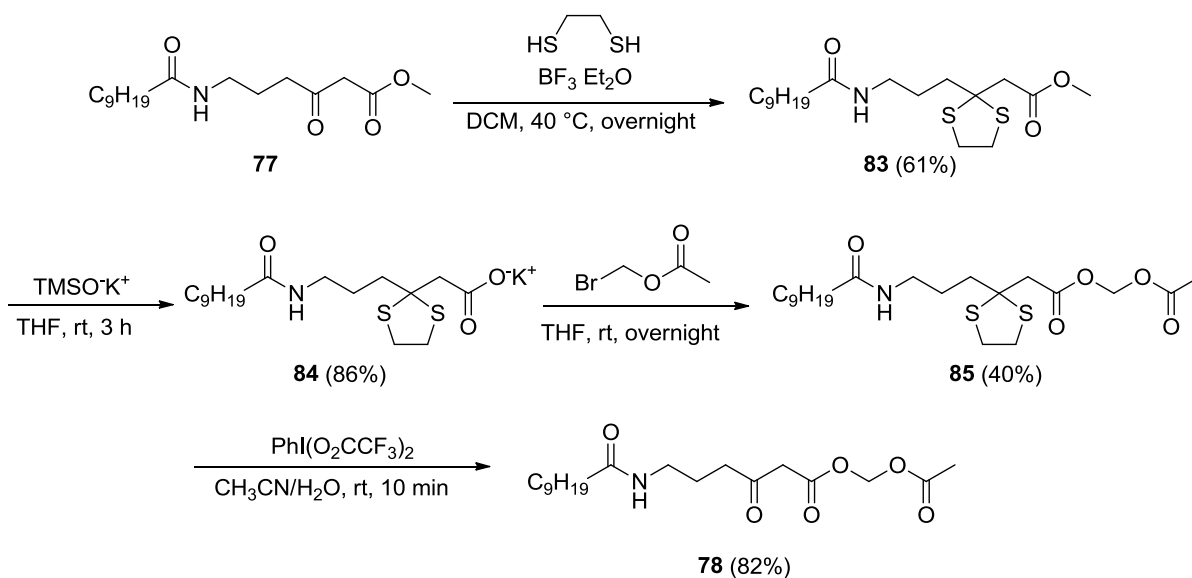
AM esters are known to spontaneously hydrolyse over time, even in neutral conditions. Therefore **78** was promptly purified by HPLC and stored for a limited amount of time at low temperature and in a lyophilised form prior to its use.

7.3.2. Feeding experiments with methyl ester *77*

The malonyl-carba(dethia)-cysteamine analogue **77** was then employed as substrates in small-scale fermentations (10 mL) of ACP mutant strains of *Streptomyces lasaliensis*. The strains, constructed from *S. lasaliensis* NRRL 3382 by point mutation of the active serine of ACP12 and ACP5 to alanine residues as previously reported,[129] do not produce the natural polyketide product lasalocid A. However, they still harbour enzyme-bound biosynthetic intermediates.

In the ethyl acetate extracts of the wild-type *Streptomyces lasaliensis* grown over 4 days in the presence of the methyl ester substrate **77** (supplemented daily to reach a 4.0 mM final concentration), the putative unnatural polyether undecaketide intermediate **77a** was identified as the major polyketide products off-loaded from the lasA PKS (Scheme 38).

Scheme 38

The postulated nature of this compound is supported by HRMSn experiments, and several careful repetition of these experiments and LC-MS analyses optimisation have allowed us to estimate that up to 10 times more of **77a** is captured using the deca-probe **77** rather than the methyl ester of **73a** (Figure 63).

a)   **b)**

Figure 63: **a)** LC-ESI-HRMS analysis of two organic extracts of *S. lasaliensis* ACP12 (S970A) grown in the presence of probe **77** and the counterpart in absence: [M+Na]+ [M+H]+ extracted ion trace for the off-loaded polyketide **77a** are shown. In both case the intensity is around 10^5. **b)** LC-ESI-HRMS analysis of the organic extract of *S. lasaliensis* ACP12 (S970A) grown in the presence of probe **73a**: [M+Na]+ [M+H]+ extracted ion trace for the off-loaded polyketide **74a** are shown with an intensity around 10^4.

Its stereochemistry is yet to be separately determined, as well as the origin of two peaks for **77a** (possibly arising from the presence of isomers/conformers).

The compound **77a** was characterized by HR-MS[2] and displayed a conserved fragmentation pattern involving McLafferty rearrangement and subsequent formation of m/z 377, a diagnostic polyether fragment. In addition, the loss of the C10 acyl chain occurring during fragmentation

afforded a m/z 260 fragment, which would correspond to a protonated cyclic imine and strongly supports the aromatic ketone nature of these derivatives (Figure 64).
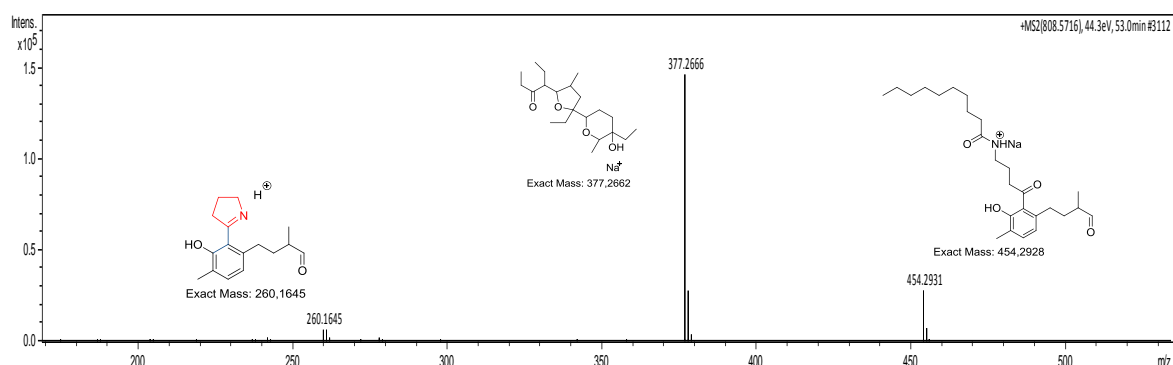
Figure 64

Interestingly, for the first time, additional formation of short-chain products (e.g., the pentaketides **77e**) was observed in quite high intensity. As well as expected species from ACP10 such as **77c** which were previously undetected, we also observed an unexpected putative dodekatide **77d**, which were unequivocally characterised by HR-MS^2. In fact this putative intermediate formally derives from KR and DH reactions taking place on the module before, and it could be due to a diffusion process into the active site of the previous module and therein processed by the KR and the DH domains to give **77d**. To the best of our knowledge this diffusion effect would be the first time that is reported. Finally, it was possible to identify unnatural polyketide deriving from other modules, like ACP2-3-5 never seen before, but the intensity of the signals were too much low to carry out a complete characterization by HR-MS^2.

7.3.3.   Feeding experiments with AM-ester **78**

In our effort to improve the titre of the off-loaded unnatural polyketides and therefore having a full kinetic picture of polyketide assembly chain, we started to investigate the attitude of the second generation of deca-probe **78** on the ACP mutant strains of *Streptomyces lasaliensis* in comparison to the first-generation methyl esters **77**. Firstly, concentration-dependent effects of **78** on bacterial cell growth and polyketide production was preliminarily evaluated on agar-plate cultures of *S. erythraea,* the soil bacterium responsible for the biosynthesis of erythromycin A. The growth of *S. erythraea* was critically affected by the presence of **78** in 10 mM and 5 mM concentration, whereas at lower concentrations (1-2 mM) normal cell growth and erythromycin production were observed (data not shown). Reasonably, the **78** toxicity on cells could be due to formaldehyde formation occurring during AM ester deprotection. To enable bacterial cells to survivor during the feeding experiments, the AM-ester **78** was added in small amounts (0.4-0.8

mM) over 5 days on bacterial liquid cultures. The overall outcome of the feeding experiments is summarized in Scheme 39.
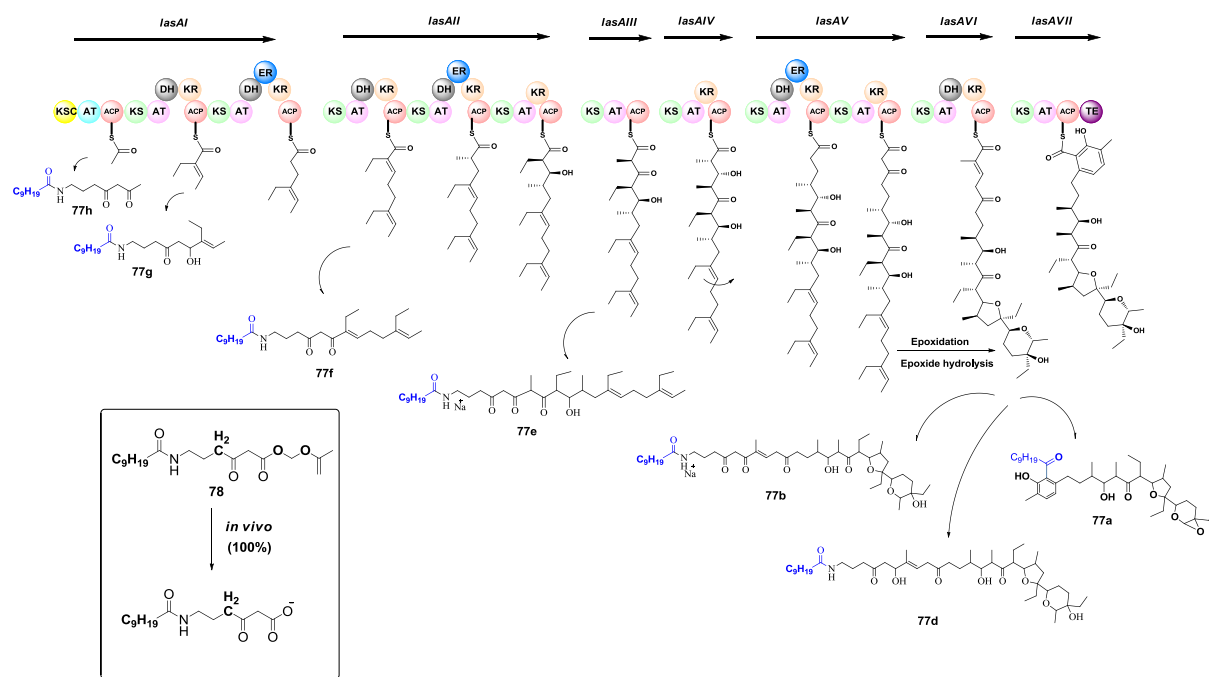
Scheme 39

LC-HRMS analyses of the ethyl acetate extracts revealed complete hydrolysis of **78** and further enhancement in the titre of the unnatural polyethers **77a,b,d-f** was clearly observed (Figure 65).
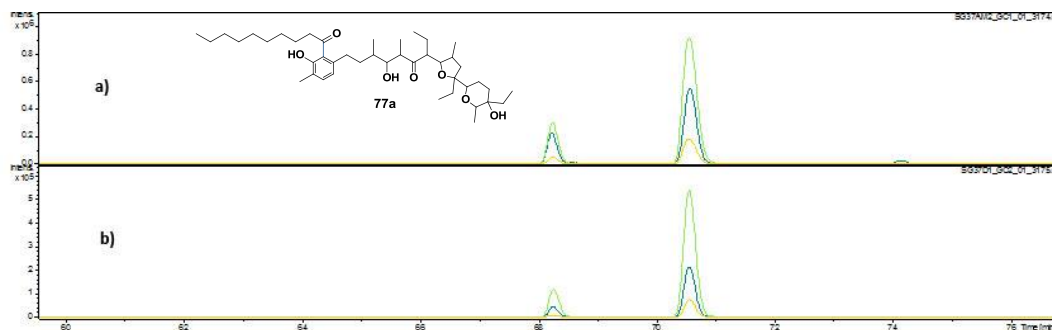

Figure 65: a) LC-ESI-HRMS analysis of an organic extract of S. lasaliensis ACP12 (S970A) grown in the presence of probe **78**: $[M+Na]^+$ $[M+H]^+$ extracted ion trace for the off-loaded polyketide **77a** is shown. The intensity is around 10^6. **b)** LC-ESI-HRMS analysis of the organic extract of S. lasaliensis ACP12 (S970A) grown in the presence of probe **77**: $[M+Na]^+$ $[M+H]^+$ extracted ion trace for the off-loaded polyketide **77a** is shown with an intensity around 10^5.

The unexpected putative dodekatide **77d**, was again identified, confirming the possibility of a diffusion effect between PKS modules. Besides, the previous experiments using this substrates *in vivo* led for the first time to the off-loading of biosynthetic short chain intermediates **77f** from the modular *lasA* polyketide assembly line. Further studies are essential to confirm the putative intermediates identified and to try to gain a complete set of biosynthetic intermediates from the modular *lasA* polyketide assembly line.

7.4. Conclusion

In summary, with this work the chemical strategy developed by Manuela Tosin *at al.* about the trapping of biosynthetic intermediates of polyketide system has been optimized. In particular, using the methyl-ester deca probe **77** on *S. lasaliensis* it has been possible to identify many intermediates never seen before, even unexpected.

Subsequently, the use of a more efficient protecting group of carboxylic moiety in term of *in situ* hydrolysis, led to obtain an evident enhancement of the titre of putative intermediates compared with the counterpart deriving from feeding with **77**. Previous experiments are really promising for having a complete set of biosynthetic intermediates from the modular *lasA* polyketide assembly line, since the identification of short-chain intermediates.

Finally, this chemical strategy represent an effective chemical biology tool for developing novel mutasynthesis and synthetic biology since its capacity to generate unnatural polyketides directly *in vivo*. Therefore this approach may give access to novel molecules of therapeutic interest, as well as helping illuminate their mechanism of action.

7.5. Experimental part

7.5.1. General methods

Unless specified otherwise, chemicals were purchased from Sigma Aldrich, Fisher Scientific, Carbosynth and Alfa Aesar and were used without further purification. Dry dichloromethane, tetrahydrofuran and *N,N*-dimethylformamide were purchased from VWR International (AR grade) and dried using solvent towers. Dry methanol and dry acetonitrile were purchased from Fisher Scientific. Reagent grade dichloromethane, ethyl acetate, methanol, acetonitrile, acetone, dimethyl sulfoxide and tetrahydrofuran were purchased from Fisher Scientific. Analytical thin-layer chromatography (TLC) was performed on aluminium sheets precoated with silica gel 60 (F254, Merck) and visualized under ultra-violet light (short and long-wave) and using potassium permanganate (KMnO4) or vanillin stains. Silica gel was purchased from Sigma Aldrich (Tech Grade, pore size 60Å, 230-400 mesh). ^{1}H and ^{13}C NMR spectra were recorded in d^4-MeOD, CDCl$_3$ or D$_2$O on the following Bruker Avance instruments: DPX-300 300 MHz, DPX-400 400 MHz, DRX-500 500 MHz, AV-600 600 MHz or AV-700 700 MHz. High-resolution mass spectra (HRMS) were obtained using electrospray ionization (ESI) on a MaXis UHR-TOF (Bruker Daltonics) or on Bruker MaXis (ESI-HR-MS). Compounds were purified by preparative or semipreparative HPLC on Phenomenex synergi™ Polar RP 80Å (250 x 21.2 mm, 4μm) and Phenomenex synergi™ Polar RP 80Å (250 x 10.0 mm, 4μm) columns respectively. The mobile phase consisted of a gradient of water and acetonitrile or methanol (HPLC grade, containing 0.1 % trifluoroacetic acid or 0.1% formic acid) at a flow rate of 20 or 2.5 mL/min, with UV detection at 210, 254 and 280 nm.

7.5.2. Synthesis

Compound 77 was prepared following the reported procedure.[61]

Synthesis of methyl-2-(2-(3-decanamidopropyl)-1,3-dithiolan-2-yl)acetate (83)
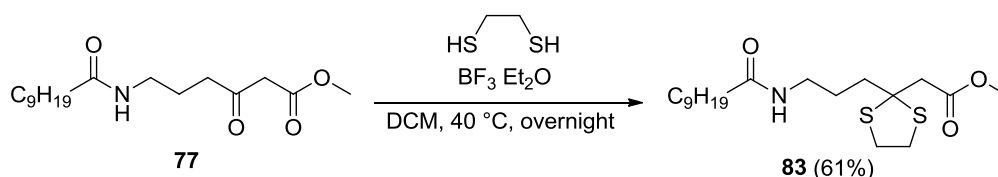
Compound **77** (800 mg, 2.55 mmol) and 1,2-ethanthiol (1.07 mL, 12.8 mmol) were dissolved in dichloromethane (16 mL) under argon atmosphere. The solution was cooled to 0 °C before BF$_3$·OEt$_2$ (1.57 mL, 12.8 mmol) was slowly added. The reaction was stirred under reflux overnight. Then, a saturated solution of NaHCO$_3$ was added at 0 °C up to pH

9 and the mixture was extracted with CH_2Cl_2 (3x10 mL) The crude product was purified by column chromatography (cyclohexane: EtOAc, 7:3 to 1:1)) and **83** was obtained as a white powder.

Yield 61%; ^1H NMR (400 MHz, CDCl$_3$): δ 5.51 (br s, 1H), 3.70 (s, 3H), 3.30 (s, 4H), 3.29 (m, 2H), 3.04 (s, 2H), 2.14 (m, 2H), 2.14 (m, 2H), 1.75 (m, 2H), 1.58 (m, 2H), 1.27 (br s, 12H), 0.87 (t, J = 6.5 Hz, 3H) ppm; ^{13}C NMR (101 MHz, CDCl$_3$): δ 173.1, 170.5, 66.6, 51.7, 48.2, 39.8, 39.4, 39.1, 36.9, 29.4, 29.4, 29.3, 29.3, 27.1, 25.8, 22.6, 22.6, 14.1 ppm; HR-ESI-MS: calculated for $C_{19}H_{35}NO_3S_2$ 412.1951, found: 412.1945 [M-H]$^-$.

Synthesis of potassium 2-(2-(3-decanamidopropyl)-1,3-dithiolan-2-yl)acetate (84)
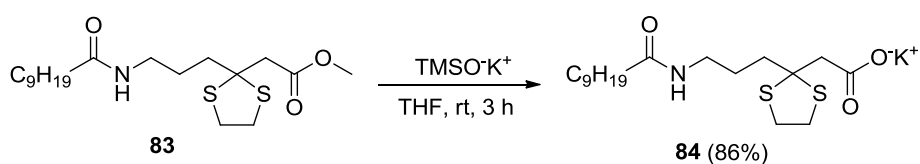
To a solution of Compound **83** (600 mg, 1.54 mmol) in dry THF (10 mL) containing 3 Å molecular sieves, was added potassium trimethilsilanolate (789 mg, 6.16 mmol). The reaction was stirred under argon atmosphere for 3 h at room temperature. Then the reaction was filtered under vacuum and concentrated. The residue was dissolved in water (5 mL), EtOAc (5 mL) was added, and the two phases were separated. The aqueous layer was freeze-dried affording **84** as a white powder.

Yield 86%; ^1H NMR (400 MHz, D$_2$O): δ 3.22 (m, 4H), 3.13 (m, 2H), 2.17 (t, J = 7.2 Hz, 2H), 2.01 (m, 2H), 1.84 (s, 4H), 1.64 (br s, 2H), 1.53 (br s, 2H), 1.22 (br s, 12H), 0.79 (br s, 3H) ppm; ^{13}C NMR (101 MHz, D$_2$O): δ 180.9, 177.4, 175.7, 67.1, 50.1, 39.4, 38.7, 38.2, 35.5, 31.1, 28.7, 28.5, 28.4, 28.2, 26.1, 25.3, 21.9, 13.2 ppm.

Synthesis of acetoxymethyl-2-(2-(3-decanamidopropyl)-1,3-dithiolan-2-yl)acetate (85)
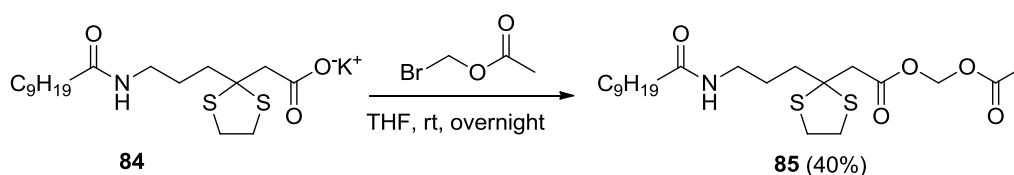
Compound **84** (545 mg, 1.32 mmol) was suspended in dry THF (9 mL) and bromoethylacetate (140 µL, 1.58 mmol) was added. The reaction was stirred at room temperature overnight and afterwards concentrated under vacuum. The crude product was purified by column chromatography (EtOAc/CycloHex 6:4) to yield **85** as a white powder (220 mg, 40%).

Yield 86%; ^{1}H NMR (400 MHz, CDCl$_3$): δ 5.75 (s, 1H), 5.55 (br s, 1H), 3.31 (s, 4H), 3.30 (m, 2H), 3.08 (s, 2H), 2.13 (m, 2H), 2.13 (m, 2H), 2.12 (s, 3H), 1.56 (m, 2H), 1.27 (m, 2H), 1.29 (br s, 12H), 0.88 (t, J = 6.4 Hz, 3H); ^{13}C NMR (101 MHz, CDCl$_3$): δ 173.2, 169.9, 168.6, 79.2, 66.4, 48.2, 39.8, 39.4, 39.1, 36.9, 29.5, 29.4, 29.3, 29.3, 27.1, 25.8, 22.7, 22.7, 20.7, 14.1 ppm. HR-ESI-MS: calculated for C$_{21}$H$_{37}$NO$_5$S$_2$ 470.2005, found: 470.2006 [M-H]$^+$.

Synthesis of acetoxymethyl-6-decanamido-3-oxohexanoate (78)
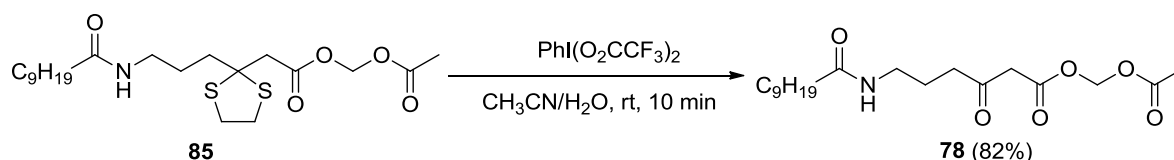
Compound **85** (200 mg, 0.45 mmol) was dissolved in acetonitrile (12 mL) and water (1.12 mL) and [bis(trifluoroacetoxy)iodo]benzene (576 mg, 1.34 mmol) was added. The reaction was stirred at room temperature for 10 minutes, quenched with H$_2$O/NaHCO$_3$ sat./Na$_2$S$_2$O$_3$ sat. solution (1:1:1, 12 mL). The organic solvent was separated and removed under reduced pressure. The final mixture was extracted with dichloromethane (3x5 mL), the organic layer was dried, filtered, concentrated and the crude was purified by column chromatography (eluent 7:3 EtOAc/CycloHex). **78** was obtained as a white powder (80 mg, 40%).

Yield 82%; ^{1}H NMR (400 MHz, CDCl$_3$): δ 5.75 (s, 1H), 5.73 (br s, 1H), 3.50 (s, 2H), 3.24 (m, 2H), 2.60 (t, J = 6.8 Hz, 2H), 2.14 (m, 2H), 2.12 (s, 3H), 1.80 (m, 2H), 1.59 (m, 2H), 1.25 (br s, 12H), 0.86 (t, J = 6.1 Hz, 3H) ppm; ^{13}C NMR (101 MHz, CDCl$_3$): δ 200.8, 173.4, 169.7, 166.1, 79.5, 48.7, 40.4, 40.4, 38.5, 31.8, 31,8, 29.4, 29.3, 29.3, 25.8, 23.9, 22.1, 20.5, 14.1 ppm; HR-ESI-MS: calculated for C$_{19}$H$_{33}$NO$_6$ 394.2200, found: 394.2202 [M-H]$^+$.

7.5.3. Feeding experiments

Microbiology methods: All media and glassware were sterilized prior to use by autoclave (Astell). Liquid cultures were grown with shaking in Innova 44 incubator/shaker (New Brunswick scientific). M79 medium: 2.5 g glucose, 2.5 g peptone, 0.5 g yeast extract, 1.5 g NaCl, 2.5 g casein hydrolysate in 250 ml of tap water adjusted to pH 7.1. MYM medium: 1.0 g maltose, 1.0 g yeast extract, 2.5 g malt extract in 250 ml of tap water adjusted to pH 7.1.

Construction of mutant strains of *Streptomyces lasaliensis*: The cultivation of the wild type lasalocid-producing strain *S. lasaliensis* NRRL3382 was carried out as previously described.[131] The construction of *S. lasaliensis* ACP12 (S970A) and ΔlasB ACP12 (S970A) mutant strains was previously reported. The ligated plasmid was transformed into *E. coli* strain DH10B and positive colonies tested by restriction mapping and sequencing before a correct clone was transferred to

---

[131]E. M. Sletten; C. R. Bertozzi; *Angew. Chem. Int. Ed.,* **2009**, *48*, 6974.

E. coli ET12567/pUZ8002. The mutant was fermented and LC-MS analysis of the ethyl acetate extracts of each culture showed that lasalocid production was completely abolished.

Growth of *S. lasaliensis* wild-type (WT), ACP12 (S970A) strain and mass spectrometry analysis:
The *S. lasaliensis* strain was grown in M79 medium (10 mL) for 3 days at 30 °C in 50 mL Erlenmeyer flasks with spring. Seed cultures (100 µL) were used to inoculate MYM liquid cultures (10 mL, in duplicate/triplicate copy, in 50 mL Erlenmeyer flasks with spring). They were incubated at 30 °C for 5 days. After the first day of incubation, the probes (**77-78**, final concentration: 2.5 mM) were added portionwise as follows: addition of 8.3 µmol dissolved in 100 µl of MeOH on day 2 and day 3; addition of 4.1 µmol dissolved in 50 µl of MeOH on day 4 and 5. Control liquid cultures in absence of **77-78** of the strains were also prepared (in duplicate/triplicate copy). After 5 days of fermentation, the liquid cultures were extracted with ethyl acetate (20 mL x 2). The extracts were concentrated and the residues were redissolved in HPLC-grade methanol (1 mL) for mass spectrometry analysis. UPLC-HR-ESI-MS analyses of *S. lasaliensis* ACP12 (S970A) strain was performed on a MaXis Impact UHR-TOF (Bruker Daltonics). Samples (5 µl) were injected onto an Acquity UPLC HSS T3 (150 mm x 1.0 mm, 1.8 µm) or Agilent Eclipse C18 (1.8um, 100 mm x 2.1 mm). The mobile phase consisted of a gradient of water and acetonitrile (HPLC grade, each with 0.1 % trifluoroacetic acid). The following solvent (A =1% TFA in H_2O, B =1% TFA in MeCN) gradient was applied:

- 10% B 0-2.7 min; 10-100% B 2.7-42.7 min; 100% B 42.7-62.7 min; 100-10% B 62.7-65.7 min; 10% B 65.7-77.7 min, using an Acquity UPLC HSS T3 column at a flow rate of 0.05 mL/min.

Spectra were recorded in positive ionisation mode, scanning from m/z 100 to 3000, with the resolution set at 45K. Selected ion search within 5 ppm was performed, as well as high resolution fragmentation (collision energy set to 15-20%) for the putative biosynthetic intermediates.

Off-loading of functionalized polyketides from *S. lasaliensis* ACP12 (S970A) via chemical probe 77

77a
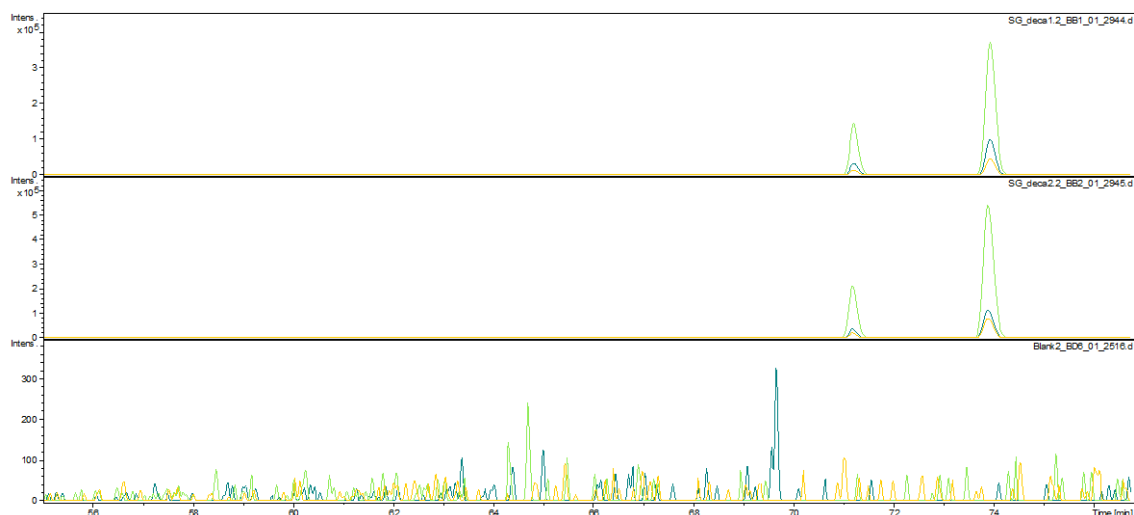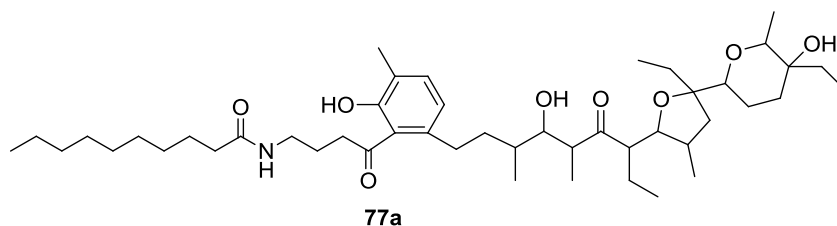
Figure 66: LC-ESI-HRMS analysis of the organic extracts of S. lasaliensis ACP12 (S970A) grown in the absence and in the presence of probe **77** (final concentration 3.0 mM; day 2 and 3: 0.01 mmol, day 4 and 5: 0.005 mmol): [M+H]$^+$, [M+Na]$^+$ and [M+NH$_4$]$^+$extracted ion traces for the off-loaded polyketide **77a** are shown.
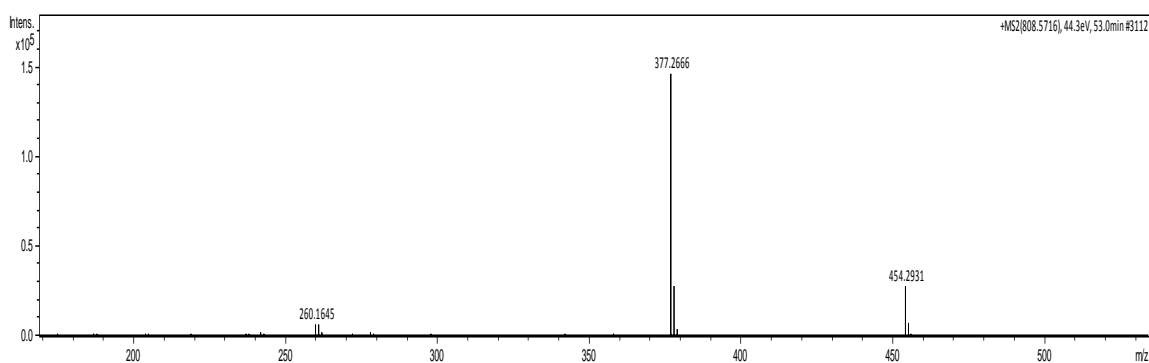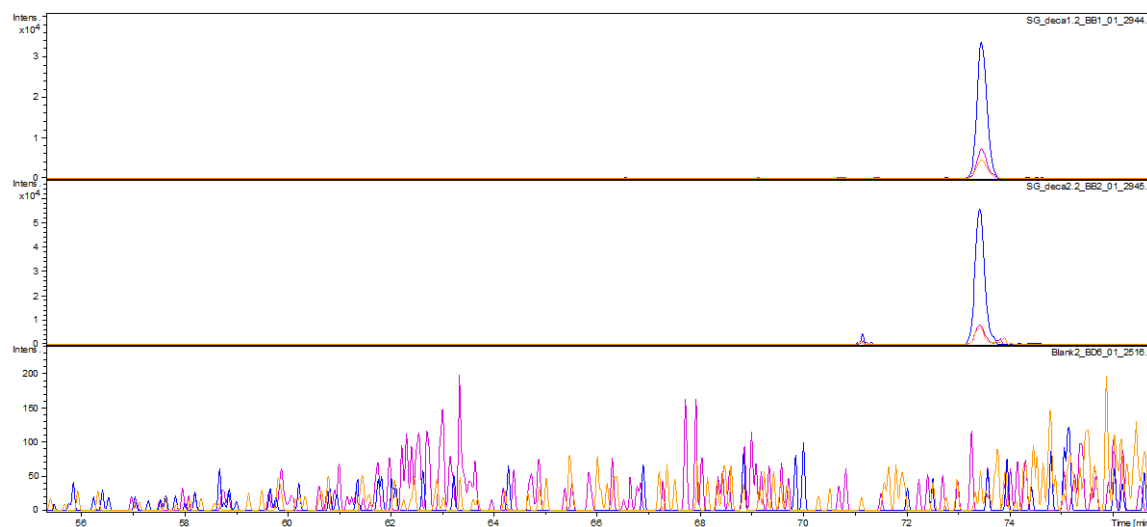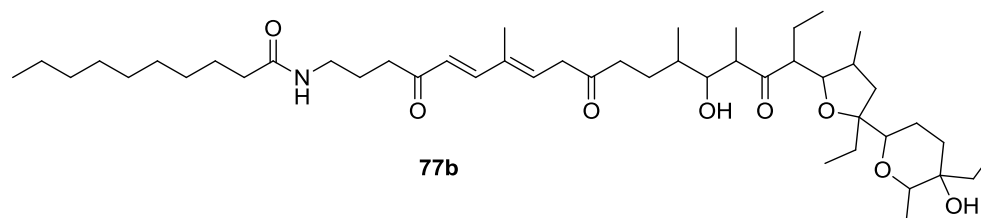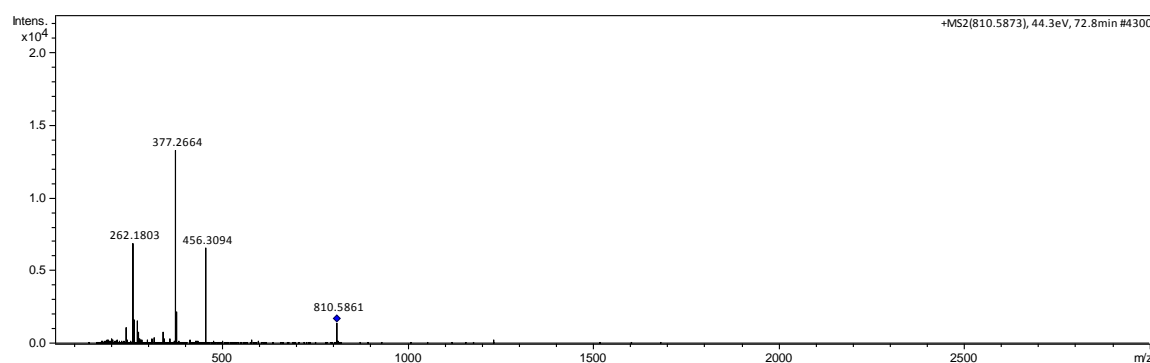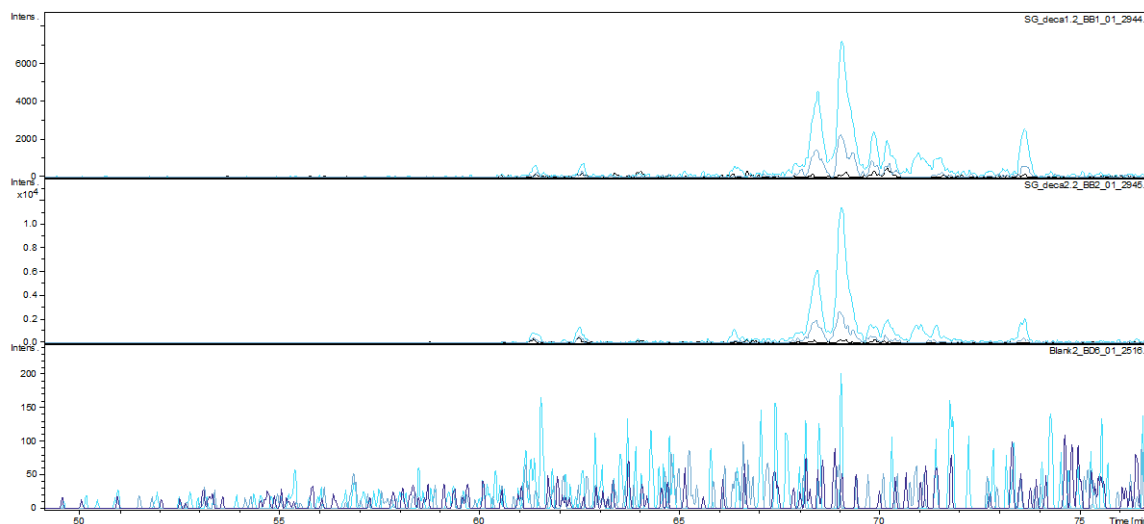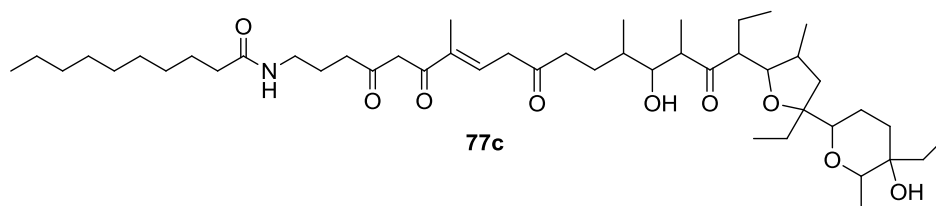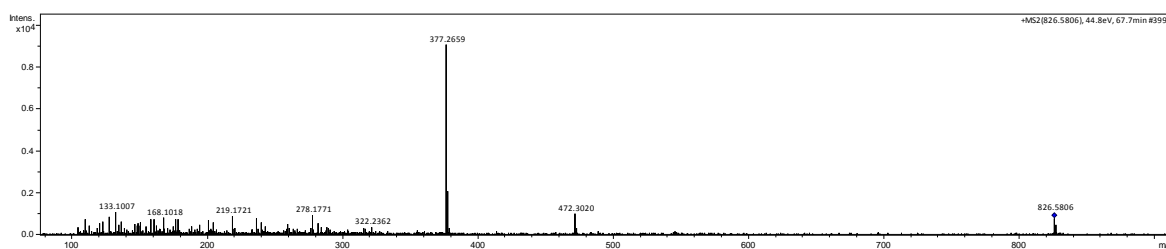

Figure 67: HR-ESI-MS^2 analysis of the off-loaded dodecaketide **77a**. McLafferty fragmentation of the [M+Na]$^+$ adduct generates a left–hand fragment of m/z 377, characteristic of lasalocid A, as well as a right-hand fragment containing the long chain moiety (m/z 454). The distinctive peak at m/z 260 corresponds to the protonated imine generated by the cyclization of the aromatic ketone and the amine derived from loss of the decanoyl chain.
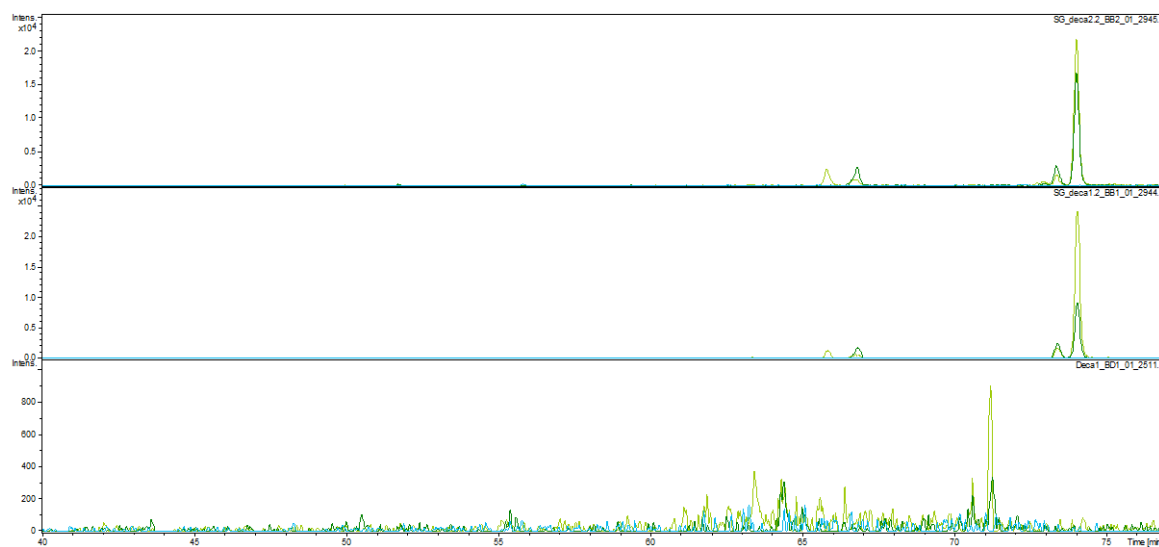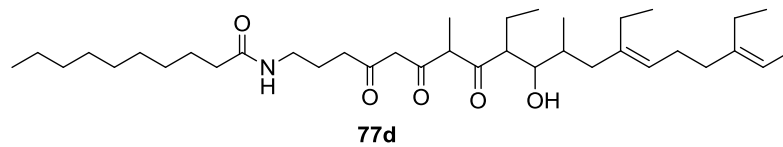
77b

Figure 68: LC-ESI-HRMS analysis of the organic extracts of S. lasaliensis ACP12 (S970A) grown in the absence and in the presence of probe **77** (final concentration 3.0 mM; day 2 and 3: 0.01 mmol, day 4 and 5: 0.005 mmol): [M+H]⁺, [M+Na]⁺ and [M+NH₄]⁺ extracted ion traces for the off-loaded polyketide **77b** are shown.

Figure 69: HR-ESI-MS² analysis of the off-loaded dodecaketide **77b**. McLafferty fragmentation of the [M+Na]⁺ adduct generates a left–hand fragment of m/z 377, as well as a right-hand fragment containing the long chain moiety (m/z 456). The distinctive peak at m/z 262 corresponds to the protonated imine generated by the cyclization of the aromatic ketone and the amine derived from loss of the decanoyl chain.
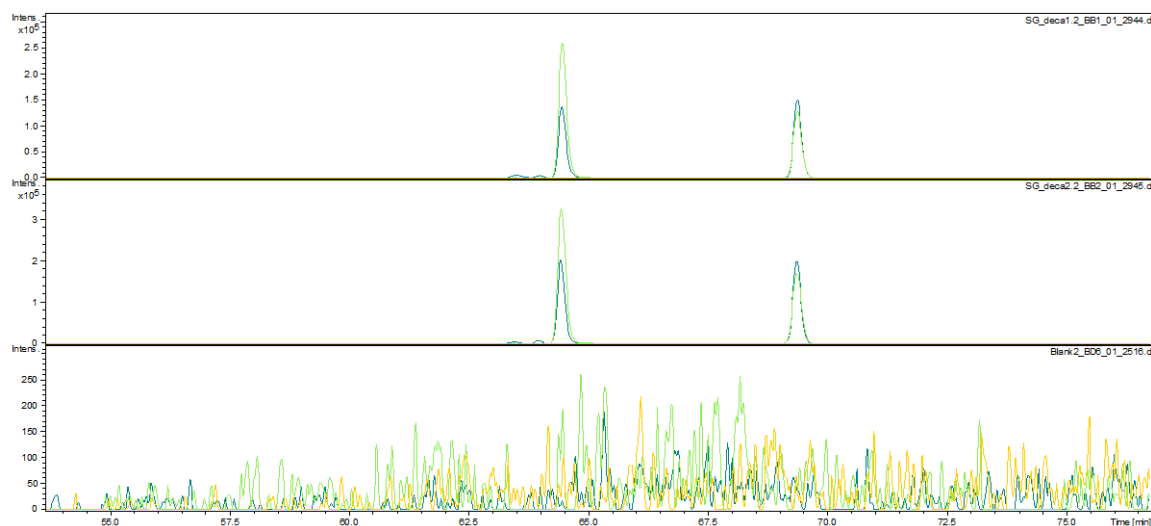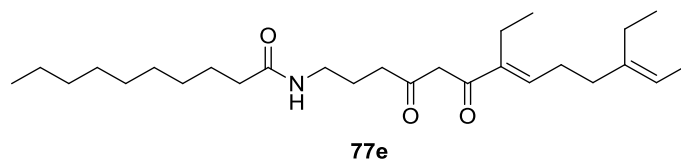
77c

Figure 70: LC-ESI–HRMS analysis of the organic extracts of S. lasaliensis ACP12 (S970A) grown in the absence and in the presence of probe **77** (final concentration 3.0 mM; day 2 and 3: 0.01 mmol, day 4 and 5: 0.005 mmol): [M+H]⁺, [M+Na]⁺ and [M+NH₄]⁺extracted ion traces for the off-loaded polyketide **77c** are shown.

Figure 71: HR-ESI-MS² analysis of the off-loaded dodecaketide **77c**. McLafferty fragmentation of the [M+Na]⁺ adduct generates a left–hand fragment of m/z 377, as well as a right-hand fragment containing the long chain moiety (m/z 472). The peak at m/z 278 corresponds to the protonated imine generated by the cyclization of the aromatic ketone and the amine derived from loss of the decanoyl chain.

77d

Figure 72: LC-ESI-HRMS analysis of the organic extracts of S. lasaliensis ACP12 (S970A) grown in the absence and in the presence of probe **77** (final concentration 3.0 mM; day 2 and 3: 0.01 mmol, day 4 and 5: 0.005 mmol): $[M+H]^+$, $[M+Na]^+$ extracted ion traces for the off-loaded polyketide **77d** are shown.
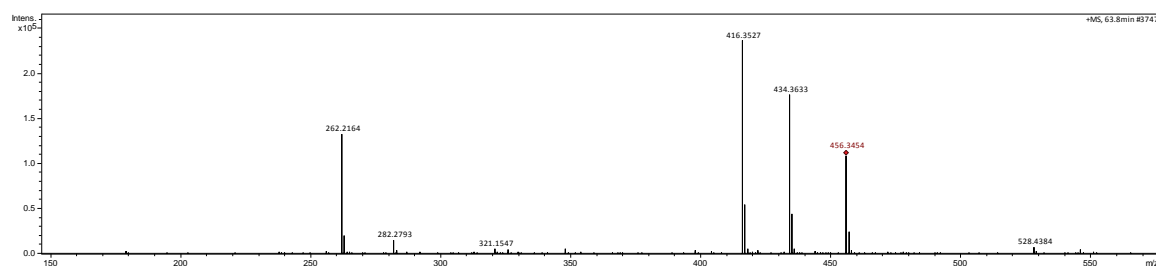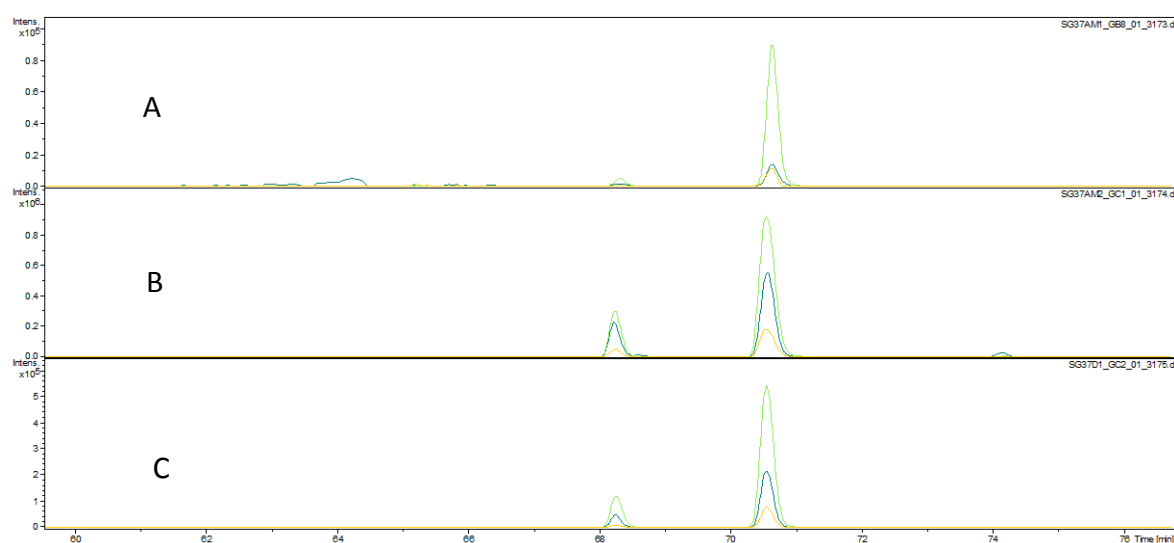
77e

Figure 73: LC-ESI-HRMS analysis of the organic extracts of S. lasaliensis ACP12 (S970A) grown in the absence and in the presence of probe **77** (final concentration 3.0 mM; day 2 and 3: 0.01 mmol, day 4 and 5: 0.005 mmol): [M+H]$^+$, [M+Na]$^+$ extracted ion traces for the off-loaded polyketide **77e** are shown.

Figure 74: HR-ESI-MS^2 analysis of the off-loaded dodecaketide **77e**. The distinctive peak at m/z 262 corresponds to the protonated imine generated by the cyclization of the aromatic ketone and the amine derived from loss of the decanoyl chain

Off-loading of functionalized polyketides from *S. lasaliensis* ACP12 (S970A) via chemical probe 78

The analysis of feeding experiments carried out with the AM ester of deca probe **78** are still under investigations. Herein I will report previous LC-ESI-HRMS analysis only.
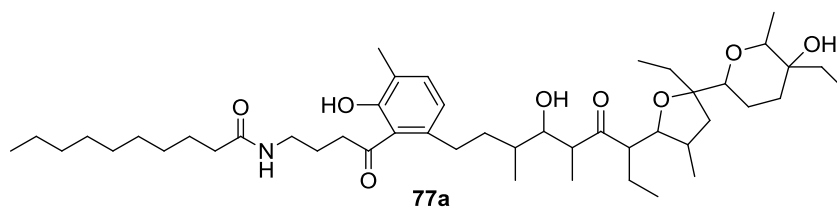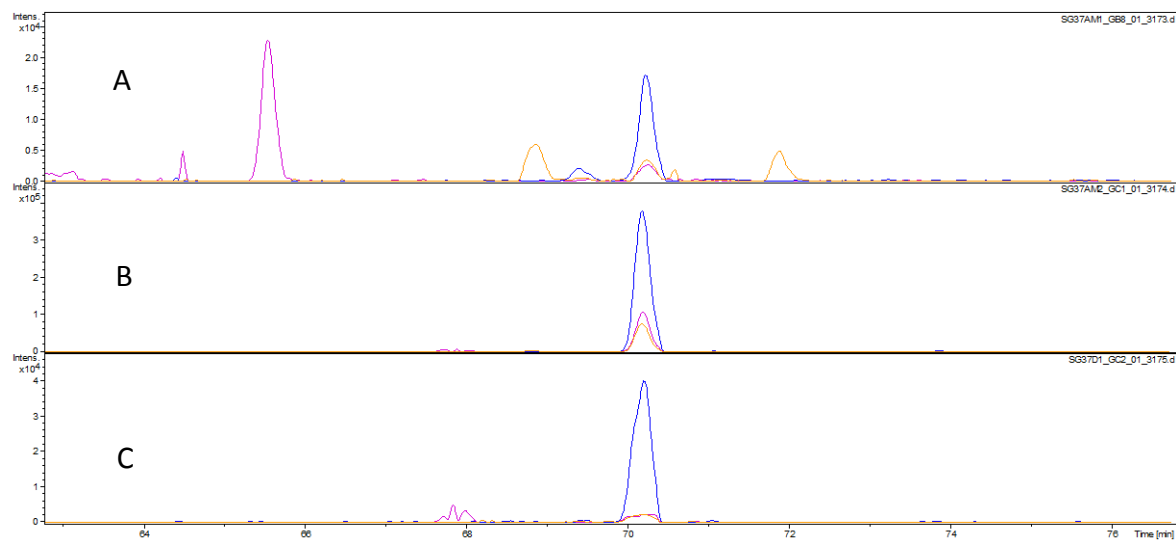

Figure 75: LC-ESI-HRMS analysis of the organic extracts of S. lasaliensis ACP12 (S970A) grown in the presence of probe **78** (**A,B**) (final concentration 3.0 mM; day 2 and 3: 0.01 mmol, day 4 and 5: 0.005 mmol) and in presence of probe **77** (**C**) as control: [M+H]$^+$, [M+Na]$^+$ and [M+NH$_4$]$^+$ extracted ion traces for the off-loaded polyketide **77a** are shown. The higher intensity is clear in the experiment (**B**).
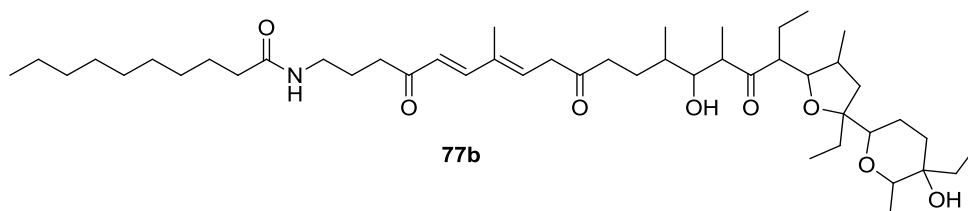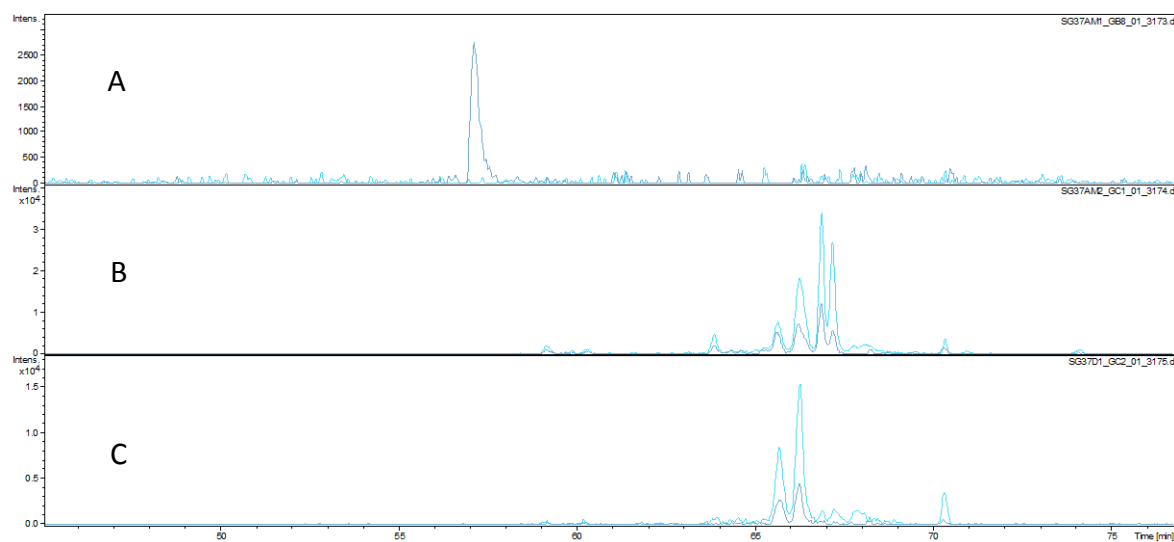
Figure 76: LC-ESI-HRMS analysis of the organic extracts of S. lasaliensis ACP12 (S970A) grown in the presence of probe **78** (**A,B**) (final concentration 3.0 mM; day 2 and 3: 0.01 mmol, day 4 and 5: 0.005 mmol) and in presence of probe **77** (**C**) as control: [M+H]$^+$, [M+Na]$^+$ and [M+NH$_4$]$^+$ extracted ion traces for the off-loaded polyketide **77b** are shown. The higher intensity is clear in the experiment (**B**).
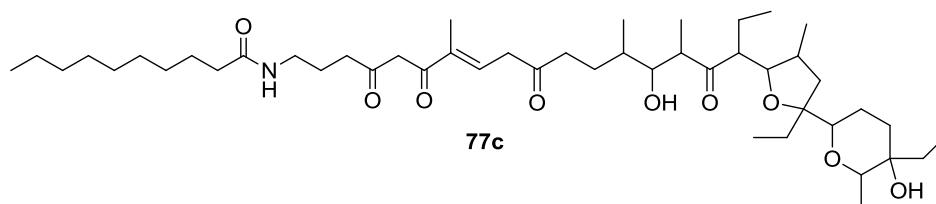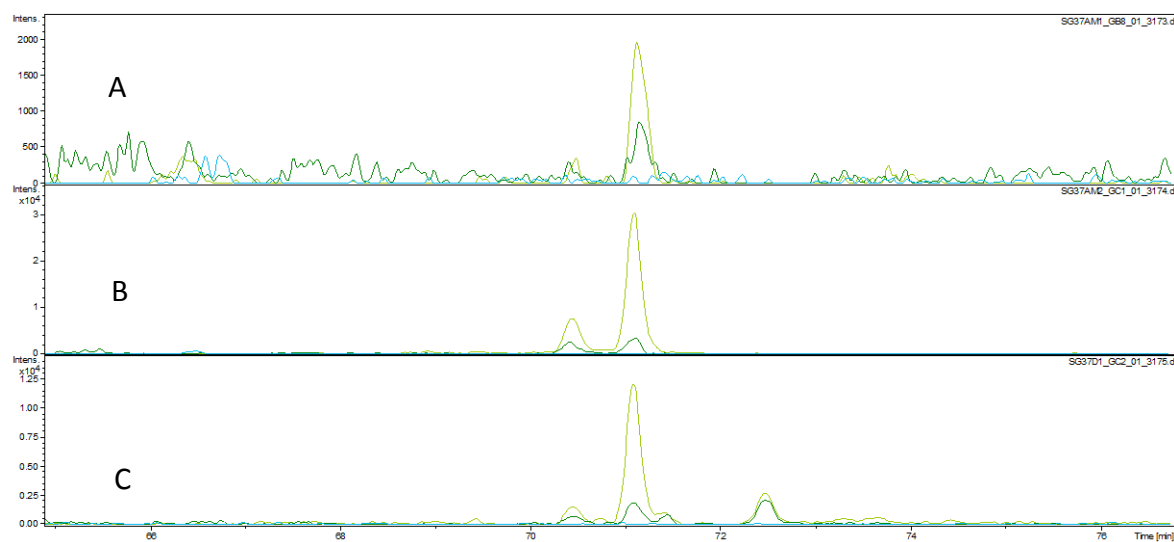
77c

Figure 77: LC-ESI-HRMS analysis of the organic extracts of S. lasaliensis ACP12 (S970A) grown in the presence of probe **78** (**A,B**) (final concentration 3.0 mM; day 2 and 3: 0.01 mmol, day 4 and 5: 0.005 mmol) and in presence of probe **77** (**C**) as control: [M+H]⁺, [M+Na]⁺ extracted ion traces for the off-loaded polyketide **77c** are shown.
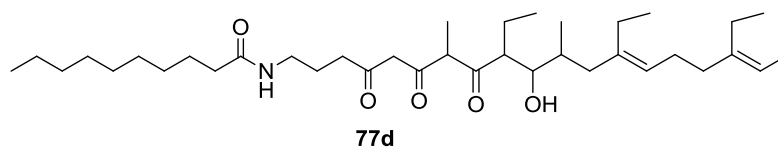
77d

Figure 78: LC-ESI-HRMS analysis of the organic extracts of S. lasaliensis ACP12 (S970A) grown in the presence of probe **78** (**A,B**) (final concentration 3.0 mM; day 2 and 3: 0.01 mmol, day 4 and 5: 0.005 mmol) and in presence of probe **77** (**C**) as control: [M+H]$^+$, [M+Na]$^+$ extracted ion traces for the off-loaded polyketide **77d** are shown.
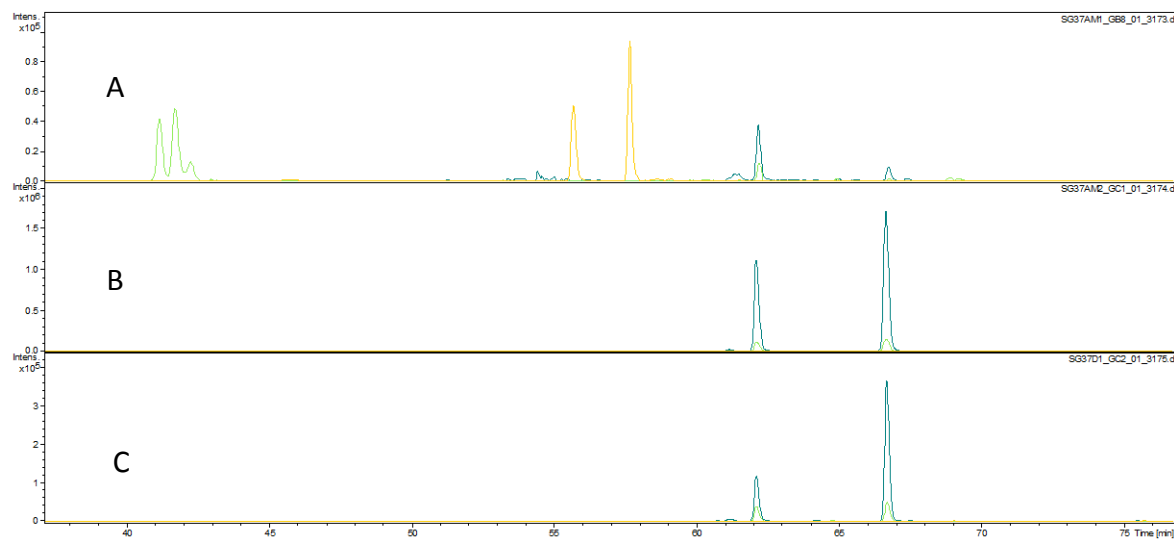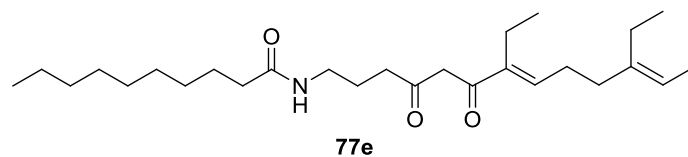
77e

Figure 79: LC-ESI-HRMS analysis of the organic extracts of S. lasaliensis ACP12 (S970A) grown in the presence of probe **78** (**A,B**) (final concentration 3.0 mM; day 2 and 3: 0.01 mmol, day 4 and 5: 0.005 mmol) and in presence of probe **77** (**C**) as control: [M+H]$^+$, [M+Na]$^+$ and [M+NH$_4$]$^+$ extracted ion traces for the off-loaded polyketide **77e** are shown. The higher intensity is clear in the experiment (**B**).
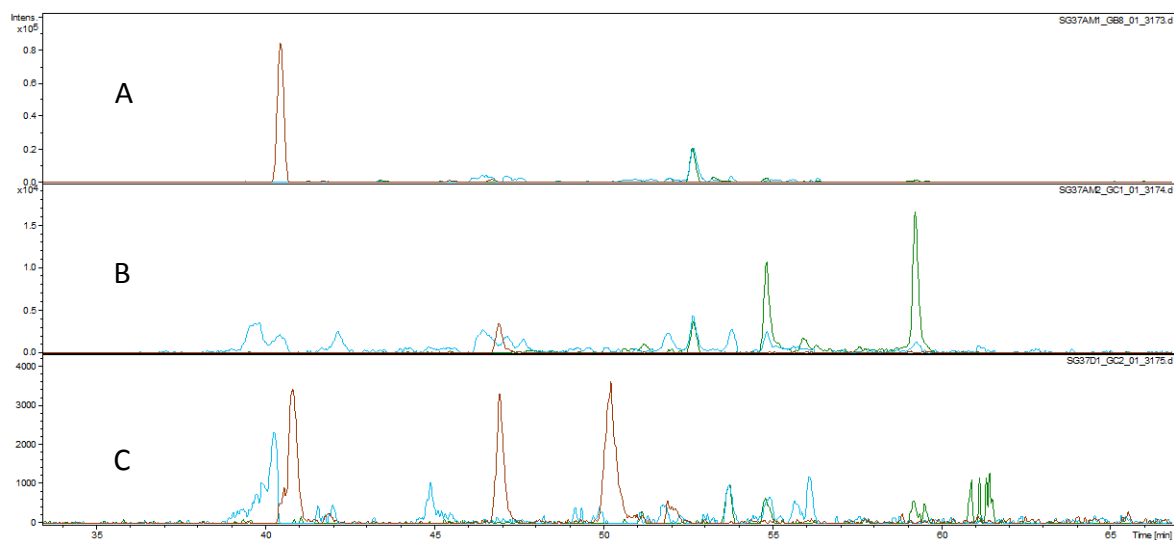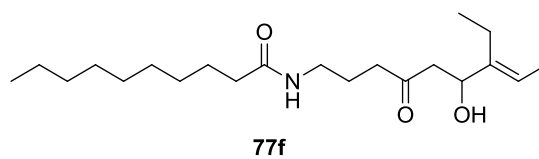
77f

Figure 80: LC-ESI-HRMS analysis of the organic extracts of S. lasaliensis ACP12 (S970A) grown in the presence of probe **78** (**A,B**) (final concentration 3.0 mM; day 2 and 3: 0.01 mmol, day 4 and 5: 0.005 mmol) and in presence of probe **77** (**C**) as control: [M+H]⁺, [M+Na]⁺ extracted ion traces for the off-loaded polyketide **77f** are shown. The putative intermediate is identifiable in the experiment (**B**).
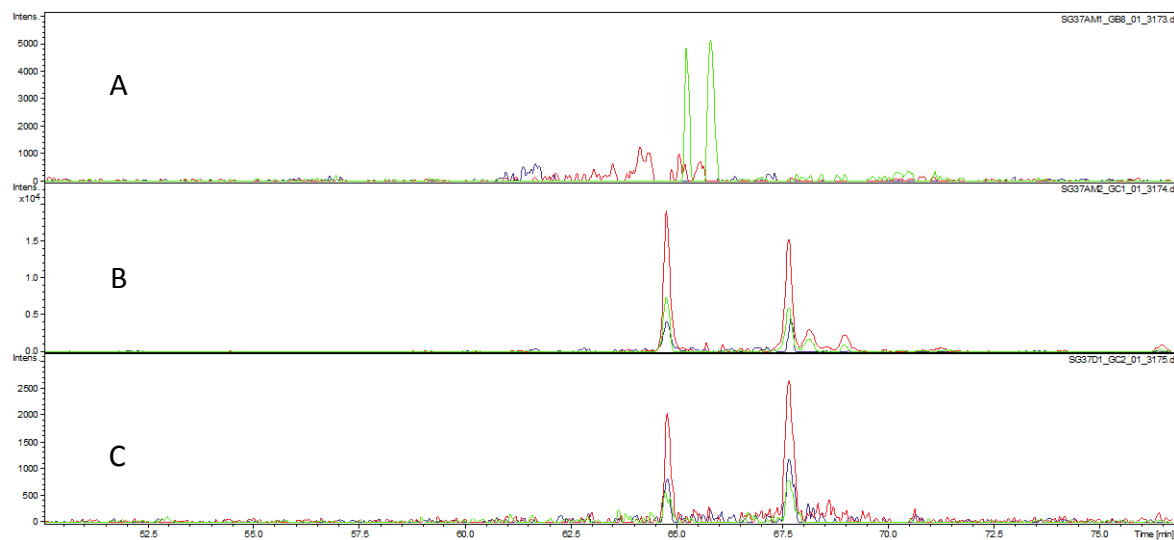
77g

Exact Mass: 805,6068

Figure 81: LC-ESI-HRMS analysis of the organic extracts of S. lasaliensis ACP12 (S970A) grown in the presence of probe **78** (**A,B**) (final concentration 3.0 mM; day 2 and 3: 0.01 mmol, day 4 and 5: 0.005 mmol) and in presence of probe **77** (**C**) as control: $[M+H]^+$, $[M+Na]^+$ and $[M+NH_4]^+$ extracted ion traces for the off-loaded polyketide **77g** are shown. The higher intensity is evident in the experiment (**B**).
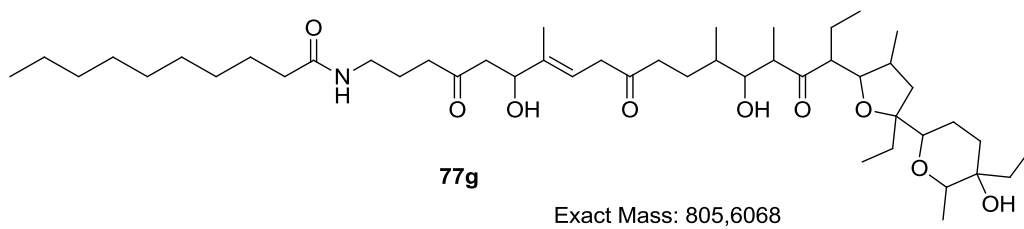
Conclusion

The main topic of my PhD is the investigation of several privileged scaffolds arising from natural compounds, with the idea to prepare from them new potential anticancer compounds.

Interesting results in term of anticancer activity were obtained either with the oxazole-pyridine series, through an effective double intramolecular domino palladium catalyzed process, or with pironetin-dumetorin hybrids, which come from modelling studies that confirmed a probable interaction with α-tubulin.

The development of two new synthetic approaches toward the synthesis of the racemic mixture and both enantiomers of boehmeriasin A, a potent alkaloid with high antiproliferative activity against several cancer cell lines, represents an additional issue to make more available novel topoisomerase and SIRT-2 inhibitors based on the boehmeriasin A scaffold.

The disegn and synthesis of a new epothilone derivative (triazole-epothilone) is today a big challenge in the research for new cancer treatments, since the efficacy of epothilones against tumour cells. Many efforts will be spend to obtain the molecule, and to evaluate it as inhibitor of microtubule activity.

Finally, the foreign period in Manuela Tosin group allowed to gain insight to one of the most efficient natural machine represented by type one polyketide synthase. The chemical strategy to isiolate biosynthetic intermediates from *Streptomices lasaliensis,* may represent an effective chemical biology tool to access to novel molecules of therapeutic interest through mutasynthesis and synthetic biology.

To conclude, Nature has been a source of medicinal products for millennia, and during the past century, an impressive number of anti-cancer drugs have been developed from natural sources, particularly plants. It is clear that Nature will continue to be a major source of new drug leads. The drug potential of the marine environment remains relatively unexplored, but it is becoming increasingly evident that the microorganisms offers a vast untapped potential. However, only a multidisciplinary collaboration between chemists, biologists and biochemists will allow to discovery and optimize new effective drugs based on the incredible fantasy of Mother Nature.

Aknowledgement

Alla fine di questi 3 lunghi, difficili e appassionanti anni, ci tengo molto adire un immenso GRAZIE a tutte quelle persone che ne hanno fatto parte.

In primo luogo il mio tutor Broggini, o amichevolmente Gianni, che mi accompagnata nella mia crescita lavorativa dandomi sempre consigli indispensabili per farmi fare il meglio che potessi.

Rngrazio ovviamente i commissari A. Goti, O. Reiser e D. Passarella che gentilmente hanno accettato di presenziare alla mia discussione di dottorato.

E ringrazio anche il prof. Piarulli che mi ha aiutato quando ho avuto bisogno, e mi ha anche tirato delle gran sberle in teste come buongiorno quasi ogni mattina per 3 anni ☺, e la prof. Manuela Tosin, perche´con la sua passione ha alimentato la mia voglia di continuare nel mondo della ricerca.

E poi ci sono tutti quelli che hanno fatto parte di questo percorso, chi più chi meno, dell'Università e ringrazio davvero tutti, dal primo all'ultimo. Un ringraziamento speciale però lo vorrei fare a:

- Filippo, che negli anni è passato da compagno di corso, a quello che non veniva alle cene universitarie, a un amico su cui ho sempre potuto contare;
- Sara G., che con le sue battuttacce ha sempre rallegrato anche le giornate più buie e che con la sua calma mi riusciva sempre a tranquillizzare;
- Pangherina, che ho adorato dal primo giorno che l'ho incontrata con quella fantistica affermazione: "ah, ma farai per forza il libero così bassa", a quando mi ha chiamato il giorno prima della mia partenza per Francoforte tutta malata solo per salutarmi. Ti adorerò sempre.. Grazie.
- Leila, che mi ha sempre incoraggiata e stimata incomprensibilmente☺ E la ringrazio per la sua spalla, sempre presente negli ultimi mesi, quelli più ardui.
- Daria, semplicemente per la sua amicizia fedele e schietta, e ovviamente per le nostre seratone indimenticabili.
- Andre e Raffa che con la loro allegria (e cinismo) hanno sempre portato un po' di brio al lab ma soprattutto ai nostri pranzi☺

Concludendo con la "gente universitaria" vorrei ringraziare anche Cekka, che pure lui mi è sempre stato vicino.

E poi c'è la gente di fuori, non meno importante. Cristina, amica da sempre, e per sempre (spero!);) Elena, insostituibile.. sempre presente.. non potrei mai fare a meno della sua amicizia.

Un ringraziamento importante va anche a Cora, una persona che mi ha fatto anche da sorella oltre che da amica da quando l'ho consciuta.

E infine alla mia famiglia… perché senza il loro sotegno morale non sarei mai potuta arrivare fino a qui.

Grazie